AFRL-RH-WP-TR-2008-0008

Human Information Processing in the Dynamic Environment (HIPDE)

Richard A. McKinley
Lloyd D. Tripp, Jr.
Jacob Loeffelholz
Robert L. Esken
Kathy L. Fullerton

Biosciences and Protection Division
Biobehavioral Performance Branch

Chuck Goodyear

General Dynamics Advanced Information Systems
5200 Springfield Pike Suite 200
Dayton OH 45431-1289

January 2008
Final Report for October 2002 to December 2007

Air Force Research Laboratory
Human Effectiveness Directorate
Biosciences and Protection Division
Biobehavioral Performance Branch
Wright-Patterson AFB OH 45433

NOTICE AND SIGNATURE PAGE

This report was cleared for public release by the 88th ABW Public Affairs Office and is available to the general public, including foreign nationals. Copies may be obtained from the Defense Technical Information Center (DTIC) (http://www.dtic.mil).

THIS REPORT HAS BEEN REVIEWED AND IS APPROVED FOR PUBLICATION IN ACCORDANCE WITH ASSIGNED DISTRIBUTION STATEMENT.

AFRL-RH-WP-TR-2008-0008

//signed//	//signed//
Richard A. McKinley Work Unit Manager Biobehavioral Performance Branch	Mark M. Hoffman, Deputy Chief Biosciences and Protection Division Human Performance Wing Air Force Research Laboratory

REPORT DOCUMENTATION PAGE

Form Approved
OMB No. 0704-0188

1. REPORT DATE *(DD-MM-YYYY)*	2. REPORT TYPE	3. DATES COVERED *(From - To)*
30 Jan 2008	Final	Oct 2002 – Dec 2007

4. TITLE AND SUBTITLE
Human Information Processing in the Dynamic Environment

5a. CONTRACT NUMBER
F41624-97-D-6004

5b. GRANT NUMBER
N/A

5c. PROGRAM ELEMENT NUMBER
62202F

6. AUTHOR(S)
Richard A. McKinley
Kathy L. Fullerton
Lloyd D. Tripp
Chuck Goodyear
Jacob Loeffelholz
Robert L. Esken

5d. PROJECT NUMBER
7184

5e. TASK NUMBER
03

5f. WORK UNIT NUMBER
05

7. PERFORMING ORGANIZATION NAME(S) AND ADDRESS(ES)
General Dynamics Advance Information Systems
5200 Sprinfield Pike Suite 200
Dayton OH 45431-1289

8. PERFORMING ORGANIZATION REPORT NUMBER

9. SPONSORING / MONITORING AGENCY NAME(S) AND ADDRESS(ES)
Air Force Materiel Command
Air Force Research Laboratory
Human Effectiveness Directorate
Biosciences and Protection Division
Aircrew Performance and Protection Branch
Wright-Patterson AFB OH 45433

10. SPONSOR/MONITOR'S ACRONYM(S)
AFRL/RHPG

11. SPONSOR/MONITOR'S REPORT NUMBER(S)
AFRL-RH-WP-TR-2008-0008

12. DISTRIBUTION / AVAILABILITY STATEMENT
Approved for public release; distribution is unlimited

13. SUPPLEMENTARY NOTES
88th ABW/PA Cleared 23 January 2008, WPAFB-08-0131

14. ABSTRACT

Flight in modern fighter aircraft often subject pilots to arduous acceleration profiles that can have traumatic consequences on their ability to perform certain cognitive tasks. The Human Information Processing in Dynamic Environments (HIPDE) program was developed to assess the extent of cognitive deficits during operationally relevant +Gz loading and provide a validated model of these effects for use in modeling, wargaming, and simulation. A total of 10 experiments were conducted to assess cognitive performance during Gz acceleration including tracking, motion inference, precision timing, peripheral information processing, relative motion, visual monitoring, short term memory, pitch-roll capture, unusual attitude recovery, situational awareness, and rapid decision making. Because each task involved multiple cognitive abilities, the results were weighted and summed across individual cognitive skills to assess the overall performance decrement. Overall, simple decision making, tracking, motion inference (fast and slow) and perception of speed are negatively affected. The findings were then compared to a model known as G-TOP to ensure its validity.

15. SUBJECT TERMS
Cognitive Performance, Acceleration, G, Cerebral Oxygen Saturation, Cognition

16. SECURITY CLASSIFICATION OF:			17. LIMITATION OF ABSTRACT	18. NUMBER OF PAGES	19a. NAME OF RESPONSIBLE PERSON
a. REPORT	b. ABSTRACT	c. THIS PAGE			Richard A. McKinley
U	U	U	SAR	257	19b. TELEPHONE NUMBER *(include area code)* N/A

Standard Form 298 (Rev. 8-98)
Prescribed by ANSI Std. 239.18

THIS PAGE LEFT BLANK INTENTIONALLY

TABLE OF CONTENTS

LIST OF FIGURES

Figure Page

LIST OF TABLES

PREFACE

The work covered in the following report was completed under the Human Information Processing in Dynamic Environments (HIPDE) program. The project/task/work unit number began as 71840303 and was then changed to 71840305. The program manager for HIPDE is currently Mr. Andy McKinley (AFRL/HEPG). The work covered in this report began in October of 2002 and was completed in December of 2007. It includes a comprehensive analysis of results and findings from all ten experiments conducted during the course of this program. Each study is separated into its own individual chapter.

This project would not have been possible were it not for the expert technical support contributed by several sources. First, the authors would like to thank the Dynamic Environment Simulator (DES) operations crew (Jeff Bird, Marvin Roark, Greg Bathgate, Doug Coppess, and Steve Bolia) for their support during this experiment. In addition, significant contributions were made by NTI, Inc. by identifying the critical cognitive skills needed in the flight environment.

HUMAN INFORMATION PROCESSING IN THE DYNAMIC ENVIRONMENT

CHAPTER 1: INTRODUCTION

Aviation related sustained acceleration research has been conducted for many years resulting in a fairly robust understanding of its negative effects on human physiology and anatomical structures. Of principle interest has been the phenomenon known as Acceleration Induced Loss of Consciousness (G-LOC) due to its propensity to cause loss of aircraft and/or aircrew deaths. Recent research conducted by Tripp et al. (2002) and Tripp et al. (2003) have also discussed the cognitive deficits directly resulting from such events. The lack of oxygen supply caused by the inertial forces of the high-G environment that can ultimately result in a G-LOC event may also contribute to other cognitive complications that can significantly reduce the overall performance of the pilot in the execution of critical tasks. For example, it is well-known that "almost loss of consciousness" (A-LOC) is accompanied by euphoria, apathy, weakness, localized uncontrollable motor activity or paralysis, loss of short-term memory, dream-like states, confusion and loss of situational awareness, abnormal sensory manifestations, sudden inappropriate flow of emotion, and inability to respond to alarms or radio calls even though the participant appreciates them at the time and desires to respond (Morrissett & McGowan, 2000). Hence, it is reasonable to hypothesize that these impairments do not materialize suddenly and all at once. As the blood (hence oxygen) supply is depleted, it is likely that specific cognitive functions are ceased in a graded fashion to devote the limited metabolic resources to those critical to survival.

Human Cognition and Cortical Metabolism

Human cognition encompasses such processes as thought, perception, problem solving, and memory. The ability to maintain these cognitive processes during high-G combat is critical to the survival of the pilot/aircraft and the achievement of mission success. Unfortunately, this task is rather difficult due to the fact that modern high-performance aircraft are capable of reaching accelerations that exceed the limits of human physiology. An increase in acceleration in the z-axis (head-to-foot) increases the inertial force acting upon the body and causes an increase in the apparent weight of the blood. As this apparent weight continues to increase, the heart must attempt to add compensating pressure to pump the blood to the upper extremities, including the head. However, this is ultimately a losing battle. In fact, each additional $+1G_z$ applied translates into a 22 mmHg decrease in eye-level blood pressure (Naval Aerospace Medical Institute, 1991). Once the apparent weight of the blood exceeds the ability of the cardiovascular system to generate compensating pressure, the flow of blood in the intracranial arteries significantly decreases, thereby causing the blood to pool in the lower extremities and reducing oxygenated blood flow to the cerebral tissues (Ernsting, Nicholson, and Rainford, 1999). Consequently, task performance and decision-making abilities can be seriously impaired during the most critical elements of air combat, such as tight turns or climbing maneuvers.

The amount of available oxygenated blood in the cerebral tissue likely drives and/or limits cognitive ability. In fact, previous work has suggested that decreases in eye-level blood pressure and cerebral oxygen saturation (rSO_2) lead to decreased motor function and cognitive ability (Ernsting, Nicholson, and Rainford, 1999; Newman, White, and Callister, 1998; Tripp, Chelette, and Savul, 1998). It is likely that these deficits are caused primarily by a global lack of metabolic resources available to the cortical tissues during high-G maneuvers. These resulting

deficits can seriously impede the pilot's ability to successfully navigate the aircraft and perform other mission essential tasks.

The brain requires an exorbitant amount of oxygen to function properly. In fact, the brain receives about 15-20 percent of the body's total blood supply, thus 15-20 percent of the total amount of inhaled oxygen. The principal reason for this is that the brain cannot metabolize fat or carbohydrates for energy. Therefore, neurons cannot store a large amount of energy. They typically utilize only glucose for energy due to the fact that a large quantity of energy is required for several functions. Glucose is converted to usable energy through aerobic respiration, which produces about 19 times more energy than anaerobic respiration. A considerable amount of this energy is used to repair or replace various cell components due to the fact that neurogenesis (creation of new neurons) is relatively sparse and occurs only in certain areas of the brain (e.g. the hippocampus). This ensures the cells survive the lifespan of an individual human being. In addition, neurons must use energy for the interneuron communication activities which include packaging, transporting, producing, secreting, and signaling the reuptake of neurotransmitters. The remainder of the neuron's energy is devoted its primary function of transmitting electrical energy (action potentials) from the dendrites to the axon.

As positive acceleration in the head-to-foot direction (G_z) increases, the oxygenated blood is drawn away from neural tissues. Without adequate oxygen, the brain cannot produce enough energy (ATP) to sustain all cognitive processes. Therefore, many of the higher-order cognitive functions begin to dissipate or arrest all together so that critical functions (such as breathing) can be maintained. A detailed investigation of the extent to which cognitive performance is affected by increases in acceleration is therefore necessary to attain a complete understanding of the overall pilot performance and effectiveness for a given mission.

Effects of Acceleration on Cognition

Acceleration research has been conducted for well over fifty years, and in that time much has been learned regarding the effect of the high-G environment on the human body and the resulting changes in physiology. These efforts have aided in the understanding of the principal phenomena that affect vision, endurance, consciousness, and performance, while leading to the development of superior G protective measures such as advanced G-suits and anti-G straining maneuvers. Still, the effects of acceleration stress on cognitive performance are largely unknown. Although several studies have been conducted that examine task performance, relatively few have been accomplished that probe the level of degradation in specific cognitive skills. A listing of the available literature detailing effects of acceleration on cognitive abilities is provided below.

Some studies have investigated the effects of acceleration on spatial disorientation (SD) (Albery, 1990) and image mental rotation/orientation (Nethus, et al., 1993). However, because SD typically occurs at low G levels, there is little available evidence of cognitive effects on perception of orientation above 3.5 G_z. Repperger, Frazier, Popper, and Goodyear (1990) conducted a study to investigate the perception of both fast and slow motion at G-levels between 1 and 5 G_z using a time estimation task. The results seem to indicate a general slowing of the perceived time for the target to reach its destination. Furthermore, although the ability to find and track targets is important to any aircraft hostile environment, only one study has attempted to truly investigate how acceleration might affect this ability (Rogers, et al., 1973). This study required subjects to fire on a target once it was in the crosshairs following a G_z profile ranging between 1 and 8 G_z. Results indicated that performance decreases significantly from baseline

performance (as much as 77% at 8 G_z). Additional studies have evaluated visual acuity during acceleration using various G profiles and metrics (Frankenhauser, 1958; McCloskey, et al., 1992; Repperger Frazier, Popper, & Goodyear, 1990; Warrick & Lund, 1946; White, 1960; White, 1962). Until now, virtually no emphasis has been placed on providing predictive tools or models that could yield pilot task performance decrements based on the decreased cognitive ability at higher accelerations.

Human Information Processing In the Dynamic Environment Program

The program entitled, "Human Information Processing in the Dynamic Environment" (HIPDE) was created to provide constructed representations of fighter pilots to the modeling and simulation (M&S) community that include validated algorithms to modify the agents' performance and cognition based on the stress of the inertial environment. The first goal of the HIPDE program concerned the development of a custom task battery to probe specific cognitive functions. This work was completed by NTI, Inc. (Dayton, OH), who identified eleven critical cognitive skills required in the flight environment through discussions with pilots. The identified cognitive abilities included instrument reading, simple decision making, visual acuity, complex decision making accuracy, complex decision making reaction time, complex decision making efficiency, tracking, slow motion inference, fast motion inference, spatial orientation, and perceptual speed.

To investigate the effects of G_z on the aforementioned list of cognitive abilities, NTI, Inc. also developed software containing twelve performance tasks. Many of the tasks focus on probing the performance of a particular cognitive skill; however, they actually test several other cognitive abilities to a lesser extent. For example, the test designed to measure the pilot's

perception of speed may also consequently probe their visual acuity to a small degree. Therefore, subject matter experts (SME's) were consulted to determine the extent to which each skill is tested in each of the twelve performance tasks. The SME's rated the level at which each of the cognitive skills is used for each of the twelve tasks with a value between 0 and 9 (9 corresponds to a cognitive skill that is highly used in the task, 0 represents a skill that is not used at all). A matrix (T-Matrix) was created from these values that can be used to weight the performance data recorded from acceleration studies across the eleven critical cognitive skills. The resulting table can be found on the following page. The performances for each of the twelve tasks identified by NTI, Inc. were studied separately during various G_z profiles.

Table 1: T-Matirx: SME values for each cognitive ability across the provided cognitive tasks

	Instrument Reading	Simple Decision Making	Visual Acuity	Complex Decision Making Accuracy	Complex Decision Making RT	Complex Decision Making Efficiency	Tracking	Slow Motion Inference	Fast Motion Inference	Spatial Orientation	Perceptual Speed
Perception of Relative Motion	0	1	0	0	0	0	4	3	4	7	6
Precision Timing	0	4	0	0	0	0	8	6	5	0	9
Motion Inference	0	6	0	0	0	0	4	9	9	0	7
Pitch/Roll Capture	0	3	0	0	0	0	8	2	2	3	2
Peripheral Processing	5	6	9	0	0	0	0	0	0	0	7
Decision Making	0	2	4	9	9	9	0	1	3	0	1
Basic Flying Skills	7	3	0	0	0	0	2	0	0	4	0
Gunsight Tracking	0	1	4	0	0	0	9	5	7	0	4
Situation Awareness	6	1	5	5	2	2	3	2	2	8	0
Unusual Attitude Recovery	9	3	0	6	3	8	0	0	0	9	2
Short Term Memory w/ Distraction	0	4	0	3	1	3	0	0	0	3	0
Visual Monitoring	4	1	6	0	0	0	6	0	0	0	3

NTI, Inc. Cognitive Model

As a final deliverable to the Air Force, NTI, Inc. developed a cognitive performance model that predicts cognitive performance among all eleven attributes for any given profile. Specifically, a database was generated for each of the critical cognitive abilities taken from the existing literature. Each for the data values was then normalized using the equation below.

$$\text{Normalized } G_z \text{ Value} = 100 - \left(\frac{([nG_z value] - [1.0G_z value])}{[1.0G_z value]} \times 100 \right) \qquad \textbf{\textit{(Equation 1)}}$$

The complete set of data pulled from existing literature is provided in Table 2. It is readily apparent in the table that experimentation had not been completed for each of the eleven abilities at every G_z level between 1 and 9. As a result, it was necessary to make some assumptions to fill in the gaps. NTI, Inc. utilized a linear extrapolation to generate the missing data points. The resulting extrapolations were separated according to cognitive ability. Each included normalized cognitive performance values for G_z between 1.0 and 9.0 with a 0.1 G_z interval.

Next, a validated model was needed that could accurately predict the physiologic effects of positive G_z acceleration. NTI, Inc. contracted with Dr. Dana Rogers to utilize his "G-effective" model developed to explain the reaction of human physiology to increased G-load (Rogers, 2003). Essentially, the model uses the G_z values and G_z history to make a prediction concerning the internal cardiovascular physiology in the human. This is done by calculating the resulting strain on the human, or "effective G" through the use of a standard first-order transfer function (see equation 2). The first step was to generate the dynamic stress function, F(s), in the frequency domain.

Table 2: Normalized Data from Literature across Cognitive Abilities

Reference	*Dependent Measure*	*1Gz*	*2Gz*	*3Gz*	*4Gz*	*5Gz*	*6Gz*	*7Gz*	*8Gz*	*9Gz*
Dial Reading (Instrument Reading)										
Warrick & Lund, 1946	Errors	100.00		64.27						
Choice Reaction Time (Simple Decision Making)										
McCloskey et al., 1992	Reaction Time (msec)	100.00	87.50							
Frankenhauser, 1958	Reaction Time (sec)	100.00		91.99						
Visual Acuity										
White. 1960	Absolute Threshold (Peripheral)	100.00	95.82	86.87	82.99					
	Absolute Threshold (Focal)	100.00	98.50	96.10	92.04					
Chambers & Hitchcock,1963	Contrast Sensitivity	100.00	84.04	77.66		34.04				
White, 1962	Contrast Sensitivity	100	100	80	74					
Frankenhauser, 1958	Percent Error of visual acuity	100		83.66						
Decision Making (Complex Decision Making)										
Cochran, 1953	Average Percent Accuracy	100.00	97.50	96.50	95.00	100.00	90.00			
	Average Reaction Time	100.00	94.00	87.50	73.50	75.00	76.50			
	Average Throughput	100	58.89	45.43	26.98	32.76	31.34			
Tracking										
Rogers et al., 1973	% Accuracy	100	97	90	85	80	65	50	23	
Motion Inference										
Repperger et al., 1990	Motion Inference, Slow Velocity	100		89.29		26.79				
	Motion Inference, Fast Velocity	100		114.29		80.95				
Spatial Orientation										
Albery, 1990	+30 Degree manipulation	100.00	55.00	35.00						
Nethus et al., 1993	Manikin Error rate, 14 FIO2 (%)	100.00				60.00				
Perceptual Speed										
Comrey et al., 1951	T-score equiv. for raw number correct	100.00	98.61		90.55					
Frankenhauser, 1958	Reaction Time (sec)	100.00		80.10						

$$F(s) = \frac{1 + as}{1 + bs + cs^2} \qquad \textit{(Equation 2)}$$

The F(s) function (e.g. the values of variables a, b, and c) was developed using data from the Stoll curve (Stoll, 1956). When F(s) is converted back to the time domain, it can be denoted as the time series dynamic stress function for the human operator or pilot. To model the "effective" G_z, Dr. Rogers developed the algorithm denoted by equation 3. It uses the time series effective stress function, F(t) convoluted with the actual G_z time series to generate the G-effective (Ge) data.

$$G_e(t) = G_z(t) * F(t) \qquad \textit{(Equation 3)}$$

Essentially, the "effective" G is the G_z equivalent the human experiences based on internal physiologic reaction. It is the culmination of many aspects of cardiovascular changes and adaptations equated to a single value. For example, the actual G_z level may only be 6, whereas G-effective value may be closer to 7 (see figure 1).

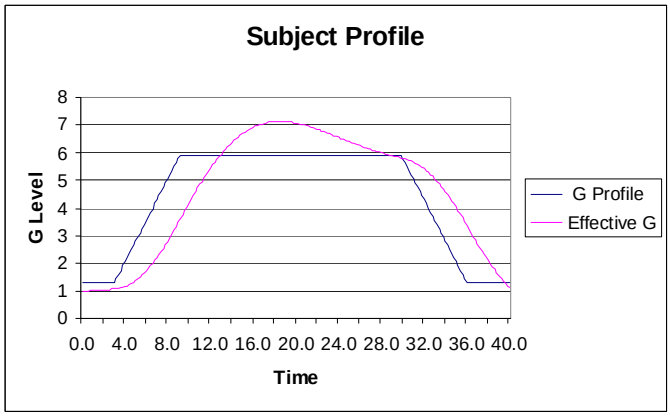

Figure 1: Ge compared to Gz profile for a single plateau (Courtesy of NTI, Inc.)

This is due to the fact that the cardiovascular system cannot react quickly to compensate for large changes in acceleration. To generate adequate counter pressure, the vessels must constrict and the heart must beat harder and more rapidly. This reaction exceeds the time required for a high-performance aircraft to generate hefty changes in acceleration.

The G-Tool to Optimize Performance (G-TOP)

The final step in the NTI, Inc. modeling effort (G-TOP) was to integrate the Ge algorithm with the normalized data tables extracted from the available literature. Once extrapolated to 9 G_z in 0.1 G increments, the performance data was separated into a matrix for each of the 11 cognitive abilities. Because the Ge model utilized the actual time series of the G_z profile as input, it was possible to predict an "effective" G value to drive the predictions for cognitive performance. Hence, the Ge data was synchronously fed to each of the "look-up" tables to select the relative performance across all 11 cognitive abilities. Once captured, the G-TOP model generates a final table of the G_z and Ge profiles with the resulting performance values depicted as a percent change from the baseline performance (baseline is shown as 100%).

In an effort to provide the user with a graphical mechanism to attain a comprehensive representation of cognitive performance during G_z loading and potential problem areas, the tabular data is presented in a series of web-like diagrams (termed cognitive vulnerability maps or CVMs). Each of these maps represents a single point in time (typically 1 second intervals). An example can be found in figure 2 below. To view changes over time, the user advances through each chart in sequence.

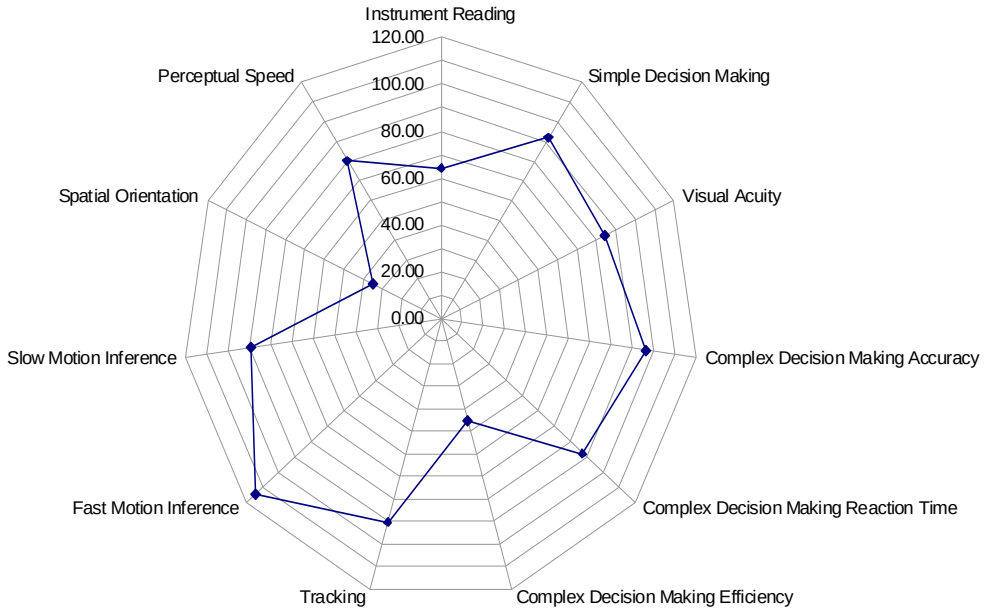

Figure 2: G-TOP Example CVM Output

Model Validation

Although the G-TOP model is based on data and results from previous acceleration studies, the methodologies utilized in each experiment were not uniform and often the tasks did not directly probe a specific task. As a result, much of the data used in the generation of the "look-up" tables was used because it was the only data in existence. Furthermore, much of the data had to be extrapolated to the higher G_z levels due to the fact that much of the existing literature focused on acceleration below 5 G_z. Consequently, it was important to verify and validate the model with a series of 10 experiments that are discussed in the subsequent chapters of this report. It should be noted that the "Basic Flying Skills" task was not tested due to the fact it is inherent to several other tasks. Hence, a lack of significant changes during pitch-roll capture, or unusual attitude recovery, would indicate that basics flying skills remain unaltered during $+G_z$ acceleration. To provide an alternative modeling technique, AFRL/HEPG scientists developed a new modular computational model based on the data from each of the experiments.

This effort served as a feasible alternative should the G-TOP model fail to effectively and accurately model the true effects of G_z on human cognition. Details of the AFRL/HEPG model will be discussed in a subsequent report.

CHAPTER 2: TASK 1 - GUNSIGHT TRACKING

Introduction

Of the cognitive proficiencies required in the flight combat environment, the ability to proficiently track and destroy an enemy/target is arguably the most critical skill for pilots to maintain to achieve mission success. As such, it is vitally important to gain a thorough understanding of the negative effects of acceleration stress on cognitive abilities that may encumber this ability. Principally, the task of tracking an enemy involves the ability to successfully navigate the aircraft such that the enemy is transfixed in the gunsight crosshairs. More specifically, the pilot's visual-motor coordination is utilized in concert with his/her working memory. The movement of the target is stored in the pilot's short term memory, allowing him/her to generate a corrective response. A motor response derived from the efferent neural pathway from the motor cortex to the muscles in the hand and arm is elicited to deliver a compensating input to the aircraft. This brings the crosshairs back to bear on the target until it alters its vector.

As previously stated, the increased acceleration generated by the aircraft subsequently increases the apparent weight of the blood making it more difficult for the heart to pump oxygenated back to the upper extremities. Because the part of the motor cortex responsible for hand and arm movements resides in the most dorsal section of the brain (furthest from the heart), it is likely that decreases in blood pressure and cerebral oxygen saturation would impact this area first. As a result, the coordination between muscles of the hand/arm and the conscious efforts of the pilot to generate a movement of the flight stick may become significantly impaired at relatively moderate G_z levels. The present study was designed to investigate this phenomenon and quantify the effects G_z on tracking performance.

Methods

Subjects

Eight active duty members of the United States Air Force (one woman and seven men) volunteered to participate in the study. They ranged in age from 28 to 38 years, with a mean age of 32 years. All participating subjects were members of the sustained acceleration stress panel at Wright-Patterson AFB, OH. As part of the requirement for membership on the stress panel, each completed the Air Force's extensive centrifuge G-training program to ensure that their tolerance to acceleration and their vestibular responses under acceleration were similar to those of pilots flying high performance aircraft.

In order to qualify for service in the study, each subject had to meet Air Force flying class III medical, height, and weight standards and have no history of neurological pathology. In addition, all participants were required to have normal or corrected-to-normal vision and a normally functioning vestibular system. Information concerning these qualifying factors was obtained from screening the participant's medical records. Prior to final acceptance into the study, all participants underwent a rigorous physical examination including x-rays of the skull and spine, tests of the integrity of the cardiovascular, pulmonary, and nervous systems, and a comprehensive blood chemistry work-up. On the basis of this examination, all of this study's participants were determined to be in excellent health by a flight surgeon.

Facilities

All training and data collection for this study was performed at the Air Force Research Laboratory's Dynamic Environment Simulator (DES) centrifuge facilities at Wright Patterson AFB (Figure 3).

Figure 3: Dynamic Environment Simulator, Wright-Patterson AFB, OH

The DES is a human rated centrifuge with an arm radius of approximately 19 feet. It is capable of attaining and sustaining accelerations up to 20 G in either of three independent axes: x, y and z. The DES has a maximum G onset and offset rate of approximately 1 G/sec. The gondola of the centrifuge was equipped with an F-22-like ACES II ejection seat with a seatback reclined to 15^{o} from vertical. As illustrated in Figure 2, the seat had adjustable lap and shoulder restraints.

An aircraft IC-10 communication system was used to provide two-way voice-communication between the research participant and the investigator. The participant's microphone was fixed in the open position to allow the participant "hands-free" communication. Participants were also provided with an emergency abort switch that enabled them to stop the centrifuge at any time during testing. Participants wore a standard Air Force issue Nomex® flight suit and a standard G-suit during all testing runs.

The gondola was outfitted with a simulated fighter cockpit. The cockpit incorporated a Thrustmaster Hotas Cougar flight stick (Guillemot, Montreal, Canada) mounted on the participant's right side, and a corresponding throttle control mounted on the participant's left

side. This was used to secure responses to the tracking performance task. A six foot hemispherical shell viewing screen, representing a 130^{o} (vertical) x 180^{o} (horizontal) visual field, mounted directly in front of the participant, was used to display the terrain. A separate projector was used to display the head-up-display (HUD) in the center of the subjects' field-of-view. In addition, a 23-inch (diagonal) LCD screen was used to display the instrument panel. Figure 4 provides an illustration of the entire visual system. Figure 5 presents a photo of the tracking task flight simulation projection onto the dome screen within the DES cab.

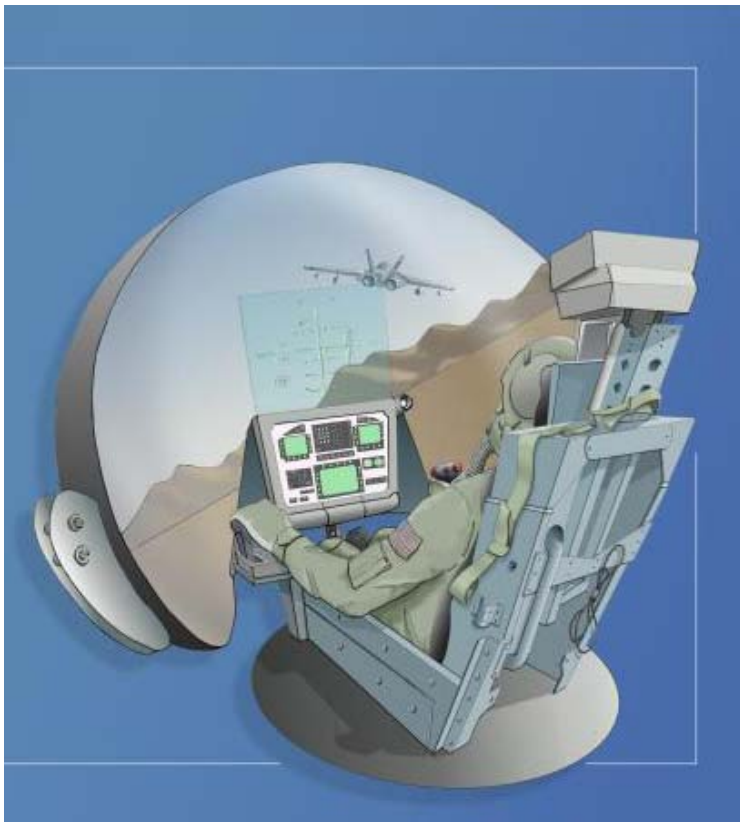

Figure 4: Illustration of ACES II Ejection Seat with Hotas Thrustmaster Flight Stick and Throttle with Dome Visual Display

Continuous surveillance of participants was provided by two closed-circuit infrared television cameras. The cameras offered a close-up view of the participant's head and a wide-angle view of the participant from head-to-foot. Research personnel housed in a control room

observed the video images. A video mixer was used to generate a composite picture of the two views of the participant along with the time, date, electrocardiogram (ECG) data, and G_z acceleration in a given run. Video data were stored on ½ inch VHS videotape for later analysis.

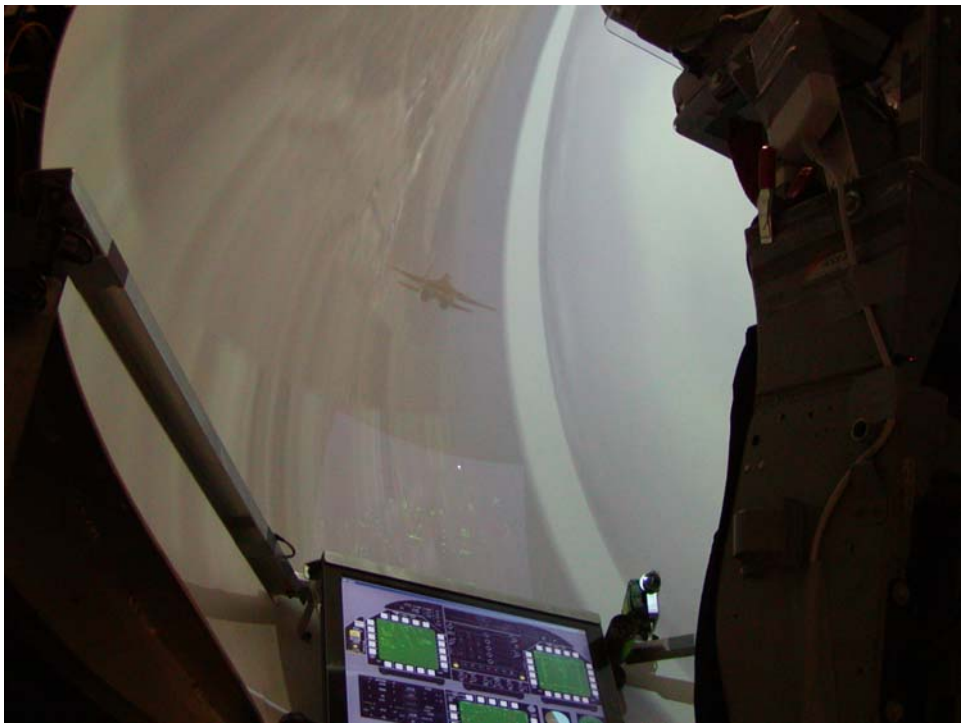

Figure 5: Hemispherical Shell Viewing Screen

Acceleration Profiles

A total of four G_z acceleration profiles were generated for use in this study. All G_z exposures were started from a baseline acceleration of 1.5 G_z. The first three profiles comprised of a 1 G/sec onset ramp to a 15-sec plateau followed by a G_z offset ramp of 1 G/sec down to the baseline acceleration level. The plateaus were 3, 5, and 7 G_z, respectively. The final acceleration exposure was a simulated aerial combat maneuver (SACM). This profile consisted of two 5-sec G_z peaks to 7 G_z with several intermittent peaks to 3 and 5 G_z. Figure 6 displays an example of a G_z plateau profile, while Figure 7 presents the SACM profile.

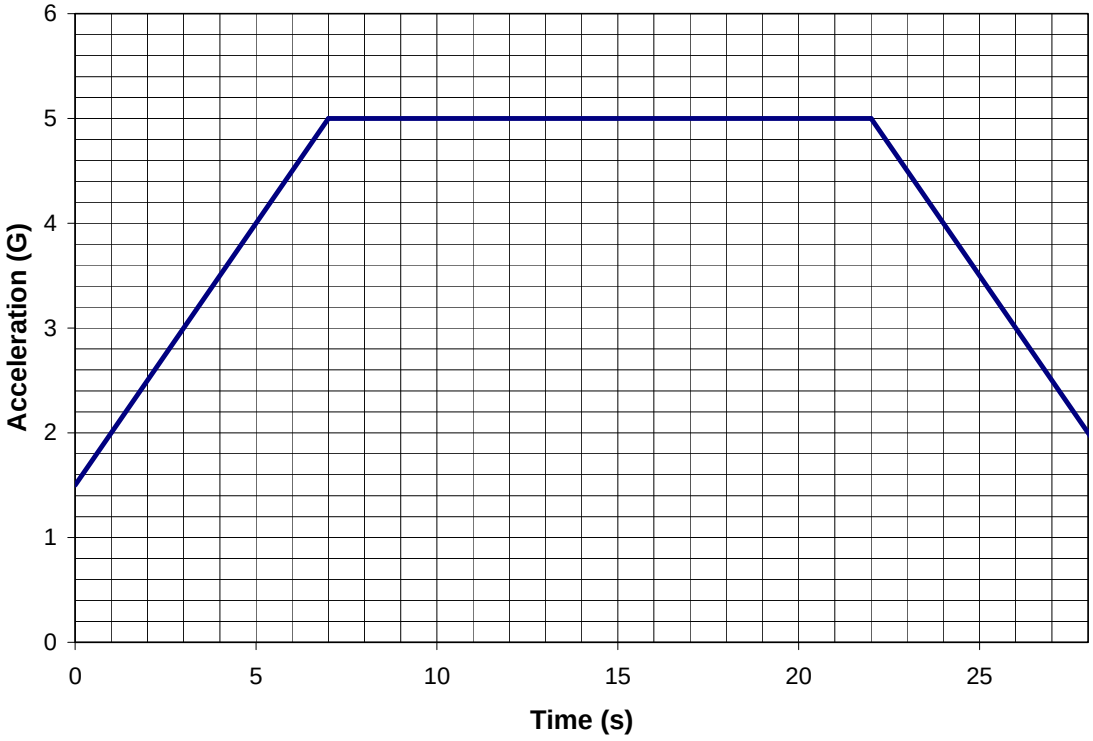

Figure 6: 15sec G_z Plateau Profile Example (5 G_z)

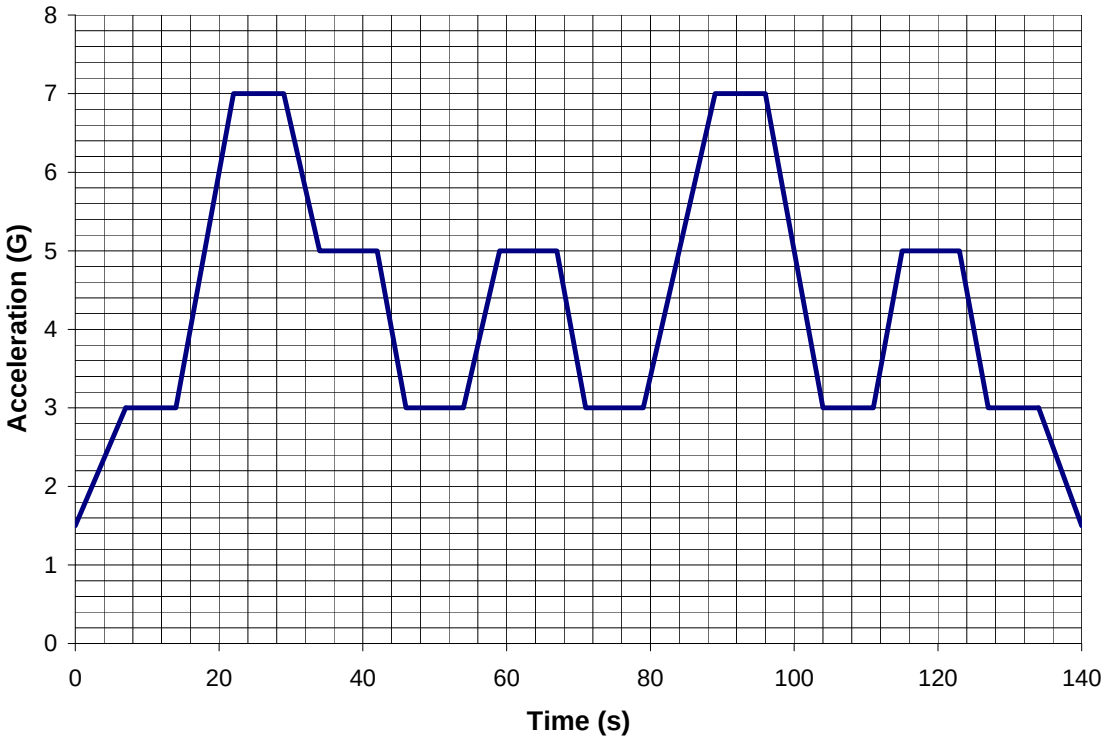

Figure 7: 7 G_z SACM Profile

Stimuli

A pursuit tracking task was created to evaluate the subjects' ability to successfully track a target in varying G_z environments. A simulated SU-37 flew a random flight profile that included left and right turns varying between 4.5 and 7 G_z. This target aircraft was placed under several restraints to reduce the overall difficulty of the task. First, the altitude was limited to a range of 1,500 to 10,000 ft. In addition, the target was tied to the subjects' aircraft to limit the maximum distance between the two jets. An additional restraint was placed on the task that set the subjects' airspeed to 470 knots. The task software calculated the root mean square error (RMSE) between the target and the subject aircraft at a sample frequency of 32 Hz. In addition, G_z and time data from the centrifuge were recorded in the same data files for later analysis.

Static Training

All subjects were trained statically on the performance task prior to dynamic training and experimental data collection. Static training was performed in an F-16 mock-up fuselage equipped with an ACES II aircraft seat with a 15 degree seat-back angle. The task was projected onto a 48-in (vertical) x 64-in (horizontal) screen. Subjects performed the task for three minutes followed by a one minute rest period. This was repeated three times per static training day. An average RMSE score was calculated by the tracking task software for each three-minute interval. The subjects were considered trained once their average RMSE score deviated less than 10% between training days.

Dynamic Training

Each subject also completed dynamic blend training on the centrifuge. This was done to eliminate any training effect associated with performing the task while in a motion environment.

It is believed that differences in performance may be exhibited due to vestibular cueing and changes in forces acting on the control stick and the subjects' arms/hands. The dynamic training served as a platform for each participant to experience and compensate for these new interactions.

Hence, subjects performed the tracking task in the DES while completing the same 3, 5, 7, G_z plateau and 7 G_z SACM profiles that were administered during the experimental test days. A one-minute rest period was given after each G_z profile. In addition, they performed the task at 1 G_z for 3 minutes prior to the G_z profile on each training day to provide a baseline profile for comparison. Subjects were considered trained once their performance on the task deviated less than 10% between training days. Performance was measured in root mean square error between the position of the target and the gunsight crosshairs.

Procedures

On a typical experimental test day, participants arrived at the laboratory, donned a flight suit and a standard G-suit, and were instrumented with electrocardiogram leads. The flight surgeon performed a brief medical examination and reviewed the subject's medical history. The participant then proceeded to the centrifuge where he/she donned a parachute harness. After entering the gondola of the centrifuge the participant was secured to the ACES II aircraft seat (with a 15-degreee seat back angle) using a three-point aircraft restraint system. The ECG leads were connected and the signals were verified prior to securing the gondola of the centrifuge. At this point, the tracking task was started and baseline performance data were collected for 3 min. Following the collection of baseline data the participant experienced his/her first G-exposure.

The subject experienced each of the four G_z exposures on three different test days in the following order: 3 G_z 15sec plateau, 5 G_z 15sec plateau, 7 G_z 15sec plateau, and 7 G_z SACM. The subject began the tracking task approximately 8 sec prior to each G_z exposure and continued for approximately 8 sec after the acceleration had returned to the baseline G_z level of 1.5 G_z. A 1-minute rest period was provided between each G_z exposure during which the task was not performed and the subject was permitted to relax at the baseline G_z level. This was accomplished to allow the physiology to return to the pre-acceleration exposure levels. Following the completion of the four G_z exposures, the participant egressed the centrifuge and was immediately examined by the flight surgeon and then released to return to his/her normal duties. These procedures were repeated over three experimental test days.

Data Analysis

For the post hoc analysis, the tracking RMSE data were determined approximately every 4 seconds. The value of 4 seconds was used due to the fact that it eliminated much of the noise in the signal and yet represented gross changes in performance. These RMSE data values were then logged for analysis to account for the positive skewing associated with tracking data. The data were then averaged across subjects and then across subjects and replications. The latter was used in the development of the model. The data were later transformed into percent change from the baseline values.

Next, tracking RMSE data were converted into values that represent the proportion of time that the target aircraft was closely tracked by the subject. The target aircraft was determined to be outside acceptable range limits once the RMSE score deviated more than 10% from the average baseline RMSE score. A value of one was assigned to RMSE values outside

this limit and a zero was assigned to RMSE values within the limit for each data point. Therefore, values close to 0 signify that the target aircraft is within a reasonable shooting range, whereas values closer to 1 refer to the situation where the target is out-maneuvering the subject's aircraft. The proportion data were then averaged across subjects and replications.

Results

The collected RMSE tracking data were first averaged across subjects. A plot of these results from the 3, 5, and 7 G_z plateau profiles is included in Figure 8 below. Dots represent data points that were significantly different than baseline values ($p<0.05$).

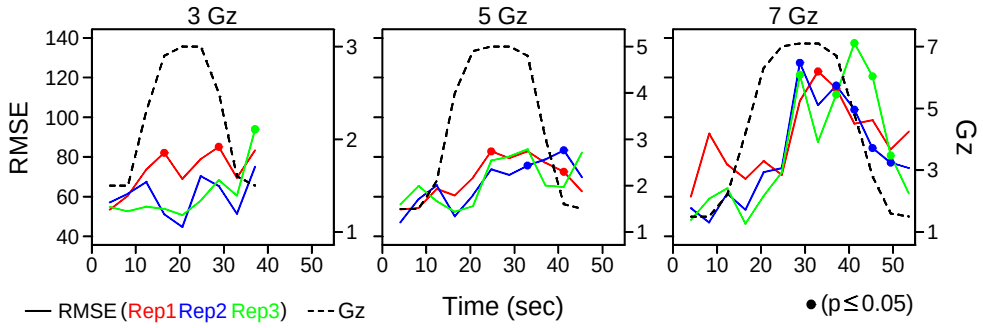

Figure 8: RMSE for Each G_z Plateau Averaged Across Subjects

Next, the data were averaged across subjects and replications. This is illustrated in Figure 9.

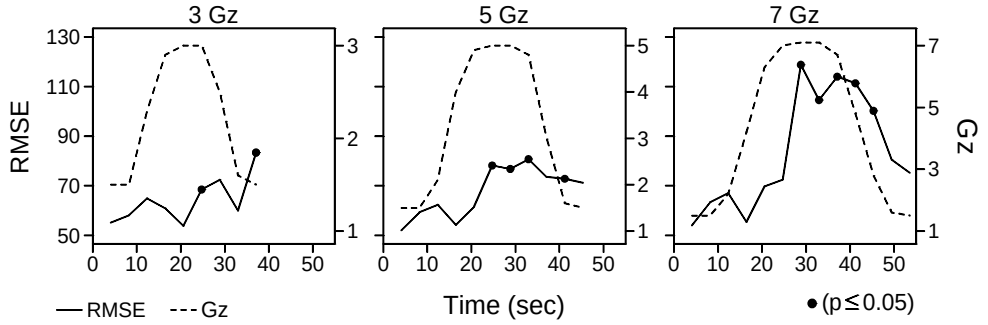

Figure 9: RMSE for Each G_z Plateau Averaged Across Subjects and Replications

RMSE tracking data collected during the 7 G_z SACM were also averaged across subjects and replications. The resulting plot can be found in Figure 10.

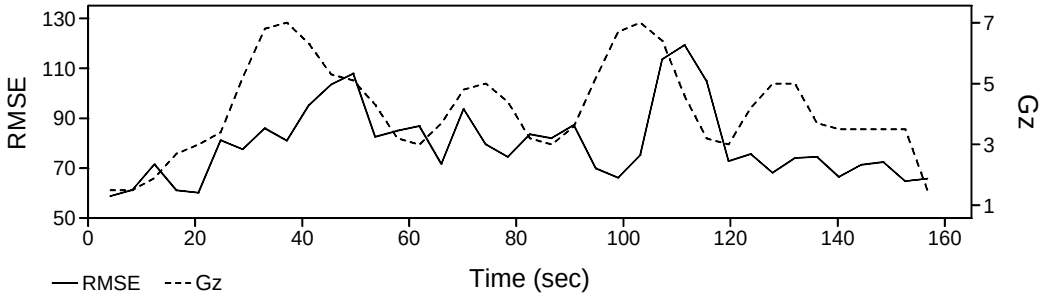

Figure 10: RMSE during SACM Averaged Across Subjects and Replications

Discussion & Conclusions

The level of cognitive function and performance can greatly influence the outcome of an air combat mission. The ability to successfully navigate the aircraft, make critical decisions, recall procedures from memory, track a target, correctly perceive motion, and maintain situational awareness can all be affected by decreases in cognitive performance. Evidence has been shown previously by Tripp et al (2002) and Tripp et al (2003) that reduced arterial blood flow to the brain is one of the principal causes for these reductions in cognitive task performance. This is mainly due to the fact that the brain requires a large amount of energy (obtained through aerobic processes) to operate at normal levels. Without oxygen, glucose metabolism is decreased producing far less usable energy. Hence, higher order cognitive processes are sacrificed to maintain critical life-preserving functions. The extent of these decrements and the subsequent ability to create an operationally relevant model is the current focus of study. Such a model would prove to enhance the wargaming and simulation software currently employed.

The results of this study show statistically significant ($p \leq 0.05$) decreases in tracking performance as the acceleration level increases. This is denoted primarily by the increases in RMS error which correspond to the target aircraft becoming further away from the crosshairs of the subject's aircraft. However, the calculated significant RMSE increases during the 3 G_z plateau may not be meaningful due to the fact that the largest increases occurred after the G_z exposure was over. This was most likely caused by subjects prematurely arresting their performance on the task, mistakenly believing that data collection was over and the 1-minute rest period had begun. Negating this final extraneous data point for the $3G_z$ profile, task performance only degraded approximately 25% at the peak. Performance degraded by about 40% during the 5 G_z plateau and approximately 100% during the 7 G_z plateau. These data reveal that pilots lose much of their ability to successfully and accurately track a target at G levels of approximately 7 or above when protected in the standard anti-G suit, only. Even at 5 G_z, their ability to track has degraded to a degree that would start to produce serious problems in successfully aligning the target in their crosshairs.

Although it is interesting to discover the magnitude of cognitive performance decrements for various discrete, single-peak G_z profiles, it does not represent the majority of the acceleration profiles pilots generally experience during combat engagements. Therefore, it is perhaps more operationally relevant to investigate performance trends over time with multiple G_z peaks at various levels. To accomplish this objective, the 7 G_z SACM was employed in this study. Perhaps one of the more interesting results from the data analysis is that the tracking performance is degraded to a greater extent for subsequent peaks to high (≥ 7) G_z levels. This is most likely a product of several phenomena. Primarily, the SACM contained G_z levels and

durations sufficient to produce significant levels of fatigue. This would most certainly warrant further decrements to the performance on the task.

In addition, oxygen dissociation in the cerebral tissue frequently continues to persist even at relatively low G_z levels (including accelerations as low as 3 G_z) during long, multiple peak profiles (Warrick & Lund, 1946). That is to say, large recoveries in cerebral oxygen saturation (rSO_2) do not take place until the acceleration has reached a level close to 1 G_z. The trend for rSO_2 in protected subjects (those equipped with a G-suit and who use the anti-G straining maneuver) during a SACM is a slow linear decay throughout the entire profile. This is most likely a result of the fact that even at 3 G_z, the eye level blood pressure could be degraded by as much as 66 mmHg (Naval Aerospace Medical Institute, 1991). Consequently, a considerable reduction in oxygenated blood delivered to the cerebral tissue remains. However, the brain continues to use the same amount of energy (hence oxygen) at 3-7 G_z as it used at 1 G_z. Therefore, oxygen continues to dissociate from the cerebral tissue to combine with glucose to be converted into usable energy. Based on this information, it is reasonable to conclude that the greater degree of depleted oxygen in the cerebral tissue at the second 7 G peak contributed to the greater decrease in tracking performance due to the fact that less energy was available for the higher order cognitive ability.

This study was a crucial first step in compiling a complete data set exhibiting cognitive performance decrements pilots experience in high G_z maneuvers. The collected data clearly illustrate the fact that cognitive performance is affected to a great extent by high-G_z stress. Once validated, the model should prove to be extremely beneficial to providing more realistic representations of the pilot to the modeling and simulation community.

CHAPTER 3: TASK 2 – PRECISION TIMING

Introduction

The perception of speed (product of time and distance) is often believed to be analogous to target tracking (see chapter 2). However, it is a separate critical cognitive ability in the respect that is requires temporal processing rather than working memory and motor coordination. The ability to successfully perceive time and speed is required for a variety of tasks such as take-off, landing, the prediction of any moving object's position at a future point in time, and the perception of time in general. The later is very important in controlling the timing on an anti-G straining maneuver (AGSM) during high acceleration turns and climbs. The AGSM is designed to increase pressure in the chest to assist the heart in pumping blood to the upper extremities such as the brain. Essentially, the pilot takes a deep breath and forces the air in the lungs against the closed glottis by performing an isometric compression of the chest cavity. After 3 seconds, the pilot executes a rapid air exchange by expelling his/her lung volume as quickly as possible and inhaling a new breath to rejuvenate the oxygen supply. Should the breath be held longer than three seconds, the body begins to become starved of oxygen causing muscles to fatigue and neural processes to shut down. If held less than three seconds, the pilot begins to hyperventilate, thereby increasing the oxygen content of the blood. This serves as a vasodilator that further limits the supply of blood to the cerebral tissue and exacerbates the difficulty of pumping oxygenated blood to the brain. Hence, it is readily apparent that the AGSM relies heavily on the ability of the pilot to successfully time his/her breathing rate precisely.

In the course of completing mission objectives, it is often necessary for pilots to fire upon and destroy enemy targets. Often, the targets move and the human operator must correctly perceive its speed so as to determine when it will cross the gunsight or "crosshairs." Again,

timing is critically important due to the fact that a misperception of speed/time will often result in a missed kill opportunity. Such an event would compromise any potential element of surprise and may lead to a mission failure. To date, little research has been conducted to evaluate this cognitive ability at high-G. Frankenhauser (1958) evaluated reaction times in a stimulus identification task at accelerations reaching 3 G_z. He discovered that reaction times tended to increase suggesting that processing times had elongated and reactions had slowed. Further, Comery et al. (1951) used a visual matching task when a center stimulus had to be matched to one of four stimuli surrounding it. The results indicated that the number of correct responses began to decline at the 4 G_z level. However, testing was not performed at higher G_z levels in either study. Although neither experiment directly investigated precision timing or speed perception, they provide the only evidence available that temporal abilities may be degraded as a result of G-induced hypoxia. The goal of this study was to focus solely on the effects of G_z (up to 7 G_z) on the precision timing ability.

Methods

Subjects

A total of eight male active duty members of the United States Air Force volunteered to participate in this study. They ranged in age from 24 to 29 years, with a mean age of 26 years. All participating subjects were members of the sustained acceleration stress panel at Wright-Patterson AFB, OH. As part of the requirement for membership on the stress panel, each completed the Air Force's extensive centrifuge G-training program to ensure that their tolerance to acceleration and their vestibular responses under acceleration were similar to those of pilots flying high performance aircraft.

In order to qualify for service in the study, each subject had to meet Air Force flying class III medical, height, and weight standards and have no history of neurological pathology. In addition, all participants were required to have normal or corrected-to-normal vision and a normally functioning vestibular system. Information concerning these qualifying factors was obtained from screening the participant's medical records. Prior to final acceptance into the study, all participants underwent a rigorous physical examination including x-rays of the skull and spine, tests of the integrity of the cardiovascular, pulmonary, and nervous systems, and a comprehensive blood chemistry work-up. On the basis of this examination, all of this study's participants were determined to be in excellent health by a flight surgeon.

Facilities

All training and data collection for this study was performed at the Air Force Research Laboratory's Dynamic Environment Simulator (DES) centrifuge facilities at Wright Patterson AFB (ref. Chap. 2, Figure 3). The DES is a human rated centrifuge with an arm radius of approximately 19 feet. It is capable of attaining and sustaining accelerations up to 20 G in either of three independent axes: x, y and z. The DES has a maximum G onset and offset rate of approximately 1 G/sec. The gondola of the centrifuge was equipped with an F-22-like ACES II ejection seat with a seatback reclined to 15^{o} from vertical. As illustrated in Figure 2 (ref. Chap. 2), the seat had adjustable lap and shoulder restraints.

An aircraft IC-10 communication system was used to provide two-way voice-communication between the research participant and the investigator. The participant's microphone was fixed in the open position to allow the participant "hands-free" communication. Participants were also provided with an emergency abort switch that enabled them to stop the

centrifuge at any time during testing. Participants wore a standard Air Force issue Nomex® flight suit and a standard G-suit during all testing runs.

The gondola was outfitted with a simulated fighter cockpit. The cockpit incorporated a Thrustmaster Hotas Cougar flight stick (Guillemot, Montreal, Canada) mounted on the participant's right side. The red trigger button on the stick was used to secure responses to the performance task. A six foot hemispherical shell viewing screen, representing a 130^{o} (vertical) x 180^{o} (horizontal) visual field, mounted directly in front of the participant. A separate projector was used to display the performance task in the center of the subjects' field-of-view with a projected image of 22.5" (width) by 18.5" (length). The large dome display was used to present two red dots located at approximately 60^{o} of visual angle to the right and left of the center of the dome and approximately 5^{o} in diameter. In addition, a red circle was displayed just above the HUD that represented 10^{o} of visual angle. The dots served as a reference to the subject of his/her visual loss. Should the smaller dots not be visible in the periphery, the subject was instructed compensate by increasing their AGSM. They were to abort the test should their vision degrade to the point that only the center red dot was visible. Figure 4 (ref. chapter 2) provides an illustration of the entire visual system.

Continuous surveillance of participants was provided by two closed-circuit infrared television cameras. The cameras offered a close-up view of the participant's head and a wide-angle view of the participant from head-to-foot. Research personnel housed in a control room observed the video images. A video mixer was used to generate a composite picture of the two views of the participant along with the time, date, electrocardiogram (ECG) data, and G_z acceleration in a given run. Video data were stored on ½ inch VHS videotape.

Acceleration Profiles

A total of four G_z acceleration profiles were generated for use in this study. All G_z exposures were started from a baseline acceleration of 1.5 G_z. The first three profiles comprised of a 1 G/sec onset ramp to a 15-sec plateau followed by a G_z offset ramp of 1 G/sec down to the baseline acceleration level. The plateaus were 3, 5, and 7 G_z, respectively. The final acceleration exposure was a simulated aerial combat maneuver (SACM). This profile consisted of two 5-sec G_z peaks to 7 G_z with several intermittent peaks to 3 and 5 G_z. Figure 6 (ref. chap. 2) displays an example of a G_z plateau profile, while Figure 7 (ref. chap. 2) presents the SACM profile.

Stimuli

The subjects completed a performance task during each G_z profile on each experimental test day. It was projected on a 22.5" (width) by 18.5" (length) screen located approximately 3 feet in front of the subject. The task display encompassed roughly 36^o horizontally, and 28^o vertically of the subjects' field of view. A screenshot is provided in figure 11.

The task used was referred to as the 'precision timing task' and consisted of a semicircular arc, a moving target light, and a hash mark/stopping point. The target light traversed a curved, semicircular path from left to right. Each participant was instructed to stop this target on the stopping point (hash mark) by depressing the trigger button on the flight stick. The stopping point appeared in a random location along the arc, although the software included limits to prevent it from appearing in the first half or last one-eighth of the curved pathway. The velocity of the target light was also randomized within a set of predetermined limits. This variable was selected in the set-up file within the software's program files. Velocity confines

were set by limiting the amount of time for the target to traverse the entire arc. Thus, shorter times resulted in faster velocities. For this experiment, the time limits were 1.25 seconds for the fastest target light and 2.25 seconds for the slowest. The software could randomly choose any time between these limits (including the limits) at 0.25 second intervals.

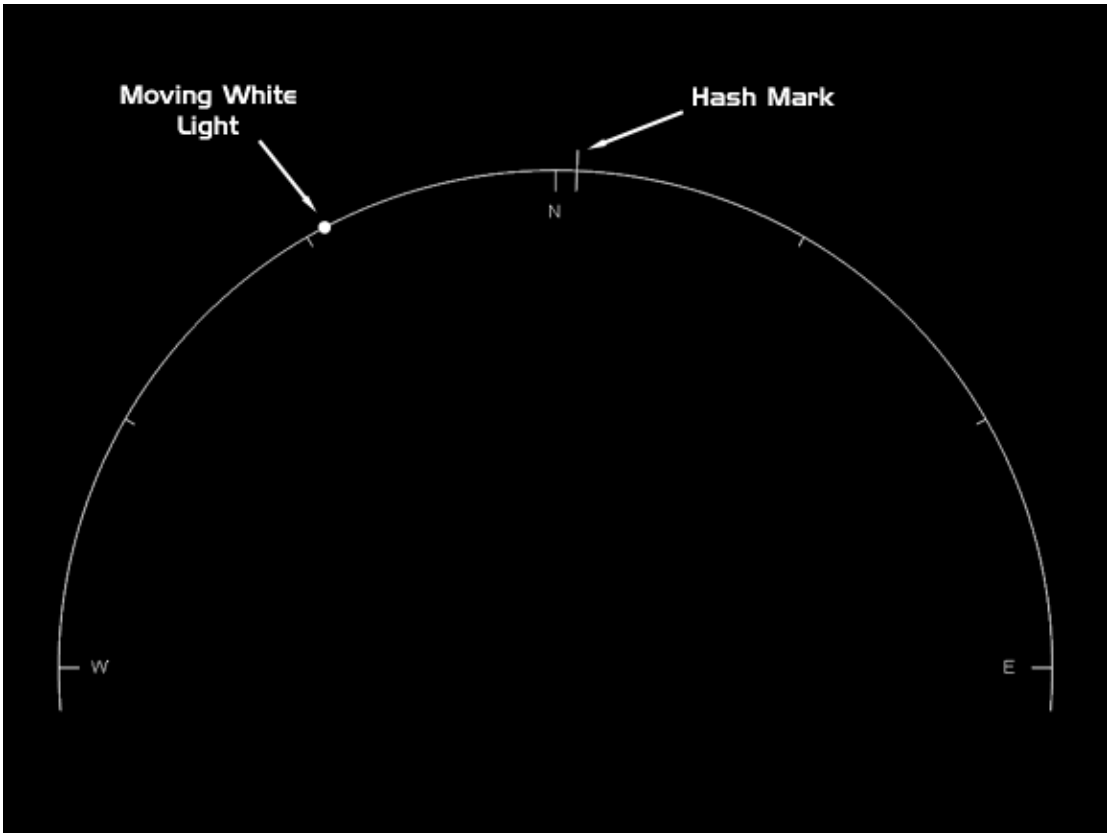

Figure 11: Screenshot of the Precision Timing Task

Performance was measured by the accuracy of the subject's response calculated by the absolute angle error between the ideal stopping point and the location where the subject stopped the target light.

Static Training

All subjects were trained statically on the precision timing performance task prior to dynamic training and experimental data collection. Static training was performed in an F-16 mock-up fuselage equipped with an ACES II aircraft seat with a 15 degree seat-back angle. The task was projected onto a 48-in (vertical) x 64-in (horizontal) screen. Subjects were given 30 presentations of the task followed by a one minute rest period. This was repeated three times per static training day. An average absolute error score was calculated by determining the angle difference between the stopping point (hash mark) position and the point at which the subject stopped the hash mark for both tasks. Participants were considered trained once their average absolute error score was $\leq$ 5 degrees and deviated less than 10% between training days.

Dynamic Training

Each subject also completed dynamic blend training on the centrifuge. This was done to eliminate any training effect associated with performing the task while in a motion environment. It is believed that differences in performance may be exhibited due to vestibular cueing and changes in forces acting on the control stick and the subjects' arms/hands. The dynamic training served as a platform for each participant to experience and compensate for these new interactions.

Hence, subjects performed the precision timing task in the DES while completing the same 3, 5, 7, G_z plateau and 7 G_z SACM profiles that were administered during the experimental test days. A one-minute rest period was given after each G_z profile. In addition, they performed the task at 1 G_z (30 presentations) each training day to provide a baseline profile for comparison. Subjects were considered trained once their performance on the task deviated less than 10%

between training days. Performance was measured in absolute angle error for the precision timing task and absolute angle error and percentage of correct responses to the letterset for the motion inference task. This was accomplished to ensure that no training effects were present in the final data that may have resulted from acclimation to performing the task in the high G environment.

Procedures

On a typical experimental test day, participants arrived at the laboratory, donned a flight suit and a standard G-suit, and were instrumented with electrocardiogram leads. The flight surgeon performed a brief medical examination and reviewed the subject's medical history. The participant then proceeded to the centrifuge where he/she donned a parachute harness. After entering the gondola of the centrifuge the participant was secured to the ACES II aircraft seat (with a 15-degreee seat back angle) using a three-point aircraft restraint system. The ECG leads were connected and the signals were verified prior to securing the gondola of the centrifuge. At that point, the performance task was initiated and baseline performance data were collected (30 presentations in total).

Subjects were instructed to watch the target light traverse the semicircular arc segment and stop the target using the trigger button on the flight stick once it intersected with the hash mark. A labeled photo of the control stick is given in figure 12 below. There was a 1-2 second random interstimulus interval between each presentation of the target light. Due to the initial difficulty level of the task, feedback was given to the subjects during training. For example, the software would display the target light once the subject had pressed the trigger button to indicate the actual position of the light. These features were disabled during data collection.

Figure 12: Labeled Photo of Control Stick for the Precision Timing Task

Following the collection of baseline data, the participant experienced his/her first G-exposure. Each of the four G_z exposures was administered on three different test days in the following order: 3 G_z 15sec plateau, 5 G_z 15sec plateau, 7 G_z 15sec plateau, and 7 G_z SACM. The subject began the performance task approximately 5 sec prior to each G_z exposure and continued until the acceleration had returned to the baseline G_z level of 1.5 G_z. A 1-minute rest period was provided between each G_z exposure during which the task was not performed and the subject was permitted to relax at the baseline G_z level. This was accomplished to allow the physiology to return to the pre-acceleration exposure levels. Following the completion of the four G_z exposures, the participant exited the centrifuge and was immediately examined by the

flight surgeon and then released to return to his/her normal duties. These procedures were repeated over all three experimental test days.

Data Analysis

Performance on the precision timing performance task was assessed by analyzing the error between the computer generated stop point (hash mark) and the point where the subject stopped the target with the trigger. The first analysis involved a comparison of the absolute angle difference during the plateaus of the 3 G_z, 5 G_z, and 7 G_z plateau runs and the 7 G_z plateau of the SACM run. The second analysis involved a comparison of angle errors during the first half vs. the second half of the SACM. Repeated measures analyses of variance (ANOVA) were performed with the mean angle error change from baseline for each subject as a dependent variable.

Results

A comparison of the angle errors during each of the treatment conditions (3 G_z, 5 G_z, and 7 G_z plateau runs and the 7 G_z plateau of the SACM) and the baseline performance data was completed. A malfunction of the flight stick occurred during the third day of data collection for subject five. This prohibited some of the responses to the task from being processed. Therefore, this data was omitted from the analysis. Figure 13 contains the angle error percent change from baseline for each subject and plateau. The dashed horizontal reference line represents the mean baseline angle error. Baseline angle error statistics (min, mean, max) are given above the top right of each plot. For the SACM, only trials during the 7 G_z plateau were used.

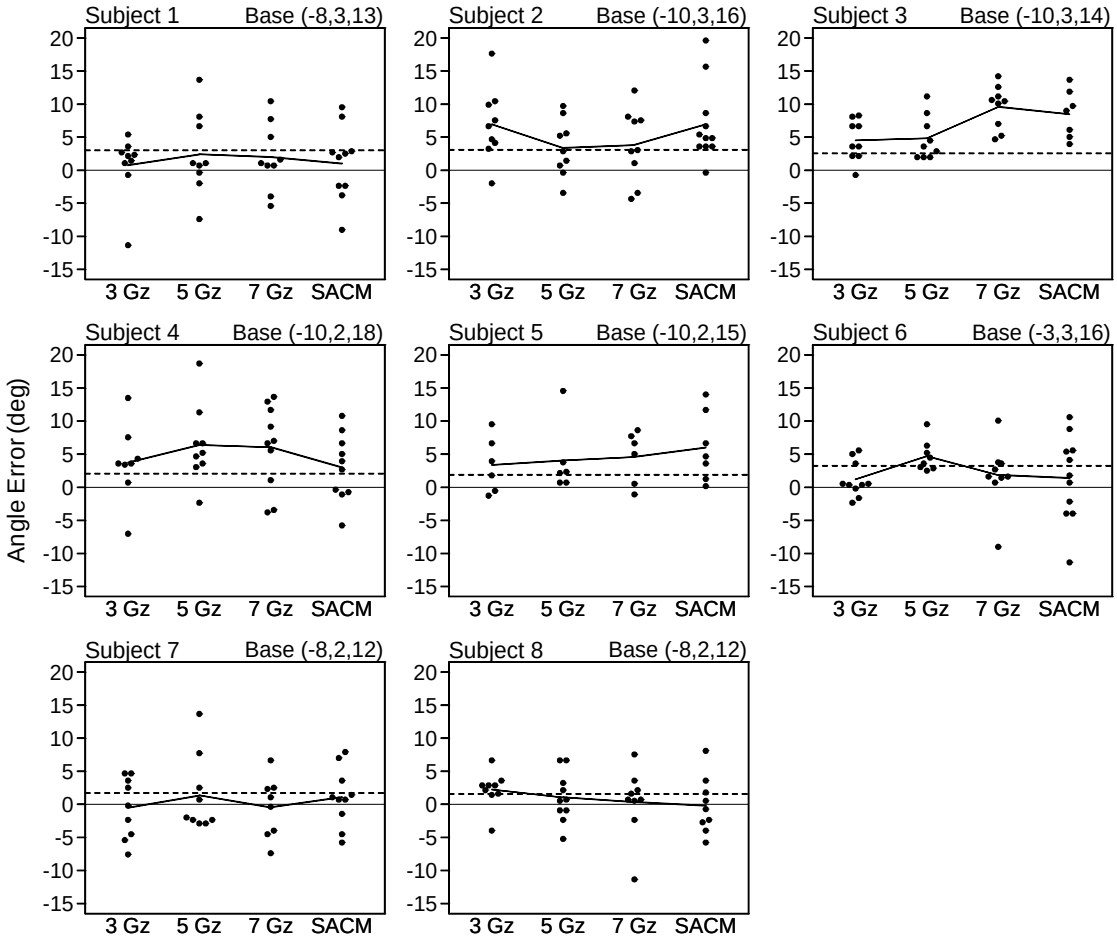

Figure 13: Angle errors for each subject and plateau

A second analysis compared performance during the first half of the 7 G_z SACM with the second half (see Figure 14). Again, baseline angle error statistics (min, mean, max) are displayed above each plot and the dashed horizontal reference line represents the mean baseline angle error. The mean angle error change from baseline was calculated for each subject during the 3 G, 5G, 7 G, (peaks only) and 7G SACM (7 G peaks only) profiles and are plotted in figure 15. In addition, the mean angle change from baseline was calculated for each half of the SACM. This data is plotted for each subject in figure 16 below. The mean angle error is shown above each plot panel.

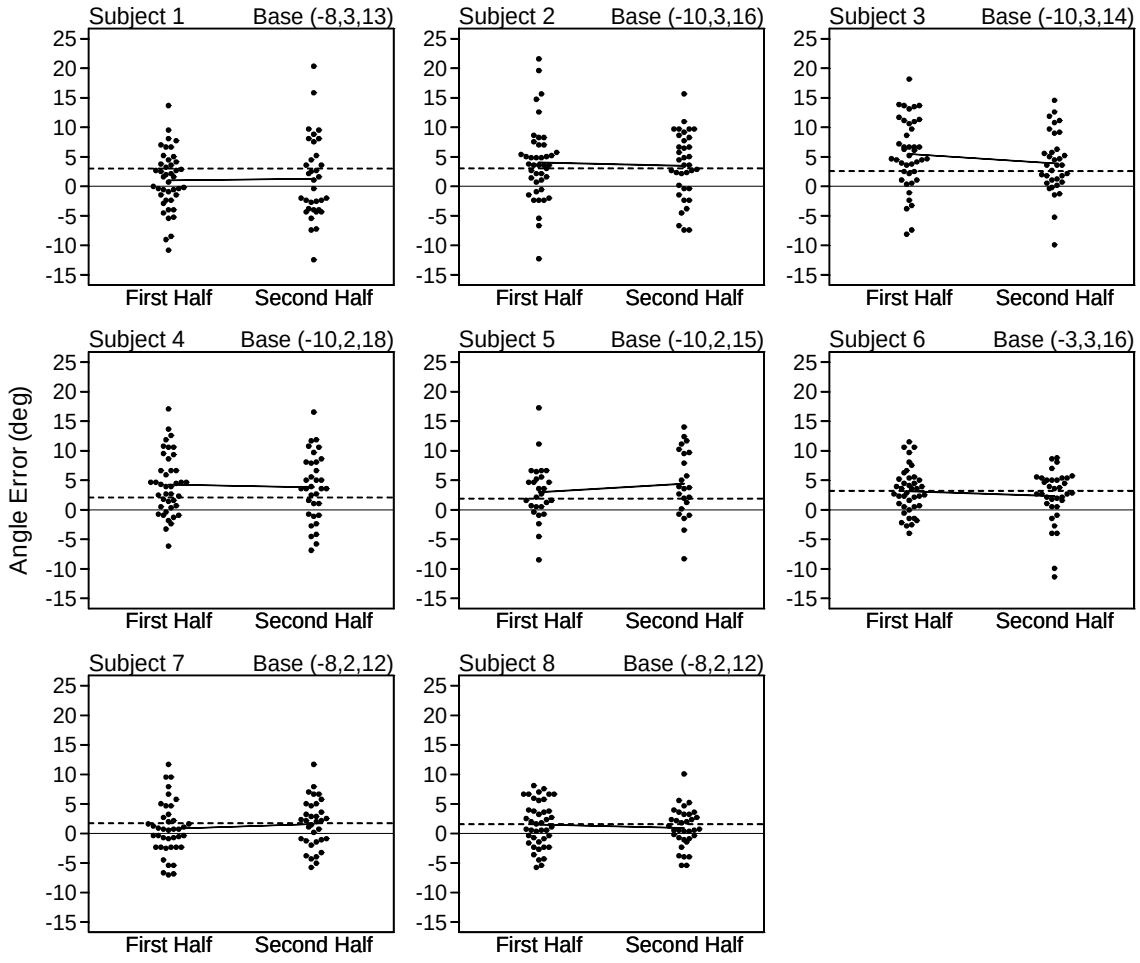

Figure 14: Angle error for each subject and SACM half

The mean angle error change from baseline was determined across subjects, from figures 15 and 16 and is presented in figure 17. The overall baseline mean angle error was 2.4^{o}.

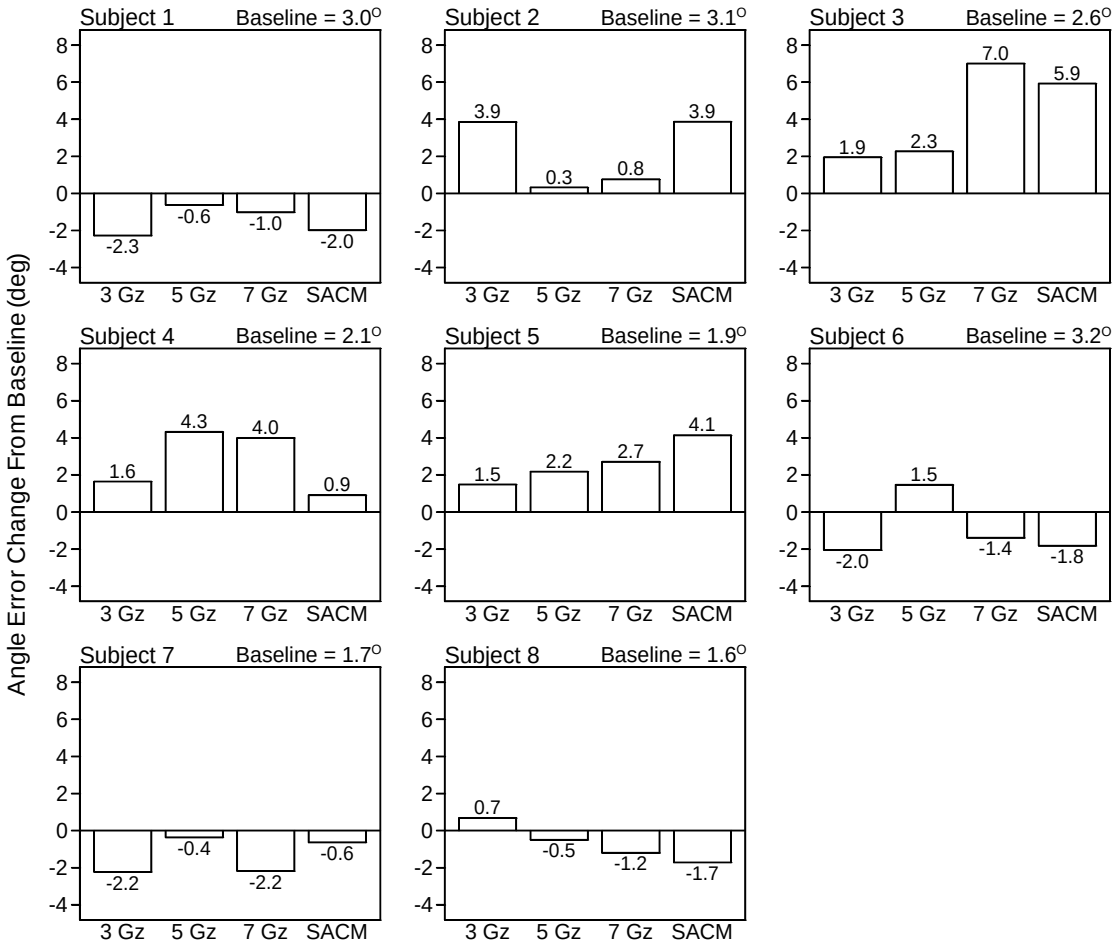

Figure 15: Mean angle error change from baseline for each subject and plateau of each Gz profile

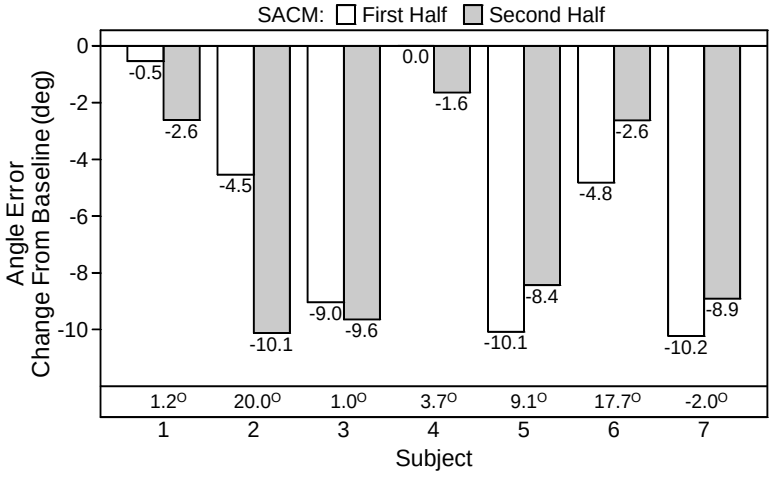

Figure 16: Mean angle error change from baseline for each subject and SACM half

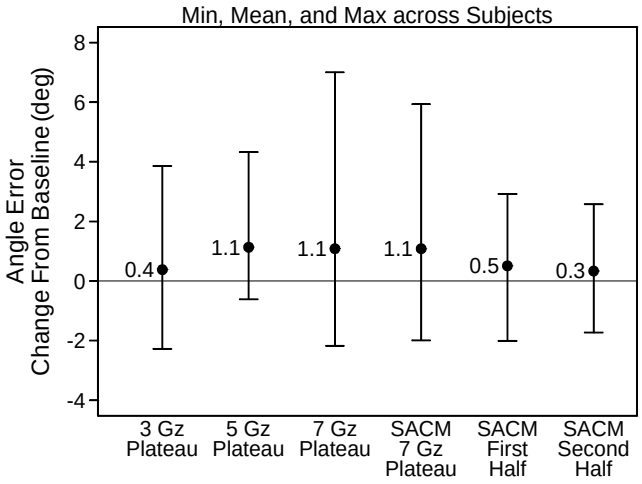

Figure 17: Minimum, mean, and maximum angle error change from baseline across subjects (N = 8)

Repeated measures analyses of variance were performed using the mean angle error change from baseline for each subject. A first analysis employed the mean angle error change from baseline for each subject and plateau during each G_z profile (Figure 15). The F-test did not find a significant difference among the 3 Gz plateau, 5 Gz plateau, 7 Gz plateau, and SACM 7 Gz plateau ($p = 0.7622$). Two-tailed t-tests using the subject means (no pooling) did not show any of the plateau means to be significantly different from 0 ($p > 0.1082$).

A second analysis used the mean angle error change from baseline for each subject and SACM half (Figure 16). The F-test did not find a significant difference between the first half and second half of the SACM ($p = 0.6304$). Two-tailed t-tests using the subject means (no pooling) also did not show either mean to be significantly different from 0 ($p > 0.4036$).

Discussion and Conclusions

The theory that acceleration induced hypoxia generates degradations in cognitive performance appears to be highly dependent on the type of task in question and, not surprisingly, the magnitude of the acceleration itself. Chapter 1 of this report illustrated the rather severe

consequences of moderate to high G_z levels on tracking ability. It is likely that the substantial losses observed were highly influenced by the relative position of the area of the cortex (primary motor cortex responsible for arm and hand movements) primarily needed to complete the given task. In that task, the cortical tissue was located at the extreme dorsal end of the brain, making it the area furthest from the heart and above the eye-level. The arterial system of the human body can be conceptually modeled as a hydrostatic column of blood using Pascal's Law (Eqn. 7).

$$P = \rho g h \qquad \textbf{(Equation 7)}$$

where P denotes pressure, ρ is the density of the liquid, g is the acceleration due to earth's gravitational pull, and h is in the height of the fluid. The traditional coordinate system is for the height (z-axis) to be 0 at the level of the heart, positive in the direction of the feet, and negative in the direction of the head. Using this equation and coordinate system, it becomes clear that blood pressure in the upper extremities is lower than that of the lower extremities at +1 G_z. As the acceleration (g) increases, the pressure in the upper extremities and head continue to decrease in a graduated fashion. Hence, blood pressure at the dorsal end of the brain is lower than that at ventral sections. By further decomposing the areas active during temporal processing, it is possible to further elucidate the rationale for the findings of the present study.

The "precision timing task" used in this study required subjects to process precise and accurate temporal relationships between a target and a stationary object (hash mark). Available literature suggests that humans process timing information both in the cerebellum and in the prefrontal cortex (Mangels et al., 1998; Nichelli, et al., 1996). The study by Mangles and colleagues (1998) attempted to further define the roles of both brain areas and noted an important

difference. Specifically, patients that had lesions in neocerebellar regions performed significantly worse in a timing task for the short duration (millisecond and second) trials, whereas patients with prefrontal cortex lesions had difficulty with long duration trials (Mangels et al., 1998). Fraisse (1984) and Mangels et al. (1998) suggest this fundamental difference in apparent function is a direct result of long duration time perception requiring the aid of memory.

The cerebellum is often referred to as the internal clock of the human body and is largely responsible for circadian rhythms and time interval perception. However, long duration time perception (more than a few seconds) is more than the cerebellum can handle alone and must engage the working memory functions in the prefrontal cortex to maintain awareness of the stimuli and track its progression. This theory is further supported with a study by Nichelli, et al. (1996) which suggested the cerebellum was responsible only for shorter duration time interval processing.

Based on those findings, it can be reasonably concluded that the cerebellum was primarily responsible for the precision timing perception in the present study due to the fact that the maximum time interval used was 2.25 seconds. The results show that there were no statistically significant differences in performance during any G_z plateau from the baseline taken at 1 G_z. Likely, this is a result of hydrostatics alluded to earlier in this section. The cerebellum lies in the ventral posterior of the brain, which places it lower (less negative value of h – see equation 7) relative to the frontal cortex allowing it to maintain higher pressure and receive oxygenated blood longer than areas above it. In addition, subjects were instructed to perform the AGSM to the extent that their vision was not significantly affected. Hence, they endeavored to maintain adequate eye-level blood pressure using their visual cues as a guide. However, there were no obvious indications to the subjects of blood pressure losses in the cortical tissue above

eye-level. As a result, it is possible that cortical tissue residing above eye-level may have experienced more pronounced declines in oxygen saturation due to relatively lower blood pressure values in these areas.

It should be noted that blood supply to the eyes begins to subside earlier than areas of the nervous system during $+G_z$ acceleration due to the intraocular pressure. Essentially, the resting arterial blood pressure in the eyes must be greater than that of surrounding tissue to compensate for the existing intraocular pressure. Hence, perfusion to the eyes will decrease first as a result of being acted on both by the intraocular pressure and the inertial forces caused by the added G_z. Given this phenomenon, surrounding cortical tissue will likely retain blood pressure and oxygen saturation for a short time after the subject begins to experience visual symptoms. However, the physical location of the cortical areas critical to execution of the task of interest likely influences the extent of cognitive performance degradations due to the hydrostatic pressure distribution. In essence, the arterial pressures in cortical areas remain proportional to the height of the arterial column. As a result, it is expected that areas of the brain closer to the neck will suffer less hypoxia than those residing above them.

It can therefore be reasoned that precision timing was not affected by G_z in this experiment due to the fact that it was processed primarily in the cerebellum, which resides below in the ventral portion of the brain. Because subjects were instructed to maintain adequate eye-level blood pressure (as evidenced by a lack of visual symptoms such as dimming or graying), it can be concluded that cortical areas below eye-level also maintained sufficient arterial pressure to receive a fresh supply of oxygen. When compared with task one (ref. chap. 2), it appears that areas above eye-level may experience larger declines in performance due to the hydrostatic pressure distribution. As a final note, it appears a subset of the population may experience

significant declines in the ability to precisely process timing information. Subjects 3, 4, and 5 demonstrated declines in performance on the task at higher G_z levels. It is believed that this is a product of the subject's individual G tolerance, height, and muscle composition. Thus, although the mean performance is not significant, some pilots may experience problems.

CHAPTER 4: TASK 3 – MOTION INFERENCE

Introduction

The effects of sustained acceleration can have a profound impact on the human body making even the simplest tasks excruciatingly difficult. Of principal interest are the effects of acceleration in the z-axis (G_z - directed head-to-foot) on human cognition. As stated in chapter 1 of this document, the inertial forces increase the apparent weight of the blood making it much more difficult to pump into the cortical tissues of the brain. As the blood begins to pool in the lower extremities, the oxygen supply may not be adequate to support many of the essential cognitive functions required for agile flight. However, to date little research has probed the effects of G_z on individual cognitive abilities. As a result, the objective of this effort was to investigate the effects of G_z on motion inference perception.

Although the task utilized in this study was titled motion inference, it actually encompassed both motion and time estimation. Essentially, the subject was required to process the initial velocity of a moving target while it was visible. It would then disappear, and the participant would estimate the time interval required for it to reach a target stopping point. During this time, the subject was given a secondary verbal task as a distraction. Time estimation appears to be largely dependent on the length of the time duration. As stated in chapter 3, time estimations over 5 seconds in duration invoke working memory processes in the prefrontal cortex. The prefrontal cortices of the brain in both hemispheres may "have the function of a hypothetical accumulator within an internal clock model" for tasks lasting more than a few seconds (Rubia & Smith, 2004). Their research has suggested that the dorsolateral and the inferior prefrontal cortex play a crucial role in time-perception tasks (lasting more than 5 seconds) through the interaction of working memory, attention, and timing. In addition, Zakay

(1990) found that the general tendency across normal subjects at +1 G_z is to overestimate short time intervals (few seconds or less) and underestimate much longer times (hours).

Time estimation is also influenced by the activities performed by the individual during the given time interval. This has led to such popular phrases as, "Time flies when you're having fun," and "This workday has slowed to a crawl." Overall, the time estimation seems to be tied to the level of work or effort by the individual. This is particularly true of cognitive workload and processing where higher levels lead to an underestimation of the time (Tsao, Wittlieb, Miller & Wang, 1983). Tsao and colleagues (1983) noted it was the level of engagement and demand on cognitive processes that influenced the estimation of the time interval. When given no task during the time interval, the estimation was greatly increased (38 seconds during high workload compared to 49 seconds with no task). Hence, the amounts of attention that can be allocated to interpreting the progression of time appears have a significant influence on time perception accuracy. As attention is focused on other tasks, particularly those that are cognitively demanding, less attention can be assigned to perceiving time. This generally results in a shortening of the perceived elapsed time for the given task (Zakay & Fallach, 1984).

The $+G_z$ acceleration of the agile flight environment presents yet another stressor to further influence time estimation. A study conducted by Repperger et al. (1990) determined that the perception of time is altered (perceived time faster than actual) at G_z levels higher than +5 G_z. That is, subjects underestimated the time required for a moving object to travel between two points. In addition, Ratino et al. (1988) reported that astronauts' have reported a compression of perceived time during and after a space flight mission. This phenomenon has been termed "The Time Compression Syndrome" (Ratino, et al., 1988).

Other studies have contributed to the realization that cognitive processes slow or shut down during hypoxia (Fowler & Prlic, 1995). For example, Canfield, Comrey, and Wilson (1949) concluded "that the reaction time to both light and sound stimuli becomes significantly longer under conditions of increased radial acceleration." In addition, Porlier et al. (1987) determined that subjects undergoing increased levels of hypoxia ($Sa0_2$ of 75, 70, and 65) experienced increases in P300 latency, which can be attributed to a general slowing of stimulus evaluation processes. These subjects also demonstrated increased reaction times to an oddball paradigm task (Porlier et al., 1987). A study conducted by Albery and Chelette (1998) also reported that subjects suffered increased choice reaction times when provided inferior G protection.

These studies provide evidence that the ability to process information is degraded during acute hypoxia. In addition, it should be expected that the inference of motion (time interval for an object to traverse a set path) may be compressed (underestimated) as a result of the stress of the inertial environment. In theory, this would result from time compression syndrome, the increased engagement of the task as a result of the added physical stressor, and decreased functioning of the prefrontal cortex.

Methods

Subjects

A total of seven subjects (5 male, 2 female) volunteered to participate in this study. They ranged in age from 24 to 35 years, with a mean age of 29 years. All participating subjects were members of the sustained acceleration stress panel at Wright-Patterson AFB, OH. As part of the requirement for membership on the stress panel, each completed the Air Force's extensive

centrifuge G-training program to ensure that their tolerance to acceleration and their vestibular responses under acceleration were similar to those of pilots flying high performance aircraft.

In order to qualify for service in the study, each subject had to meet Air Force flying class III medical, height, and weight standards and have no history of neurological pathology. In addition, all participants were required to have normal or corrected-to-normal vision and a normally functioning vestibular system. Information concerning these qualifying factors was obtained from screening the participant's medical records. Prior to final acceptance into the study, all participants underwent a rigorous physical examination including x-rays of the skull and spine, tests of the integrity of the cardiovascular, pulmonary, and nervous systems, and a comprehensive blood chemistry work-up. On the basis of this examination, all of this study's participants were determined to be in excellent health by a flight surgeon.

Facilities

All training and data collection for this study was performed at the Air Force Research Laboratory's Dynamic Environment Simulator (DES) centrifuge facilities at Wright Patterson AFB (ref. Chap. 2, Figure 3). The DES is a human rated centrifuge with an arm radius of approximately 19 feet. It is capable of attaining and sustaining accelerations up to 20 G in either of three independent axes: x, y and z. The DES has a maximum G onset and offset rate of approximately 1 G/sec. The gondola of the centrifuge was equipped with an F-22-like ACES II ejection seat with a seatback reclined to 15^{o} from vertical. As illustrated in Figure 2 (ref. Chap. 2), the seat had adjustable lap and shoulder restraints.

An aircraft IC-10 communication system was used to provide two-way voice-communication between the research participant and the investigator. The participant's microphone was fixed in the open position to allow the participant "hands-free" communication.

Participants were also provided with an emergency abort switch that enabled them to stop the centrifuge at any time during testing. Participants wore a standard Air Force issue Nomex® flight suit and a standard G-suit during all testing runs.

The gondola was outfitted with a simulated fighter cockpit. The cockpit incorporated a Thrustmaster Hotas Cougar flight stick (Guillemot, Montreal, Canada) and throttle. The flight stick was mounted on the participant's right side and the throttle was positioned on the left. A six foot hemispherical shell viewing screen, representing a 130^{o} (vertical) x 180^{o} (horizontal) visual field, mounted directly in front of the participant. A separate projector was used to display the performance task in the center of the subjects' field-of-view with a projected image of 22.5" (width) by 18.5" (length). The large dome display was used to present two red dots located at approximately 60^{o} of visual angle to the right and left of the center of the dome and approximately 5^{o} in diameter. In addition, a red circle was displayed just above the HUD that represented 10^{o} of visual angle. The dots served as a reference to the subject of his/her visual loss. Should the smaller dots not be visible in the periphery, the subject was instructed compensate by increasing their AGSM. They were to abort the test should their vision degrade to the point that only the center red dot was visible. Figure 4 (ref. chapter 2) provides an illustration of the entire visual system.

Continuous surveillance of participants was provided by two closed-circuit infrared television cameras. The cameras offered a close-up view of the participant's head and a wide-angle view of the participant from head-to-foot. Research personnel housed in a control room observed the video images. A video mixer was used to generate a composite picture of the two views of the participant along with the time, date, electrocardiogram (ECG) data, and G_z acceleration in a given run. Video data were stored on ½ inch VHS videotape.

Acceleration Profiles

A total of four G_z acceleration profiles were generated for use in this study. All G_z exposures were started from a baseline acceleration of 1.5 G_z. The first three profiles comprised of a 1 G/sec onset ramp to a 15-sec plateau followed by a G_z offset ramp of 1 G/sec down to the baseline acceleration level. The plateaus were 3, 5, and 7 G_z, respectively. The final acceleration exposure was a simulated aerial combat maneuver (SACM). This profile consisted of two 5-sec G_z peaks to 7 G_z with several intermittent peaks to 3 and 5 G_z. Figure 6 (ref. chap. 2) displays an example of a G_z plateau profile, while Figure 7 (ref. chap. 2) presents the SACM profile.

Stimuli

The subjects completed a "motion inference" performance task during each G_z profile on each experimental test day. It was projected on a 22.5" (width) by 18.5" (length) screen located approximately 3 feet in front of the subject. The display encompassed roughly 36^o horizontally, and 28^o vertically of the subjects' field of view. The motion inference performance task contained two separate tasks. The primary task contained a semicircular arc, a moving target light, and a hash mark/stopping point as in the precision timing task. As in the precision timing experiment (ref. chapter 3), the target light traversed the curved path from left to right at a constant velocity, however, the target would disappear after it had negotiated approximately one-third of the arc-segment (see Figure 18). The objective was to stop the target on the predetermined stopping point (hash mark) by estimating time interval required for the target to intersect this point based on its velocity before it disappeared.

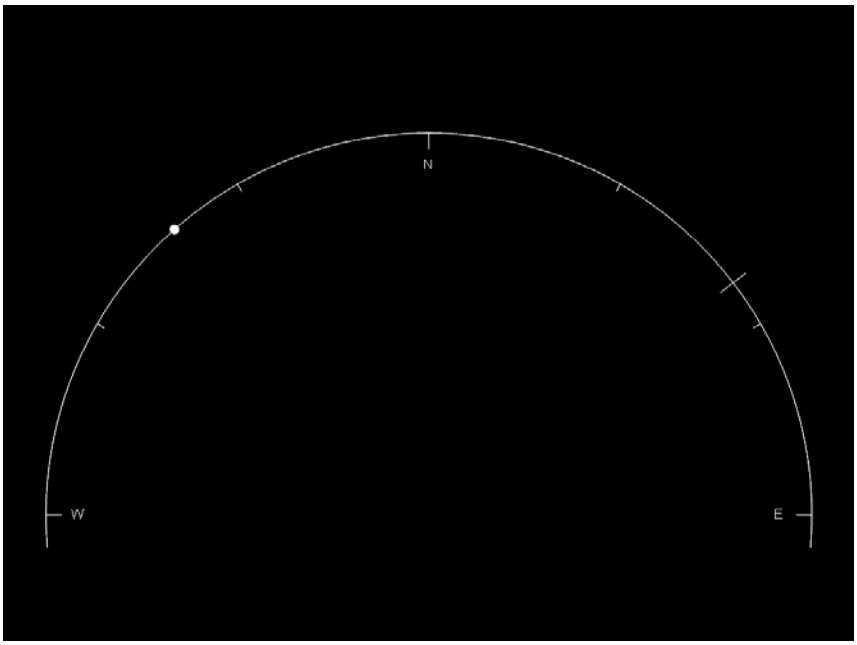

Figure 18: Motion Inference Task – Moving Target Shortly Before Disappearing

Once the target light disappeared, a secondary task would appear in the bottom, center of the display screen that consisted of four letters inside a box. The objective was to determine whether or not the letter set contained a vowel. A screen shot illustrating this secondary task can be found in Figure 19.

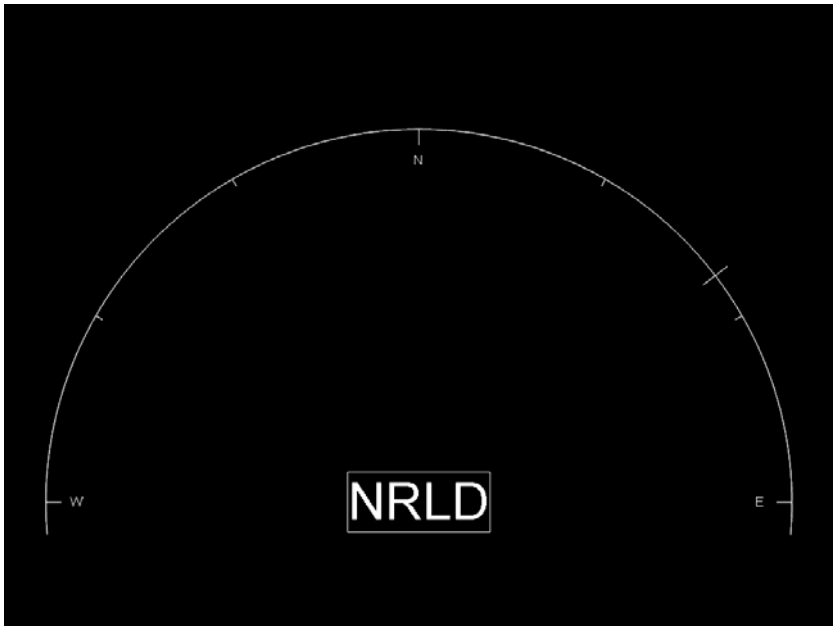

Figure 19: Motion Inference Task – Moving Target Disappeared; Letterset is now Visible

Static Training

All subjects were trained statically on the motion inference performance task prior to dynamic training and experimental data collection. Static training was performed in an F-16 mock-up fuselage equipped with an ACES II aircraft seat with a 15 degree seat-back angle. The task was projected onto a 48-in (vertical) x 64-in (horizontal) screen. Subjects were given 30 presentations of the task followed by a one minute rest period. This was repeated three times per static training day. An average absolute error score was calculated by determining the angle difference between the stopping point (hash mark) position and the point at which the subject stopped the hash mark. In addition, responses to the lettersets were compiled and analyzed. The subjects were considered trained once their average absolute error score was $\leq$ 5 degrees and deviated less than 10% between training days. In addition, subjects had to respond correctly to 90% of the lettersets, on average, to be considered trained.

Dynamic Training

Each subject also completed dynamic blend training on the centrifuge where they were required to perform the motion inference task in the DES while completing the same 3, 5, 7, G_z plateau and 7 G_z SACM profiles that were administered during the experimental test days. A one-minute rest period was given after each G_z profile. Prior to the centrifuge runs, subjects performed the task at 1 G_z (30 presentations) each training day to provide a baseline for comparison. Subjects were considered trained once their performance on the task deviated less than 10% between training days. Performance was measured in absolute angle error and percentage of correct responses to the letterset. This was accomplished to ensure that no training

effects were present in the final data that may have resulted from acclimation to performing the task in the high G environment.

Procedures

On a typical experimental test day, participants arrived at the laboratory, donned a flight suit and a standard G-suit, and were instrumented with electrocardiogram leads. The flight surgeon performed a brief medical examination and reviewed the subject's medical history. The participant then proceeded to the centrifuge where he/she donned a parachute harness. After entering the gondola of the centrifuge the participant was secured to the ACES II aircraft seat (with a 15-degreee seat back angle) using a three-point aircraft restraint system. The ECG leads were connected and the signals were verified prior to securing the gondola of the centrifuge. At this point, the motion inference performance task was initiated and baseline performance data were collected over 30 presentations.

Each participant was instructed to watch the target light as it traversed the semi-circular arc segment. Once the target disappeared and the letterset appeared, the subject was to determine whether a vowel was present. The response was secured with the toggle switch located below the red button on the top of the flight stick (see figure 20). Subjects were also told to keep track of where they believed the invisible target light was at all times based on the velocity it was traveling at the beginning of the trial. Once they believed it had reached the hash mark, participants were to respond by depressing the trigger button on the flight stick. They were also instructed to treat the target light as the primary task and the letterset as a secondary task. If at any time they felt that they could not respond to both tasks, they were not to respond to the letterset task.

Figure 20: Joystick Response Switches for Motion Inference Task

Due to the difficulty level of the task, feedback was given to the subjects during training. For example, after responding to the letterset, the software would display the word 'correct' or 'incorrect' at the bottom of the screen. In addition, the target light would reappear once the subject had pressed the trigger button to show where they had stopped the target. These features were disabled during data collection.

Following the collection of baseline data, the participant experienced his/her first G-exposure. Each of the four G_z exposures was administered on three different test days in the following order: 3 G_z 15sec plateau, 5 G_z 15sec plateau, 7 G_z 15sec plateau, and 7 G_z SACM. The subject began the performance task approximately 5 sec prior to each G_z exposure and continued until the acceleration had returned to the baseline G_z level of 1.5 G_z. A 1-minute rest period was provided between each G_z exposure during which the task was not performed and the

subject was permitted to relax at the baseline G_z level. This was accomplished to allow the physiology to return to the pre-acceleration exposure levels. Following the completion of the four G_z exposures, the participant was removed from the centrifuge and immediately examined by the flight surgeon. Afterwards, they were released to return to their normal duties. These procedures were repeated over all three experimental test days.

Results

Two separate analyses were completed with regard to the mean angle error. Due to a computer problem on the second day of data collection for subject 3, the entire data set did not get recorded. Therefore, this data was omitted from all analyses. The first analysis was completed to determine whether there were significant main effects of G_z level on degree of angle error. This included data from the plateaus of the 3 Gz, 5 Gz, and 7 Gz runs and the two 7 Gz plateaus of the SACM run. Plots of the data for each of the seven subjects can be found in figure 21. The solid horizontal line connects the mean values of angle error for each of the G_z exposures. The dotted line represents the average baseline value for that particular subject. In addition, the angle error statistics for the baseline data (min, mean, max) are shown above each data plot.

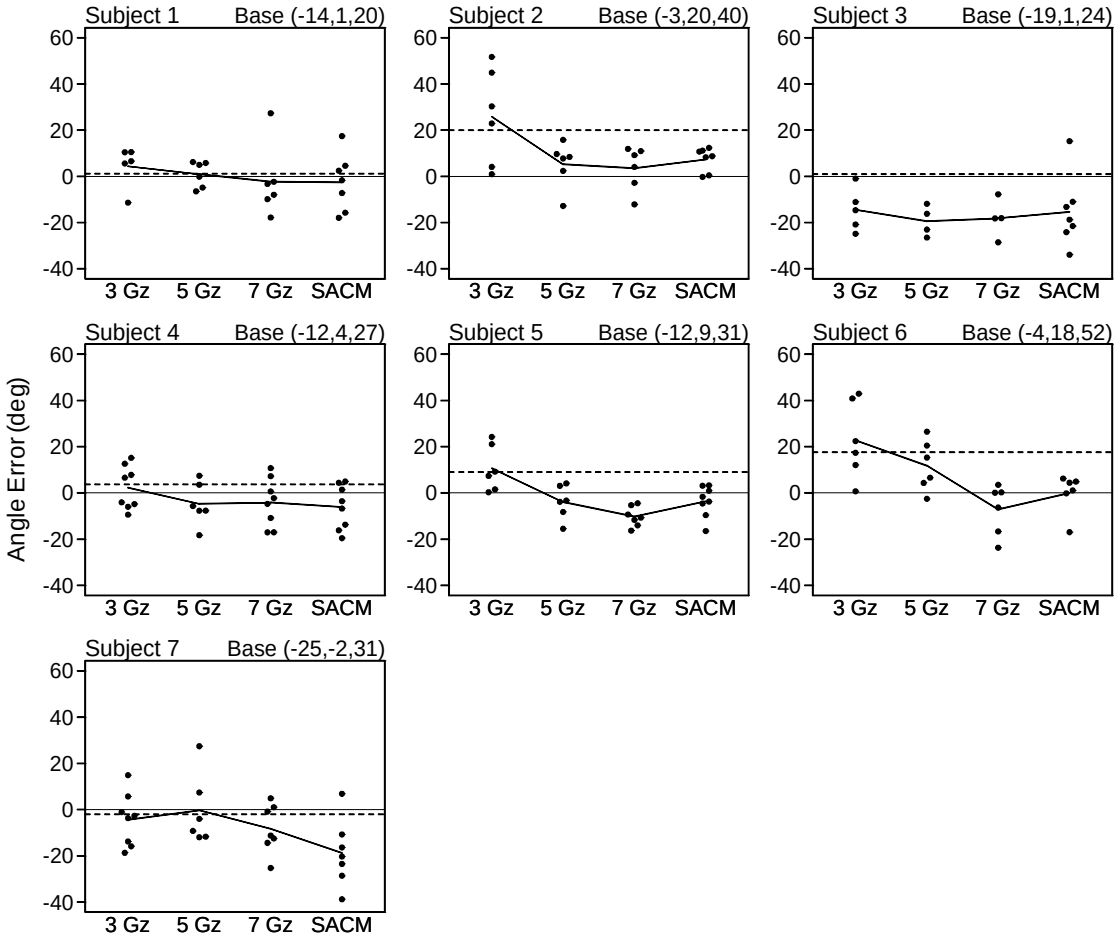

Figure 21: Motion Inference mean angle error change from baseline for each subject and G_z plateau

The angle error change from baseline was also calculated for each subject and averaged across experimental test days. The plots of these data for each subject can be found in Figure 22. The average angle error baseline value for each subject is displayed above each plot panel.

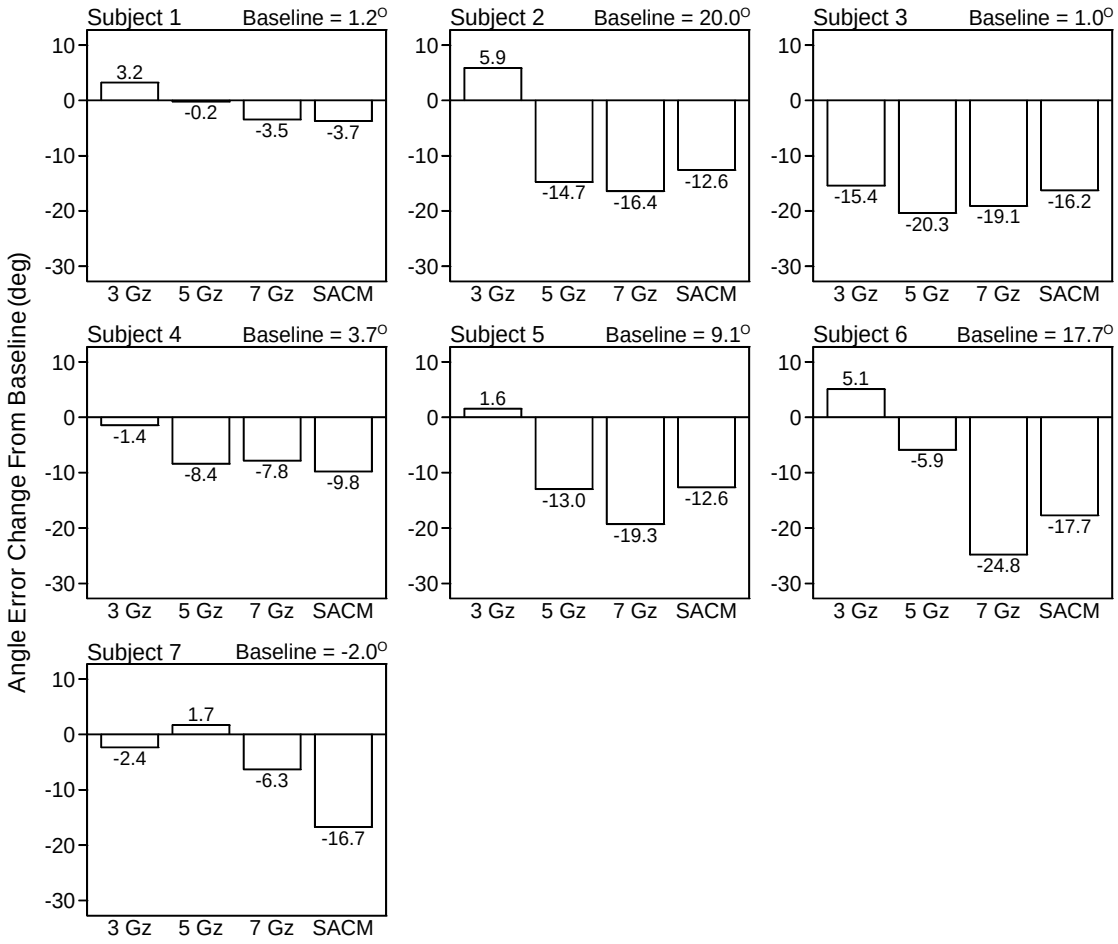

Figure 22: Motion inference mean angle error change from baseline for each subject and G_z plateau

The second analysis involved a comparison of angle errors during the first half vs. the second half of the SACM. This analysis was completed to determine task performance changed as the SACM progressed. The data used in this analysis can be found in Figure 23. The lines and legends on these data plots have the same denotations as the plots in Figure 21.

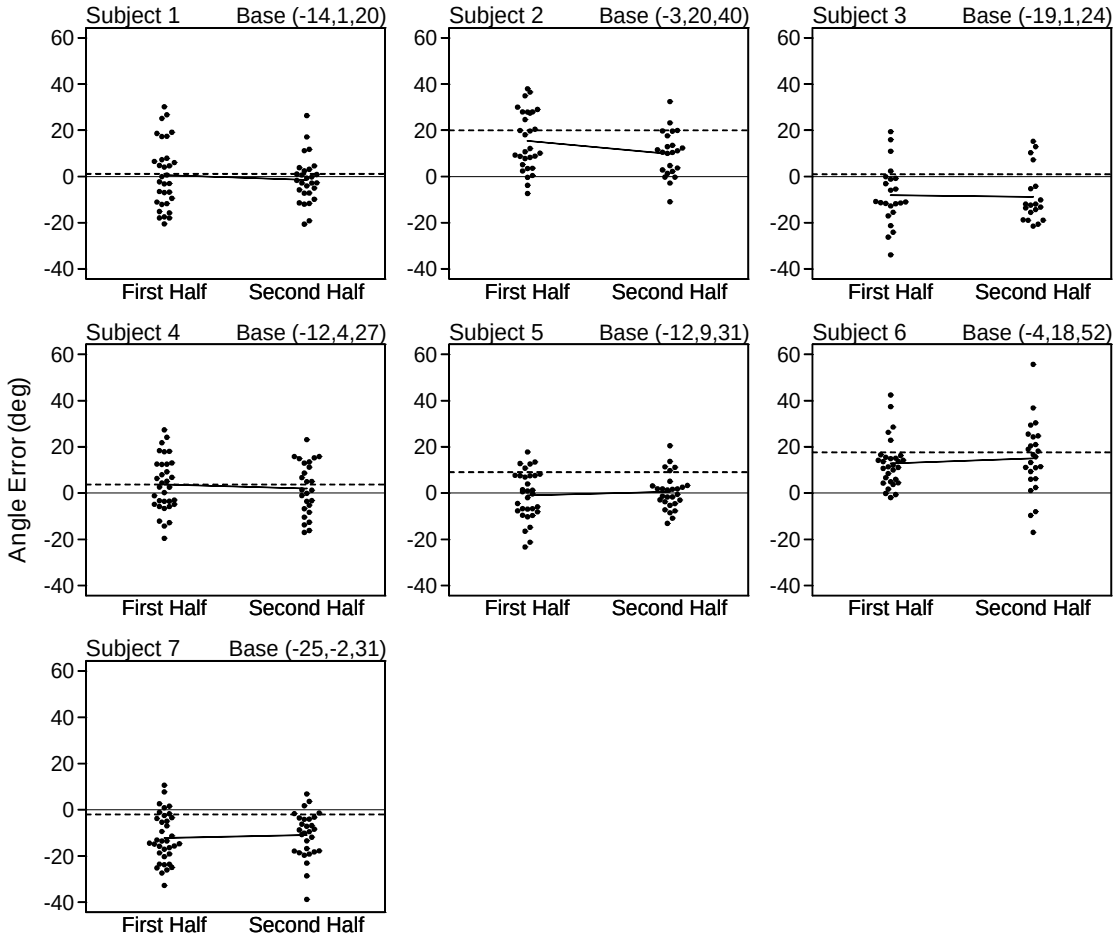

Figure 23: Motion Inference angle error for each subject for the first or second half of SACM.

Likewise, a second plot of the mean angle error change from baseline was created for this analysis (see Figure 24). The mean baseline angle error is displayed above the subject number in on the X-axis. Figure 25 displays the mean error change from baseline averaged across subjects and experimental days. The overall baseline mean angle error across subjects and test days was 7.2^{o}. The bars emanating from each point represent the minimum and maximum angle error changes from baseline.

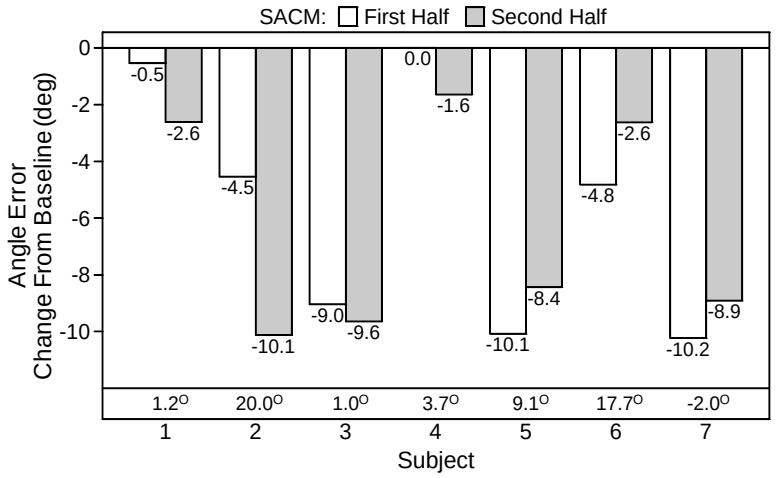

Figure 24: Motion Inference mean angle error change from baseline for each subject and SACM half

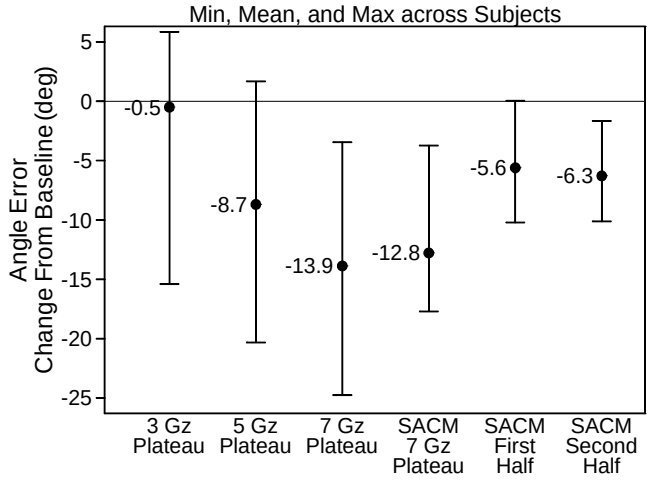

Figure 25: Motion Inference minimum, mean, and maximum angle error change from baseline across subjects (N = 7)

A repeated measures ANOVA was performed for the mean angle error change from baseline performance metric. The F-test found a significant difference among the 3 G_z plateau, 5 G_z plateau, 7 G_z plateau, and SACM 7 G_z plateau (p = 0.0013: Greenhouse-Geisser epsilon = 0.69, adjusted p = 0.0053). The Bonferroni paired comparison procedure with a 0.05 family-wise error level showed the mean angle error change from baseline at the 3 G_z plateau to be significantly different than the other three plateaus, with the 5 G_z, 7 G_z, and SACM 7 G_z plateaus

not different from each other. Two-tailed t-tests using the subject means (no pooling) did not find the 3 Gz plateau mean to be significantly different from 0 (p = 0.8638) but did find the 5 Gz (p = 0.0274), 7 Gz (p = 0.0037), and SACM 7 Gz (p = 0.0005) plateau means to be significantly different from 0.

The second analysis (SACM halves comparison) used means from Figure 24. Here, the F-test did not find a significant difference between the first half and second half of the SACM (p = 0.5305). Two-tailed t-tests using the subject means (no pooling) found the mean for the first half (p = 0.0141) and second half (p = 0.0046) of the SACM to be significantly different from 0.

Discussion and Conclusions

Time and velocity estimation (motion inference) are essential functions that need to be maintained during agile flight combat. Primarily, failure of these cognitive abilities impedes the ability of a pilot to track a moving target should he/she temporarily lose site of it. Operationally, a pilot may need to track a target aircraft moving across his/ her line-of-sight. Should it fly into a cloud or behind another visual obstacle, the pilot would need to estimate when it would emerge on the other side. An accurate estimation would allow him/her to quickly fire on the target when it again became visible. Due to the fact that G_z acceleration is an integral aspect of the combat flight environment, it is important to quantify any changes to the performance of this cognitive ability so that countermeasures and/or improved training techniques can be employed to overcome this challenge.

The results from the present study suggest that the ability to infer motion and accurately estimate a time interval is significantly affected by the forces of the inertial environment. The mean angle error values became significantly more negative as the G_z acceleration level was

increased. Angle errors are vector quantities where negative values denote the angle was to the left of the target hash mark. Because the target light moved from left to right, negative values indicate that the subjects were significantly *early* in their estimation of the time interval. Declines in performance were also found by Repperger et al. (1990). Subjects in his study also exhibited a chronic underestimation for the time interval required for a moving target light to travel between two points. However, these changes were only found at G_z levels of +5. The difference here was that Repperger et al. (1990) used time as a metric of performance whereas the present study utilized stopping point position errors measured in degree of arc angle. However, the data can be standardized in terms of the percent change from baseline. A comparison of the results can be found in table 5 below. The negative values denote that the change from baseline was greater than 100%. That is, the *difference* between the performance values at the given G_z level and the average baseline was greater that the average baseline value.

Table 3: Comparison of Motion Inference Performance Data

Reference	***Dependent Measure***	***1Gz***	***2Gz***	***3Gz***	***4Gz***	***5Gz***	***6Gz***	***7Gz***
Repperger et al., 1990	Motion Inference, Slow Velocity	100		89.29		26.79		
Repperger et al., 1990	Motion Inference, Fast Velocity	100		114.29		80.95		
Current Study	Motion Inference, Fast/Slow Combined	100		93.05		-20.83		-93.06

Table 5 provides a clear illustration that the changes in performance at G_z were much greater in this study. This could have been due to the fact that performance measures for motion inference accuracy differed between the two studies. In addition, the non-counting time estimation task used by Repperger, et al. (1990) did not provide a distracter task, hence making it somewhat easier to perform. By distracting the subject with a secondary task (as done in the

present study) during the time interval, it is very difficult to attempt to count or keep track of time during the time interval. The important similarity in both studies is that subjects experienced what is now known as "The Time Compression Syndrome," where the pilot underestimates the time for the target to reach its destination (Ratino, et al., 1988). Operationally, this indicates that under G_z stress in a hard turn or climb, pilots could be prone to fire on a target too early should it temporarily disappear behind an obstruction such as a cloud or mountain.

Nevertheless, it appears that the findings by Repperger et al. (1990) that performance only begins to decline at +5 G_z or more may still hold true. In the present study, subjects habitually o*verestimated* the time for the target light to reach the hash mark at +1 G_z, evidenced by the positive 7.2^o average value. Hence, at +3 G_z, subjects technically performed better than baseline due to the fact that they stopped the target closer to the hash mark. It is important to note that a different subject pool using pilots experienced in firing on targets may yield a more accurate baseline (angle error closer to zero). However, it is theorized that the percentage changes will be relatively similar due to the decline in oxygen delivered to the prefrontal cortex.

As stated in chapter 3, "Precision Timing," the cerebellum is believed to be the body's internal clock. It controls circadian rhythms and available evidence has shown it to be responsible for short time interval estimation (Nichelli, et al., 1996). Given that the precision timing task used in chapter 2 of this report used a maximum time for 2.25 sec, it is theorized that the cerebellum was largely responsible for the perception of the time interval. The motion inference task used in the present study elongated this time interval to a maximum of 6 seconds to incorporate some slow velocity/time estimation. Slow time estimation is believed to invoke the prefrontal cortex to access working memory. In addition, the fact that the target light in the

motion inference task of the present study disappeared indicates that subjects had to store the initial velocity of the target in short term memory.

Because the prefrontal cortex lies dorsal to the cerebellum, it is likely that it received less blood and oxygen. This phenomenon is caused by the pressure gradient along the z-axis (head-to-foot) of the human body, which is further exacerbated by increased apparent gravity (refer to chapter 3's "Discussion and Conclusions" section). As a result, metabolic demands of the prefrontal cortex are hypothesized to overextend the available oxygen resources thereby causing many of its functions to shut down. Consequently, the cerebellum was not able to access the working memory functions at high G_z, which caused the performance on the primary task to suffer.

The NTI, Inc. look-up table data generated from the Repperger et al. (1990) study appear to be an underestimation based on the data collected in the present study. Whether due to the higher difficulty of the task or the difference in performance metrics, the current motion inference task provides a more conservative estimate of performance at G_z and should be used in place of the NTI, Inc. look-up tables.

CHAPTER 5: TASK 4 – RELATIVE MOTION

Introduction

The ever-emerging threats facing today's military require agile and adaptable responses in disparate environments spanning a multitude of geographical boundaries. Ongoing operations in Iraq and Afghanistan have required extensive, long duration air missions that often exceed the range of many aircraft in the U.S. Air Force inventory. As a result, many pilots are required to regularly perform air-to-air refueling as part of their mission to ensure they can attack the target and return to base safely. Furthermore, others complete missions in "flights" where aircraft travel in formation. Formation flying refers to the condition where aircraft are strategically positioned close to one another to conceal the true number of aircraft from radar imaging and provide support to their wingmen. Finally, avoiding moving targets, such as surface-to-air or air-to-air missiles is critical to the pilot's survival. Refueling, formation flying, and projectile countermeasures all essentially encompass the notion of collision avoidance. This requires the pilot to be aware of his/her aircraft position and motion *relative* to another object in 3-dimensional space. As a result, it is important to understand potential effects of increased acceleration on the ability to process relative motion and optic flow information.

Motion perception is a rather complex process that is not entirely understood by today's psychologists and neuroscientists. Nevertheless, it is generally accepted that the capacity for humans to perceive motion is housed in a few key areas of the brain. The act of interpreting and reconstructing input data from the eyes is initially performed in the primary visual cortex (V1). To sense the movement of an object, the brain must interpret speed and direction while interpolating over time. The V1 area contains specialized neurons that respond to directional shifts aptly named directional selective (DS) cells (Bair and Movshon, 2004). Neurons in the V1

area have relatively small receptive fields and therefore respond only to local stimuli (Bair and Movshon, 2004). Hence, the discrete visual and directional information must be sent from V1 to another area of the brain, referred to as the medial temporal visual area (MT or V5), to be integrated into a cohesive reconstruction of the entire visual scene (Maunsell & Van Essen, 1983).

To adequately perceive motion of potential harmful objects (e.g. missiles, fast moving aircraft, etc.), the brain must have a high baud rate of information delivery to V5 to ensure the visual reconstruction of the scene (including proximate objects) is accurate and current. As a result, V5 neurons are densely packed and are heavily coated in myelin, a substance that enhances the speed of action potentials down the axon (Carlson, 2007). Research has shown that the V5 (MT) area appears to be crucial for the perception of optic flow (Peuskens, et al., 2001). Accurate optic flow perception is vital to the awareness of one's own velocity relative to another moving or stationary object. Temporary lesions on V5, created by transcranial magnetic stimulation, demonstrated that when this area is not properly functioning, human participants cannot distinguish moving objects from those that are stationary (Walsh, et al., 1998). This leads to the hypothesis that a lack of V5 function caused by hypoxia may lead to similar results.

Perception of relative motion also requires the human to be aware of his/her spatial position as well as the position of other objects. Carlson (2007) suggests that the dorsal stream of the visual cortex *must* be involved in the spatial perception of objects due to the findings by Goodale and colleagues (Goodale and Milner, 1992; Goodale et al. 1994; and Goodale and Westwood, 2004) suggesting that its primary role is to guide actions and movements in 3-D space. Carlson (2007) noted, "…how else could it direct movements toward [the location of these objects]?" Given that aircraft are controlled via inputs to the flight stick, it is important to

note that the posterior parietal lobe of the visual cortex has various connections to the frontal lobe (Carlson, 2007). These primarily serve to perform control movements including grasping and reaching. Hence, hypoxic conditions in the frontal lobe may inhibit the human's ability to navigate the aircraft to avoid obstacles even if they are detected.

The task designed for this study is a "join-up" between an F-16 fighter jet and a KC-135 refueling tanker. Essentially, the subject must process the motion of the tanker relative to his/her ownship (the F-16) and successfully control the closure rate between the two objects. This performance task appears rather specific to the aerial refueling task typical to many Air Force missions. However, it probes the basic cognitive ability to perceive the motion of one object relative to another, thereby providing results that can be extrapolated to similar tasks such as flying in tight formations.

Methods

Subjects

Eight subjects (7 male, 1 female) volunteered to participate in this study and ranged in age from 25 to 33 years, with a mean age of 27 years. All participating subjects were members of the sustained acceleration stress panel at Wright-Patterson AFB, OH. Requirements to qualify for participation in this study are identical to those of chapter 2 (ref chapter 2, Methods section).

Facilities

All training and data collection for this study was performed at the Air Force Research Laboratory's Dynamic Environment Simulator (DES) centrifuge facilities at Wright Patterson AFB (ref. Chap. 2, Figure 3). The DES is a human rated centrifuge with an arm radius of approximately 19 feet. It is capable of attaining and sustaining accelerations up to 20 G in either

of three independent axes: x, y and z. The DES has a maximum G onset and offset rate of approximately 1 G/sec. The gondola of the centrifuge was equipped with an F-22-like ACES II ejection seat with a seatback reclined to 15^{o} from vertical. As illustrated in Figure 2 (ref. Chap. 2), the seat had adjustable lap and shoulder restraints.

An aircraft IC-10 communication system was used to provide two-way voice-communication between the research participant and the investigator. The participant's microphone was fixed in the open position to allow the participant "hands-free" communication. Participants were also provided with an emergency abort switch that enabled them to stop the centrifuge at any time during testing. Participants wore a standard Air Force issue Nomex® flight suit and a standard G-suit during all testing runs.

The gondola was outfitted with a simulated fighter cockpit. The cockpit incorporated a Thrustmaster Hotas Cougar flight stick (Guillemot, Montreal, Canada) mounted on the participant's right side that was used to secure responses to the performance task. A six foot hemispherical shell viewing screen, representing a 130^{o} (vertical) x 180^{o} (horizontal) visual field, mounted directly in front of the participant. A separate projector was used to display the performance task in the center of the subjects' field-of-view with a projected image of 22.5" (width) by 18.5" (length). The large dome display was used to present two red dots located at approximately 60^{o} of visual angle to the right and left of the center of the dome and approximately 5^{o} in diameter. In addition, a red circle was displayed just above the HUD that represented 10^{o} of visual angle. The dots served as a reference to the subject of his/her visual loss. Should the smaller dots not be visible in the periphery, the subject was instructed compensate by increasing their AGSM. They were to abort the test should their vision degrade

to the point that only the center red dot was visible. Figure 4 (ref. chapter 2) provides an illustration of the entire visual system.

Continuous surveillance of participants was provided by two closed-circuit infrared television cameras. The cameras offered a close-up view of the participant's head and a wide-angle view of the participant from head-to-foot. Research personnel housed in a control room observed the video images. A video mixer was used to generate a composite picture of the two views of the participant along with the time, date, electrocardiogram (ECG) data, and G_z acceleration in a given run. Video data were stored on ½ inch VHS videotape.

Acceleration Profiles

A total of four G_z acceleration profiles were generated for use in this study. All G_z exposures were started from a baseline acceleration of 1.5 G_z. The first three profiles comprised of a 1 G/sec onset ramp to a 15-sec plateau followed by a G_z offset ramp of 1 G/sec down to the baseline acceleration level. The plateaus were 3, 5, and 7 G_z, respectively. The final acceleration exposure was a simulated aerial combat maneuver (SACM). This profile consisted of two 5-sec G_z peaks to 7 G_z with several intermittent peaks to 3 and 5 G_z. Figure 6 (ref. chap. 2) displays an example of a G_z plateau profile, while Figure 7 (ref. chap. 2) presents the SACM profile.

Stimuli

The performance task in this experiment was a two-dimensional "join-up" task where subject were to join an F-16 with the simulated fueling boom on the tail of a KC-135 tanker aircraft. The F-16 was fixed at the bottom, center of the viewing screen and represented the

subject's "own" aircraft. Once the task began, the KC-135 tanker would appear from infinity and draw closer to the subject's aircraft (F-16) over time. A fueling boom extended from the tail of the tanker and was divided into two sections: one colored red and the other colored green. Figure 26 provides a screenshot where both aircraft and the boom are visible. The task provided subjects with aileron and throttle control combined with simplified flight equations. The objective was to close in on the tanker aircraft as quickly as possible. Once in range, the controls were to be manipulated in such a way as to maneuver the nose of the F-16 to the posterior end (green section) of the fueling boom. Once the F-16 was touching the green section of the boom for 2 seconds, the "join-up" was considered successful and the trial ended.

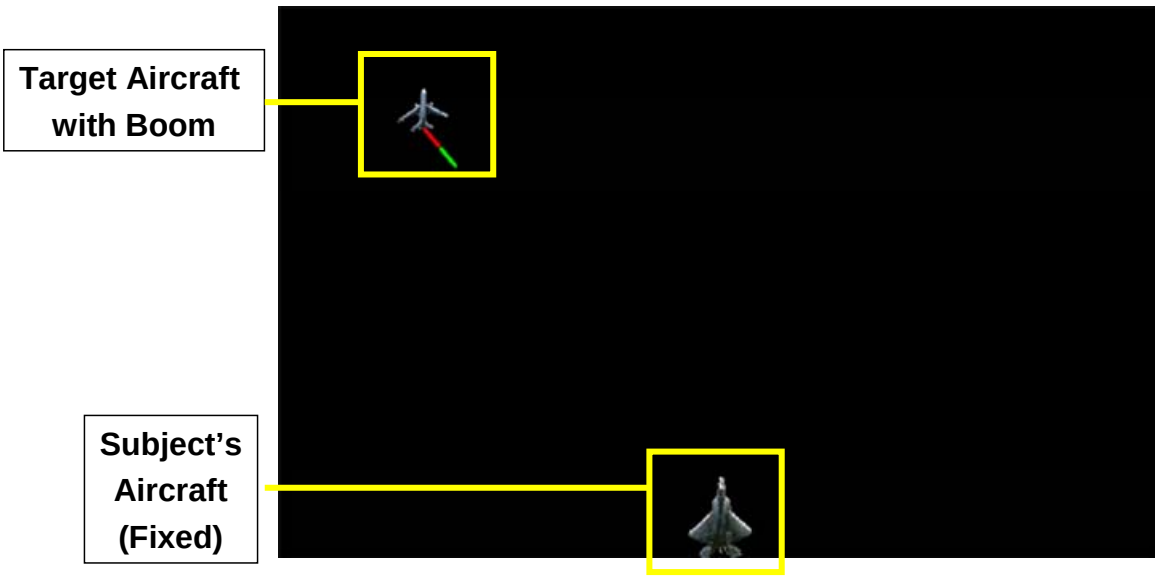

Figure 26: Relative Motion Performance Task Screenshot

The green section of the boom would shrink should the F-16 continue to draw closer to the KC-135. If the subject's aircraft impacted the red section of the boom, the "join-up" was considered a crash and recorded as an error. It was also possible for the subject to fly past the

KC-135 tanker, which constituted an improper join-up and was also recorded as an error. Trial completion time and result (error or success) were recorded by the software each trial.

Static Training

All subjects were trained statically on the relative motion "join-up" performance task prior to dynamic training and experimental data collection. Static training was performed in an F-16 mock-up fuselage equipped with an ACES II aircraft seat with a 15 degree seat-back angle. The task was projected onto a 48-in (vertical) x 64-in (horizontal) screen. Subjects were given 30 presentations of the task followed by a one minute rest period. This was repeated three times per static training day. An average trial completion time and error rate was calculated and tabulated for each session. The subjects were considered trained once their average trial completion time ("capture time") deviated less than 10% between training days. In addition, subjects had to demonstrate successful "join-ups" with the tanker boom for 90% of the trials.

Dynamic Training

As in the previous experiments for this program, dynamic blend training was completed in the centrifuge where subjects were required to perform the relative motion "join-up" task during the 3, 5, 7, G_z plateau and 7 G_z SACM acceleration profiles. A one-minute rest period was given after each G_z profile. Prior to the centrifuge runs, subjects performed the task at 1 G_z (30 presentations) each training day to provide a baseline for comparison. Subjects were considered trained once their performance on the task deviated less than 10% between training days. Performance was measured in capture time and percentage of successful join-up

maneuvers. Dynamic blend training was designed to eliminate training effects resulting from acclimation to performing the task with the presence of motion and acceleration.

Procedures

On a typical experimental test day, participants arrived at the laboratory, donned a flight suit and a standard G-suit, and were instrumented with electrocardiogram leads. The flight surgeon performed a brief medical examination and reviewed the subject's medical history. The participant then proceeded to the centrifuge where he/she donned a parachute harness. After entering the gondola of the centrifuge, the participant was secured to the ACES II aircraft seat (with a 15-degreee seat back angle) using a three-point aircraft restraint system. The ECG leads were connected and the signals were verified prior to securing the gondola of the centrifuge. At this point, the relative motion performance task was initiated and baseline performance data were collected over 10 trials (join-ups).

Each participant was instructed to accelerate toward the target tanker boom as quickly as possible. Once relatively close, participants were to rapidly decelerate and carefully maneuver the nose of their aircraft until it contacted the green section of the boom for a total of two seconds. Subjects were instructed that the tanker would disappear and a new trial would begin once the "join-up" was successful. Aileron control was secured with the HOTAS Cougar flight stick while acceleration was controlled with the throttle (see figure 27). Subjects were told to complete the task as quickly and accurately as possible. Recorded performance data included the mean capture time and the number of errors.

Figure 27: Thrustmaster HOTAS Cougar Flight Stick and Throttle

Following the collection of baseline data, each of the four G_z exposures was administered on three different test days in the following order: 3 G_z 15sec plateau, 5 G_z 15sec plateau, 7 G_z 15sec plateau, and 7 G_z SACM. The performance task was initiated approximately 5 sec prior to the onset of each G_z exposure and continued until the acceleration had returned to the baseline G_z level of 1.5 G_z. A 1-minute rest period was provided between each G_z exposure during which the task was not performed and the subject was permitted to relax at the baseline G_z level. This was accomplished to allow the physiology to return to the pre-acceleration exposure levels. Following the completion of the four G_z exposures, the participant was removed from the centrifuge and immediately examined by the flight surgeon. Afterwards, they were released to return to their normal duties. These procedures were repeated over all three experimental test days.

Results

The mean capture time and percent error data from the relative motion performance task were analyzed separately. Trials that resulted in the subject flying past the KC-135 tanker or colliding with the red section of the boom were considered errors. Two-tailed paired t-tests were used to determine if the mean percentage of trials with errors was significantly different than baseline. Due to a large number of errors relative to the other seven subjects, it was decided that subject 4 was not able to perform the task at a sufficient proficiency and was not included in any analysis. The results from the t-tests showed the percent error was significantly different than the mean baseline during the 7 Gz ($p = 0.0239$) and the SACM ($p = 0.0166$) profiles. However, the 3 Gz ($p = 0.6729$) and 5 Gz profile ($p = 0.2797$) failed to differ at a statistically significant level. Table 6 contains error counts across subjects not including subject 4.

Table 4: Relative Motion Task Percent Error across Trials, Subjects, and Days

		Number of Trials		Percent Error		
Profile	Total Trials	No Contact	Improper Contact	No Contact	Improper Contact	Overall
Baseline	210	2	6	1.0	2.9	3.8
3 Gz	42	0	2	0.0	4.8	4.8
5 Gz	42	0	4	0.0	9.5	9.5
7 Gz	43	3	5	7.0	11.6	18.6
SACM	154	4	18	2.6	11.7	14.3

A second analysis was performed to determine if the mean percent change in capture time changed significantly during any of the G_z profiles. Due to the fact that trials resulting in an error required considerably less time, only trials resulting in a successful "join-up" were included in this analysis. As before, subject 4 was not included in the analysis due to the fact that he/she was an outlier. Subject baseline means ($N = 7$) ranged from 14.3 to 15.6 sec with mean of 14.9 sec. Repeated measures analysis of variance did not show a significant difference among the profiles ($p = 0.2170$). Two-tailed t-tests revealed a mean percent change significantly different

from 0 for SACM (p = 0.0350) but not for the other 3 profiles (p > 0.1634). Figure 28 displays the mean and range of capture times across subjects for each profile.

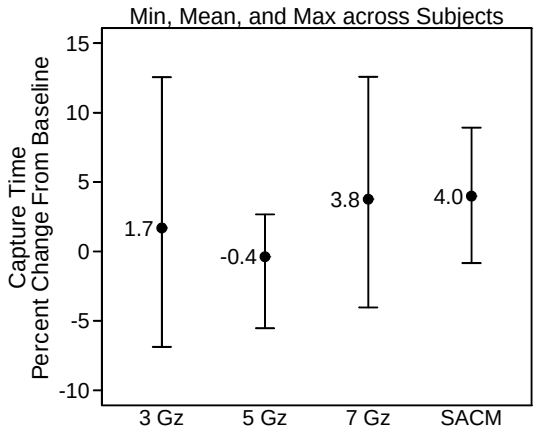

Figure 28: Minimum, mean, and maximum percent change in capture time from baseline

Lastly, mean performance in the first half of the 7 G_z SACM was compared to mean performance in the second half. This was done to determine if performance was further degraded as a result of physical fatigue resulting from performing the anti-G straining maneuver (AGSM). The SACM was separated at the midpoint, which occurred at 85 seconds. For each subject, the mean capture time percent change from baseline was determined for trials ending at or before 85 seconds (first part) and for trials ending after 85 seconds (second part). Two-tailed paired t-tests did not find a significant difference between these two profile segments (p = 0.4722) with means: first half = 3.1%, second half = 5.1%.

Discussion and Conclusions

The results of this experiment indicate that the ability to accurately perceive the motion of objects *relative* to other objects may be impeded at G_z levels of 7 or higher. As previously stated, visual images are initially perceived by V1 DS neurons. These relatively small, local

pictures of the outside world are then coalesced in the V5 (MT) section of the temporal lobe to generate a larger, global depiction. In addition, V5 appears to be necessary for the perception of optic flow, which is vital in ascertaining the relative velocity of the moving projectiles or obstacles in the human's visual field. Furthermore, the visual cortex of the posterior parietal lobe communicates extensively with the frontal lobe to control movement including hand grasping, arm movements, and other limb/eye control (Goodale and Milner, 1992; Goodale et al. 1994; and Goodale and Westwood, 2004). The data from this experiment suggests that oxygen levels may not be adequate to support the metabolic processes of these key areas of the brain at G_z levels of 7 or higher.

The V5 area resides in the striate cortex of the occipital lobe and terminates in the dorsal end of the parietal lobe and is integral to the perception of motion. In terms of height, it is relatively dorsal to eye-level and would likely have a smaller amount of blood profusion than other cortical tissues at or below eye-level. However, to supply oxygenated blood to the eyes, the cardiovascular system must generate compensating pressure not only to overcome the increased apparent weight of the blood arising from the centripetal forces, but also to overcome the intraocular pressure. This indicates that blood pressure must be somewhat higher to maintain profusion to retinal tissue than for neural tissues at the same distance from the heart. Given this phenomena and the fact that subjects were instructed to perform the AGSM to the extent that their vision was not impeded, it is reasonable to expect that the neural tissues at or below eye-level received adequate blood supply.

Additionally, anecdotal evidence gleaned from verbal comments suggests that many of the subjects sacrificed their peripheral vision by performing a less intense strain during the 7 G_z plateau profile in order to conserve energy for the AGSM in the subsequent SACM maneuver. A

quote by Burns and Balldin (1988) summarizes the AGSM effort level quite well, "…performance of the AGSM is very fatiguing and cannot be maintained for very long." A significant reduction in peripheral light loss indicates that oxygen supply within the eye was not adequate to support its metabolic processes. Subsequently, the neural tissue at the same or modestly higher (dorsal) position in the z-axis (distance from heart) may not have sustained adequate oxygen supply during this profile. Without adequate oxygen, the neurons would not be able to continue aerobic metabolic processes to convert glucose to usable energy and would greatly reduce their firing rate. Without V5 neurons firing properly, the ability to decipher the movement of objects on the screen, such as the KC-135 and the attached boom, would be greatly inhibited. This is substantiated by Walsh et al. (1998) who discovered that inhibition of V5 via transcranial magnetic stimulation (TMS) caused subjects lose the ability to decipher moving objects from stationary objects.

The posterior end of the temporal lobe (termination point of visual area V5) extends connections to the frontal lobe to coordinate limb movements (Goodale and Milner, 1992; Goodale et al. 1994; and Goodale and Westwood, 2004). Examples are reaching for a ball located on a table, swatting a fly, catching a ball, or simple eye movements (Carlson, 2007). In this study, subjects were required to move a displacement stick to control their simulated F-16 as it joined with the refueling boom on a moving KC-135. As a result, communication between the frontal and parietal lobes was essential to coordinate movements of the hand and arm with the movements of the aircraft on the screen. Because many of the cortical areas of the frontal lobe are located in dorsal areas of the brain, it is likely that the cerebral perfusion and oxygen supply was reduced.

In summary, it is hypothesized that at the lower G_z levels (e.g. 3 G_z and 5 G_z), the subjects' cardiovascular system combined with the anti-G suit and the AGSM were adequate to supply compensating pressure to overcome the increased apparent weight of the blood. However, it is likely that the 7 G_z profiles presented forces that would too much for the cardiovascular system to surmount. As a result, adequate blood pressure to both the V5 and the frontal lobe could not be sustained. Hence, a preponderance of subjects endured difficulties both in correctly perceiving the motion of the aircraft relative to each other *and* in generating correct movements of the control stick to position the aircraft in the proper location. This inevitably led to the decline in successful join-ups at higher G_z levels.

This theory is not supported by the results from the capture time performance metric. The mean time to complete a trial was nearly 15 seconds, which was largely spent approaching the KC-135. Once in range, the join-up required only a few seconds, thus the differences in capture time may be hidden by the time necessary to approach the KC-135. However, the time was not segregated during the experiment, and there is no possibility of performing such an analysis post hoc. In future studies, the capture time should start once the F-16 is in range to begin the join-up process with the refueling tanker.

CHAPTER 6: TASK 5 – PERIPHERAL INFORMATION PROCESSING

Introduction

Engaging enemies in fast-fighter aircraft involves accelerations that could severely impede neural processes, motor functions, and vision. Often, it is impossible to keep targets within the foveal visual field at all times. As a result, it is imperative to maintain peripheral awareness to ensure the enemy is not able to maneuver to a position that would pose a threat to the pilot. In addition, peripheral vision is important to maintain spatial awareness and monitor critical instruments within the cockpit. Because high acceleration often results in the inhibition or elimination of peripheral vision, an assessment of information processing from stimuli residing in the peripheral field is necessary to account for potential pilot performance decrements.

Vision is possible when light, focused by the lens, is projected on the retina located in the back of the eye. Within the retina are two types of photoreceptors called rods and cones. The cones are located in the center of the retina and are therefore responsible for sensing visual information from the central receptive field. Primarily, these photoreceptors are responsible for daytime, color vision and provide a high level of visual acuity (Carlson, 2007). Rods are particularly sensitive to low levels of light and are primarily located in the peripheral sections of the retina. They are not able to process color and provide relatively low visual acuity (Carlson, 2007). However, rods are predominantly sensitive to detecting motion, lines, and edges. This makes them ideal for finding areas of interest to draw the attention of the foveal vision.

As positive centripetal acceleration forces blood to pool in the lower extremities, the blood pressure at the level of the eye begins to rapidly decline. At +1 $G_{z,}$ the average human eye-level blood pressure is approximately 98 mmHg. Without G_z countermeasures such as the

anti-G straining maneuver (AGSM) or a standard G-suit, eye-level blood pressure will decrease 22 mmHg for every additional +1 G_z of acceleration (Naval Aerospace Medical Institute, 1991). As blood perfusion to the eye fails, the photoreceptors within the eye begin to shut down due to the fact that oxygen (carried by red blood cells) is needed to transmit the visual data to the bipolar cells. In addition, the intraocular fluid exacerbates the issue due to the fact that its pressure opposes efforts of the cardiovascular system by increasing the pressure gradient. The arterial supplies to the foveal photoreceptors (mainly the cones) are larger than those supplied to the periphery. As a result, the peripheral vision generally is the first to shut down, which is apparent to the human subject in the form of "tunnel vision." Here, the visual field collapses into a narrow circle in the center (fovea) of the subject's point-of-gaze. This phenomenon is also readily apparent in color vision due to the fact that cone distributions sensitive to blue, red, and green wavelengths vary based on the distance from the center of the retina (Carlson, 2007). In particular, blue photoreceptors are located furthest on the periphery, which leads to difficulties viewing shades of blue at G_z. However, the color red appears to be rather "G tolerant" due to the relative high densities of red sensitive cones located in the fovea.

The eyes transmit information to the primary visual cortex (V1) located in the occipital lobe. This is further processed in the various areas (V2-V5) of the extrastriate cortex, a portion of the visual association cortex (Carlson, 2007). The visual association cortex divides into two sections for analysis called the dorsal stream and the ventral stream (Baizer, Ungerleider, and Desimone, 1991). Classically, the ventral stream is known as interpreting the "what" (color, form, etc.) whereas the dorsal steam is responsible for motion and position information (Carlson, 2007). Given that the photoreceptive cells in the peripheral vision are more sensitive to high contrast and movement, it is likely most of the information in the peripheral field is processed in

the dorsal stream. Because this stream proceeds from the occipital lobe toward the posterior parietal cortex (more dorsal = toward the top of the head), it is more likely to be effected by the adverse consequences of high G_z. This is due to the fact that blood pressure at the dorsal end of the brain is lower than that at ventral sections as a result of the graduated pressure distribution. The purpose of this study was to quantify these effects on peripheral information processing abilities across a wide range of G_z levels.

Methods

Subjects

Ten active duty members of the United States Air Force (8 male, 2 female) volunteered to participate in this study and ranged in age from 24 to 36 years, with a mean age of 29 years. One female was medically disqualified and did not complete data collection for this study. Hence, all analyses for this experiment include data from only 9 subjects (8 male, 1 female). All participating subjects were members of the sustained acceleration stress panel at Wright-Patterson AFB, OH. Requirements to qualify for participation in this study are identical to those of chapter 2 (ref chapter 2, Methods section).

Facilities

All training and data collection for this study was performed at the Air Force Research Laboratory's Dynamic Environment Simulator (DES) centrifuge facilities at Wright Patterson AFB (ref. Chap. 2, Figure 3). The DES is a human rated centrifuge with an arm radius of approximately 19 feet. It is capable of attaining and sustaining accelerations up to 20 G in either of three independent axes: x, y and z. The DES has a maximum G onset and offset rate of approximately 1 G/sec. The gondola of the centrifuge was equipped with an F-22-like ACES II

ejection seat with a seatback reclined to 15^{o} from vertical. As illustrated in Figure 2 (ref. Chap. 2), the seat had adjustable lap and shoulder restraints.

An aircraft IC-10 communication system was used to provide two-way voice-communication between the research participant and the investigator. The participant's microphone was fixed in the open position to allow the participant "hands-free" communication. Participants were also provided with an emergency abort switch that enabled them to stop the centrifuge at any time during testing. Participants wore a standard Air Force issue Nomex® flight suit and a standard G-suit during all testing runs.

The gondola was outfitted with a simulated fighter cockpit. The cockpit incorporated a Thrustmaster Hotas Cougar flight stick (Guillemot, Montreal, Canada) mounted on the participant's right side that was used to secure responses to the performance task. A six foot hemispherical shell viewing screen, representing a 130^{o} (vertical) x 180^{o} (horizontal) visual field, mounted directly in front of the participant. This screen was used to display the peripheral information performance task. A separate projector was used to display a red "x" with a horizontal red bar located directly above it. The projected image of the bar was 20" wide and 1" in height, whereas the "x" was 4" wide and 4" in height. The red bar served as a visual reference to ensure the subject did not lose consciousness while performing the task at G. Should any portion of the red bar become not visible during the G_z profile, the subject was instructed to depress the emergency abort switch. The centrifuge was also stopped immediately if the participant reported verbally that the bar became shorter or could no longer see the "x". The "x" also acted as the subject's fixation point, meaning the subject's eyes were to remain focused on the "x" at all times while the task was running. To ensure the subject was not "cheating" by taking his/her eyes off the "x," an Eye Tracker monitored the subject's point-of-gaze.

The Eye Tracker utilized in this experiment was the ViewPoint by Arrington Research, Inc. A photo of the device can be found in Figure 29 below. Resembling a pair of glasses with no lenses, the Eye Tracker utilized a camera over the right eye to record the subject's field of view. A second camera focused directly into the subject's eye and was paired with a moveable infra-red light that illuminated the image of the subject's eye. A drawstring encircling the subject's head served to keep the Eye Tracker securely in place during the task. The Eye Tracker was calibrated for each individual at the start of each experimental run in order for the program to lock onto the subject's pupil (see Figure 30). The ViewPoint program continually recorded data indicating the position of the subject's pupil during the task; thus, any changes in the subject's focus could be observed.

Figure 29: ViewPoint Eye Tracker by Arrington Research Inc.

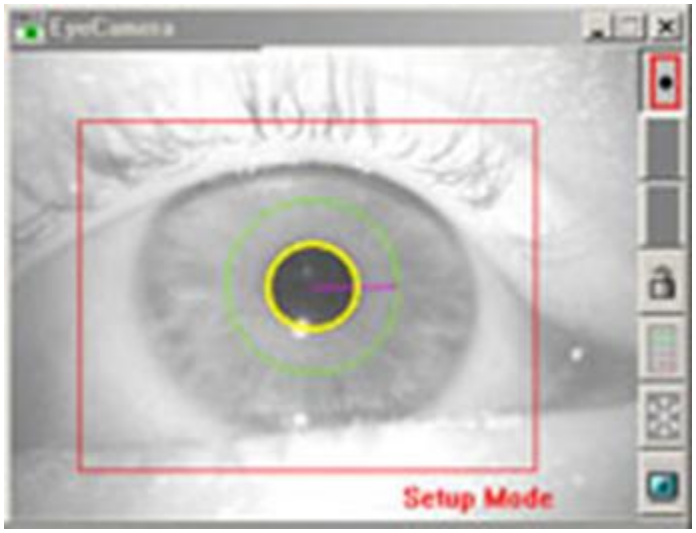

Figure 30: Eye Tracker calibration for an individual subject

Lastly, continuous video surveillance of participants was provided by two closed-circuit infrared television cameras. The cameras offered a close-up view of the participant's head and a wide-angle view of the participant from head-to-foot. Research personnel housed in a control room observed the video images. A video mixer was used to generate a composite picture of the two views of the participant along with the time, date, electrocardiogram (ECG) data, and G_z acceleration in a given run. Video data were stored on ½ inch VHS videotape.

Acceleration Profiles

A total of four G_z acceleration profiles were generated for use in this study. All G_z exposures were started from a baseline acceleration of 1.5 G_z. The first three profiles comprised of a 1 G/sec onset ramp to a 15-sec plateau followed by a G_z offset ramp of 1 G/sec down to the baseline acceleration level. The plateaus were 3, 5, and 7 G_z, respectively. The final acceleration exposure was a simulated aerial combat maneuver (SACM). This profile consisted of two 5-sec G_z peaks to 7 G_z with several intermittent peaks to 3 and 5 G_z. Figure 6 (ref. chap.

2) displays an example of a G_z plateau profile, while Figure 7 (ref. chap. 2) presents the SACM profile.

Stimuli

The peripheral information performance task used for this study consisted of a single white dot. This dot would appear either to the left side or right side of the red "x" at eye level (Figure 31). The starting position of the dot could be as close as six inches from the "x" to as far as six inches from the edges of the shell. The dot would remain stationary for a predetermined amount of time and then began to move either up, down, left or right at a constant speed.

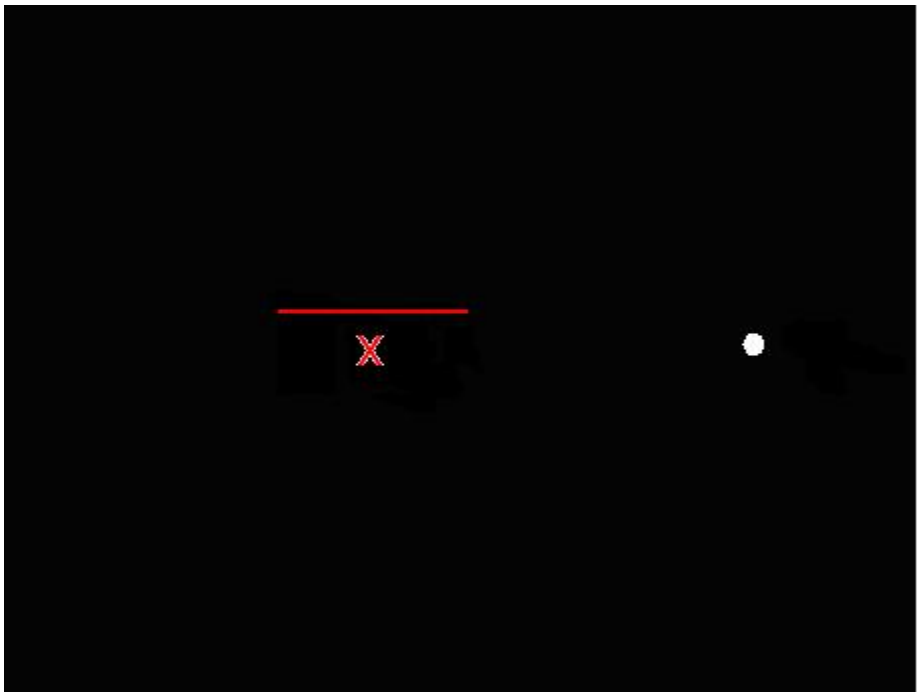

Figure 31: Freeze frame of the white dot before it begins to move.

The time limit for the dot to start moving after it appeared was randomly selected from 0.75-2.25 seconds in 0.25 second intervals. At that time, the subject was to move the top-right hat switch in the direction he/she believed the dot was moving while keeping focus on the red "x." Once

the subject chose a direction, the dot would disappear and another would reappear after an interstimulus period of 0.75- 1.5 seconds, in 0.25 second intervals. If the subject did not push the hat switch in any direction, the dot would continue to move until it was no longer on the projected screen. A new dot would appear after the previous dot was no longer visible.

Static Training

Each subject was trained statically on the Peripheral Information Processing task prior to dynamic training and data collection. Due to the fact this task required the use of the 180^{o}, 6-ft diameter dome projector to stimulate the subjects' peripheral vision, static training was performed in the DES. Subjects were given 30 presentations of the task followed by a one minute rest period. This was repeated three times per static training day. The subjects were considered trained when they had responded correctly to 90% of the presentations and had attained a 100% response rate.

Dynamic Training

After each subject successfully met the requirements for static training, they performed dynamic blend training in the DES prior to data collection. The subjects performed the task in the DES at 1 G_z each day to provide a baseline profile. Baseline metrics were compared to the subject's performance at the same 3, 5, 7, G_z plateau and 7 G_z SACM profiles administered during the experimental test days. Each acceleration profile was followed by a one minute rest period. Subjects were considered trained once their performance on the task deviated less than 10% between training days. Performance was measured by the percentage of correct responses

to the task. This was accomplished to ensure that no training effects were present in the final data that may have resulted from acclimation to performing the task in the high G environment.

Procedures

On a typical experimental test day, participants arrived at the laboratory, donned a flight suit and a standard G-suit, and were instrumented with electrocardiogram leads. The flight surgeon performed a brief medical examination and reviewed the subject's medical history. The participant then proceeded to the centrifuge where he/she donned a parachute harness. After entering the gondola of the centrifuge the participant was secured to the ACES II aircraft seat (with a 15-degree seat back angle) using a three-point aircraft restraint system. The ECG leads were connected and the signals were verified prior to removing the cab support bar from the gondola of the centrifuge. Next, the cerebral oximeter was placed around the subject's head. The investigator started the oximeter data collection computer program to record the subject's oxygen saturation levels during the experiment. Next, the Eye Tracker was placed over the subject's eyes using the supplied frames similar to normal glasses. The camera and infrared light were adjusted for a clear picture of the subject's eye. Again, the investigator ran the eye tracker software, which locked onto the pupil of the eye. At this point, the peripheral information processing task was initiated and baseline performance data was collected over 30 presentations.

Subjects were instructed to maintain focus on the red "x" located in the center of the screen at all times. A white dot would appear between 0.5 and 1.5 seconds following initial execution of the trial. Once present, it would remain stationary for a random length of time ranging from 2.0 to 3.0 sec. Next, the dot would begin to move in one of four directions (up, down, left, or right). At this point, the subject was to indicate the direction of displacement by

pushing the top-right hat switch on the joystick in the corresponding direction (as shown in Figure 32 below). The interstimulus interval was a random duration ranging from 1.0-2.0 seconds.

Figure 32: Joystick Response Switch for Peripheral Information Processing Task

Following the collection of baseline data, the participant experienced his/her first G-exposure. Subjects were instructed to perform an AGSM sufficient to maintain full peripheral vision throughout each G_z profile. Each of the four G_z exposures was administered on three different test days in the following order: 3 G_z 15 sec plateau, 5 G_z 15 sec plateau, 7 G_z 15 sec plateau, and 7 G_z SACM. The subject began the performance task approximately 5 sec prior to each G_z exposure and continued until the acceleration had returned to the baseline level of 1.5 G_z. Between each G_z exposure, a one-minute rest period was administered, during which the task was not performed and the subject was permitted to relax at the baseline G_z level. This rest period allowed the subject's physiology to recover. Following the completion of the four G_z exposures, the participant was removed from the centrifuge and immediately examined by the

flight surgeon. Afterwards, he/she was released to return to his/her normal duties. These procedures were repeated over all three experimental test days.

Data Analysis

Performance on the peripheral information processing task was assessed by comparing the response time percent change from baseline. The first analysis compared response time percent change from baseline during the plateau of the 3 G_z, 5 G_z, and 7 G_z plateau runs, and from the 7 G_z plateau of the SACM run. Only trials ending within 0.5 G_z of the plateau level were included in data analysis. The second analysis compared response time percent change from baseline during the first half of the SACM run vs. the last half of the SACM run. Only trials after the start of the first onset and before the end of the last offset were used.

Results

The mean percent change in response time was calculated for individual subjects during each of the four G_z profiles (see Figure 33). For the SACM profile, only data occurring during the two 7 G_z peaks were used. The geometric mean of baseline response time is shown in the top right corner of each panel in the figure below.

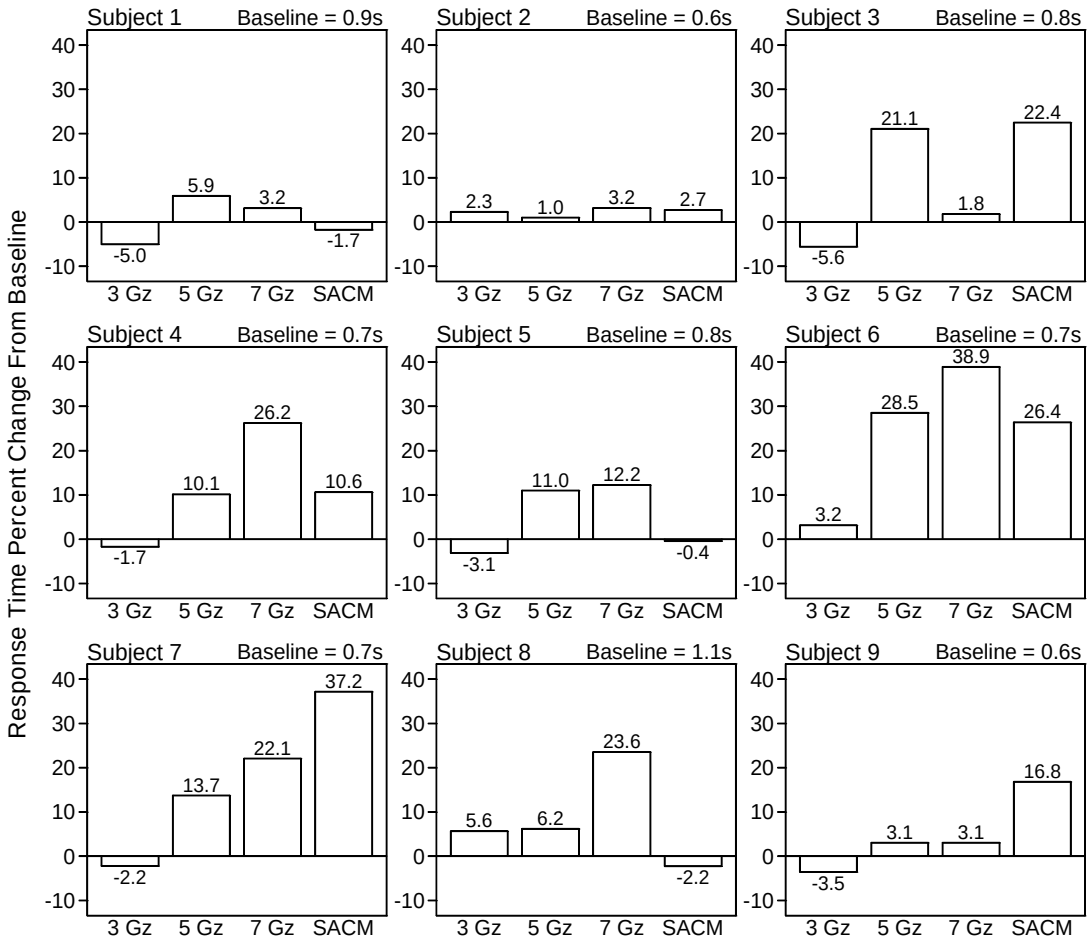

Figure 33: Mean response time percent change from baseline for each subject and G_z profile plateau.

In addition, the mean response time percent change from baseline was calculated across subjects and is presented in figure 34. The bars represent the minimum and maximum value for the G_z profile across all trials and subjects. The overall geometric mean of response time for the baseline data was 0.75 seconds. However, the percent change of from baseline was calculated for each individual subject using their own mean baseline value.

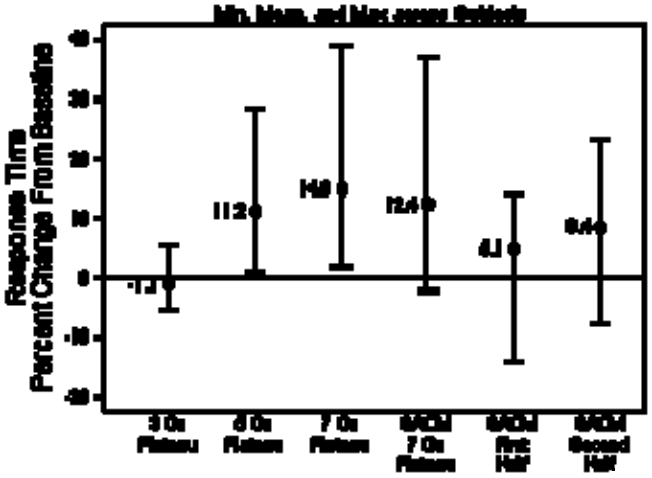

Figure 34: Minimum, mean, and maximum response time percent change from baseline across subjects (N = 9)

Repeated measures analyses of variance (ANOVA) were performed using the response time percent change from baseline for each subject as the dependent variable. The F-test found a significant mean difference among the 3 G_z plateau, 5 G_z plateau, 7 G_z plateau, and SACM 7 G_z plateau ($p = 0.0042$: Greenhouse-Geisser epsilon = 0.75, adjusted $p = 0.0098$). A Bonferroni paired comparison procedure with a 0.05 family wise error level showed the mean at the 3 G_z plateau to be significantly different than the other three plateaus, with the 5 G_z, 7 G_z, and SACM 7 G_z plateau means not significantly different from each other. Two-tailed t-tests using the subject means (no pooling) did not find the 3 G_z plateau mean to be significantly different from 0 ($p = 0.4181$) but did find the 5 G_z ($p = 0.0054$), 7 G_z ($p = 0.0100$), and SACM 7 G_z ($p = 0.0300$) plateau means to be significantly different from 0.

The second analysis compared response time percent change from baseline during the first half of the SACM vs. the last half of the SACM. Only trials after the start of the first G_z acceleration onset ramp and before the end of the last G_z deceleration were used to ensure that

trials beginning or ending outside near the baseline G_z level were excluded from the analysis. This resulting data can be found in figure 35 below.

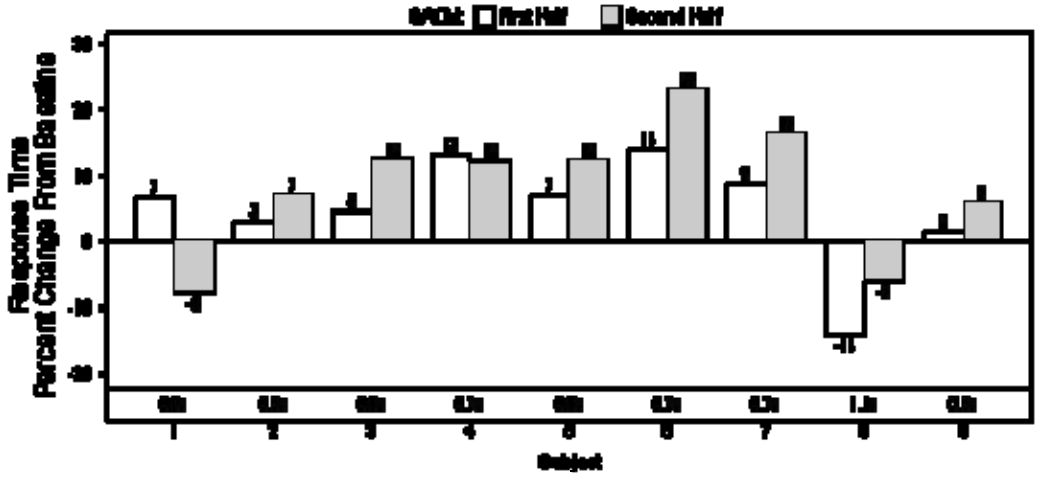

Figure 35: Mean response time percent change from baseline for each subject during each SACM half

A second repeated measures ANOVA was performed to compare performance during each SACM half using data from figure 35. The F-test did not find a significant difference between the first half and second half of the SACM ($p = 0.2070$). However, two-tailed t-tests using the subject means (no pooling) did not find the mean for the first half ($p = 0.1050$) but did find the mean for the second half ($p = 0.0354$) of the SACM to be significantly different from 0.

Prior to experiencing any acceleration profiles, custom software collected 30 seconds of rSO_2 data from the INVOS 4100 cerebral oximeter. The mean of this static data was used as the baseline value for that day. The software then calculated the percent change from this baseline for each data point (sample rate = approximately 0.5 Hz) during the acceleration profiles. These calculated values were then averaged across subjects and days and can be found in Figure 36. The bars indicate the minimum and maximum rSO_2 values for each profile. The overall mean baseline rSO_2 value was 61.6.

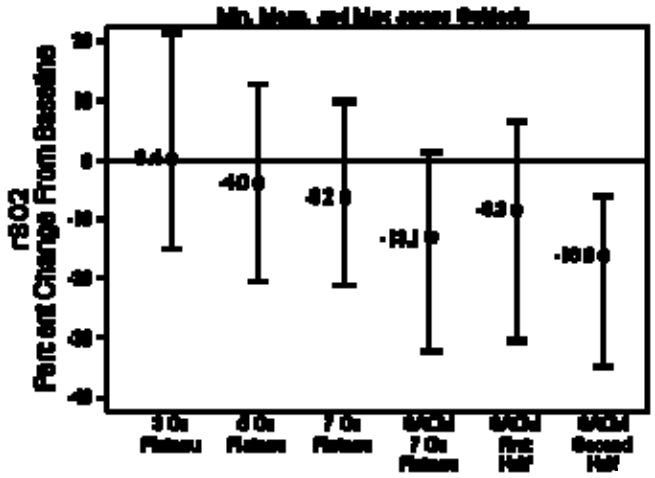

Figure 36: Minimum, mean, and maximum rSO2 percent change from baseline across subjects (N = 9).

Repeated measures analyses of variance were performed using the rSO_2 percent change from baseline for each subject as the dependent variable. The F-test found a significant mean difference among the 3 G_z plateau, 5 G_z plateau, 7 G_z plateau, and SACM 7 G_z plateau (p = 0.0001: Greenhouse-Geisser epsilon = 0.66, adjusted p = 0.0001). The Bonferroni paired comparison procedure with a 0.05 family wise error level showed the means at each plateau to be significantly different from each other with the exception of 5 G_z vs. 7 G_z. Two-tailed t-tests using the subject means (no pooling) did not find the plateau means to be significantly different from 0 at 3 G_z (p = 0.9292), 5 G_z (p = 0.3083), or 7 G_z (p = 0.1318), but did find the mean at the SACM 7 G_z plateau (p = 0.0116) to be significantly different from 0.

The second analysis used means from each SACM half. The F-test found a significant difference between the first half and second half of the SACM (p = 0.0011). Two-tailed t-tests using the subject means (no pooling) did not find the mean for the first half (p = 0.0806) but did find the mean for the second half (p = 0.0035) of the SACM to be significantly different from 0.

Discussion and Conclusions

The results of this study support the hypothesis that the ability to perceive and process information in the peripheral visual field is significantly degraded during G_z acceleration. In particular, the comparison of the response time percent change from baseline during each profile plateau showed the performance at 3 G_z was significantly different than the performance at 5 G_z, 7 G_z. However, the 7 G_z and 7G_z SACM plateaus did not differ significantly from one another. Given that the t-test showed the 3 G_z mean was not significantly different from zero, it can be concluded that performance at 3 G_z was similar to that of performance at 1 G_z. Similarly, t-test showed performance at 5 G_z or higher was significantly different (greater) than zero, indicating that accelerations between 5 and 7 G_z leads to significantly longer response times to moving targets in the periphery. In fact, the overall mean change from baseline was 12.8% or 0.096 sec. during these plateaus. Although significant, it is not clear that such a small difference constitutes degradations that are operationally relevant.

The mechanisms that are responsible for the relatively mild performance changes during high G_z acceleration likely originate from physiological changes. As arterial blood flow to the body's upper extremities begins to deteriorate as a result of the increased apparent weight of the blood, the aerobic metabolic processes used by neurons begin to subside due to the lack of fresh oxygen resources. As the neurons quickly run out of available adenosine tri-phosphate (ATP), neural communication and action potential propagation arrest and the cortical tissue is not capable of properly processing and interpreting sensory information. This hypothesis is substantiated with the relative cerebral oxygen saturation measures obtained from the cerebral oximeter in this experiment. As expected, the results show that the mean %rSO_2 value decreases as the G_z magnitude increases. In addition, a decrease in %rSO_2 was noted between the first and

second half of the SACM, which is similar to findings by Tripp, Chelette, Savul, and Widman (1998). This indicates that oxygen saturation to cortical tissue does not recover instantaneously at lower G_z levels (e.g. 3 G_z) and continues to deteriorate during multiple-peak acceleration profiles.

The dorsal stream of the visual association cortex is primarily responsible for processing high contrast objects and stimuli that are moving. As a result, much of the information detected by the photoreceptors on the peripheral regions of the retina is sent to the dorsal stream for processing. The cerebral oximeter sensors were not placed directly over these areas due to the fact that accurate readings cannot be obtained through the hair. As a result both sensors were placed on the subject's forehead and recorded data from the frontal lobe. However, much of the dorsal stream lies approximately on the same horizontal plane as the measures sites on the frontal lobe. It can therefore be reasoned that arterial perfusion to the dorsal stream would mimic that of the frontal lobe. This phenomenon can be explained using Pascal's Law (Eqn. 7 – see chapter 3), which stipulates that the pressure distribution of a hydrostatic column is influenced by the height. Hence, the brain areas closer to the top of the arterial tree (hydrostatic column of blood) will have contain less pressure than those areas that reside at lower heights. Those at the same height should theoretically have the same pressure. Given that the frontal lobe experienced significant changes in oxygen saturation, it is likely that the dorsal stream of the visual association cortex suffered similar oxygen shifts. Therefore, it can be concluded that declines in cerebral oxygen saturation in the dorsal stream contributed to reduced cortical function resulting in the significant performance degradations during the high acceleration profiles.

Visual symptoms including visual loss, visual tunneling, and loss of color perception are all common to high acceleration exposure. These signals are a direct result of decreased blood

flow to the retina and photoreceptor cells. Typically, the blood flow to the eyes is even lower than that of surrounding cortical tissue due to the fact that intraocular fluid exerts additional pressure that opposes incoming arterial blood. To prevent such symptoms from influencing the performance on the cognitive task, subjects in this experiment were instructed to perform an AGSM sufficient to maintain peripheral vision throughout each of the profiles. However, the duration of each plateau was 15 seconds, making it difficult to maintain an adequate strain during the entire profile, especially at 7 G_z. Furthermore, the duration of the SACM profile was 180 sec, which is certainly longer than the average human can sustain a full AGSM. As stated in the previous chapter, "…performance of the AGSM is very fatiguing and cannot be maintained for very long," (Burns and Balldin, 1988). Consequently, it is possible that degradations in peripheral vision contributed to the decreased performance on the task at high G. Regardless of this potential confound, the goal of this experiment was to quantify the performance changes resulting from acceleration stress. The alterations observed, whether influenced by visual symptoms or not constitute a statistically significant change from baseline performance and should be noted. The operational significance is still debatable and highly depends on the specific task in question.

It is theorized that oxygen saturation in the dorsal stream of the visual association cortex was not adequate at G_z levels greater than or equal to 5 G_z to support the processing of peripheral information. Particularly during the7 G peaks of the SACM profile, it is possible that muscle fatigue prevented subjects from exerting a full AGSM to maintain their peripheral vision. As such, performance may have been also influenced by temporary vision tunneling. In addition, vision tracking confirmed that the subjects did not "cheat" by moving their point of gaze to the peripheral sections of the dome display.

CHAPTER 7: TASK 6 – PITCH-ROLL CAPTURE

Introduction

Survival in the flight combat environment, heavily hinges on the timely detection of a potential threat coupled with an immediate and deliberate action to counter that threat. Rapid maneuvers at the high speeds characteristic of modern fighter aircraft typically involve significant sustained accelerations that can compromise the body's ability to deliver fresh oxygen to the cortical tissue. As a result, the pilot may respond inappropriately or at a reduced rate to the new perceived threats. Available evidence also suggests that cognitive abilities do not immediately recover following an acceleration-induced ischemic insult (Tripp, et al., 2002). This reveals that recently completed high-G_z maneuvers may greatly reduce the reaction time of the pilot when confronted with a new target.

The detection of objects depends on the ability of the visual cortex to correctly perceive and interpret information originating from the photoreceptive cells housed in the retina of the eye. The pilot's field of view (FOV) is traditionally decomposed into the foveal and peripheral visual regions. A discussion of the effects of acceleration on the ability to process visual information in the peripheral field was provided in the previous chapter. Therefore, this chapter will only refer to information in the foveal vision.

The processing of foveal imagery and object detection is largely processed in the ventral stream of the visual association cortex. The pathway feeds information from the primary visual cortex areas (V1 and V2) to the ventral stream areas including V3, V4, V8, the lateral occipital complex, fusiform face area, etc. (Wang, et al, 1999; Carlson, 2007). The ventral stream terminates in the ventral section of the temporal lobe, which is further segmented into the posterior area (TE and the anterior area (TEO) (Carlson, 2007). This vital section is responsible

for interpreting and merging important information concerning objects and their identity, such as color, form, shape, location recognition, and face recognition (Wang, et al., 1999). These neurons are well acquainted with processing complex, colorful, three-dimensional objects, but are not so attuned to simple objects such as lines and dots (Carlson, 2007). As the name implies, the ventral stream largely lies ventral to (closer to the neck) the primary visual cortex. This positioning indicates it may be more "G tolerant" than the dorsal stream due to the fact it is closer to the heart. Maintaining function of this cortical region is crucial to detecting objects and determining whether they pose a significant threat to the pilot.

Once the threat has been established, the pilot must execute the proper maneuver to position his/her aircraft in a firing position or evade an incoming attack. Many maneuvers are constructed with a set list of procedures that must be accomplished in a specific order to be successful. For example, to drastically reduce altitude, the pilots often cannot simply nose-over and descend due to the fact that it generates high negative G_z. Modern aircraft are designed to tolerate up to positive 9 G_z, but cannot structurally handle high negative loading. As a result, the proper maneuver involves inverting the aircraft, pulling up (which now angles the aircraft toward the ground), leveling the aircraft in the pitch axis, and then rolling back to an upright orientation. Therefore, standard maneuvers require a few cognitive processes including procedural memory and perception of orientation.

Available evidence suggests that orientation perception may be disturbed during high-G_z. For example, a study conducted by Nethus et al. (1993) found slight performance decline when performing a visual orientation manipulation task. Subjects were presented with a "manikin" or stick figure representation that would appear in a variety of spatial orientations (forward facing, backward facing, upside down, right-side up, etc). The goal was to indicate if an object was on

his left or right side. Nethus et al. (1993) found that reaction times increased during G_z loading only for trials that were incongruent between the side the object was located and the response button (e.g. right side, left button). However, the declines in performance were mere milliseconds, and may not indicate operational significance.

The purpose of this study was to quantify the effects of acceleration on detecting a target, then executing a procedure to acquire and fire upon the target. The subjects must remain aware of their orientation to properly execute the maneuver. Once the target appeared on the screen, participants were required to first roll the aircraft until the target was in the center of the screen and then pitch until it was centered in the gunsight crosshairs. At this point the subjects fired their weapon.

Methods

Subjects

Ten active duty members (7 male, 3 female) volunteered to participate in this study and ranged in age from 22 to 34 years, with a mean age of 26 years. All participating subjects were members of the sustained acceleration stress panel at Wright-Patterson AFB, OH. Requirements to qualify for participation in this study are identical to those of chapter 2 (ref chapter 2, Methods section).

Facilities

All training and data collection for this study was performed at the Air Force Research Laboratory's Dynamic Environment Simulator (DES) centrifuge facilities at Wright Patterson AFB (ref. Chap. 2, Figure 3). The DES is a human rated centrifuge with an arm radius of approximately 19 feet. It is capable of attaining and sustaining accelerations up to 20 G in either

of three independent axes: x, y and z. The DES has a maximum G onset and offset rate of approximately 1 G/sec. The gondola of the centrifuge was equipped with an F-22-like ACES II ejection seat with a seatback reclined to 15^{o} from vertical. As illustrated in Figure 2 (ref. Chap. 2), the seat had adjustable lap and shoulder restraints.

An aircraft IC-10 communication system was used to provide two-way voice-communication between the research participant and the investigator. The participant's microphone was fixed in the open position to allow the participant "hands-free" communication. Participants were also provided with an emergency abort switch that enabled them to stop the centrifuge at any time during testing. Participants wore a standard Air Force issue Nomex® flight suit and a standard G-suit during all testing runs.

The gondola was outfitted with a simulated fighter cockpit. The cockpit incorporated a Thrustmaster Hotas Cougar flight stick (Guillemot, Montreal, Canada) mounted on the participant's right side that was used to secure responses to the performance task. A six foot hemispherical shell viewing screen, representing a 130^{o} (vertical) x 180^{o} (horizontal) visual field, mounted directly in front of the participant. A separate projector was used to display the performance task in the center of the subjects' field-of-view with a projected image of 22.5" (width) by 18.5" (length). The large dome display was used to present two red dots located at approximately 60^{o} of visual angle to the right and left of the center of the dome and approximately 5^{o} in diameter. In addition, a red circle was displayed just above the HUD that represented 10^{o} of visual angle. The dots served as a reference to the subject of his/her visual loss. Should the smaller dots not be visible in the periphery, the subject was instructed compensate by increasing their AGSM. They were to abort the test should their vision degrade

to the point that only the center red dot was visible. Figure 4 (ref. chapter 2) provides an illustration of the entire visual system.

Continuous surveillance of participants was provided by two closed-circuit infrared television cameras. The cameras offered a close-up view of the participant's head and a wide-angle view of the participant from head-to-foot. Research personnel housed in a control room observed the video images. A video mixer was used to generate a composite picture of the two views of the participant along with the time, date, electrocardiogram (ECG) data, and G_z acceleration in a given run. Video data were stored on ½ inch VHS videotape.

Acceleration Profiles

A total of four G_z acceleration profiles were generated for use in this study. All G_z exposures were started from a baseline acceleration of 1.5 G_z. The first three profiles comprised of a 1 G/sec onset ramp to a 15-sec plateau followed by a G_z offset ramp of 1 G/sec down to the baseline acceleration level. The plateaus were 3, 5, and 7 G_z, respectively. The final acceleration exposure was a simulated aerial combat maneuver (SACM). This profile consisted of two 5-sec G_z peaks to 7 G_z with several intermittent peaks to 3 and 5 G_z. Figure 6 (ref. chap. 2) displays an example of a G_z plateau profile, while Figure 7 (ref. chap. 2) presents the SACM profile.

Stimuli

The performance task in this experiment was a two-dimensional flight task with medium-fidelity flight characteristics. The subject was provided with a generic out-the-window scene inclusive of the interior instrument panel. Atmospheric conditions were clear with no clouds or

other visual obstructions. A static target aircraft would appear somewhere in the subject's field of view following a random interval of 1.5-3.0 seconds (random times were chosen in half-second intervals). Targets could appear in a total of eight different positions that were randomly assigned each presentation. Figure 37 provides a screenshot of the out-the-window view with the target aircraft visible.

Figure 37: Pitch-Roll Capture out-the-window view with target visible

The task provided subjects with aileron and elevator control only and with simplified flight equations. Subjects first had to roll the aircraft until the target was located in the center of the two vertical white lines. A visual representation of this can be found in the figure 38. Next he/she would pitch the aircraft until the aircraft was centered in gunsight reticule. At that point, the subject would depress the "trigger" button on the flight stick, which would indicate the target was "captured" and conclude the trial.

Figure 38: Pitch-Roll Capture: target centered between white vertical lines

Static Training

To ensure training effects did not influence experimental results, all subjects were trained statically on the pitch-roll capture performance task prior to dynamic training and experimental data collection. Static training was performed in an F-16 mock-up fuselage equipped with an ACES II aircraft seat with a 15 degree seat-back angle. The task was projected onto a 48-in (vertical) x 64-in (horizontal) screen. Subjects were given 30 presentations of the task followed by a one minute rest period. This was repeated three times per static training day. Vector error magnitude measured from the final target position to the center of the crosshairs was calculated for each trial. Those resulting in a distance of more than 41.5 pixels were determined to be outside the crosshairs and termed “unsuccessful.” An average target capture time and capture success rate were tabulated for each session. The subjects were considered trained once their performance deviated less than 10% between training days.

Dynamic Training

As in the previous experiments for this program, dynamic blend training was completed in the centrifuge where subjects were required to perform the pitch-roll capture task during the 3, 5, 7, G_z plateau and 7 G_z SACM acceleration profiles. A one-minute rest period was given after each G_z profile. Prior to the centrifuge runs, subjects performed the task at 1 G_z (30 presentations) each training day to provide a baseline for comparison. Subjects were considered trained once their performance on the task deviated less than 10% between training days. Again, performance was measured in capture time and capture success rate. Dynamic blend training was designed to eliminate training effects resulting from acclimation to performing the task with the presence of motion and acceleration.

Procedures

On a typical experimental test day, participants arrived at the laboratory, donned a flight suit and a standard G-suit, and were instrumented with electrocardiogram leads. The flight surgeon performed a brief medical examination and reviewed the subject's medical history. The participant then proceeded to the centrifuge where he/she donned a parachute harness. After entering the gondola of the centrifuge, the participant was secured to the ACES II aircraft seat (with a 15-degreee seat back angle) using a three-point aircraft restraint system. The ECG leads were connected and the signals were verified prior to securing the gondola of the centrifuge. At this point, the pitch-roll capture performance task was initiated and baseline performance data were collected over 30 presentations.

Each participant was instructed to continuously scan the visual environment for target aircraft. Once spotted, participants performed a series of maneuvers in a specific order. First, they rapidly rolled the aircraft to the left or right until the target was between the two vertical, white lines (see figure 38). Subjects were instructed to then pitch the aircraft to bring the enemy aircraft within the gunsight crosshairs. They were told that the ideal placement was for the center of the aircraft to be aligned with the center of the gunsight. Control of their simulated aircraft was secured with the HOTAS Cougar flight stick (see figure 12). The throttle was not needed due to the fact that the aircraft were static in regards to airspeed. Subjects were to complete the task as quickly and accurately as possible. Recorded performance data included the capture time and the number of successful captures.

Following the collection of baseline data, each of the four G_z exposures was administered on three different test days in the following order: 3 G_z 15sec plateau, 5 G_z 15sec plateau, 7 G_z 15sec plateau, and 7 G_z SACM. The performance task was initiated approximately 5 sec prior to the onset of each G_z exposure and continued until the acceleration had returned to the baseline G_z level of 1.5 G_z. A 1-minute rest period was provided between each G_z exposure during which the task was not performed and the subject was permitted to relax at the baseline G_z level. Following the completion of the four G_z exposures, the participant was removed from the centrifuge and immediately examined by the flight surgeon. Afterwards, they were released to return to their normal duties. These procedures were repeated over all three experimental test days.

Results

All distances for the pitch-roll capture task were measured in pixels. In this experiment, the size of the gunsight crosshair was determined to have a radius of 41.5 pixels. Therefore, trials concluding with center of the target aircraft lying more than 41.5 pixels from the center crosshair were determined to be "unsuccessful." Analyses of capture time (distance of target from center crosshair at the end of each trial) only used trials with successful "captures." In addition, only trials after the start of the first acceleration onset and before the end of the final deceleration back to baseline were used in the analyses.

The first comparison evaluated the number of unsuccessful captures (error rate) during each of the acceleration profiles. Table 5 contains the percent of unsuccessful trials (i.e., vector error > 41.5 pixels) for each subject and Gz profile. Three subjects (2, 5, and 8) had no unsuccessful trials and one subject (9) had only one unsuccessful trial. Due to these four subjects, testing for significance among the conditions for the percent of unsuccessful trials would have little meaning.

Capture times from each profile were compared to the mean baseline performance within each subject. The data were normalized by calculating the percent change in capture time from the baseline and then collapsed across data days. For the SACM, only trials during the 7 G_z plateaus were used. Figure 39 summarizes the results mean capture time percent change in baseline for each of the subjects during each profile. The geometric mean of baseline capture time is shown above each panel.

As in the other experiments discussed in previous chapters, performance during the first half of the SACM was compared to performance in the second half. The mean capture time

percent change from baseline is shown for each subject and SACM half in figure 40. Here, the geometric mean of baseline capture time is shown above the subject X-axis labels.

Table 5: Percent of unsuccessful trials for each subject and Gz profile.

	Percent of Unsuccessful Trials				
Subject	**Baseline**	**3 Gz**	**5 Gz**	**7 Gz**	**SACM**
1	27.8	22.2	33.3	47.1	36.8
2	0.0	0.0	0.0	0.0	0.0
3	3.3	0.0	16.7	27.8	6.1
4	0.0	0.0	0.0	16.7	6.5
5	0.0	0.0	0.0	0.0	0.0
6	1.4	11.1	7.7	27.8	13.8
7	0.0	0.0	0.0	29.4	12.3
8	0.0	0.0	0.0	0.0	0.0
9	0.0	0.0	0.0	0.0	1.5
10	2.2	0.0	9.1	7.1	3.7

Data were then collapsed across subjects and data days. Figure 41 provides a graph of the minimum, maximum, and means for each profile and SACM half. The overall baseline geometric mean of capture time was 3.04 sec.

Repeated measures analyses of variance were performed with the capture time percent change from baseline for each subject as the dependent variable. The F-test did not find a significant difference among the 3 Gz plateau, 5 Gz plateau, 7 Gz plateau, and SACM 7 Gz plateau ($p = 0.2518$: Greenhouse-Geisser epsilon = 0.90, adjusted $p = 0.2551$). Two-tailed t-tests using the subject means (no pooling) did not find any of the plateau means to be significantly different from 0 ($p > 0.2966$).

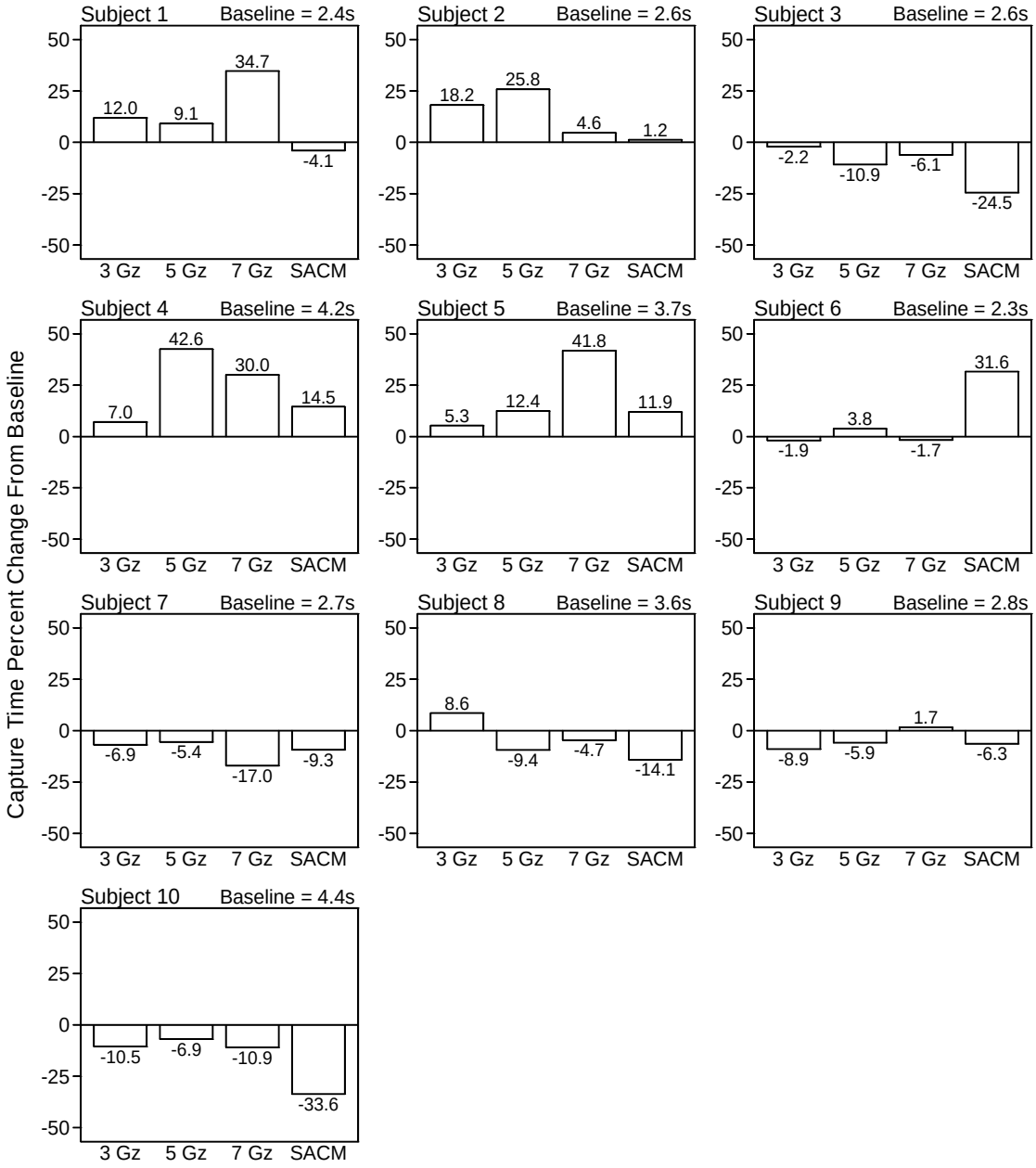

Figure 39: Mean capture time percent change from baseline for each subject and

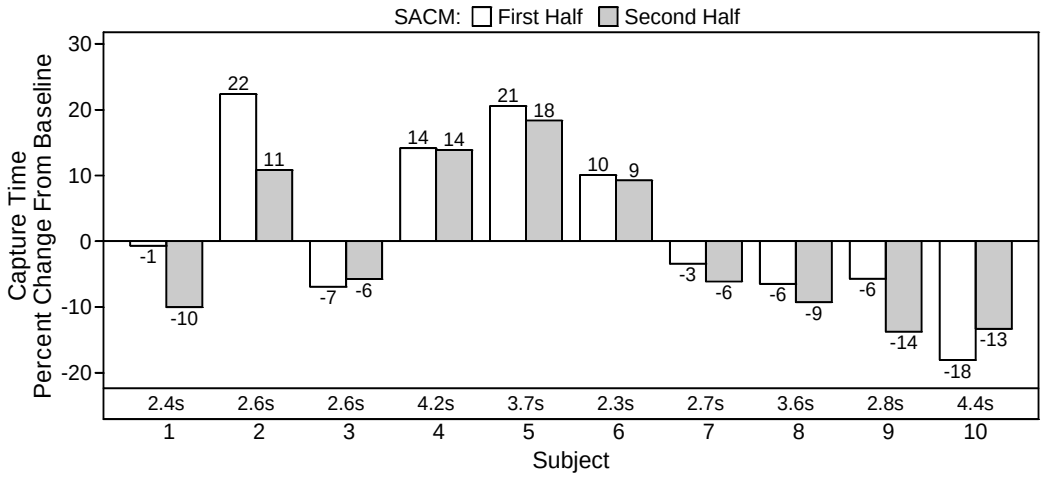

Figure 40: Mean capture time percent change from baseline for each subject and SACM half.

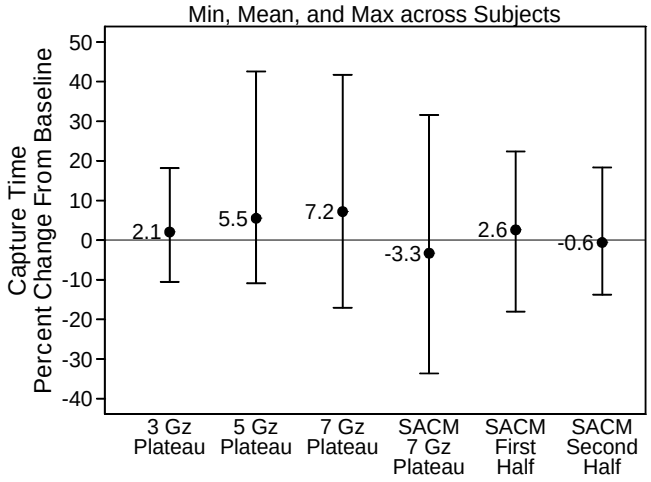

Figure 41: Minimum, mean, and maximum capture time percent change

A second analysis utilized a repeated measures ANOVA to compare means between the first and second half of the SACM. The F-test did not show a significant difference between the two halves ($p = 0.0770$). Two-tailed t-tests using the subject means (no pooling) did not find the mean for either half of the SACM to be significantly different from 0 ($p > 0.5552$).

Discussion and Conclusions

The data analyses indicate that performance on the pitch-roll capture task is not significantly affected by positive G_z acceleration stress. Target capture success rates may have been affected by a few of the subjects, but at least half showed almost no errors for any of the G_z profiles. Hence a test of the significance was not meaningful due to the fact the findings may not apply to the overall population. In addition, the capture time data did not show any differences from the mean baseline indicating that subjects had no difficulty in maneuvering in the prescribed manner to acquire the target in the gunsight reticule. A review of the video tape surveillance confirmed the proper procedures (roll first, then pitch toward target) were executed during data collection by each of the subjects.

Given the lack of significant alterations in performance, it is important to decompose the pitch-roll capture task to discover the mental processes utilized. In this way, it is possible to discover the principle areas of the brain required to execute said tasks and evaluate the effects of G_z on their metabolic rates based on anatomic position. The procedures of the pitch-roll capture task were presented over the course of approximately 6 different training days (combining static and dynamic training). Such extensive training on this task indicates that the act of maneuvering the aircraft was stored in implicit or episodic memory. Traditionally, episodic memory relates to memorizing a series of events that are perceived or described verbally. This type of memory requires the subject to recall the individual stimuli *and* the order of occurrence (Carlson, 2007). Carlson (2007) also points out that at first, the procedures must be attended to vigorously with little distractions. As the movements or process becomes automatic, the memories shift to the basil ganglia (Carlson, 2007). Hence, the neural circuits of the basil ganglia progressively

control more and more of the necessary processes until the subjects are no longer required actively engage high-level, trans-cortical circuits to complete the task (Carlson, 2007).

The basal ganglia traditionally include a variety of nuclei including the caudate, putamen, nucleus accumbens, globus pallidus, substantia nigra, and subthalamic nucleus. The caudate lies caudal to the frontal lobe and ventral to the corpus callosum. The stained section of the image in figure 42 depicts the caudate structure. Next, the putamen lies just caudal to the rostral end of the caudate and is largely involved in coordinating motor responses and behaviors that are automatic (e.g. driving, swinging a golf club, etc,). The globus pallidus positioned just inside (medial) to this structure and the nucleus accumbens resides slightly ventral to the globus pallidus. Lastly, the substantia nigra is the most ventral (lowest) of the basal ganglia nuclei and is located just below (ventral to) the thalamus.

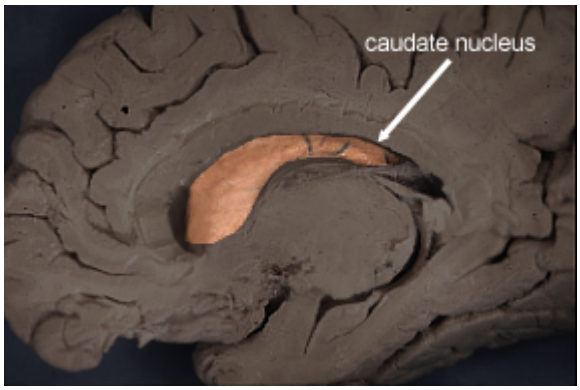

Figure 42: Caudate nucleus as seen along the sagittal plane (White, et al., 2007).

Given that the basal ganglia structures are located within the midbrain and are generally associated with low-level functions (e.g. primitive brain operations), they are generally more resistant to shutting down due to lack of adequate oxygenated blood, theoretically due to lower metabolic needs. It is traditionally the higher-order cognitive functions housed in the cerebral cortex that are sacrificed to allow autonomic and automatic functions to remain operational as

long as possible. Additionally, the anatomic position of these structures is largely ventral to many of the high-order cortical tissues. Given that the activity generally decreases from the superior areas of the cortex to the inferior or internal areas of the brain, it follows that the basal ganglia areas will remain highly G tolerant.

The fact that sequential procedures vital to the task were stored in episodic memory indicates the processing for the task was achieved solely in the basal ganglia. This implies the subjects did not have to actively think about what they were doing (Carlson, 2007). The performance changes observed in previous chapters was largely due to a lack of oxygen to the dorsal regions of the cerebral cortex. Because the higher cortical functions were theoretically not engaged in this task, a lack of oxygen supply to those sites would not be expected to negatively impact performance on the task.

Another aspect to consider is the possibility that the task was overtly simple. This coupled with extensive training could have lead to a ceiling effect. The hypothesis that the task became automatic for the subjects prior to data collection lends itself to the conclusion that the task was not sufficiently sensitive to elicit changes during the positive accelerations provided in this experiment. Anecdotal comments from the subjects seem to confirm this line of reasoning, although subjective measures and comments were not formally recorded. It is the opinion of the authors that the task must include additional variables to increase the difficulty including a greater number of procedures, moving targets, and a smaller gunsight reticule in order to make the task viable for human performance research under various stressors.

Operationally, the results of this experiment indicate procedures that are repeated to the extent that they become “automatic” (that is, housed in episodic memory) will not suffer performance degradations during positive G_z acceleration profiles up to and including 7 G_z.

Such tasks may include emergency procedures, flight maneuvers, communication protocols, etc. This seems to support the assertions of many pilots that numerous functions in the cockpit become so automatic, acceleration or other stressors should not affect their performance. As a result, this element is is eliminated from the suite of cognitive tasks identified as potentially affected by G_z acceleration (up to +7 G_z). However, it is important to note that it is unknown whether higher +G_z (e.g. 8 or 9 G_z) levels induce significant changes in performance. These levels were not included into this study as they were deemed not operationally relevant. Data obtained from Operation Red Flag showed the peak G_z levels rarely if ever exceed +7 G_z. Given that the Red Flag exercise is an extremely realistic air combat environment, it can be concluded that its G_z levels would be indicative of those experienced in theatre.

CHAPTER 8: TASK 7 & 8 – UNUSUAL ATTITUDE RECOVERY AND SITUATIONAL AWARENESS

Introduction

The dynamic nature of the flight environment creates forces and motion that can distort perceptions of orientation in the absence of visual cues. High mental workload coupled with a plethora of disparate tasks such radio calls, target searches, visual/audio warnings, instrument crosschecks can lead to attention tunneling or loss of situational awareness. As a result, the aircraft can enter into what is known as an "unusual attitude," and is typically associated with spatial disorientation (SD). The accepted department of defense (DoD) definition of SD is "the failure to correctly sense the position, motion, or attitude of one's aircraft with respect to the earth or other object." SD is typically caused by either visual illusions or vestibular illusions. The human vestibular system is not inherently well-suited for the flight environment, and can therefore provide the brain with inconsistent or incorrect cues in the presence of the unique dynamics of flight.

One such example has been termed the "pitch-up" illusion. It is typified by significant linear acceleration (e.g. during take-off) followed by an increase in pitch angle and will generally occur in low visibility conditions. Because the linear acceleration causes the otoconia within the otoliths to shift dorsally, the pilot's brain perceives this as a pitch up. When the pilot lifts off, this real increase in pitch angle is added to the false pitch perceived during the acceleration down the runway. As a result, the pilot may attempt to correct the false "over pitch" by nosing over and pitching down. At this point, the pilot has entered an unusual attitude and will need to both perceive the error and correct it as quickly as possible if he/she hopes to survive.

The prevalence of SD in the DoD merits special attention. In fact, SD related incidents cost the DoD an average of over $300 million per year in accident investigations alone (Wickens, et al., 2007). Given that many SD illusions are elicited by accelerations, it is important to quantify cognitive deficits caused by the resulting inertial forces that may negatively affect the pilots' ability to recognize an unusual attitude and then appropriately maneuver back to straight and level flight. In addition, the ability of the pilot to maintain situational awareness is imperative to preventing the unusual attitude event from occurring. The purpose of this experiment was to measure cognitive performance in both of these abilities to determine if G_z acceleration compounds the negative effects of SD illusions on flight performance.

The perception of spatial locations is largely handled in the parietal lobe and receives input from the vestibular, somatosensory, and visual systems (among others). One of its primary jobs is to integrate these sensory inputs and coordinate the perception of spatial location, orientation, and distances to objects in the immediate vicinity. Within the dorsal stream, the medial temporal/medial superior temporal sections appear to be responsible for the perception of motion and optic flow (Carlson, 2007). Additionally, subjects with Turner syndrome (TS) exhibited reduced performance on a spatial cognition task (Kessler, et al., 2004). Functional magnetic resonance imaging (fMRI) results indicated decreased activation in the inferior parietal lobe, which is important for spatial encoding and memory (Kessler, et al., 2004). Kessler et al. (2004) also discovered that the perception of spatial orientation is a complex interchange between the parietal lobe, frontal lobe and occipital lobe. However, major structures noted indicate the inferior parietal lobules, the middle occipital gyri, and the superior parietal lobules.

Reduced oxygen supply to these functional areas of the brain could render them inoperable making recovery from SD event very difficult for the pilot. As stated in the previous

chapters, neurons cannot metabolize fats or carbohydrates for energy making energy storage difficult. Without oxygen, these cells are forced to resort to anaerobic metabolism, which is unable to sustain the mental demands of flight. As a result, it is important to investigate which cognitive processes are compromised and quantify the extent of the effects. With respect to the basic cognitive skills identified as crucial to the flight environment, the situational awareness task probes *monitoring under high workload*. As the name stipulates, the unusual attitude recovery task primary corresponds to *unusual attitude recovery* but also explores *monitoring under high workload*.

Methods

Subjects

Ten active duty members (8 male, 2 female) volunteered to participate in this study and ranged in age from 24 to 35 years, with a mean age of 27 years. All participating subjects were members of the sustained acceleration stress panel at Wright-Patterson AFB, OH. Requirements to qualify for participation in this study are identical to those of chapter 2 (ref chapter 2, Methods section).

Facilities

All training and data collection for this study was performed at the Air Force Research Laboratory's Dynamic Environment Simulator (DES) centrifuge facilities at Wright Patterson AFB (ref. Chap. 2, Figure 3). The DES is a human rated centrifuge with an arm radius of approximately 19 feet. It is capable of attaining and sustaining accelerations up to 20 G in either of three independent axes: x, y and z. The DES has a maximum G onset and offset rate of approximately 1 G/sec. The gondola of the centrifuge was equipped with an F-22-like ACES II

ejection seat with a seatback reclined to 15^{o} from vertical. As illustrated in Figure 2 (ref. Chap. 2), the seat had adjustable lap and shoulder restraints.

An aircraft IC-10 communication system was used to provide two-way voice-communication between the research participant and the investigator. The participant's microphone was fixed in the open position to allow the participant "hands-free" communication. Participants were also provided with an emergency abort switch that enabled them to stop the centrifuge at any time during testing. Participants wore a standard Air Force issue Nomex® flight suit and a standard G-suit during all testing runs.

The gondola was outfitted with a simulated fighter cockpit. The cockpit incorporated a Thrustmaster Hotas Cougar flight stick (Guillemot, Montreal, Canada) mounted on the participant's right side that was used to secure responses to the performance task. A six foot hemispherical shell viewing screen, representing a 130^{o} (vertical) x 180^{o} (horizontal) visual field, mounted directly in front of the participant. A separate projector was used to display the performance task in the center of the subjects' field-of-view with a projected image of 22.5" (width) by 18.5" (length). The large dome display was used to present two red dots located at approximately 60^{o} of visual angle to the right and left of the center of the dome and approximately 5^{o} in diameter. In addition, a red circle was displayed just above the HUD that represented 10^{o} of visual angle. The dots served as a reference to the subject of his/her visual loss. Should the smaller dots not be visible in the periphery, the subject was instructed compensate by increasing their AGSM. They were to abort the test should their vision degrade to the point that only the center red dot was visible. Figure 4 (ref. chapter 2) provides an illustration of the entire visual system.

Continuous surveillance of participants was provided by two closed-circuit infrared television cameras. The cameras offered a close-up view of the participant's head and a wide-angle view of the participant from head-to-foot. Research personnel housed in a control room observed the video images. A video mixer was used to generate a composite picture of the two views of the participant along with the time, date, electrocardiogram (ECG) data, and G_z acceleration in a given run. Video data were stored on ½ inch VHS videotape.

Acceleration Profiles

A total of four G_z acceleration profiles were generated for use in this study. All G_z exposures were started from a baseline acceleration of 1.5 G_z. The first three profiles comprised of a 1 G/sec onset ramp to a 15-sec plateau followed by a G_z offset ramp of 1 G/sec down to the baseline acceleration level. The plateaus were 3, 5, and 7 G_z, respectively. The final acceleration exposure was a simulated aerial combat maneuver (SACM). This profile consisted of two 5-sec G_z peaks to 7 G_z with several intermittent peaks to 3 and 5 G_z. Figure 6 (ref. chap. 2) displays an example of a G_z plateau profile, while Figure 7 (ref. chap. 2) presents the SACM profile.

Stimuli

The subjects completed two performance tasks during each G_z profile on each experimental test day. The "unusual attitude recovery" task utilized both a simulated view of out-of-window terrain and a heads-up-display (HUD). The HUD incorporated standard F-16 symbology and can be found in Figure 43. Only airspeed, pitch, heading, and altitude displays for were relevant for the unusual attitude recovery task.

The subject was instructed to remain aware of their aircraft's airspeed, heading, and altitude at all times. He/she was also instructed to maintain level flight without changing the plane's pitch, heading, or air speed. After a predetermined time of straight and level flight, the secondary task ("situational awareness task") would be presented. This task replaced the out-of-window view and HUD with a black screen. Next, a written statement commenting on the subject's altitude, heading, or air speed, appeared. The statement claimed that an individual reading was above or below a specific number. As a result, the subject had to determine if the statement was true or false and indicate their decision by pushing the top right hat switch forward or backward, respectively (Figure 44).

After the subject responded true or false, the situational awareness task was complete for that trial and the unusual attitude task began. First, the out-of-window view and HUD instrumentation reappeared but with the aircraft positioned in an unusual attitude. The unusual attitude of the aircraft varied, with roll angles between -71 and 70 degrees and pitch between -74 and 70 degrees. The pitch and roll settings were predetermined by the operator, but the subject assumed random generation. Upon placement in an unusual attitude, the subject's first task was to recover the plane so that its pitch and roll were each within 5 degrees of zero in either direction.

Each subject was assigned three combinations of pitch and roll for the unusual attitude. This was done so that percent changes from baseline involved recovery from the same unusual attitude. The four possibilities of directional change for a pitch-roll combination are positive pitch-positive roll, positive pitch-negative roll, negative pitch-positive roll, and negative pitch-negative roll. Each subject was assigned three of the four possibilities. Training runs eliminated pitch-roll combinations that were too difficult or too easy, relative to all combinations used,

based on time to recovery. The pitch and roll combinations assigned to each subject are listed in Table 6.

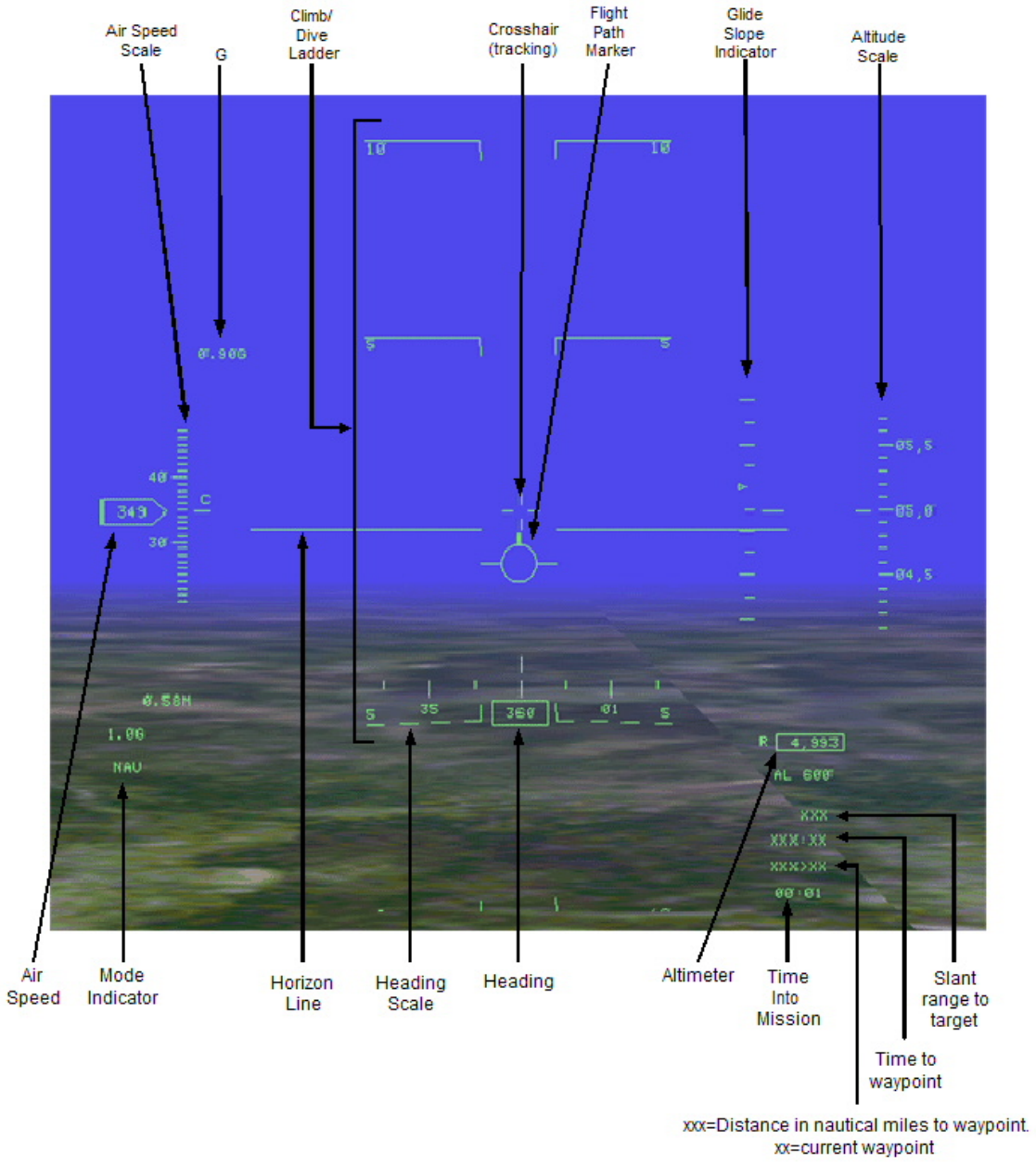

Figure 43: Unusual Attitude Recovery Task Heads Up Display.

Figure 44: Joystick Response Switch for Situational Awareness Task

Table 6: Combinations of pitch and roll assigned to each subject ordered from left to right based on positive pitch. The legend for subject 1, most positive pitch is 23P,-53R = 23° pitch and -53° roll.

Subject	Most Positive Pitch	Middle Pitch	Most Negative Pitch
1	23P,-53R	-39P,-49R	-74P,60R
2	39P,-26R	33P,21R	-69P,-13R
3	51P,31R	-16P,49R	-38P,-65R
4	30P,-54R	-21P,-71R	-49P,41R
5	40P,25R	16P,-53R	-66P,26R
6	29P,-50R	-32P,-66R	-38P,23R
7	43P,51R	30P,-24R	-61P,70R
8	46P,50R	23P,-53R	-43P,-22R
9	35P,-70R	-64P,-67R	-69P,53R
10	64P,-29R	-42P,-44R	-70P,51R

Depending on the position of the aircraft's pitch, the subject had certain rules to follow. The first step was to roll the aircraft to "wings-level" as quickly as possible. This required the subject to identify the direction of roll that would result in the shortest rotational distance. Hence, if the roll angle was +30 degrees, the subject would need to roll left. Should they roll

right, it would require a rotation of 330 degrees rather than 30, which was incorrect. Next the subjects were to correct their pitch angle by returning to 0 degrees. Again, there were specific rules to follow. If the pitch of the aircraft was + 15 degrees or less, the subject could simply level the aircraft. If the pitch was above 15 degrees, the subject had additional maneuvers to complete. The first was to roll to a fully inverted attitude. Again, subjects were to roll in the direction that resulted in the shortest rotational distance. Once the aircraft was inverted, the subject then pulled back on the stick to bring the plane to 0 ± 5 degrees of pitch. Next, the subject could roll the aircraft either direction to bring it to an upright attitude determined by achieving a roll angle of 0 ± 5 degrees. Recoveries taking more than 20 seconds were recorded as a "timed out" trial.

Static Training

Each subject was trained statically on the Unusual Attitude and Situational Awareness task prior to dynamic training and data collection. Static training was performed in an F-16 mock-up fuselage equipped with an ACES II aircraft seat with a 15-degree seatback angle. The task was projected onto a 48-in. (vertical) x 64-in. (horizontal) screen. Subjects were given 9 unusual attitudes and situational awareness questions followed by a one minute rest period. This was repeated nine times per static training day. A subject was considered trained when they responded correctly to 90% of the situational awareness questions, attained a 100% response rate, and when their ability to recover the plane from an unusual attitude deviated less than 10 percent between training days.

Dynamic Training

After each subject passed the requirements for static training, dynamic blend training was completed. The subjects performed the both the situational awareness and unusual attitude tasks in the DES at 1 G_z each day to provide a baseline performance metric. They then performed the tasks during the same 3 G_z, 5 G_z, and 7 G_z plateaus and 7 G_z SACM profiles that were administered during the experimental test days. A one-minute rest period was given after each G_z profile. Subjects were considered trained once their performance on the task deviated less than 10% between training days. Performance was measured by the percentage of correct responses to the situational awareness questions and ability to recover the plane quickly and correctly. Dynamic training was conducted in order to ensure that no training effects were present in the final data that may have resulted from acclimation to performing the task in the high G environment.

Procedures

On a typical experimental test day, participants arrived at the laboratory, donned a flight suit and a standard G-suit, and were instrumented with electrocardiogram leads. The flight surgeon performed a brief medical examination and reviewed the subject's medical history. The participant then proceeded to the centrifuge where he/she donned a parachute harness. After entering the gondola of the centrifuge the participant was secured to the ACES II aircraft seat (with a 15-degree seat back angle) using a three-point aircraft restraint system. The ECG leads were connected and the signals were verified prior to securing the gondola of the centrifuge. Following this, the cerebral oximeter was secured around the subject's forehead. The operator started the computer program to keep track of changes in the subject's oxygen saturation levels.

At this point, the Unusual Attitude task was started and baseline performance data was collected over 9 presentations. After the baseline data was collected, the subject was then ready for the four G_z exposures.

The subject experienced each of the four G_z exposures on three different test days in the following order: 3 G_z 15-sec plateau, 5 G_z 15-sec plateau, 7 G_z 15-sec plateau, and 7 G_z SACM. The subject began the task approximately 8 sec prior to each G_z exposure and continued for approximately 8 sec after the acceleration had returned to the baseline G_z level of 1.5 G_z. A 1-minute rest period was provided between each G_z exposure, during which the task was not performed and the subject was permitted to relax at the baseline G_z level. This was accomplished to allow the physiology to return to the pre-acceleration exposure levels. During the SACM profile, performance data was collected for 6 presentations to measure the first half of the SACM against the second half. Following the completion of the four G_z exposures, the participant exited the centrifuge and was immediately examined by the flight surgeon and then released to return to his/her normal duties. These procedures were repeated over three experimental test days.

Results

Situational Awareness

The dependent variables used for the analyses were the response time percent change from baseline. Repeated measures analysis of variance (ANOVA) were used with factor condition and levels (3 G_z plateau, 5 G_z plateau, 7 G_z plateau, first half of SACM, second half of SACM). The plateaus and SACM halves were used in separate analyses.

Across all trials (n = 540), the response times ranged from 1.07 to 6.12 sec with median = 2.01 sec. There were three trials from subject 3 that were too fast to be considered legitimate (< 100 msec) and were therefore deemed to be computer errors. These data were not included in the analysis. Across all trials there were 53 errors (9.8%) with the distribution of errors for each condition shown in Table 7.

Table 7: Situational awareness response percent error for each treatment condition

Condition	# Errors	Total Trials	Percent Error
Baseline	13	270	4.8
3 Gz Plateau	1	30	3.3
5 Gz Plateau	8	30	26.7
7 Gz Plateau	2	30	6.7
SACM first half	9	90	10.0
SACM second half	20	90	22.2
Total	53	540	9.8

The results for the situational awareness question response time percent change from baseline are contained in figure 45. Data are separated by subject and treatment condition. The mean baseline value is shown above each panel. S1 and S2 refer to the first and second half of the SACM. Figure 46 contains the minimum, mean, and maximum values across subjects for response time percent change from baseline. The overall mean baseline was 2.46 sec.

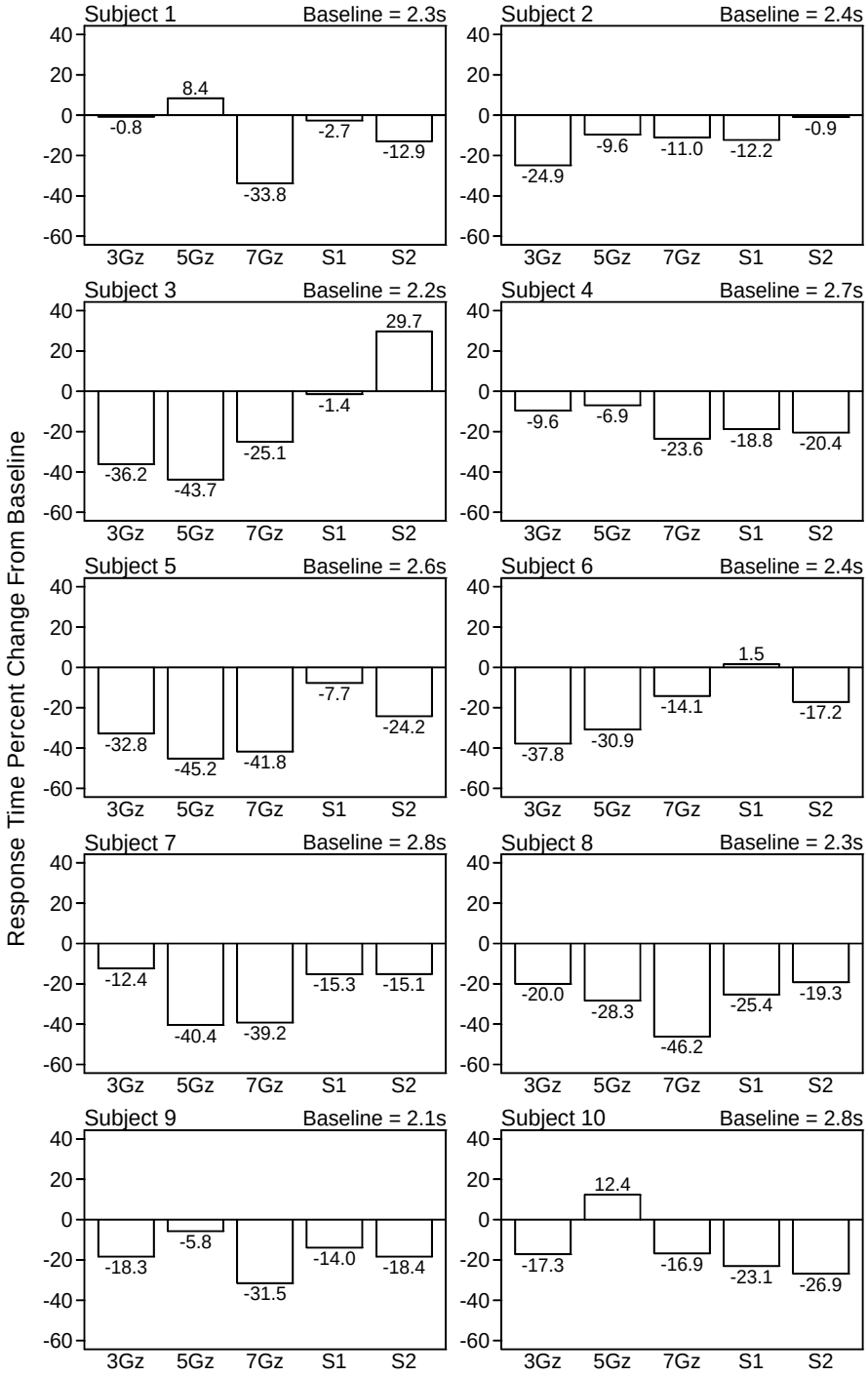

Figure 45: Mean response time percent change from baseline for each subject and condition.

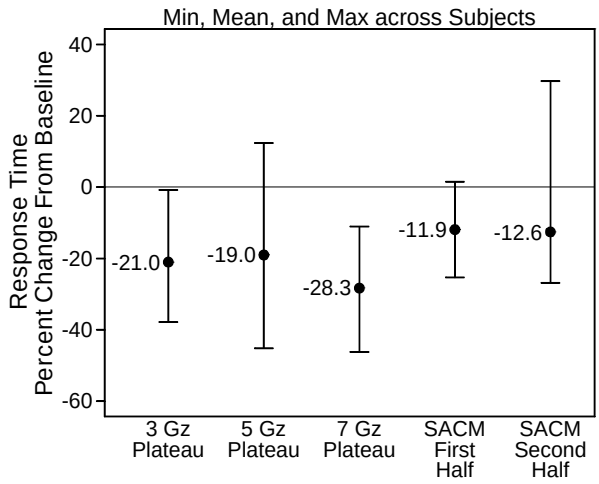

Figure 46: Minimum, mean, and maximum response time percent change from baseline across subjects.

Repeated measures analyses of variance were performed with response time percent change from baseline as the as dependent variable. The first analysis compared the 3 G_z, 5 G_z, and 7 G_z plateaus whereas the second analysis compared the first and second half of the SACM. To determine if a particular condition mean was significantly different from 0, two-tailed t-tests were performed using only data from that condition (i.e., test did not use pooled error across conditions). The F-test did not find a significant mean difference among the 3 G_z, 5 G_z, and 7 G_z plateaus {$F(2,18) = 1.38$, $p = 0.2771$} or between the two halves of the SACM {$F(1,9) = 0.02$, $p = 0.8894$}. All five conditions did show a mean percent change significantly different from 0: 3 G_z ($p = 0.0004$), 5 G_z ($p = 0.0205$), 7 G_z ($p = 0.0001$), first half of SACM ($p = 0.0027$), second half of SACM ($p = 0.0389$).

Unusual Attitude Recovery

The dependent variable in the unusual attitude recovery task was the recovery time percent change from baseline. Again, repeated measures analysis of variance (ANOVA) were

performed with factor condition and levels (3 G_z plateau, 5 G_z plateau, 7 G_z plateau, first half of SACM, second half of SACM). The plateaus and SACM halves were used in separate analyses.

Across all trials (n = 540), the times to recovery times ranged from 1.10 to 19.74 sec with median = 6.56 sec. There was 1 trial from subject 3 that was too fast to be considered legitimate (52 msec) and nine trials across all subjects resulting in a timeout (> 20 sec). During baseline, the 3 combinations assigned to each subject were presented 3 times following a Latin square design (i.e., 3 blocks of 3 trials with each block a different combination of trials) with a constraint that the same combination was never used twice in a row (i.e., end of one block different combination that start of the next block). The presentation of the 3 combinations among the 3 plateau conditions across the 3 days followed a 3x3 Latin square design. That is, across the 3 days each combination was used once for each plateau condition and within a day a different combination was used for each plateau condition.

For the SACM condition, each combination was presented once in the first half of the SACM and once in the second half of the SACM, in a random fashion, with a constraint that the last combination in the first half was different than the first combination in the second half. The following procedure was used to determine a percent change for each subject and condition.

(1) Assign a value of 20 sec to the nine timeout trials. Don't use the one trial from subject 3 that was too fast to be considered legitimate (52 msec).
(2) Within each day, determine the baseline mean time to recovery for each of the three pitch-roll combinations.
(3) For each pitch-roll combination, separately determine the percent change from baseline for all non-baseline values.
(4) Average the percent changes for each condition across pitch-roll combinations and days.

The mean recovery time for each subject and treatment condition can be found in figure 47. The mean baseline value is shown above each panel. S1 and S2 refer to the first and second

half of the SACM. Figure 48 contains the minimum, mean, and maximum values across subjects for recovery time percent change from baseline. The overall mean baseline was 7.09 sec.

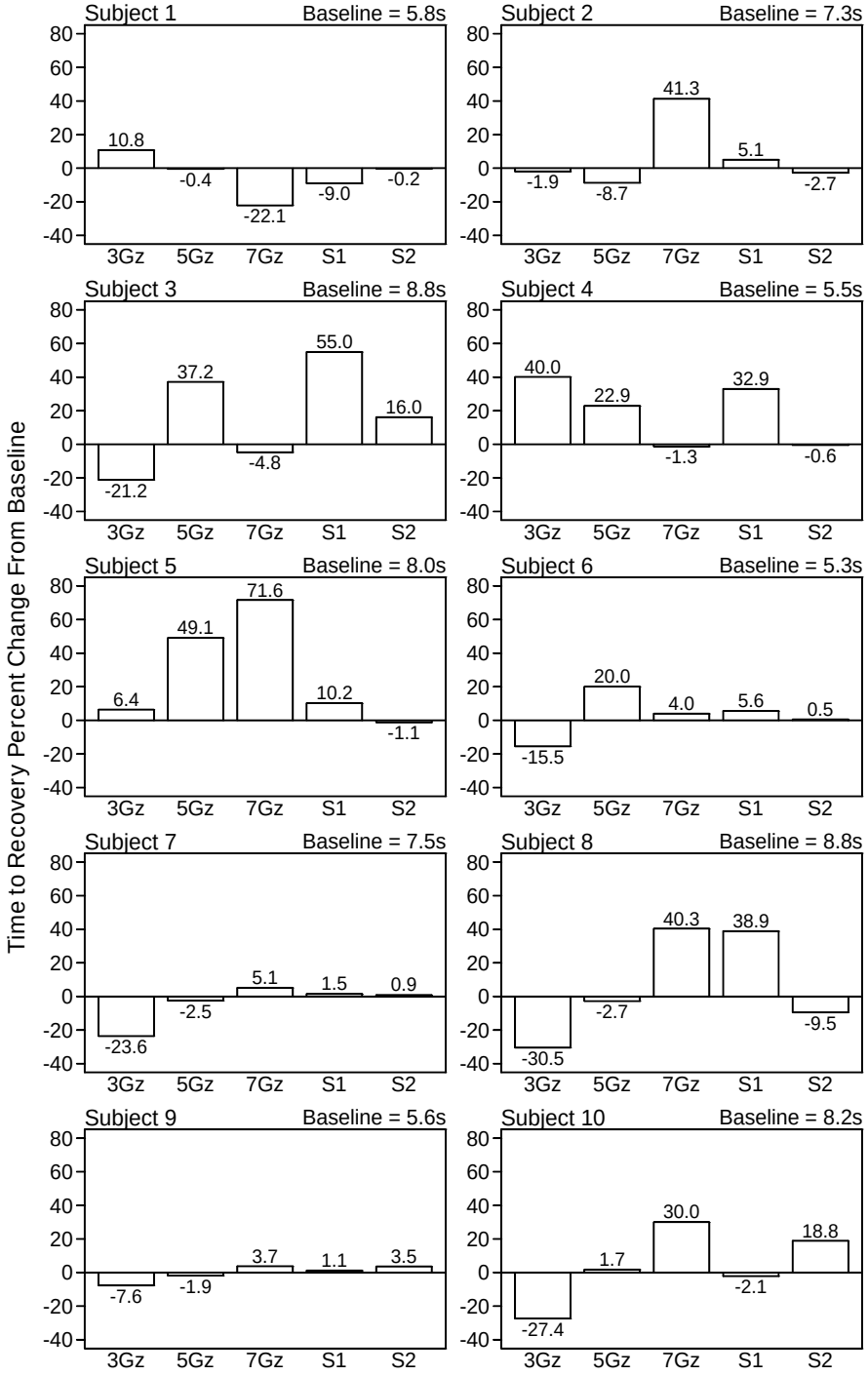

Figure 47: Mean time to recovery percent change from baseline for each subject and condition.

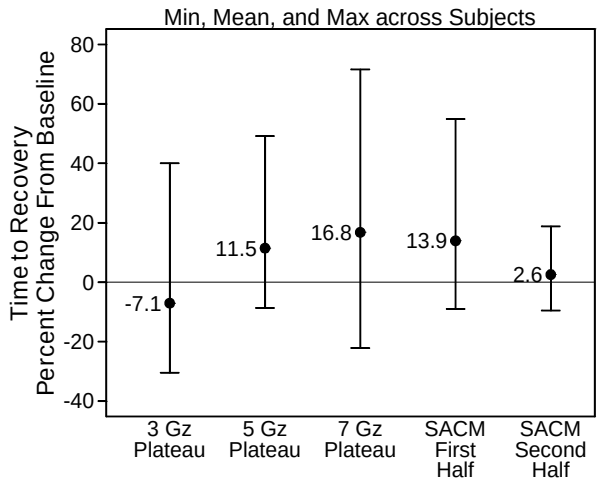

Figure 48: Minimum, mean, and maximum time to recovery percent change from baseline across subjects.

Repeated measures analyses of variance were performed with recovery time percent change from baseline as the as dependent variable. The first analysis compared the 3 G_z, 5 G_z, and 7 G_z plateaus whereas the second analysis compared the first and second half of the SACM. To determine if a particular condition mean was significantly different from 0, two-tailed t-tests were performed using only data from that condition (i.e., test did not use pooled error across conditions). The F-test did not find a significant mean difference among the 3 G_z, 5 G_z, and 7 G_z plateaus {$F(2,18) = 3.10$, $p = 0.0699$} or between the two halves of the SACM {$F(1,9) = 2.63$, $p = 0.1395$}. None of the five conditions showed a mean percent change significantly different from 0 ($p > 0.0640$).

Discussion and Conclusions

Upon further inspection of the data results, it appears rather odd that the error rate for the situational awareness question was elevated during the 5 G_z plateau profile (ref. Table 11). It is possible that because this profile was the first in the series that required use of the straining maneuver. All of the subjects participating in this experiment did not perform the breathing

portion of the anti-g straining maneuver (AGSM) during the 3 G_z plateau profile due to the fact that it was not necessary to maintain their vision. Hence, the addition of this portion of the AGSM during the 5 G_z onset may have led to an increase number of errors as a result of more attention being placed on both recalling AGSM procedures and performing it correctly. However, the overall performance across conditions, with the exception of the 5 G plateau and second half of the SACM, indicated subjects were performing within the training specifications of a 90% success rate. The increased error during the second half of the SACM signifies that the ability to maintain situational awareness following a series strenuous flight maneuvers may be compromised.

The response time percent change from baseline for the situational awareness question showed no differences among the 4 treatment conditions. However, the mean values for each condition were significantly lower than zero, indicating that performance actually got better under G_z acceleration. Part of this phenomenon can be explained by the increased arousal created by the stress of the G_z environment. It is possible to observe performance increases to a certain plateau as arousal increases often caused by environmental or physiologic factors. This plateau is often referred to as the "optimal level of arousal." The concept of arousal influencing task performance was initially introduced by Hebb in 1955 (Hebb, 1955). His theory modeled performance as a bell shaped curve with respect to arousal, indicating there is a value for arousal at which performance is at its peak. It is likely that in the static environment, the repetitive questions concerning situational awareness both preceded and eventually followed by periods of relative boredom created a low level of stimulation for the subjects. This environment is hypothesized to produce levels of arousal below the optimal threshold. When placed in a more stressful situation (e.g. +G_z acceleration), the sympathetic nervous system was stimulated, as

well as other sensory systems (e.g. tactile). The new sensory input coupled with the body's "flight-or-flight" response to the added physiologic stress likely increased level of arousal closer to the optimal point. It is this greater level of arousal that is believed to have caused, in part, the performance improvements during the G_z acceleration.

The fact that the task duration was directly linked to the amount of time the subjects took to complete the task suggests that they may have attempted to respond more rapidly in an effort to finish the task and focus on the AGSM. Given that the performance on the situational awareness task was measured in terms of response time or how quickly the subjects answered the question, this provides a potential explanation of why their performance improved.

Overall, the results did *not* suggest that situational awareness and unusual attitude recovery is significantly influenced by positive G_z acceleration. From a purely anatomic perspective, the crucial brain areas responsible for processing and controlling behaviors and responses appropriate to these tasks are disparate and anatomically distributed. However, the major structures identified for spatial location and awareness appear to be the inferior parietal lobules, the middle occipital gyri, and the superior parietal lobules. The inferior parietal lobules lie dorsal to the intraparietal sulcus and just rostral to the parieto-occipital fissure. They are dorsal to the superior parietal lobules and rostral of the middle occipital gyri. All of these structures reside at or below the horizontal plane within the brain. Hence, it appears that the G_z acceleration was not sufficient to reduce cerebral blood flow to brain areas below the horizontal plane. As seen in previous chapters, those positioned dorsal to the horizontal plane appear to experience marked reductions in oxygenated blood supply evidenced by reduced oxygen saturation values recorded by the cerebral oximeter. Because many of the lower or primitive processing areas of the brain responsible for autonomic functions reside near the horizontal

plane, it is theorized that loss of consciousness occurs as the blood supply to these areas becomes compromised. Given that the subjects in this experiment did not experience an acceleration-induced loss of consciousness event (G-LOC), it is believed that arterial blood pressure did not reduce to the extent that it could not be pumped to these areas. Further evidence can be found in the lack of visual symptoms of the subjects. Should the oxygen be absent from the occipital lobe (residing near the horizontal plane), the visual scene could not have been processed. Hence it is believed that performance differences were not found due to the fact that the anatomic position of the brain structures critical to situational awareness and unusual attitude recovery were sufficiently ventral (low) to maintain adequate oxygenated blood supply.

CHAPTER 9: TASK 9 – RAPID DECISION MAKING

Introduction

It is well known that pilots must make an abundance of decisions in a timely fashion during any given mission ranging from deciding what information is appropriate to view on their multifunction displays (MFDs) to when to eject from the aircraft. Unfortunately, it is the decisions that ensure the survival of the aircraft and aircrew that require the greatest precision and the shortest timeframes for response. Decisions typically involve the perception of the sensory input, high-order processing of the input and comparison to information stored in memory, choice among two or more alternatives, and a motor response. For example, the pilot interprets visual symbols referencing potential targets on a display and then compares this data with rules or knowledge stored in memory. Next, he/she selects the most threatening target and provides motor inputs to the flight controls to engage and/or fire upon the target.

The brain areas involved in each of the aforementioned processes are varied and anatomically distributed. Visual sensory information is initially interpreted in the striate cortex (V1), which in turn sends the information to other areas (e.g. ventral and dorsal streams) for further processing. Object recognition, such as identification of targets, is completed in the lateral occipital complex (L0). This area of the brain is located within the ventral stream that extending to the posterior parietal cortex. As a result, L0 is located lower than or ventral to V1. Other activities such as the control of eye movements (V7, lateral intraparietal area) and visual attention (V7, lateral intraparietal area) are handled in the dorsal stream. Hence, they are housed higher than, or dorsal to area V1.

Once the visual stimulus was recognized, the subject was required to make a decision based on the relative threat level. This requires interaction with procedural and declarative

memories (e.g. how to respond to the recognized stimulus) indicating the induction of hippocampal activity. Such activity is important to note due to the fact that hippocampal pyramidal cells (particularly those housed in area CA1) are extremely sensitive to ischemic insults and the subsequent lack of oxygen (Krnjevic, 1999). In fact, available evidence suggests they are among the first to arrest function (Sugar & Gerard, 1938). This phenomenon has been attributed to the high metabolic need of the hippocampal cells and is believed to be a protective mechanism aimed at preserving energy (Krnjevic, 1999).

Additionally, the decision making process appears to involve both the ventromedial prefrontal cortex (Smith et al, 2002) and the amygdala (Bechara, 2006). Bechara (2006) notes that "real life" decisions appear to be significantly affected by the emotional weight associated with a particular alternative. Hence, some decisions (e.g. impulse purchases) may be evaluated simply on an emotional level rather than an objective weighting of the alternatives (Bechara, 2006). However, damage to the ventrolateral prefrontal cortex will also adversely affect the individual's ability to resolve conflicts and make effective calculations of choice consequences (Smith, et al, 2002). Ultimately, this reduces the ability to achieve an appropriate decision supporting the attainment of a goal.

The final output from the subjects was in the form of a motor response in which one of the choice alternatives was selected by depressing a button. This process involves the frontal cortex (planning), cerebellar cortex (movement coordination), and the motor cortex (control of the hand/fingers). Of particular note is the fact that the cerebellar cells (Purkinje Fibers) are also extremely sensitive to oxygen deprivation (Krnjevic, 1999).

The varied and disparate nature of the brain during the decision-making process denotes a somewhat complex process which is difficult to delineate. As a result, it is unclear whether

positive acceleration will have a benign or cataclysmic effect on the decision making process. Although, it is possible that cognitive deficits may manifest during G_z loading due to the potential failure of highly oxygen-sensitive areas such as the hippocampus and cerebellum, and high-level processing areas such as the ventromedial prefrontal cortex, visual association cortices, motor cortex, etc., other areas such as L0 and the amygdala may be protected due to the relatively low anatomical position or smaller metabolic need. As a result, this study examines a simple, but rapid decision-making task under positive acceleration stress.

Methods

Subjects

Ten active duty members of the United States Air Force (9 male, 1 female) volunteered to participate in this study. They ranged in age from 24 to 31 years, with a mean age of 27 years. All participating subjects were members of the sustained acceleration stress panel at Wright-Patterson AFB, OH. Requirements to qualify for participation in this study are identical to those of chapter 2 (ref chapter 2, Methods section).

Facilities

All training and data collection for this study was performed at the Air Force Research Laboratory's Dynamic Environment Simulator (DES) centrifuge facilities at Wright Patterson AFB (ref. Chap. 2, Figure 3). The DES is a human rated centrifuge with an arm radius of approximately 19 feet. It is capable of attaining and sustaining accelerations up to 20 G in either of three independent axes: x, y and z. The DES has a maximum G onset and offset rate of approximately 1 G/sec. The gondola of the centrifuge was equipped with an F-22-like ACES II

ejection seat with a seatback reclined to 15^{o} from vertical. As illustrated in Figure 2 (ref. Chap. 2), the seat had adjustable lap and shoulder restraints.

An aircraft IC-10 communication system was used to provide two-way voice-communication between the research participant and the investigator. The participant's microphone was fixed in the open position to allow the participant "hands-free" communication. Participants were also provided with an emergency abort switch that enabled them to stop the centrifuge at any time during testing. Participants wore a standard Air Force issue Nomex® flight suit and a standard G-suit during all testing runs.

The gondola was outfitted with a simulated fighter cockpit. The cockpit incorporated a Thrustmaster Hotas Cougar flight stick (Guillemot, Montreal, Canada) mounted on the participant's right side that was used to secure responses to the performance task. A six foot hemispherical shell viewing screen, representing a 130^{o} (vertical) x 180^{o} (horizontal) visual field, mounted directly in front of the participant. A separate projector was used to display the performance task in the center of the subjects' field-of-view with a projected image of 22.5" (width) by 18.5" (length). The large dome display was used to present two red dots located at approximately 60^{o} of visual angle to the right and left of the center of the dome and approximately 5^{o} in diameter. In addition, a red circle was displayed just above the HUD that represented 10^{o} of visual angle. The dots served as a reference to the subject of his/her visual loss. Should the smaller dots not be visible in the periphery, the subject was instructed compensate by increasing their AGSM. They were to abort the test should their vision degrade to the point that only the center red dot was visible. Figure 4 (ref. chapter 2) provides an illustration of the entire visual system.

Continuous surveillance of participants was provided by two closed-circuit infrared television cameras. The cameras offered a close-up view of the participant's head and a wide-angle view of the participant from head-to-foot. Research personnel housed in a control room observed the video images. A video mixer was used to generate a composite picture of the two views of the participant along with the time, date, electrocardiogram (ECG) data, and G_z acceleration in a given run. Video data were stored on ½ inch VHS videotape.

Acceleration Profiles

A total of four G_z acceleration profiles were generated for use in this study. All G_z exposures were started from a baseline acceleration of 1.5 G_z. The first three profiles comprised of a 1 G/sec onset ramp to a 15-sec plateau followed by a G_z offset ramp of 1 G/sec down to the baseline acceleration level. The plateaus were 3, 5, and 7 G_z, respectively. The final acceleration exposure was a simulated aerial combat maneuver (SACM). This profile consisted of two 5-sec G_z peaks to 7 G_z with several intermittent peaks to 3 and 5 G_z. Figure 6 (ref. chap. 2) displays an example of a G_z plateau profile, while Figure 7 (ref. chap. 2) presents the SACM profile.

Stimuli

The subjects completed a "rapid decision making" performance task during each G_z profile on each experimental test day. This task was projected on a six foot hemispherical shell viewing screen, representing a 130^o (vertical) x 180^o (horizontal) visual field. However, the task utilized a projector that produced a smaller image on the screen directly in front of the subject spanning 18" x 18". The task used for this experiment employed a visual Radar Warning

Receiver (RWR), comprised of three colored concentric circles. The outermost ring was colored green, the intermediate was yellow, and the center was red (Figure 49). Each ring represented a threat level with the red, yellow, and green regions representing high, medium, and low threat levels, respectively.

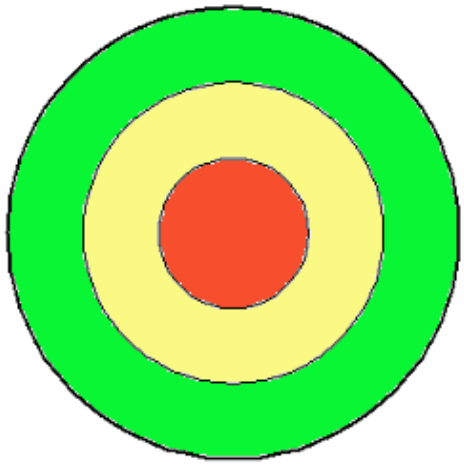

Figure 49: Rapid Decision Making Task Radar Warning Receiver

During each trial, three different symbols representing enemy targets (X, O, ?) would appear simultaneously within the RWR. A single target could only occupy one ring, but a single ring could hold up to three targets (Figure 50). Each target symbol represented a threat level, with the "X", "O", and "?" symbols representing high, medium, and low threat levels, respectively.

After the subject visually processed the targets in the RWR, he/she had to determine which posed the greatest threat at that particular moment. Prior to the task, each subject was given a particular set of rules to follow for deciding which target represented the greatest threat:

Rule 1. If the X appears in the center area, it is clearly the highest threat no matter where the others may be.

Rule 2. If the X is in the same ring as both of the other threats, or is closer to the center than both of the other threats, it represents the highest threat.

Rule 3. If the X is further away from the center than either of the other two symbols, then one of them represents the greatest threat, and your decision must depend on the following rules:

3a. If the "O" and "?" are in the same area of the RWR, the "O" represents the greatest threat.

3b. If the "O" is in the center or middle ring of the RWR, and the "?" is in the outer ring, the "O" represents the greatest threat.

3c. If the "?" is in the center or middle ring of the RWR, and the "O" is in the outer ring, the "?" represents the greatest threat.

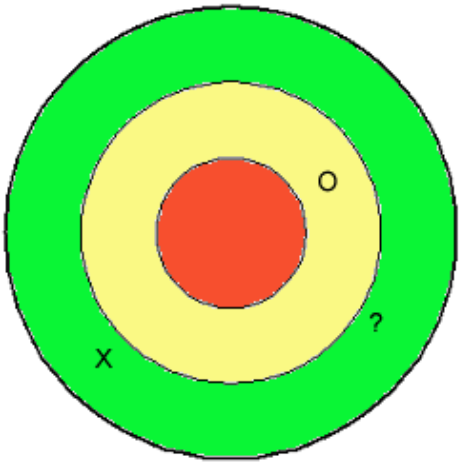

Figure 50: Targets randomly placed in RWR

After using these rules to analyze the threats, the subject pressed the appropriate direction on the top right hat switch to represent which threat he/she determined to be greatest for that stimulus presentation (Figure 51). The subject was instructed to push the hat switch left to indicate "X," right to indicate "?," and down to indicate "O." The presentation would "time out" and immediately cease if no response was made within a five second time period. No response was recorded for those trials. After the subject either made a decision response or the trial timed

out at five seconds, there was a two-second interstimulus interval before a new randomized presentation of the target symbols appeared in the RWR.

Figure 51: Joystick response switch for rapid decision making task

Static Training

To ensure training effects were eliminated from the experimental data set, each subject was trained statically on the Rapid Decision Making task prior to dynamic training (see next section) and data collection. Static training was performed in an F-16 mock-up fuselage equipped with an ACES II aircraft seat with a 15-degree seatback angle. The task was projected onto a 48-in. (vertical) x 64-in. (horizontal) screen. Subjects were given 50 trials of the task followed by a one minute rest period. This was repeated three times per static training day. A

subject was considered trained when they responded correctly to 90% of the presentations and attained a 100% response rate.

Dynamic Training

After each subject passed the requirements for static training, dynamic blend training was completed. The subjects performed the Rapid Decision Making task in the DES at 1 G_z each day to provide a baseline performance metric. They then performed the tasks during the same 3 G_z, 5 G_z, and 7 G_z plateaus and 7 G_z SACM profiles that were administered during the experimental test days. A one-minute rest period was given after each G_z profile. Subjects were considered trained once their performance on the task deviated less than 10% between training days. Performance was measured by the percentage of correct responses to the task as well as response time. Dynamic training was conducted in order to ensure that no training effects were present in the final data that may have resulted from acclimation to performing the task in the high G environment.

Procedures

On a typical experimental test day, participants arrived at the laboratory, donned a flight suit and a standard G-suit, and were instrumented with electrocardiogram leads. The flight surgeon performed a brief medical examination and reviewed the subject's medical history. The participant then proceeded to the centrifuge where he/she donned a parachute harness. After entering the gondola of the centrifuge the participant was secured to the ACES II aircraft seat (with a 15-degree seat back angle) using a three-point aircraft restraint system. The ECG leads were connected and the signals were verified prior to securing the gondola of the centrifuge.

Following this, the cerebral oximeter was secured around the subject's forehead. The operator started the computer program to keep track of changes in the subject's oxygen saturation levels. At this point, the Rapid Decision Making task was started and baseline performance data was collected over 50 presentations. After the baseline data was collected, the subject was then ready to begin the four G_z exposures.

The subject experienced each of the four G_z exposures on three different test days in the following order: 3 G_z 15-sec plateau, 5 G_z 15-sec plateau, 7 G_z 15-sec plateau, and 7 G_z SACM. The subject began the task approximately 8 sec prior to each G_z exposure and continued for approximately 8 sec after the acceleration had returned to the baseline G_z level of 1.5 G_z. A 1-minute rest period was provided between each G_z exposure, during which the task was not performed and the subject was permitted to relax at the baseline G_z level. This was accomplished to allow the physiology to return to the pre-acceleration exposure levels. During the SACM profile, performance data was collected for 6 presentations to measure the first half of the SACM against the second half. Following the completion of the four G_z exposures, the participant exited the centrifuge and was immediately examined by the flight surgeon and then released to return to his/her normal duties. These procedures were repeated over three experimental test days.

Results

There were 3908 total trials performed in the study (including baseline profiles). Of these, only 56 (1.4%) resulted in an error (subject pressed a button indicating a target that was not the most threatening). The errors did not occur more frequently in one profile over another

and in fact, 14 occurred during baseline. As a result, no significant findings could be found for the error rate performance metric.

The Rapid Decision Making task was also assessed by comparing the response time percent change from baseline. Presentations ending in an error were omitted from the data set. The first analysis compared response time percent change from baseline during the plateau of the 3 G_z, 5 G_z, and 7 G_z plateau runs, and from the 7 G_z plateau of the SACM run. Only trials ending within 0.5 G_z of the plateau level were used for data analysis. The second analysis compared response time percent change from baseline during the first half of the SACM run vs. the last half of the SACM run. Only trials after the start of the first onset and before the end of the last offset were used for data analysis.

The response time percent change from baseline was calculated for each subject during the peaks from the 3 G_z, 5G_z, 7 G_z, and 7G_z SACM (7 G_z peaks only) profiles. These values are plotted in Figure 52. In addition, the response time percent change from baseline was calculated for each half of the SACM. This data is plotted for each subject in Figure 53 where geometric mean is shown above each plot panel. The mean response time percent change from baseline was determined across subjects and is presented in Figure 54. The overall baseline geometric mean of response time was 0.99 seconds.

Repeated measures analyses of variance were performed with the response time percent change from baseline for each subject as the dependent variable. The F-test did not find a significant mean difference among the 3 G_z plateau, 5 G_z plateau, 7 G_z plateau, and SACM 7 G_z plateau ($p = 0.7642$: Greenhouse-Geisser epsilon = 0.72, adjusted $p = 0.7004$). Two-tailed t-tests using the subject means (no pooling) did not find any of the G_z plateau means to be significantly different from 0 ($p > 0.3790$).

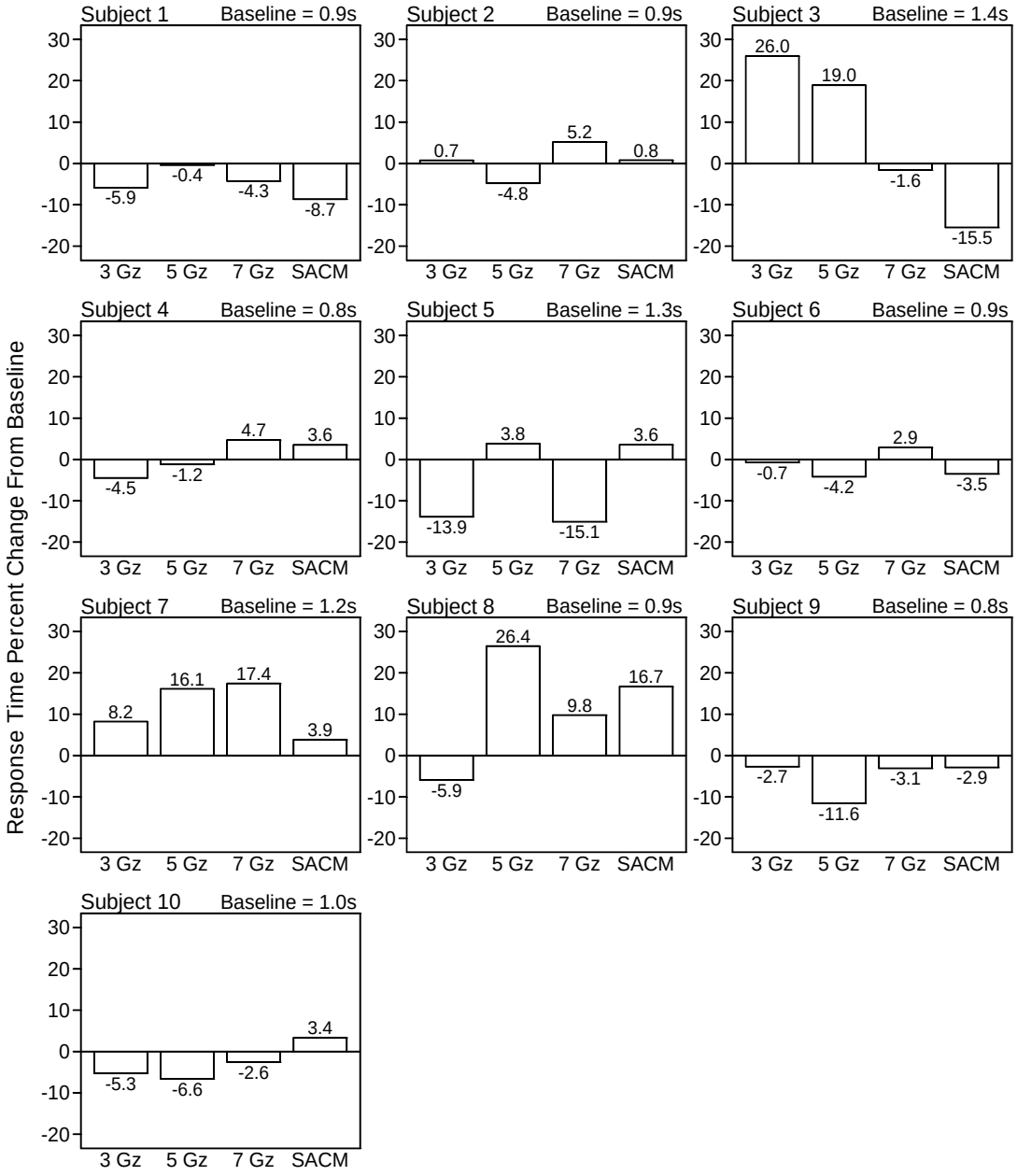

Figure 52: Mean response time percent change from baseline for each subject and Gz profile.

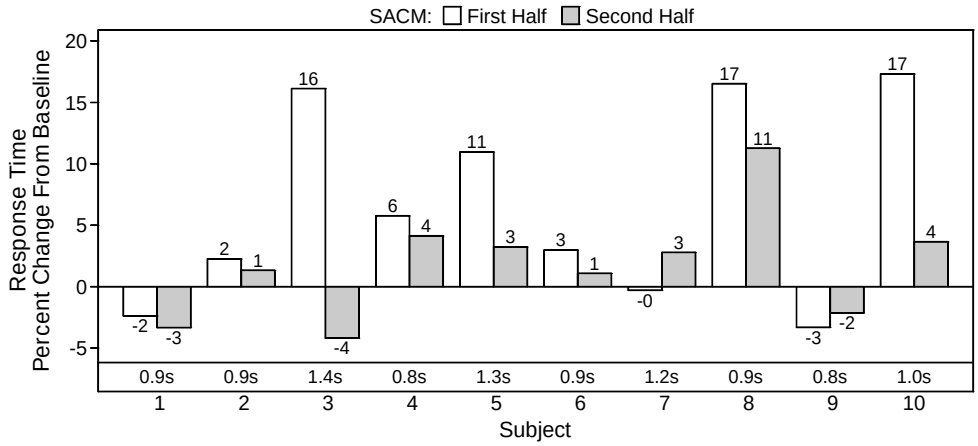

Figure 53: Mean response time percent change from baseline for each subject and SACM half

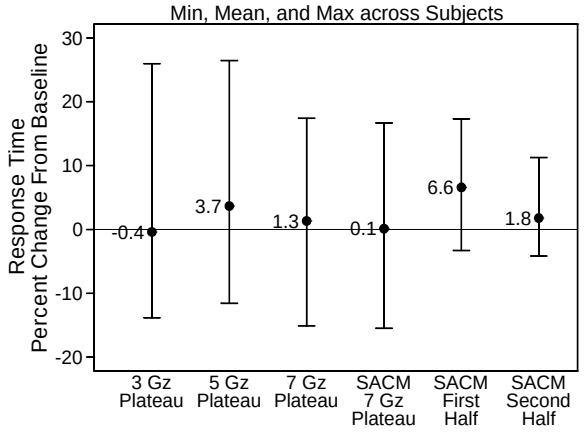

Figure 54: Min, mean, and max response time percent change from baseline across subjects (N = 10)

The F-test for the second analysis did not find a significant difference between the first half and second half of the SACM ($p = 0.0656$). Two-tailed t-tests using the subject means (no pooling) found the mean for the first half ($p = 0.0290$) but did not find the mean for the second half ($p = 0.2374$) of the SACM to be significantly different from 0. Figure 55 contains rSO_2 percent change from baseline across subjects for each G_z profile. For the SACM, only recordings during the 7 G_z plateau were used.

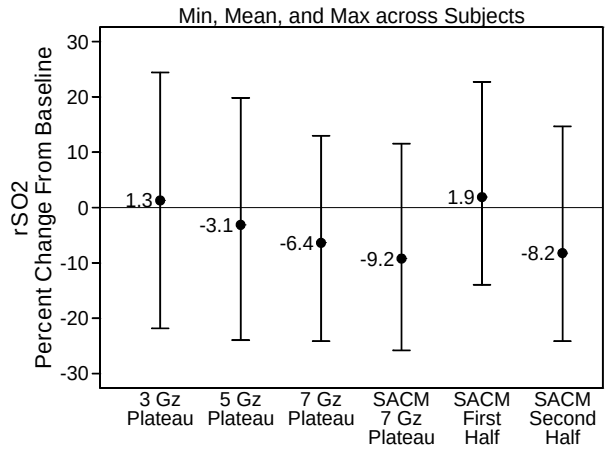

Figure 55: Min, mean, and max rSO_2 percent change from baseline across subjects (N=10)

Repeated measures analyses of variance were performed with the rSO_2 percent change from baseline for each subject as the dependent variable. The F-test found a significant mean difference among the 3 G_z plateau, 5 G_z plateau, 7 G_z plateau, and SACM 7 G_z plateau (p = 0.0001: Greenhouse-Geisser epsilon = 0.57, adjusted p = 0.0001). The Bonferroni paired comparison procedure with a 0.05 family-wise error level showed the means at each plateau to be significantly different from each other with the exception of 7 G_z vs. SACM 7 G_z. Two-tailed t-tests using the subject means (no pooling) did not find the plateau means to be significantly different from 0 at 3 G_z (p = 0.7354), 5 G_z (p = 0.3975), or 7 G_z (p = 0.0831), but did find the mean at the SACM 7 G_z plateau (p = 0.0140) to be significantly different from 0.

The second analysis used means from each SACM half. The F-test found a significant difference between the first half and second half of the SACM (p = 0.0006). Two-tailed t-tests using the subject means (no pooling) did not find the mean for the first half (p = 0.5609)

Discussion and Conclusions

Air combat missions often require the pilot to make critical decisions at a moment's notice that could significantly impact the success of the mission and/or the survivability of the pilot/aircrew. Because such missions often involve high $+G_z$ stress, blood supply needed to sustain high-order cognitive function can begin to pool in the lower extremities making it very difficult for the heart to pump a fresh supply of oxygen and nutrients to the cortical tissues. Hence, it was necessary to study the effects of inertial forces on the pilot's ability to maintain critical cognitive abilities such as rapid decision making. Overall, the performance measured in terms of both error rate and response time did not significantly alter during any of the G_z conditions.

Response times were normalized by computing a percent change from the baseline (1 G_z) data to ensure a fair and equal comparison across subjects. Even when further delineated by subject, performance remained stable across all G_z plateaus. Only subjects 7 and 8 experienced significant decrements in response times as a result of increased G_z stress. However, the performance data did not correlate directly with the regional oxygen saturation (rSO_2) data measured at the forehead. In addition, less than 2% of the task presentations resulted in an error. When compared across profiles, no particular pattern could be found and there was no correlation with physiologic data. In fact, 14 errors occurred during the baseline (1 G_z) profile.

The model developed by NIT, Inc. utilized a previous study performed by Cochran (1953) to develop the look-up table database for complex decision making. The results were decomposed categorically into three subcomponents referred to as accuracy, reaction time, and throughput/efficiency. Essentially, subjects endured accelerations up to 6.0 G_z (generated in a centrifuge) in complete darkness. Once the target acceleration magnitude was achieved, the

lights would be turned on indicating the subject should execute an emergency aircraft ejection. The reaction time was measured as the interval between the activation of the lights and the completion of the ejection procedures. The success or failure of the ejection maneuver was equated to accuracy. "Throughput" or efficiency was measured as the percent accuracy divided by the average response time. Although relatively simplistic, significant declines in performance were noted for both the accuracy and throughput measures. Table 8 below provides the specific performance values at each G_z level.

Table 8: Complex Decision Making Performance Utilized in NTI, Inc. Data Tables (Cochran, 1953).

	1 G_z	2 G_z	3 G_z	4 G_z	5 G_z	6 G_z
Average Percent Accuracy	100.00	97.50	96.50	95.00	100.00	90.00
Average Reaction Time	100.00	94.00	87.50	73.50	75.00	76.50
Average Throughput	100.00	58.89	45.43	26.98	32.76	31.34

The lack of significant declines in performance in this study lends itself to the question of why this cognitive ability was not affected. First, it should be noted that the performance task described in Cochran (1953) required subjects to raise their arms above their heads to grasp the face curtain handles. Given that the increased acceleration results in an increased apparent weight of the entire body, it is not surprising that additional time was required to perform the task. Primarily, this elongation of the "reaction time" was likely a direct result of the arms being up to 6 times heavier than at baseline, indicating the performance declines may have been almost entirely a product of increased muscle resistance rather than cognitive deficiency.

Additionally, it is possible that the simplicity of the task created a paradigm by which subjects were able to successfully complete it without the benefit of higher order cognitive

influence. The repetitive and lengthy training regime coupled with the simplicity of the task may have led to a conditioned stimulus-response model whereby the initial recognition of the target led directly to the trained (and reinforced) correct motor response requiring little preprocessing. Evidence suggests that learned complex behaviors that require instruction and adhering to a set of rules eventually becomes automatic following intense or prolonged training (Carlson, 2007). This is referred to as instrument learning. Initially, the task is performed slowly due to the large amount of cortical areas involved in executing the task correctly and the lack of strong synaptic connections in areas responsible for generating the favorable outcomes (Carlson, 2007). As the task is presented more and more, it becomes routine and automatic. In terms of neural circuitry, the behaviors become "transferred to the basal ganglia," which takes over many of the functions leading to the intended output or action (Carlson, 2007). It follows that visual stimuli from L0 and other sensory association cortices may have been sent to the motor cortex through the basal ganglia and thalamus (Carlson, 2007). Because acute oxygen deprivation seems to affect high-order cognitive circuits more drastically than those involved in autonomic and automatic functions due to the greater consumption of energy, it is expected that tasks involving conditioned or automatic responses to stimuli would remain resistant to functional shutdown resulting from anoxia or hypoxia (Krnjevic, 1999). Similar to the "pitch-roll-capture" study described in chapter 7, the automation of the response to the task likely resulted in stimulation of areas requiring lower energy resources to function and they were therefore not greatly affected by a relatively short lack of fresh oxygen supply.

The rSO_2 data suggest that cerebral oxygen was significantly reduced during the tasks. In fact, the mean decrease during the 7G profile was 6.4% of the baseline value. This value increased to over 9% during the SACM due to the longer overall duration and multiple G_z peaks.

However, it is possible that these levels of rSO_2 were not sufficient to elicit changes in brain function; particularly those regions alluded to above. It is known that loss of consciousness tends to occur once rSO_2 values decline 19% from the baseline value (McKinley, et al., 2005). However, it is not known at what level of rSO_2 that decision making functionality begins to decline. In addition, it should be noted that the task used in this study was a simple choice among three alternatives. Operationally, pilots will likely have more complex decisions with many alternatives and no clear-cut optimal choice. As a result, the results from this study primarily pertain to decisions involving set procedural alternatives to a given stimuli. However, it is believed that such situations are frequent in emergency situations such as the decision of when to eject, how to respond to a new target, and what procedures to employ to address warnings within the cockpit.

Pilots are trained extensively to deal with threats both within the cockpit and outside the cockpit. Often there are trained procedures and maneuvers from which the pilot can quickly select to deal with the situation at hand. It is the opinion of the authors that the extensive training leads to the transfer of many processes engaged in these responses to basal ganglia control via connections with the stimuli association cortices and the motor cortex. Hence, the pilots do not have to think about the response, it is an automated reflex resulting from repetition and experience. The conclusions of this study are that $+G_z$ up to 7 G_z does not negatively affect the pilot's ability to execute simple decisions. This is ultimately caused by the omission of oxygen-sensitive cortices responsible for high-order cognition from the execution of the task. Although the rSO_2 values declined, the magnitude and duration of the hypoxia were not sufficient to cause the basal ganglia to reduce its activity.

CHAPTER 10: TASK 10 – VISUAL MONITORING

Introduction

Military aircraft cockpits are highly saturated with various types of visual displays ranging from analog "round gages" to advanced multifunction digital displays. With the deluge of information from these visual stimuli all competing for the pilot's undivided attention, several studies have been aimed at discovering the methods and strategies aircrew employ to process the data and the corresponding mental workload ascribed to this procedure (Casali & Wierwille, 1984; Hayashi, 2003; Phillips, et al., 2007; Wilson, 2002). One question is whether pilots process information in parallel or serially.

Cognitive architectures such as Adaptive Control of Thought, Rational (ACT-R), and Executive-Process Interaction Control (EPIC) provide a platform on which to simulate human cognition by utilizing a central cognitive processor and sets of productions rules to execute tasks, retrieve information, process sensory data, etc. Often, multiple procedures can run in parallel within the architecture based on Wicken's (1984) multiple resource theory that there are different resource allocations for different types of tasks. However, within the same modality (e.g. vision), information may or may not be able to be processed in parallel. Simple features, line detection, and sudden motion can be detected and processed in peripheral vision while the subject focuses on more detailed information located in the foveal field-of-view. Nevertheless, Hayashi (2003) posits instrument reading must occur serially due to the fact that accurate readings require visual fixation. Thus visual instrument scans advance one-at-a-time with brief pauses on each to decipher the information or data values presented.

Typically, displays have normative values or ranges for which no corrective action is necessary. For example, the engine temperature will have a normative or "safe" region whereby

the pilot is not required to initiate emergency procedures. Others such as airspeed, altitude, pitch angle, etc. will have expected values and ranges for which corrective action is not necessary. Should the pilot wish to maintain 20,000 ft of altitude and the display presents feedback indicating the aircraft is presently at the specified altitude, the visual attention will then move onto the next instrument in the scan pattern. Therefore, the instrument scanning can take place rapidly at steady state, with the pilot primarily looking for abnormalities in each display.

This study attempted to evaluate the pilot's visual scanning performance under operationally relevant $+G_z$ stress. The performance task utilized in this experiment attempted to mirror the paradigm described above by presenting 4 different displays and allotting a normative value range to each. The values oscillated around the normative value continuously within the "safe" range to ensure the abnormal readings would not be solely discovered in the peripheral vision. Hence, the subjects were forced to monitor each display in a serial fashion and press a button corresponding to the display should its value deviate from the normative range.

Visual processing is initiated by the primary visual cortex (V1) located in the occipital lobe. As stated in chapter 6, the visual association cortex divides into two sections to further analyze the sensory data. These separate segments are classically referred to as the dorsal stream and the ventral stream (Baizer, Ungerleider, and Desimone, 1991). As the name implies, the "ventral stream" extends from the striate cortex in the ventral direction (towards the base of the skull) to the inferior temporal cortex. The ventral stream is believed to interpret the "what" (color, form, etc.) of the object(s) in the visual field (Carlson, 2007). Specifically, V3 (visual processing of visual scene), V4 (analysis of form), V8 (color perception), and L0 (object recognition) areas of the ventral stream are believed to be the primary active areas during execution of this task. As the blood supply is diverted from the cortical areas, neurons

responsible for higher order information processing will reduce their firing as a protective mechanism. Each action potential requires additional energy in the form of ATP, which becomes scarce in the absence of oxygen ferried by the red blood cells. However, it is not known whether visual attention and instrument scanning processes are inhibited during $+G_z$. This study was aimed at determining the existence and extent of the cognitive decrements in an instrument reading task at high $+G_z$.

Methods

Subjects

Ten active duty members (7 male, 3 female) volunteered to participate in this study and ranged in age from 23 to 28 years, with a mean age of 26 years. All participating subjects were members of the sustained acceleration stress panel at Wright-Patterson AFB, OH. Requirements to qualify for participation in this study are identical to those of chapter 2 (ref chapter 2, Methods section). One of the female participants declined to complete her final day of data collection due to increased demands of her job.

Facilities

All training and data collection for this study was performed at the Air Force Research Laboratory's Dynamic Environment Simulator (DES) centrifuge facilities at Wright Patterson AFB (ref. Chap. 2, Figure 3). The DES is a human rated centrifuge with an arm radius of approximately 19 feet. It is capable of attaining and sustaining accelerations up to 20 G in either of three independent axes: x, y and z. The DES has a maximum G onset and offset rate of approximately 1 G/sec. The gondola of the centrifuge was equipped with an F-22-like ACES II

ejection seat with a seatback reclined to 15^{o} from vertical. As illustrated in Figure 2 (ref. Chap. 2), the seat had adjustable lap and shoulder restraints.

An aircraft IC-10 communication system was used to provide two-way voice-communication between the research participant and the investigator. The participant's microphone was fixed in the open position to allow the participant "hands-free" communication. Participants were also provided with an emergency abort switch that enabled them to stop the centrifuge at any time during testing. Participants wore a standard Air Force issue Nomex® flight suit and a standard G-suit during all testing runs.

The gondola was outfitted with a simulated fighter cockpit. The cockpit incorporated a Thrustmaster Hotas Cougar flight stick (Guillemot, Montreal, Canada) mounted on the participant's right side that was used to secure responses to the performance task. A six foot hemispherical shell viewing screen, representing a 130^{o} (vertical) x 180^{o} (horizontal) visual field, mounted directly in front of the participant. A separate projector was used to display the performance task in the center of the subjects' field-of-view with a projected image of 22.5" (width) by 18.5" (length). The large dome display was used to present two red dots located at approximately 60^{o} of visual angle to the right and left of the center of the dome and approximately 5^{o} in diameter. In addition, a red circle was displayed just above the HUD that represented 10^{o} of visual angle. The dots served as a reference to the subject of his/her visual loss. Should the smaller dots not be visible in the periphery, the subject was instructed to compensate by increasing their AGSM. They were to abort the test should their vision degrade to the point that only the center red dot was visible. Figure 4 (ref. chapter 2) provides an illustration of the entire visual system.

Continuous surveillance of participants was provided by two closed-circuit infrared television cameras. The cameras offered a close-up view of the participant's head and a wide-angle view of the participant from head-to-foot. Research personnel housed in a control room observed the video images. A video mixer was used to generate a composite picture of the two views of the participant along with the time, date, electrocardiogram (ECG) data, and G_z acceleration in a given run. Video data were stored on ½ inch VHS videotape.

Acceleration Profiles

A total of four G_z acceleration profiles were generated for use in this study. All G_z exposures were started from a baseline acceleration of 1.5 G_z. The first three profiles comprised of a 1 G/sec onset ramp to a 15-sec plateau followed by a G_z offset ramp of 1 G/sec down to the baseline acceleration level. The plateaus were 3, 5, and 7 G_z, respectively. The final acceleration exposure was a simulated aerial combat maneuver (SACM). This profile consisted of two 5-sec G_z peaks to 7 G_z with several intermittent peaks to 3 and 5 G_z. Figure 6 (ref. chap. 2) displays an example of a G_z plateau profile, while Figure 7 (ref. chap. 2) presents the SACM profile.

Stimuli

The "visual monitoring" performance task developed by NTI, Inc. was utilized in this experiment to assess the subjects' instrument reading and scanning abilities under G. The task was presented on the smaller, foveal projection measuring 22.5" (width) by 18.5" (length) on the 6-ft dome shell. The projection provided an outside-the-window representation for the F-PASS flight simulator developed by NTI, Inc. Subjects were to fly a simulated aircraft straight and

level while monitoring four generic instrument displays. The displays were presented in the four corners of the out-the-window scene as shown in figure 69 below. The displays are numbered in a clockwise fashion as follows: Display 1 - Top Left; Display 2 - Top Right; Display 3 - Lower Right; Display 4 - Lower Left. Each display contained both “safe” areas and “unsafe areas”. The instructions were to monitor each display and indicate the display that moves into an “unsafe area” with the hat switch on the HOTAS Cougar flight stick depicted in figure 70.

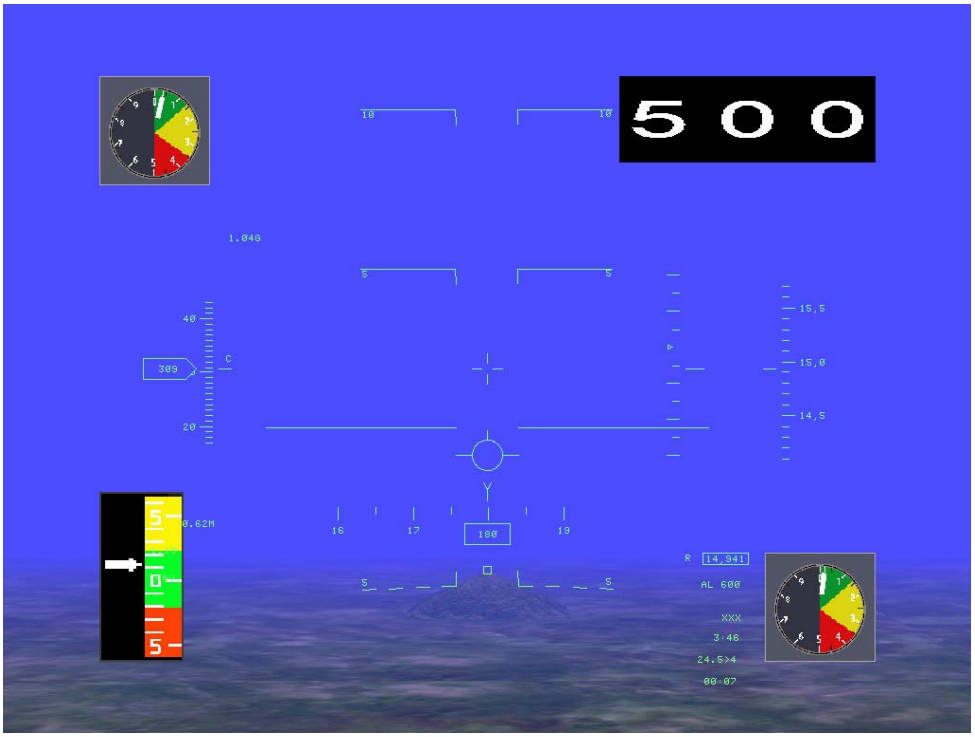

Figure 56: Visual Monitoring Task Out-The-Window View with Four Instrument Display Overlays

Figure 57: Joystick switches for resetting the 4 displays to be monitored

Display 1 was a round dial with three colored regions: green, yellow, and red. The green section indicated the "safe zone" whereby no input was required from the subject. Should the dial venture into the yellow or red areas, the subject was required to indicate that there was a problem by moving a hat button on the control stick in the "up" direction. The needle would remain in the yellow/red areas until either the correct stick input was recognized or 15 seconds had elapsed. Once selected, the display would reset back to the "safe zone." The dial needle moved continuously to prevent the subject from perceiving changes solely with peripheral visual cues. Therefore, he/she was required to fixate on the display and determine to what area the needle was pointing.

Display 2 was a digital display presenting a continuously and sequentially changing three-digit number. The "safe zone" was any value between 450 and 550. Should the value read greater than 550 or less than 450, the reading was determined to be in the "unsafe zone" requiring immediate input from the subject. Participants were told to move the hat button on the control stick to the left to indicate display 2 had displayed an unsafe value. Again, the value would remain in the unsafe region until the proper input from the subject was recorded or 15 sec had transpired. At this point, the display would reset back to its nominal range (450-500).

Display 3 was identical to display 1. Instructions were the same with the exception that subjects had to move the hat switch on the flight stick downward to indicate display 3 had moved out of the safe area.

Display 4 was a vertical "tape" display that contained a green, yellow, and red area. As in display 1, the green area represented the "safe zone," although it was located in the center of the display rather than the top. The display contained a continuously moving needle that primarily oscillated within the green area. However, if the needle moved up to the yellow area, or down to the red area, the subject was required to indicate this by moving the hat switch to the left to reset the display. Figure 71 below shows display 3 in the "unsafe zone."

Subjects were not told to maintain a certain altitude, heading, or airspeed, so visual scanning of the instrument was limited to the four generic displays and an assessment of roll and pitch (easily performed via alignment with the horizon). In addition, only one of the displays would move into the "unsafe" regions for any given trial. The displays changed values rapidly to increase the difficulty of the task.

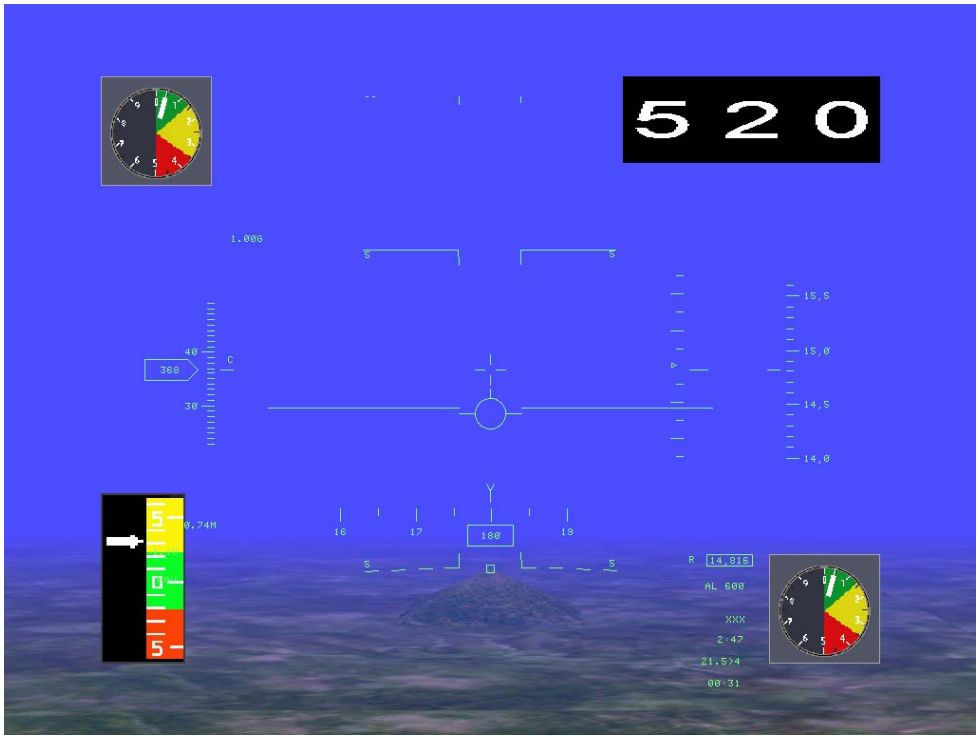

Figure 58: Display 3 has moved into the "unsafe zone"

Static Training

Each subject was trained statically on the Visual Monitoring task prior to dynamic training and data collection. Static training was performed in an F-16 mock-up fuselage equipped with an ACES II aircraft seat with a 15-degree seatback angle. The task was projected onto a 48-in. (vertical) x 64-in. (horizontal) screen. Subjects were given 30 trials of the task followed by a one minute rest period. This was repeated three times per static training day. A subject was considered trained when their performance deviated less than 10% between training days. Performance was assessed through response times and error rates.

Dynamic Training

Following the successful completion of static training, subjects were required to perform dynamic blend training over the course of several days. The subjects performed the Visual Monitoring task in the DES at 1 G_z each day to provide a baseline performance metric for comparison. They then performed the task during the same 3 G_z, 5 G_z, and 7 G_z plateaus and 7 G_z SACM profiles that were administered during the experimental test days. Each profile was given once per day in order of ascending G_z magnitude. A one-minute rest period was given after each G_z profile. Subjects were considered trained once their performance on the task deviated less than 10% between training days. Performance was measured by the percentage of correct responses to the task as well as response time. Dynamic training was conducted in order to ensure that no training effects were present in the final data that may have resulted from acclimation to performing the task in the high G environment.

Procedures

On a typical experimental test day, participants arrived at the laboratory, donned a flight suit and a standard G-suit, and were instrumented with electrocardiogram leads. The flight surgeon performed a brief medical examination and reviewed the subject's medical history. The participant then proceeded to the centrifuge where he/she donned a parachute harness. After entering the gondola of the centrifuge the participant was secured to the ACES II aircraft seat (with a 15-degree seat back angle) using a three-point aircraft restraint system. The ECG leads were connected and the signals were verified prior to securing the gondola of the centrifuge. The operator started the computer program to keep track of changes in the subject's oxygen

saturation levels. At this point, the Rapid Decision Making task was started and baseline performance data was collected over 20 presentations. After the baseline data was collected, the subject was then ready to begin the four G_z exposures.

The subject experienced each of the four G_z exposures on three different test days in the following order: 3 G_z 15-sec plateau, 5 G_z 15-sec plateau, 7 G_z 15-sec plateau, and 7 G_z SACM. The subject began the task approximately 8 sec prior to each G_z exposure and continued for approximately 8 sec after the acceleration had returned to the baseline G_z level of 1.5 G_z. A 1-minute rest period was provided between each G_z exposure, during which the task was not performed and the subject was permitted to relax at the baseline G_z level. This was accomplished to allow the physiology to return to the pre-acceleration exposure levels. During the SACM profile, performance data was collected for 6 presentations to measure the first half of the SACM against the second half. Following the completion of the four G_z exposures, the participant exited the centrifuge and was immediately examined by the flight surgeon and then released to return to his/her normal duties. These procedures were repeated over three experimental test days.

Results

Due to the fact that the G_z plateaus were only 15 seconds in duration (excluding the SACM profile), only two presentations of the task could be administered during each peak. Therefore, each subject performed, in order, a baseline run (20 trials), a 3 Gz plateau run (2 trials), a 5 Gz plateau run (2 trials), a 7 Gz plateau run (2 trials), and a SACM run (14 trials) on each of 3 experimental data collection days. A total of 13 trials resulted in a “time out,” denoting the subject did not make a response within the 15-second time limit. In addition, one trial was

found to have an abnormally fast response time of 0.03 sec and was classified as an outlier. This trial was not included in the analysis. Of the remaining 1147 trials, only 79 were incorrect (7%). When delineated across the profiles (including baseline), error rates were nearly identical. Hence, no statistical differences between the profiles could be found with respect to error rate.

Next, the data was analyzed with respect to the response time. Only trials resulting in a correct response were included in the analysis. Across all subjects and days, the baseline response time for correct trials ranged from 0.42s to 12.11s with median = 2.19s. Across all subjects and days, the response time for correct trials during the non-baseline runs (i.e., under G stress) ranged from 0.59s to 19.00s with median = 2.24s. The response times across trials were positively skewed. Therefore, geometric means of response time were generated within each subject, day, and display to account for the skew. The percent change from baseline for the same display was determined using these geometric means. A total of two analyses were peroformed. The first compared response time percent change from baseline during the 3 Gz, 5 Gz, and 7 Gz plateaus, and the 7 Gz plateaus ($G_z \geq 6.0$) of the SACM run. The second analysis compared response time percent change from baseline during the first half of the SACM run vs. the last half of the SACM profile.

In the first analysis, a repeated measures analysis of variance using the geometric means as the dependent variable found a significant difference among the displays {$F(3,27) = 10.55$, $p = 0.0001$}. The Bonferroni paired comparison procedure with a 0.05 familywise error level showed the mean for display 2 to be significantly higher than the other three displays with displays 1, 3, and 4 not significantly different from each other. Baseline geometric means were transformed back to seconds as follows: display 1 = 1.96s, display 2 = 2.85s, display 3 = 2.07s, display 4 = 2.08s.

Percent changes from baseline were averaged across day and display for each subject and Gz plateau. Figure 72 shows these percent changes from baseline for each subject and G_z profile. For the SACM, only trials during the 7 G_z plateau ($G_z \geq 6.0$) were used. The geometric mean of baseline response time is shown above each panel.

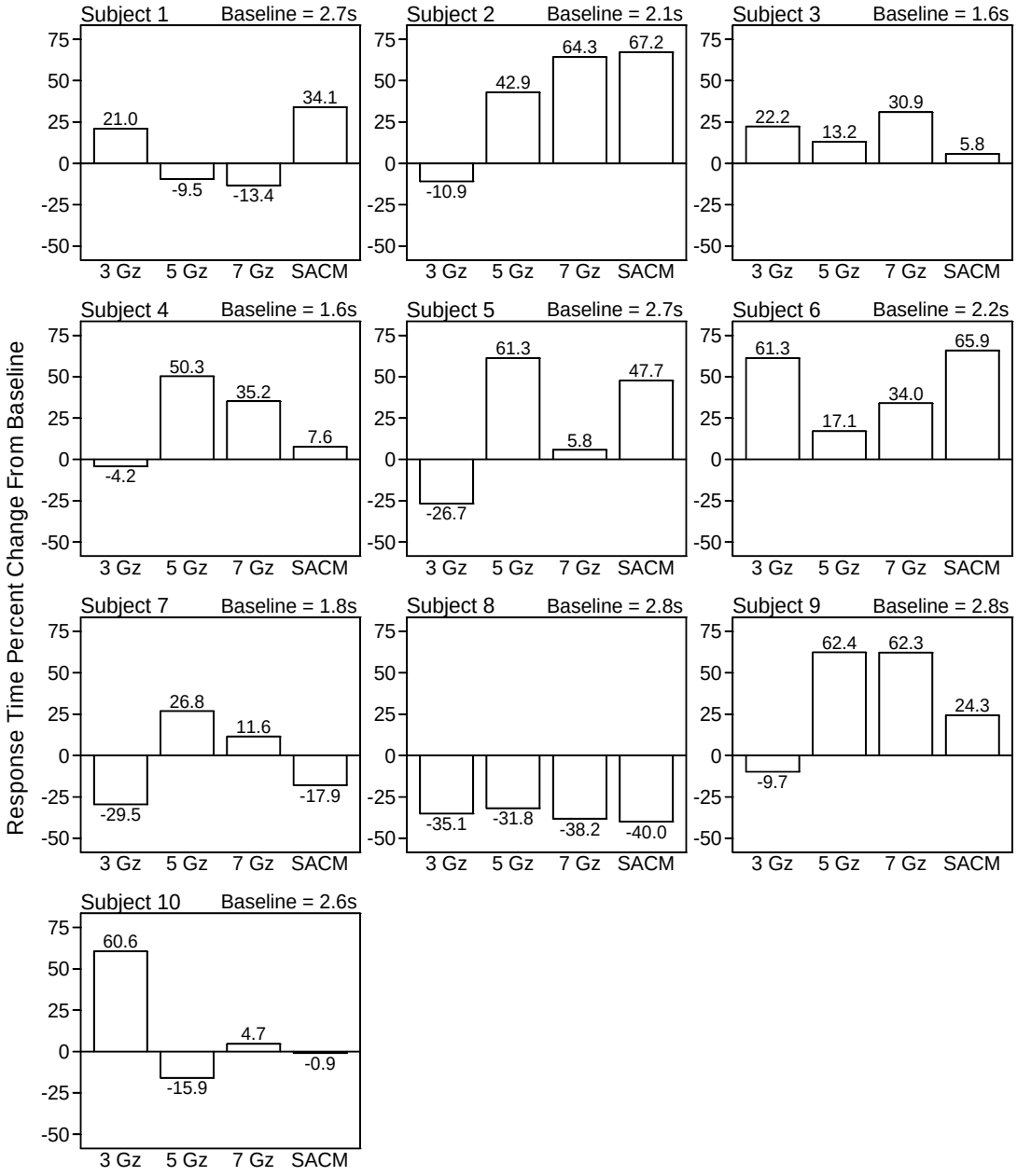

Figure 59: Mean response time percent change from baseline for each subject and Gz plateau.

Figure 73 displays the response time percent change from baseline for each subject during the first and second half of the SACM profile. The geometric mean of baseline response time is shown above the subject X-axis labels.

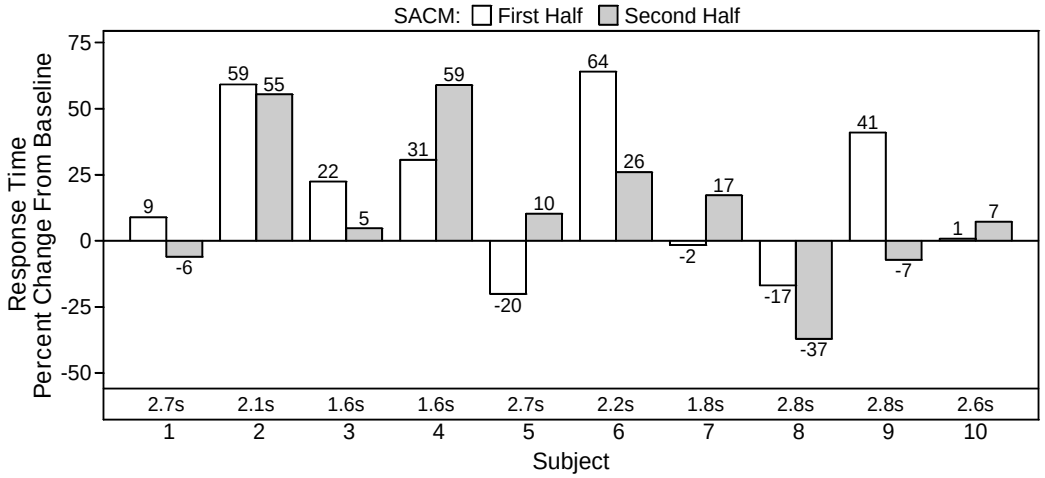

Figure 60: Mean response time percent change from baseline for each subject and SACM half.

Figure 74 contains the minimum, mean, and maximum response time percent change from baseline across subjects (N = 10). The overall baseline geometric mean of response time was 2.23s.

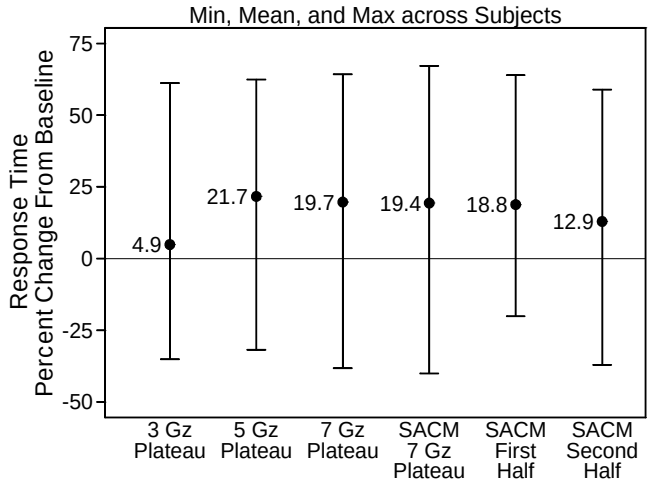

Figure 61: Minimum, mean, and maximum response time percent change from baseline across subjects.

Repeated measures analyses of variance were performed with the response time percent change from baseline as the dependent variable. In the first analysis, the F-test did not find a significant mean difference among the 3 Gz plateau, 5 Gz plateau, 7 Gz plateau, and SACM 7 Gz plateau {$F(3,27) = 0.76$, $p = 0.5285$}. Two-tailed t-tests using the subject means (no pooling) did not show the response time mean during any plateau to be significantly different from 0: 3 Gz plateau ($p = 0.6713$), 5 Gz plateau ($p = 0.0685$), 7 Gz plateau ($p = 0.0846$), and SACM 7 Gz plateau ($p = 0.1158$).

For the second analysis, the F-test did not find a significant difference between the first half and second half of the SACM {$F(1,9) = 0.48$, $p = 0.5044$}. Two-tailed t-tests using the subject means (no pooling) did not find the mean for the first half ($p = 0.0759$) or the second half ($p = 0.1896$) of the SACM to be significantly different from 0.

Discussion and Conclusions

The act of visually scanning an aircraft instrument cluster involves a variety of cortical areas that are primarily housed in the occipital lobe. Pressure, temperature, fuel readings, and other analog "round dials" are often designed to display a nominal value located either at the center or to one side of the gage to allow the pilot to perform a visual scan quickly. Here, the pilot is mainly looking for discrepancies or "oddballs," which upon detection require further scrutiny. As a result, areas such as V3 (visual processing of visual scene), V4 (analysis of form), V8 (color perception), and L0 (object recognition) are hypothesized to be the primary active areas during execution of this task. However, it should be noted that functional magnetic resonance imaging (fMRI) data is necessary to verify these hypotheses.

Evidence also suggests that instrument readings must occur serially due to the fact that they require fixation for the perception of the data in the display (Hayashi, 2003). Pilots utilize a scanning pattern formed by experience, training, and strategy in which they briefly fixate on a display A until the information contained therein is perceived. Next, they proceed to display B, fixate, perceive, and then proceed to display C, etc. This indicates that the peripheral visual field is not used to read instrument displays. It is possible that sudden changes, such as warning lights may guide the pilot's attention to a certain area or display, but this does not suggest an actual reading of the information presented. Therefore, it appears that the cortical tissues used in the visual monitoring task reside within the ventral stream (Baizer, Ungerleider, and Desimone, 1991). Even in a static +1 G_z environment, the blood pressure differs throughout the body based on the anatomic distance from the heart. Hence when standing, the blood pressure at eye level is less that the blood pressure at the level of the feet due to the force created by the product of the blood mass and the acceleration due to earth's gravitational pull. As this acceleration is increased (increasing G_z), this gradient becomes magnified and more blood begins to pool in the lower extremities. Even within the brain itself, a graded blood pressure will exist where dorsal areas (located furthest from the heart) will have lower blood pressures than ventral areas (closest to heart). Because the ventral stream would theoretically have higher blood pressures and thus higher oxygenated blood volume, it is probable that it is more resilient to increased G_z exposure than areas that are more dorsal.

The results indicate that the type of display may have an influence on the visual information processing performance. Specifically, the results indicated that the mean response time for the digital numeric display (display 2) was significantly higher than the other three. Displays 1, 3, and 4 could all be assessed by utilizing visual perceptions and comparisons.

Primarily, they relied on visual discrimination or the ability to perceive color, form, shape, and position. Hence, the subject simply had to recognize the needle and the color of the three areas. Then, he/she perceived the relative position of the needle to determine the area in which it resided. Conversely, display 2 did not provide a colored visual range for the subject to quickly assess its position (either safe or unsafe). Instead, subjects were required to recall from memory the nominal range (450-550) and compare this with the current value presented on this display. Hence, the processing of the data in display 2 likely required the engagement additional areas including the hippocampus (Carlson, 2007). This additional conscious thinking and memory retrieval likely caused the elongation of the response time. However, it should be noted that Krnjevic (1999) indicated hippocampal tissue is highly susceptible to hypoxia and anoxia. Hence, displays using numeric tables or values not only require more time to process but these response time may be further exacerbated by G_z. An analysis delineating response times for display 2 from the other 3 displays could not be completed from the data in this study due to the random selection of the display to augment during the trials coupled with the relatively few trials at G. There was simply not enough data to make any conclusions based on the type of display. Further study is necessary to explore this hypothesis.

Overall, the results of this experiment seem to suggest that monitoring of simple instruments that contain a nominal value range or "safe area" is not compromised during exposure of $+G_z$ up to +7. Both error rates and response times remained relatively unaltered across the G_z profiles and no statistically significant differences were discovered. This contradicts evidence from Warrick and Lund (1946) that noted significant declines in dial reading performance for relatively low G_z levels. Specifically, the task utilized in their experiment required subjects to view a series of 8 instrument dials, each with a corresponding

numerical reading presented above it. In some cases, the numerical reading was markedly different from the actual dial reading. In those instances, the subjects were required to denote the dial was reading incorrectly. Subjects were given a right-wrong score and an error rate (shown in the table below).

Table 9: Instrument Reading Scores Utilized in NTI, Inc.'s Look-up Tables (Warrick & Lund, 1946).

	1.5 G_z	3.0 G_z
Right-Wrong Scores	12.65	10.56
Errors	3.47	4.71

However, the task used by Warrick and Lund (1946) required subjects to make a comparison between a numerical or digital value and the dial reading. As previously stated, comparisons of digital values are more difficult than dial readings, which may have lead to the increased error rate. Additionally, it is likely that the anatomic position of the cortical areas required for this task contribute to their ability to continue to function in the presence of the stress from the inertial environment. Additionally, because the subjects were instructed to maintain clear vision throughout each of the G_z exposures by executing a stronger AGSM when necessary, it follows that cortices involved with visual processing will retain adequate blood pressure and oxygen throughout the profile.

The findings of this study suggest negative effects of acceleration do not exist in the task of visual monitoring a series of instruments. As a result, it is likely that pilots will be able to accurately assess the state of critical aircraft systems and respond appropriately even after sustained acceleration (up to 7 G_z). Visual scans appear to be protected both by the ventral anatomic position of the cortices involved in visual processing and the endeavor to maintain vision during high-acceleration maneuvering. As a result, a model of human information processing in the G_z environment will not need to account for visual monitoring.

CHAPTER 11: TASK 11 – SHORT-TERM MEMORY

Introduction

Successfully executing a mission in the flight environment certainly involves accurate perception of sensory stimuli such as enemy targets, cockpit audio warnings, and instrument readings (as described in the previous chapters). However, occasionally decisions and comparisons require the retention of sensory information for a short amount of time (typically several seconds). For example, when receiving flight instructions from air traffic control or a wingman, the pilot must not only perceive the audio sensory information, but also retain it for a short amount of time to execute the instructed procedures once the sensory stimulus has arrested. Additionally, when attempting to reconcile his/her current position with that displayed on a digital map prior to landing, he/she must first fixate on the map and then recall certain features when viewing the out-the-window scene to assess the position of the aircraft and the relative distance to the runway. This brief storage of information is commonly referred to as perceptual short term memory. It is well-known that the amount of data capable of being stored in short-term memory (STM) is limited and highly transient. In fact, the number of items that can be stored in STM (7 ± 2) was originally theorized by George Miller (1956) and is still valid today.

The brain is capable of modifying activity across a distributed neural network by mechanisms known as brain plasticity (Bliss and Lømo, 1973). Neurons are engaged in neural networks capable of dynamic change to generate adaptable, efficient responses to a changing environment. Plasticity refers to the modification of synaptic strength through biochemical or structural alterations that serve to support neural adaptation to external stimuli and is essential to the survival of the organism (Carlson, 2007; Messaoudi, et al., 2007). Hebb (1949) originally hypothesized that the modifications to synaptic strength within existing neuronal networks

constitute the formation and consolidation of new memories. Once formed, these synaptic changes are not static. In fact, it is now known that even long-term memories that were once thought to be "hardwired" are influenced by new experiences and can be revised throughout the life of the organism (Bruel-Jungerman, Davis, & Laroche, 2007). Short-term memories essentially are a result of sensory neural activity (primarily in the sensory association cortices) that remains after the stimulus has terminated or been removed. Hence, even though typical long-lasting plastic changes such as long-term potentiation (LTP) and long-term depression (LTD) have not been accomplished, the neural activity is capable of remaining between 2-30 seconds.

In addition to brief activation of the sensory association cortices, there is evidence that the frontal cortex also exhibits activity during STM in monkeys (Funahashi, Bruce, and Goldman-Rakic, 1989). Likewise, Courtney, et al. (1998) discovered the human prefrontal cortex is active during delayed match-to-sample tasks (Carlson, 2007). Other areas of the brain such as the dorsolateral prefrontal cortex and the inferior prefrontal cortex become active due to conscious thought about the information to be remembered. For example, in the retention of object information, a subject may think about the way the object appears, how the word is pronounced, what the word looks like, etc. (Carlson, 2007). Although hippocampal activation is critical in the formation of new memories and retention of information, it does not appear to be crucial for short-term memory. In fact, patients with damage to the hippocampus (diagnosed with anterograde amnesia) are not able to form new memories but can retain small amounts of information up to 30 seconds (Milner, Corkin, and Teuber, 1968; Milner, 1970).

This experiment used an audio procedural task in which subjects were forced to recall verbal instructions for a short amount of time. As a result, it is likely that in addition to regions

of the prefrontal cortex, areas of the brain responsible for the processing of speech such as Wernicke's area will be necessary for successful completion of the task. Additionally, the primary auditory cortex located in the superior temporal lobe will be actively engaged. Therefore, the ability to retain and recall the instructions from the short-term memory store under sustained acceleration will likely hinge on the ability of the heart to pump an adequate supply of oxygenated blood to sustain metabolic processes in these key regions. This study was focused on measuring objective STM performance during operationally relevant acceleration (G_z) levels.

Methods

Subjects

Seven active duty members (5 male, 2 female) volunteered to participate in this study and ranged in age from 24 to 35 years old, with a mean age of 29 years. All participating subjects were members of the sustained acceleration stress panel at Wright-Patterson AFB, OH. Requirements to qualify for participation in this study are identical to those of chapter 2 (ref chapter 2, Methods section). Subject 8 dropped out of the study early due to scheduling conflicts and did not perform day 3 of data collection.

Facilities

All training and data collection for this study was performed at the Air Force Research Laboratory's Dynamic Environment Simulator (DES) centrifuge facilities at Wright Patterson AFB (ref. Chap. 2, Figure 3). The DES is a human rated centrifuge with an arm radius of approximately 19 feet. It is capable of attaining and sustaining accelerations up to 20 G in either of three independent axes: x, y and z. The DES has a maximum G onset and offset rate of approximately 1 G/sec. The gondola of the centrifuge was equipped with an F-22-like ACES II

ejection seat with a seatback reclined to 15^{o} from vertical. As illustrated in Figure 2 (ref. Chap. 2), the seat had adjustable lap and shoulder restraints.

An aircraft IC-10 communication system was used to provide two-way voice-communication between the research participant and the investigator. The participant's microphone was fixed in the open position to allow the participant "hands-free" communication. Participants were also provided with an emergency abort switch that enabled them to stop the centrifuge at any time during testing. Participants wore a standard Air Force issue Nomex® flight suit and a standard G-suit during all testing runs.

The gondola was outfitted with a simulated fighter cockpit. The cockpit incorporated a Thrustmaster Hotas Cougar flight stick (Guillemot, Montreal, Canada) mounted on the participant's right side that was used to secure responses to the performance task. A six foot hemispherical shell viewing screen, representing a 130^{o} (vertical) x 180^{o} (horizontal) visual field, mounted directly in front of the participant. A separate projector was used to display the performance task in the center of the subjects' field-of-view with a projected image of 22.5" (width) by 18.5" (length). The large dome display was used to present two red dots located at approximately 60^{o} of visual angle to the right and left of the center of the dome and approximately 5^{o} in diameter. In addition, a red circle was displayed just above the HUD that represented 10^{o} of visual angle. The dots served as a reference to the subject of his/her visual loss. Should the smaller dots not be visible in the periphery, the subject was instructed to compensate by increasing their AGSM. They were to abort the test should their vision degrade to the point that only the center red dot was visible. Figure 4 (ref. chapter 2) provides an illustration of the entire visual system.

Continuous surveillance of participants was provided by two closed-circuit infrared television cameras. The cameras offered a close-up view of the participant's head and a wide-angle view of the participant from head-to-foot. Research personnel housed in a control room observed the video images. A video mixer was used to generate a composite picture of the two views of the participant along with the time, date, electrocardiogram (ECG) data, and G_z acceleration in a given run. Video data were stored on ½ inch VHS videotape.

Acceleration Profiles

A total of four G_z acceleration profiles were generated for use in this study. All G_z exposures were started from a baseline acceleration of 1.5 G_z. The first three profiles comprised of a 1 G/sec onset ramp to a 15-sec plateau followed by a G_z offset ramp of 1 G/sec down to the baseline acceleration level. The plateaus were 3, 5, and 7 G_z, respectively. The final acceleration exposure was a simulated aerial combat maneuver (SACM). This profile consisted of two 5-sec G_z peaks to 7 G_z with several intermittent peaks to 3 and 5 G_z. Figure 6 (ref. chap. 2) displays an example of a G_z plateau profile, while Figure 7 (ref. chap. 2) presents the SACM profile.

Stimuli

The subjects completed a "short-term memory" (STM) performance task during each G_z profile on each experimental test day. This task was projected on a six foot hemispherical shell viewing screen, representing a 130^o (vertical) x 180^o (horizontal) visual field but only directly in front of the subject spanning of 18" x 18". The task utilized both a simulated view of out-of-

window terrain and a heads-up-display (HUD) (Figure 75). The HUD instrument readings relevant to this task included the pitch ladder and the scrolling heading readout.

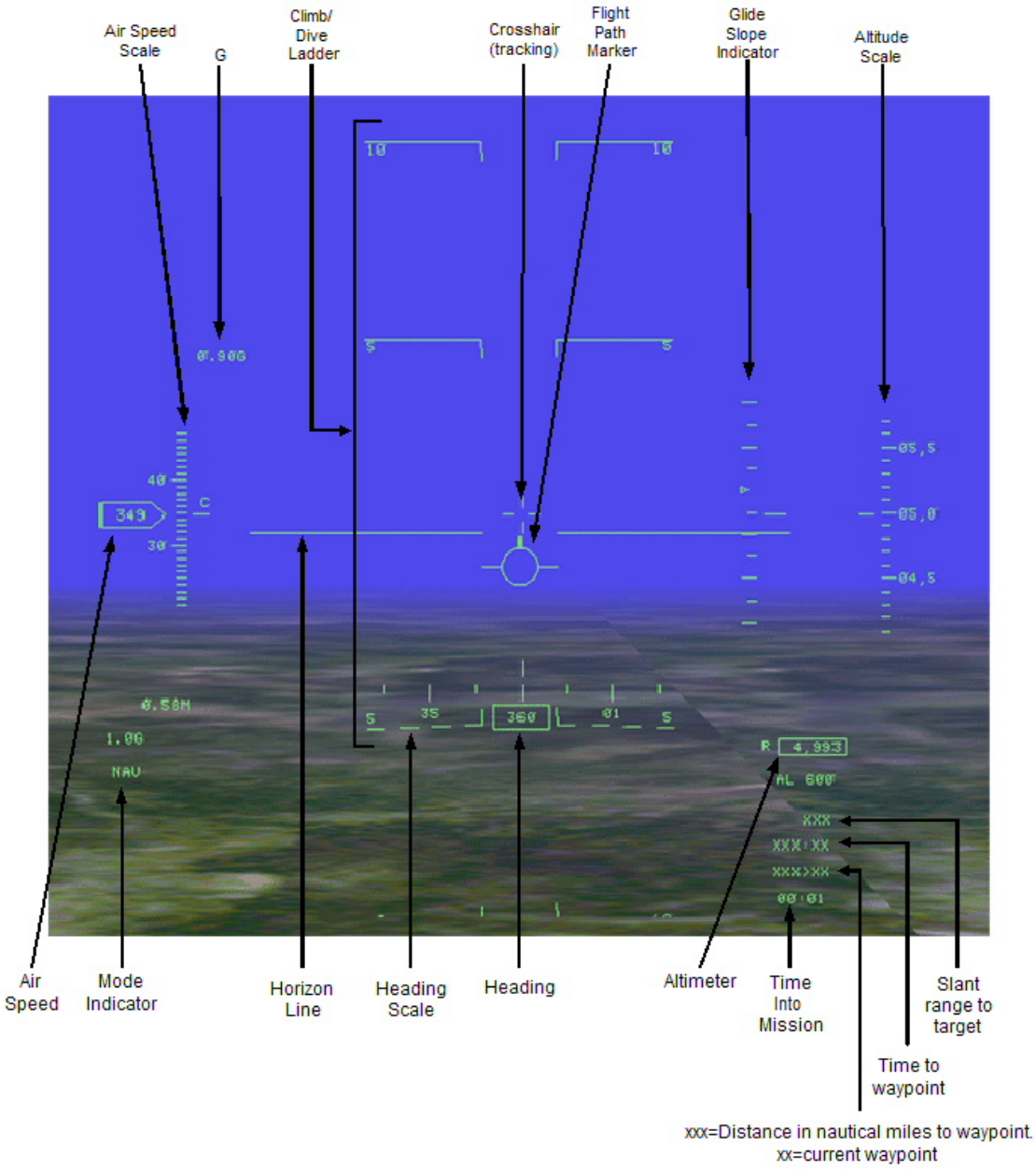

Figure 62: Short-Term Memory Out-the-Window Display with HUD

Prior to execution of the task, the subject was given a set of three instructions to remember and carry out. The instructions involved either pitching a specified number of degrees

or directing the aircraft to a specific heading. The subject was instructed to maintain level flight without changing the plane's pitch, heading, or air speed. Following 7 seconds of straight and level flight, a brief 1 kHz audio tone was presented through the headset to direct the subject to execute the first instruction in the set. Seven seconds after the first tone, the subject heard a second 1 kHz tone was presented to signify that the second instruction in the set was to be completed. Likewise, 7 seconds following the second tone, a third 1 kHz tone was played and the subject was to execute the last of the instructions. Seven seconds after the third tone was played, the task was arrested by the investigator.

The pitch and heading values in the instructions were randomly selected increments within a pre-specified value range. For pitch, values ranged from -25º and 25º (inclusive) in increments of 5º. Heading values varied between 150º and 210º (inclusive) in increments of 10º. For both pitch and heading, the subject was asked to obtain a true pitch or heading within ± 5º of the commanded value. After a subject achieved a specified pitch, he/she was required to return to straight and level flight in preparation for the next tone.

During the training days, the subject received only three sets of instructions, each consisting of three commands for the baseline profile. This was augmented to fourteen sets of instructions during baseline data collection on experimental test days. Three sets were used for data analysis; each of these sets was repeated three times within the fourteen baseline sets. The remaining five sets of instructions were randomized to avoid cue recognition and anticipation by the subject; these data points were not included in analysis. For the 3 G_z, 5 G_z, and 7 G_z plateau profiles, the same three sets of instructions that were used in the baseline data collection runs were randomized across subject and profile for each data collection day. During the 7 G_z SACM, the subject received a set of instructions consisting of four commands, the first and

second of which also served as the third and forth. These cues were also randomized across subjects for each data collection day. In each SACM, the subject was instructed to return to heading 180º at the third beep. This method was utilized in order to provide a basis for comparison of the subject's performance between the first and second halves of the SACM. For the SACM, the cues were randomized across subjects for each data collection day. Figure 76 portrays an illustration of the flight control stick utilized in this experiment.

Figure 63: Hotas Cougar Flight Stick for Short Term Memory Task

Static Training

Each subject was trained statically on the STM task prior to dynamic training and data collection. Static training was performed in an F-16 mock-up fuselage equipped with an ACES II aircraft seat with a 15-degree seatback angle. The task was projected onto a 48-in. (vertical) x 64-in. (horizontal) screen. Subjects were given 6 sets of instructions, each consisting of three different commands to execute. Following each set of instructions, the subject was given a one

minute rest period. A subject was considered trained when their performance deviated less than 10% between training days. Performance was assessed through response times and error rates.

Dynamic Training

Following the successful completion of static training, subjects were required to perform dynamic blend training over the course of several days. The subjects performed the STM task in the DES at 1 G_z each day to provide a baseline performance metric for comparison. They then performed the task during the same 3 G_z, 5 G_z, and 7 G_z plateaus and 7 G_z SACM profiles that were administered during the experimental test days. Each profile was given once per day in order of ascending G_z magnitude. A one-minute rest period was given after each G_z profile. Subjects were considered trained once their performance on the task deviated less than 10% between training days. Performance was measured by the Performance was measured by the percentage of correct aircraft manipulations performed within ±5º from the instructed values as well as response time. Dynamic training was conducted in order to ensure that no training effects were present in the final data that may have resulted from acclimation to performing the task in the high G environment.

Procedures

On a typical experimental test day, participants arrived at the laboratory, donned a flight suit and a standard G-suit, and were instrumented with electrocardiogram leads. The flight surgeon performed a brief medical examination and reviewed the subject's medical history. The participant then proceeded to the centrifuge where he/she donned a parachute harness. After entering the gondola of the centrifuge the participant was secured to the ACES II aircraft seat

(with a 15-degree seat back angle) using a three-point aircraft restraint system. The ECG leads were connected and the signals were verified prior to securing the gondola of the centrifuge. Following this, the cerebral oximeter was secured around the subject's forehead. The operator started the computer program to keep track of changes in the subject's oxygen saturation levels. At this point, the Short Term Memory task was executed and baseline performance data was collected over 14 presentations. Once complete, the subject was ready to undergo the four G_z exposures.

The subject experienced each of the four G_z exposures on three different test days in the following order: 3 G_z 15-sec plateau, 5 G_z 15-sec plateau, 7 G_z 15-sec plateau, and 7 G_z SACM. The task began approximately 8 sec prior to each G_z exposure and continued for approximately 8 sec after the acceleration had returned to the baseline G_z level of 1.5 G_z. The first beep occurred just as the subject reached the beginning of each plateau and the next two beeps after seven second breaks. A 1-minute rest period was provided between each G_z exposure, during which the task was not performed and the subject was permitted to relax at the baseline G_z level in order for the subject's physiology to return to normal, resting levels. During the SACM profile, performance data was collected over 5 presentations to measure the first half of the SACM against the second half. Following the completion of the four G_z exposures, the participant exited the centrifuge and was immediately examined by the flight surgeon and then released to return to his/her normal duties.

Results

The short term memory task performance was assessed using error rates and time to respond. Errors consisted of actions incongruent with the instructions (e.g. pitching down 15

degrees when the instruction was to pitch up 15 degrees) or a lack of action when an action was required (e.g. subject did not perform the instruction following the tone). Of the 1100 total instructions (3 instructions per trial), 62 were responded to incorrectly (6%). Segregated by run type, there were 20 incorrect baseline trials (2%), 10 incorrect 3 Gz trials (17%), 12 incorrect 5 Gz trials (20%), 8 incorrect 7 Gz trials (13%), and 12 incorrect SACM trials (15%). Although the error rates during the G_z profiles did not differ significantly from each other, there were more errors during the non-baseline runs than during baseline runs.

The response time was measured from the time the tone sounded and the instruction was completed. Completion was determined once the subject remained within $\pm$5 degrees of the desired pitch or heading. Only trials resulting in a successful action for the given instruction were utilized in this analysis. Across all subjects and days, the baseline response time for correct trials ranged from 0.92s to 7.70s with a median of 2.81s. Likewise, the response time (across subjects and days) for correct trials during the non-baseline runs ranged from 0.96s to 7.76s with a median of 2.76s. The data was normalized across subjects and days by calculating the percent change from the baseline performance values. For any particular instruction given during the non-baseline runs, the baseline value used for percent change was the mean across baseline trials of the same instruction (n = 3 or 4). Once percent changes were determined, they were averaged across instruction and day (n = 9 for plateaus with 3 instructions and 3 days, n = 6 for SACM with 2 instructions and 3 days). These mean percent changes are shown in Figure 64 (SACM halves combined). Additionally, mean percent changes from baseline response time during the first and second half of the SACM are displayed in Figure 65. Only baseline trials with the same instruction as some non-baseline trial were used to determine the baseline mean shown in Figures 64 & 65 (the value above subject label is the baseline mean).

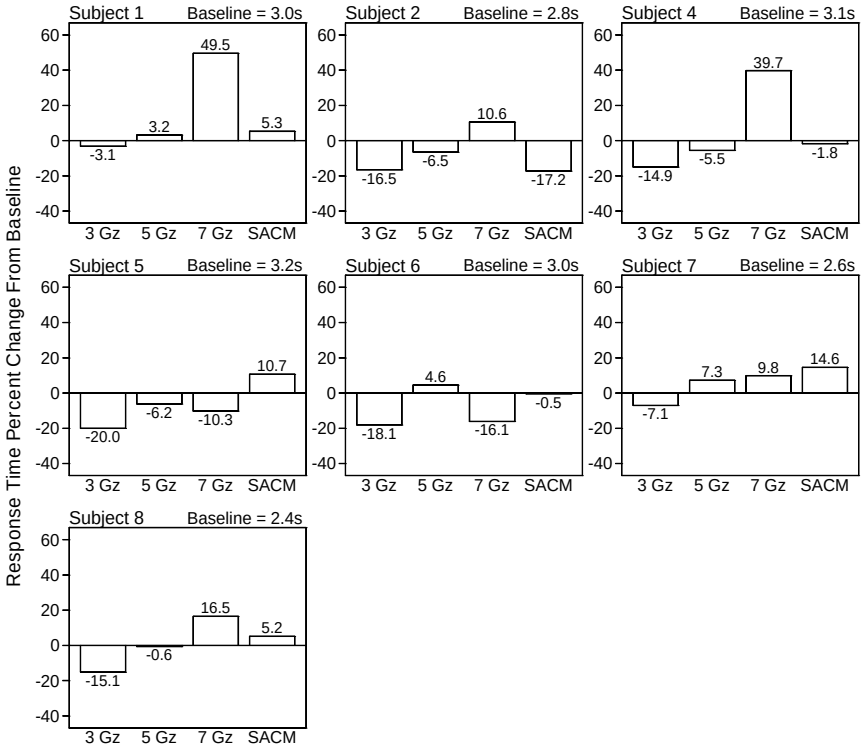

Figure 64: Short Term Memory Mean Response Time Percent Change from Baseline for Each Subject

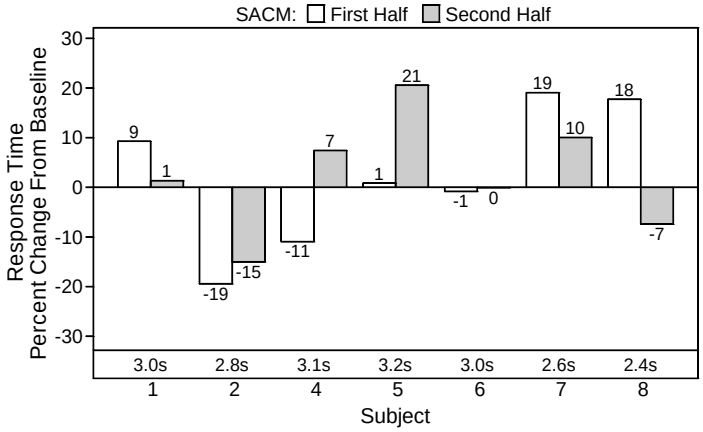

Figure 65: Short Term Memory Mean Response Time Percent Change from Baseline for Each Subject and SACM Half

Figure 66 contains the minimum, mean, and maximum response time percent change from baseline across subjects and experimental days (N = 7).

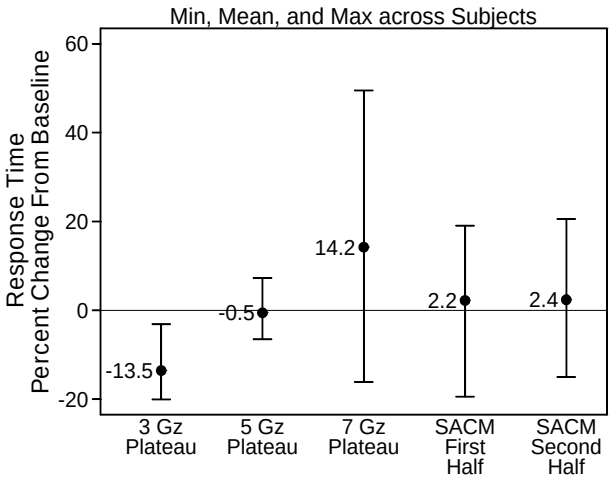

Figure 66: Minimum, Mean, and Maximum Response Time Percent Change from Baseline across Subjects (N=7)

A repeated measures analysis of variance was performed with response time percent change from baseline as the dependent variable. The factor was run type (3 Gz, 5 Gz, 7 Gz, SACM first half, SACM second half). The F-test found a significant difference among the run types {$F(4,24) = 3.96$, $p = 0.0132$}. Post-hoc paired comparisons of run type used the Bonferroni paired comparison procedure with a 0.05 experiment-wise error level. The only significant mean difference among the runs types was between 3 Gz (mean % change = -13.5) and 7 Gz (mean % change = 14.2) with $p = 0.0006$. To determine whether any run type mean percent change was significantly different from 0, two-tailed t-tests were performed using subject means with no pooling of error across run type. The only run type with a mean percent change significantly different from 0 was 3 Gz (mean % change = -13.5, $p = 0.0011$). The 14.2% change for 7 Gz was not significant ($p = 0.1672$).

Discussion and Conclusions

Positive G_z acceleration can greatly reduce regional cerebral oxygen saturation potentially leading to performance degradations (McKinley et al., 2005). Given that the hippocampus appears to be heavily involved in the formation of memories and is highly susceptible to reductions in oxygen, it was necessary to quantify the effects of high acceleration (hence, reduced oxygen supply) on short term memory. In fact, the hippocampus has been shown to be one of the first brain structures to arrest function in the absence of available oxygen (Krnjevic, 1999). This is thought to be a protective mechanism to conserve energy needed to sustain vital functions necessary to the preservation of life of the individual pyramidal cells (Krnjevic, 1999). The results of this experiment showed elevated error rates during G_z acceleration but failed to show statistically significant differences in short term memory response time. In fact, performance was actually *enhanced* during the 3 G_z plateau.

When delineating the response time data into the individual subjects (see Figure 64), five of the subjects experienced elevated response times during the 7 G_z plateau. Subjects 5 and 6 appeared to have a null or positive performance response during each of the G_z profiles with respect to response time. Hence, some subjects may have a delayed recall of memorized data or information during high acceleration (>5 G_z). It is possible that such an effect was masked by the superior performance exhibited by subjects 5 and 6 and that the effects of G_z may become significant with a much larger subject pool. However, this effect cannot be derived conclusively from the results of this experiment. Nevertheless, a model of the effects of acceleration on cognition warrants a conservative estimate given that over half of the subjects experienced degraded performance under G_z. As a result, the data will be used in model development and verification.

Although not statistically significant, the fact that over half of the subject population in this relatively small subject pool exhibited at least some short term memory deficiencies is noteworthy. In explicating the link between the cerebral physiology and metabolism with human behavior and performance metrics, it is important to describe the underlying neuronal mechanisms and the effects of hypoxic conditions on the cellular functions. Because neural pathways linked with learning and memory reengage during retrieval, it follows that the underlying mechanisms are utilized in a wide variety of cognitive abilities. Coupled with the deluge of scientific research concerning the formation and retrieval of memories, the cellular mechanisms of learning can provide a great deal of insight concerning the importance of energy and oxygen delivery to neurons.

Neural tissue consumes a large amount of energy derived exclusively from glucose due to the fact neurons are not capable of metabolizing fats or carbohydrates. To match the metabolic demands of the active tissue, glucose is converted to adenosine triphosphate (ATP) through aerobic respiration processes (glycolysis, Krebs cycle, and the electron transport system). Although the Na-K pumps utilize a considerable amount of ATP, approximately 60% is devoted to protein synthesis utilized for cell structures as well as enzymes, receptors, and neurotransmitter release, reuptake, and transport (Hochachika, 1996). These tasks are particularly relevant to mechanisms of learning and memory, namely synaptic plasticity.

A sudden loss of oxygen supply to neural tissue can be crippling at the cellular level, although not all structures are affected equally. Krnjevic (1999) attributes this trend to differing metabolic needs. Cortical tissues involved in high-order processing are more active than those ascribed to lower order functioning including autonomic functions and sustainment of the life of the organism. This is supported with evidence from Gerard (1932) that the peripheral nervous

system and lower central nervous system are not particularly sensitive to acute hypoxia. Of notable interest is the fact that the hippocampus appears to be extremely sensitive to the absence of oxygen and is often the first to arrest function (Sugar & Gerard, 1938). Given this evidence, it is compelling to investigate the cellular mechanisms that contribute to the decline in neural activity resulting from declined oxygen supply.

Hypoxia tends to illicit several predictable responses from hippocampal neurons thought to be protective measures to ensure the survival of the cell. This is critical because neurons do not replicate like other cells of the body and neuron-genesis in adults tends to be infrequent at best. One of the more pronounced changes during hypoxia is increased permeability to potassium ions (K^+) (Hansen, Hounsgaard, & Jahnsen, 1982). This allows the high concentration of K^+ inside the cell to diffuse outside into the interstitial fluid. The mass exodus of positive charge from the cell creates a hyperpolarization of the membrane. Consequently, the threshold of excitation is much greater than normal resulting in fewer action potentials that serve to assuage the need for additional ATP (Krnjevic, 1999). The cause of K^+ permeability changes can be attributed in part to an increase in Ca^{2+} ions in the cytoplasm (Krnjevic, 1975). Because oxygen is in short supply, ATP is produced exclusively from anaerobic glycolysis. NADH remains a byproduct, but it cannot be utilized to make ATP due to the absence of oxygen. As a result, it likely interacts with other structures such as inositol triphosphate ($Insp_3$) receptors (Krnjevic, 1999). $Insp_3$ are second messengers that release Ca^{2+} ions stored within the cell (Madesh, et al., 2005). The increase in internal Ca^{2+} triggers Ca^{2+}-activated K^+ (K_{Ca}) channels to open (Leblond, & Krnjevic, 1989).

Both the hippocampus (Erdemli, Xu, and Krnjevic, 1998) and Purkinje Cells (found in the cerebellum and also particularly sensitive to hypoxia) (Ballanyi, 2004), contain ATP-

sensitive K^+ channels (K_{ATP}). These channels require continuous ATP to remain closed and will open in the absence of available energy. Although the initial release of K^+ serves to decrease neuronal excitability and conserve ATP, energy levels are still reduced by approximately 15% (recorded when K^+ is elevated), indicating K_{ATP} channels aid in the release of K^+ (Lipton & Whittingham, 1982; Ballanyi, 2004). Purkinje Cells in particular were found to exhibit two rapid increases in Ca^{2+} during hypoxic conditions (Ballanyi, 2004). The findings indicate the first Ca^{2+} rise was attenuated by K^+ release through K_{ATP}. Because Ca^{2+} can initialize apoptosis or irreversible cell damage, the increase permeability to K^+ serves as a protective mechanism by decreasing cell excitability thereby reducing ATP consumption and diminishing the entry of additional Ca^{2+} caused by excitatory signals.

The increase permeability to K^+ also appears to bring forth modifications to the synapse itself. Specifically, postsynaptic excitatory postsynaptic potentials (EPSPs) decline as a direct result of a lack of neurotransmitter (glutamate) release from the presynaptic membrane (Leblond, & Krnjevic, 1989). Furthermore, adenosine accumulation is known to coincide with hypoxic conditions. The rise is caused by ATP being converted to ADP and AMP resulting from an increased lack of glucose (Centonze, et al., 2001). As adenosine binds to presynaptic adenosine A1 receptors, neural excitability is reduced resulting in less glutamate release (Centonze, et al., 2001; Krnjevic, 1999).

Alternatively, a large amount of the hippocampal formation resides below the horizontal plane within the brain. As seen in chapters 6 and 8 of this report, those structures positioned dorsal to the horizontal plane appear to experience marked reductions in oxygenated blood supply evidenced by reduced oxygen saturation values recorded by the cerebral oximeter. Therefore, oxygenated blood supply may not be compromised at the lower G_z levels (3 and 5 G_z)

and may explain the reason for the response time performance stabilization during those profiles, although error rates remain elevated. This is thought to be a result of interactions with regions of the frontal cortex (organization) that is more sensitive to G_z. Given that the hippocampus is near (some of it even above) the horizontal plane, it is likely susceptible only to the larger G_z levels (e.g. 7 G_z and higher).

Lastly, and perhaps most importantly, the two subjects experiencing no performance decrements in this experiment were the shortest individuals. As a result, the distance from the heart to the brain was smaller than the other subjects which may have permitted preservation of oxygenation to their critical brain structures. As a result, their performance was not affected by increased $+G_z$.

In conclusion, it appears that a preponderance of the subjects experienced declines in short term memory performance during extended periods at 7 G_z (~15 seconds). This is hypothesized to be a direct result of cellular mechanisms devoted to the protection of hippocampal cells. Additionally, the anatomic position of the hippocampal formation places it at the cusp of performance degradations likely resulting in adequate perfusion during the 3 and 5 G_z profiles. This produced the relatively stable performance during these profiles. The lack of performance declines during the SACM likely resulted from the fact the subjects were only required to memorize two instructions. To ensure valid statistical comparisons between the two halves of the SACM, the instructions had to be identical in each half. As a result, the task may have been overly simplified to be sensitive to hypoxic conditions caused by G_z. Future studies should incorporate a more difficult task during the SACM. Lastly, performance may be influenced by the height of the individual. Further study is necessary to ensure this is indeed a contributing factor.

CHAPTER 12: THE G-TOOL TO OPTIMIZE PERFORMANCE (G-TOP) MODEL VERIFICATION

Introduction

Under the HIPDE program, a phase II small business innovation research (SBIR) contract with NTI, Inc. was utilized to develop a cognitive model of human cognitive performance under operationally relevant positive accelerations. A description of the model can be found in chapter 1 of this report. The primary purpose of the experiments described in chapters 2-11 was an effort to verify the validity of the model predictions. Given that acceleration experimentation with human subjects is costly and presents a higher than normal level of risk to the subjects, the literature search conducted by NTI, Inc. returned many holes. In fact, the findings showed many of the studies were conducted at 5 G_z or less thereby making the generation of the model database difficult. The solution was to linearly extrapolate the data from the low G_z to the high (up to +9 G_z) to provide an approximation of the expected values. Unfortunately, many systems involving human physiology are non-linear, indicating that the approximations may not be valid. However, with no supporting data, an equation describing the non-linearity could not be derived.

Because each of the performance tasks used in the experiments described in chapters 2-11 often involved multiple cognitive abilities, the resulting data from each test had to be delineated across each cognitive factor. As stated in chapter 1, this was performed using a weighting table referred to as the T-Matrix (ref. chapter 1). This weighting had to be calculated for each ability and G_z level (3, 5, and 7). The resulting data were then compared to the data extracted from the literature as well as the linear extrapolations to ensure validity.

Methods

The findings from the studies described in chapter 2-11 were normalized by calculating the mean percent change in baseline for each of the profiles. Baseline performance was ascribed a value of 100% and reductions in performance (if found in the corresponding study) were subtracted from this value. Weighted values were then calculated using the T-Matrix estimates found in Table 1 (ref. chapter 1). Essentially the T-Matrix score for a particular task (e.g. perception of relative motion) was divided by the sum of all the scores for a specific cognitive ability (e.g. instrument reading). The result was the weighting factor that was then multiplied by the normalized data from the HIPDE experimental results. This was repeated for each G_z level, 3, 5, and 7. An example of this weighting procedure can be found in table 10 below. The table presents data from the 3 G_z plateau and only the "instrument reading" and "simple decision making" abilities for illustration purposes.

Table 10: Example of the Weighting Calculations per Cognitive Ability

3 Gz Data

	Instrument Reading				Simple Decision Making			
	T-Matrix Score	Weighting Factor	Performance [%]	Weighted Data	T-Matrix Score	Weighting Factor	Performance [%]	Weighted Data
Perception of Relative Motion	0.000	0.000	100.000	0.000	1.000	0.029	100.000	2.857
Precision Timing	0.000	0.000	100.000	0.000	4.000	0.114	100.000	11.429
Motion Inference	0.000	0.000	100.000	0.000	6.000	0.171	100.000	17.143
Pitch/Roll Capture	0.000	0.000	100.000	0.000	3.000	0.086	100.000	8.571
Peripheral Processing	5.000	0.161	100.000	16.129	6.000	0.171	100.000	17.143
Decision Making	0.000	0.000	100.000	0.000	2.000	0.057	100.000	5.714
Basic Flying Skills	7.000	0.226	100.000	22.581	3.000	0.086	100.000	8.571
Gunsight Tracking	0.000	0.000	75.000	0.000	1.000	0.029	75.000	2.143
Situation Awareness	6.000	0.194	121.000	23.419	1.000	0.029	121.000	3.457
Unusual Attitude Recovery	9.000	0.290	100.000	29.032	3.000	0.086	100.000	8.571
Short Term Memory	0.000	0.000	98.250	0.000	4.000	0.114	98.250	11.229
Visual Monitoring	4.000	0.129	100.000	12.903	1.000	0.029	100.000	2.857
T-Matrix Score Totals	31.000				35.000			
Mean Performance			99.521				99.521	
Sum of Weighted Data				104.065				99.686

Mean percent changes from baseline for each profile and HIPDE task were used as the "Performance %" (see table 10) in the weighting calculations. Only those values resulting in statistically significant percent changes from baseline were included. All others were given a value of 100% as they did not differ from baseline. The only exception to this rule was the

"short term memory" task. As detailed in chapter 11, a majority of the subjects experienced elevated response times and error rates during the non-baseline profiles. As a result, these values were included in the weighting calculations. Because G_z acceleration affected two separate metrics significantly in the "short term memory" task (error rate and response time), the percent changes from baseline were averaged. These averaged values were then used in the weighting calculations as the performance percentage.

Once the weighted scores were calculated, they were summed within each of the cognitive abilities (columns) at each G_z level. An example of the summed scores can be found in the last row of table 10 above. It is these values that constitute the final performance metrics that were then compared to the G-TOP model database (look-up table) values.

Results

Final summed scores for each of the 11 cognitive abilities across the 12 HIPDE tasks were collected and displayed in table 11 below. Values above 100 denote an improvement in performance over baseline.

Table 11: Cognitive Ability Performance for Each G_z Level

	Instrument Reading		Simple Decision Making		Visual Acuity		Complex Decision Making Accuracy	
Gz	Data	Model	Data	Model	Data	Model	Data	Model
1	100.000	100.000	100.000	100.000	100.000	100.000	100.000	100.000
3	99.686	64.000	99.686	90.000	100.179	85.000	104.337	96.000
5	101.871	46.400	94.874	72.500	94.079	34.000	102.859	100.000
7	103.016	28.800	91.451	47.500	85.925	28.400	104.313	85.000
	Complex Decision Making RT		Complex Decision Making Efficiency		Tracking		Slow Motion Inference	
Gz	Data	Model	Data	Model	Data	Model	Data	Model
1	100.000	100.000	100.000	100.000	100.000	100.000	100.000	100.000
3	102.683	87.000	101.670	45.000	96.318	90.000	97.036	89.000
5	101.883	75.000	100.398	33.000	92.323	80.000	91.418	27.000
7	102.827	69.500	100.691	28.250	80.191	50.000	79.675	20.200
	Fast Motion Inference		Spatial Orientation		Perceptual Speed			
Gz	Data	Model	Data	Model	Data	Model		
1	100.000	100.000	100.000	100.000	100.000	100.000		
3	95.844	114.000	104.787	35.000	97.561	80.000		
5	89.991	81.000	103.610	60.000	92.700	83.333		
7	75.966	52.600	105.388	46.667	85.327	70.000		

To calculate the agreement of the data with the look-up table values used in the G-TOP model, criteria described by Griffin (2001) was used. Essentially, the author states that

agreement is more than simply having high correlation (values close to 1) between two data sets. In addition, the data should be plotted on a chart of measured versus predicted values. Here, the linear best-fit slope should be close to 1.0 to ensure high agreement. Lastly, the mean percent error between the two data sets should be relatively low. Table 12 displays the agreement calculations for each of the 11 cognitive abilities.

Table 12: Agreement Results between Measured and G-TOP Look-Up Table Data

Cognitive Ability	Correlation	Slope	Mean % Error
Instrument Reading	-0.833	-16.052	40.573
Simple Decision Making	0.982	5.500	20.340
Visual Acuity	0.883	4.739	36.490
DM Accuracy	-0.631	-2.195	7.321
DM Reaction Time	-0.786	-8.196	18.518
DM Efficiency	-0.488	-22.624	48.703
Tracking	1.000	2.511	14.389
Slow Motion Inference	0.878	4.039	38.348
Fast Motion Inference	0.922	2.334	14.923
Spatial Orientation	-0.963	-11.290	41.102
Perceptual Speed	0.842	1.623	11.517

Discussion and Conclusions

Table 11 illustrates that fact that many of the extrapolations of the data found in the literature grossly overestimated the actual performance decreases found in the HIPDE experiments. As a result, the calculations found in table 12 show very poor agreement between the two data sets. Overall, the best agreement results were found in the perceptual speed, tracking, and fast motion inference cognitive abilities. The discrepancies illustrate that linear approximations are rarely accurate when dealing with human system dynamics. This is particularly true when using data on one end of a continuum ($+G_z$ in this case) to extract information concerning data on the other end of the spectrum. It is intuitively pleasing that the data sets from the literature that included G_z values of +5 or higher (particularly tracking and motion inference) resulted in higher agreement with the data sets from the HIPDE experiments.

However, all three decision making metrics (accuracy, reaction time, and throughput) did not exhibit the same degradations found in Cochran (1953). Although NTI, Inc. utilized the results of this study to denote "decision making," a careful review of the paper reveals that it actually attempted to answer the question of whether pilots could successfully eject from an aircraft at high G_z. The task required subjects to extend both arms over their head to reach for the face curtain handles. Given that the apparent weight of the arms increases with rising G_z levels, it is readily apparent that the task difficulty increases as well. In fact, comments from the subjects revealed that many of them nearly reached the point of muscle failure when reaching for the handles. However, with considerably more effort, they were often able to attain the handles. In addition, subjects were not trained on the proper techniques for reaching over their heads at $+G_z$ prior to the acceleration exposures for the experiment. The author comments that many of the errors were caused by improper techniques. Hence, the dramatic decreases in reaction time and throughput may have been solely a result of neuromuscular phenomenon rather than cognitive deficits.

Lastly, subject G_z tolerance may have added to the data depicting reduced performance. First, the subjects used in this experiment were undergoing their first indoctrination run in the centrifuge. Although all were pilots, their G_z experience cannot be ascertained from the Cochran paper. Inexperience often leads to a lower G_z tolerance as both the muscle tensing and breathing portions of the anti-G straining maneuver may be executed at a less than optimal level. Additionally, muscle tone will often increase over time as a result of the isometric contractions performed during G_z exposures. This ultimately increases blood return to the heart leading to improved G_z tolerance. Likewise, the subjects utilized a 1950's G-suit technology described as

an “anti-blackout” suit. Since that time, G-suits have improved, which may have given the subjects in the HIPDE experiments an advantage.

The spatial orientation cognitive ability also showed poor agreement with the data found in the literature. Again, this discrepancy can be explained by comparing the performance tasks by which subjects were assessed during each experiment. NTI, Inc. used results from Albery (1990) and Nethus et al. (1993) to build the data in the G-TOP model look-up tables for the spatial orientation metric. However, the study conducted by Albery (1990) attempted to answer the question of whether the Dynamic Environment Simulator (DES) centrifuge could illicit vestibular illusions. Because these illusions (specifically the G-excess illusion) were presented without visual cueing, subjects with a normally functioning vestibular system should have experienced an altered sense of orientation, given the illusion was properly administered. Hence, the results should not be ascribed a performance decrease, rather they prove that the illusion was properly presented. Given that the HIPDE experiments did not employ any vestibular illusions, the results of the two data sets should not match.

The study by Nethus et al. (1993) utilized, in part, a manikin orientation task in the cognitive assessment of the subjects during $+G_z$ acceleration. However, the G_z exposure consisted of a SACM only rather than prolonged peaks at individual G_z levels. The task involves a stick-figure of a human with outstretched arms. Below the figure a letter (A or B) is presented. Likewise the letters are displayed in the hands of the “manikin” (A is in the left hand while B is in the right hand or vice versa). The subject must match the letter presented below the manikin with the hand in which that letter is displayed (left or right). The manikin is presented in several orientations (inverted, facing forward, facing backward, facing backward inverted). Therefore, the subject must quickly perform a mental rotation of the object to assess respond

correctly. Spatial orientation in the traditional sense is an egocentric task whereby the pilot or subject views a scene or imagery from a variety of angles or orientations. This is often referred to as "perspective-taking," (Hegarty & Waller, 2004). Although data from the manikin task was used in part to build the G-TOP look-up data matrix for the spatial orientation cognitive attribute, mental rotation and perspective taking have been shown to be different and distinct (Hegarty & Waller, 2004). Specifically, these two types of spatial tests require different mental transformations to assess the object or scenery. Hegarty and Waller (2004) point out that the difference lies in the fact that spatial visualization (mental rotation of an object) requires an object-based translation where the subject's frame of reference remains constant. On the other hand, spatial orientation (Perspective-taking) requires the subject to make a transform of the egocentric frame of reference where the frames of reference for objects in the scene remain constant. Results from a study conducted by Hegarty and Waller (2004) show that mental rotation and spatial orientation are highly distinct. Because the tasks in the HIPDE experiment used spatial orientation rather than mental rotation, it is not surprising that the data did not closely align with the data from Nethus, et al (1993).

CHAPTER 13: CONCLUDING REMARKS

Although it was hypothesized that many if not all of the pilot's cognitive abilities would be affected by $+G_z$, the results from the HIPDE experiments show that only a few were significantly affected. Specifically, tracking, motion inference, peripheral information processing, and short term memory were all negatively impacted by increases in acceleration. Because these tasks probe multiple cognitive abilities to various extents, the data had to be separated into the individual abilities with a weighting factor. These weights were determined by SMEs recruited by NTI, Inc. in the SBIR contract with the Air Force Research Laboratory resulting in what is referred to as the T-Matrix. When weighted with the scores in the T-Matrix, it became readily apparent that the cognitive abilities of simple decision making, visual acuity, tracking, motion inference, and perceptual speed will all deteriorate under increased G_z stress.

It is the opinion of the authors that these decrements arise from diminished firing rates of specific regions of cortical tissue resulting from decreased blood profusion and oxygen supply. Tissues in the upper extremities of the brain (above the horizontal plane) are furthest from the heart, and therefore receive the least amount of blood/oxygen under $+G_z$. As a result, tasks requiring activation of these tissues will suffer to a greater extent than those requiring ventral brain areas. In addition, structures with high metabolic rates such as the hippocampus and the cerebellum will decrease their firing rate sooner in an effort to preserve the life of the individual neurons.

Because of the relatively small sample of data found in the literature, NTI, Inc. was forced to fill in the gaps with extrapolations of the existing data. Because these extrapolations were linear, it was uncertain whether the resulting values were valid, given that many human systems are highly nonlinear. As a result, the main purpose of the HIPDE experiments was to

verify that the NTI, Inc. approximations were valid. The resulting agreement results indicate that there were large disparities in the model approximations and the collected data. Many of these disparities can be explained by the fact that the only available data was extracted from low G_z (2 or 3). It is often the case that the further the extrapolation is extended past the collected data, the less accurate it will be. Others disparities, such as those found in the decision making abilities and the spatial orientation ability, can be explained by the fact that the data used to build the G-TOP model tables originated from tasks probing abilities that had little to do with the cognitive ability with which they were correlated. Therefore, the G-TOP look-up tables should be replaced with data from the HIPDE experiments to improve the validity of the model output.

Finally, a separate model was created by AFRL/HEPG personnel over the course of the HIPDE project. Essentially, quantitative algorithms for each cognitive test were created to model performance under G_z. This modular approach allows the user to include or dismiss the appropriate abilities based on the task he/she wishes to model. A portion of this model can be found in McKinley et al. (2005b) and McKinley (2005c). However, the model remains in development and has not yet been validated. Validation is planned for 2008, and the details of the model will be presented in the final report of the validation.

A model of the negative effects of $+G_z$ on a pilot's cognitive performance has applications to mission planning, simulation, and wargaming. By accounting for the decrements to specific cognitive abilities, adequate mitigation strategies could be employed prior to mission execution, and pilots in training would be able compete with a much more realistic adversary while simultaneously experiencing the same decrements to vision and tracking found in actual flight. The next step will be to transition either the G-TOP model or the AFRL model (once validated) to the operational community.

REFERENCES

1. Albery, W. B. (1990). Spatial disorientation research on the Dynamic Environmental Simulator (DES). AAMRL-SR-90-513.
2. Albery, W. B., Chelette, T. L. (1998). Effect of G suit type on cognitive performance. *Aviat Space Environ Med.* May; *69*(5): 474-9.
3. Ballanyi, K. (2004). Review: Protective role of K_{ATP} channels in brain hypoxia. *The Journal of Experimental Biology 207*, 3201-3212.
4. Bechara, Antoine. (2004). The role of emotion in decision-making: Evidence from neurological patients with orbitofrontal damage. *Brain & Cognition, 55*(1): 30-40.
5. Bair, W., and Movshon, J.A. (2004). Adaptive Temporal Integration of Motion in Direction-Selective Neurons in Macaque Visual Cortex. *Journal of Neuroscience, 24*(33):7305–7323.
6. Baizer, J.S., Ungerleider, L.G., and Desimone, R. (1991). Organization of visual inputs to the inferior temporal and posterior parietal cortex in macaques. *Journal of Neuroscience 11*:168-190.
7. Bliss, T.V., Lømo, T. (1973). Long-lasting potentiation of synaptic transmission in the dentate area of the anaesthetized rabbit following stimulation of the perforant path. *J Physiol (Lond) 232*:331–356.
8. Bruel-Jungerman, E., Davis, S., Laroche, S. (2007). Brain plasticity mechanisms and memory: A party of four. *The Neuroscientist, 13*(5):492-505.
9. Burns, J.W., and Balldin, U.I. (1988). Assisted positive pressure breathing for augmentation of acceleration tolerance time. *Aviat. Space and Environ. Med.*; *59*:225-33.
10. Canfield, A. A., Comrey, A. L., and Wilson, R. C., (1949). "A Study of Reaction Times to Light and Sound as Related to Increased Positive Radial Acceleration", *Aviation Medicine*, October:350-355.
11. Carlson, Neil R. (2007). In Physiology of Behavior. (9th ed.). (pp. 199-207). Boston: Allyn and Bacon.
12. Casali, J.G., Wierwille, W.W. (1984). On the measurement of pilot perceptual workload: a comparison of assessment techniques addressing sensitivity and intrusion issues. *Ergonomics, 27*(10):1033-1050.
13. Centonze, D., Saulle, E., Pisani, A., Bernardi, G., Calabresi, P. (2001). Adenosine-medicated inhibition of striatal GABAergic synaptic transmission during in vitro ischaemia. *Brain, 124*:1855-1865.
14. Cochran, L. B. (1953). Studies on the ease with which pilots can grasp and pull the ejection seat face curtain handles. *Journal of Aviation Medicine, 24*, 23-28.
15. Courtney, S.M., Petit, L., Maisog, J.M., Ungerleider, L.G., and Haxby, J.V. (1998). AN area specialized for spatial working memory in human prefrontal cortex. *Science, 279*: 1347-1351.

16. Erdemli, G., Xu, Y. Z., and Krnjevic, K. (1998). Potassium Conductance Causing Hyperpolarization of CA1 Hippocampal Neurons during Hypoxia. *J Neurophysiol, 80*: 2378–2390.

17. Ernsting, J., Nicholson, A.N., and Rainford, D.J. (eds.). Aviation Medicine 3rd edition. (1999) pp. 43-58. Butterworth Heinemann, Oxford, England.

18. Frankenhauser, M. (1958). Effects of prolonged gravitational stress on performance. *Acta Psychologica, 14*: 92-108.

19. Fraisse, P. (1984). Perception and estimation of time. *Annual Review of Psychology*, 35: 1-36.

20. Fowler, B., Prlic, H. (1995). A comparison of visual and auditory reaction time and P300 latency thresholds to acute hypoxia. *Aviat Space Environ Med,* 7: 645-50.

21. Funashi, S., Bruce, C.J., and Goldman-Rakic, P.S. (1989). Mnemonic coding in the visual space in the monkey's dorsolateral prefrontal cortex. *Journal of Neurophysiology, 61:*331-349.

22. Goodale, M.A., and Milner, A.D. (1992). Separate visual pathways for perception and action. *Trends in Neuroscience, 15*:20-25.

23. Goodale, M.A., Meenan, J.P., Bulthoff, H.H., Nicolle, D.A., Murphy, K.H., and Raciot, C.I. (1994). Separate neural pathways for the visual analysis of object shape in perception and prehension. *Current Biology, 4*:604-610.

24. Goodale, M.A., and Westwood, D.A. (2004). An evolving vision of duplex vision: Separate by interacting cortical pathways for perception and action. *Current Opinion in Neurobiology, 14:*203-211.

25. Griffin M.J. (2001). The Validation of Biodynamic Models. Clinical Biomechanics. 16 (1, Suppl.): 81S-92S.

26. Hansen, A.J., Hounsgaard, J., Jahnsen, H. (1982). Anoxia increases potassium conductance in hippocampal nerve cells. *Acta Physiol Scand, 115*:301-310.

27. Hayashi, M. (2003). Hidden Markov models to identify pilot instrument scanning and attention patterns. *In Proceedings of the IEE International Conference on Systems, Man, and Cybernetics*, Washington DC, 2889-2896.

28. Hebb, D.O. (1949). The organization of behavior. New York: John Wiley.

29. Hebb, D.O. (1955) 'Drives and the C.N.S. (Conceptual Nervous System)'. *Psychological Review, 62*: 243-254.

30. Hegarty, M. & Waller, D. (2004). A dissociation between mental rotation and perspective-taking spatial abilities. *Intelligence, 32*: 175-191.

31. Hochachika, P.W. (1996). ATP supply and demand. In: Haddad GG, Lister G. (eds.) Tissue oxygen deprivation. New York: Raven Press; 1994.

32. Kessler, S.R., Haberecht, M.F., Menon, V., Warsofsky, I.S., Dyer-Friedman, J., Neely, E.K., Reiss, A.L. (2004). Functional Neuroanatomy of Spatial Orientation Processing in Turner Syndrome. *Cerebral Cortex, 14* (2): 174-180.

33. Krnjevic, K. (1999). Early Effects of Hypoxia on Brain Cell Function. *Basic Sciences, 40*(3):375-380.

34. Krnjevic, K. (1975). Coupling of neuronal metabolism and electrical activity. InL Igvar, D.H., Lassen, N.A., (eds.). Brain Work. Proceedings of the Alfred Benzon Symposium VIII, Copenhagen: Munksgaard Press; pp 65-78.

35. Leblond, J., Krnjevic, K. (1989). Hypoxic changes in hippocampal neurons. *J Neurophysiol, 62*:1-14.

36. Lipton, P., Whittingham, T.S. (1982). Reduced ATP concentration as a basis for synaptic transmission failure during hypoxia in the in vitro guinea-pig hippocampus. *J Physiol, 325*:51-65.

37. Mangels, A J et al. (1998). Dissociable contributions of the prefrontal and neocerebellar cortex to time perception. *Cognitive Brain Research* 7:15-39.

38. Maunsell J, Van Essen D (1983). "Functional properties of neurons in middle temporal visual area of the macaque monkey. I. Selectivity for stimulus direction, speed, and orientation." *J Neurophysiol* 49 (5): 1127-47.

39. Messaoudi, E., Kanhema, T. Soule, J., Tiron, A., Dagyte, G., da Sailva, B., Bramham, C.R. (2007). Sustained Arc/Arg3.1 synthesis controls long-term potentiation consolidation through regulation of local actin polymerization in the dentate gyrus in vivo. *The Journal of Neuroscience, 27*(39):10445–10455.

40. Morrissett, K., & McGowan, D. (2000). Further support for the concept of a GLOC syndrome: A survey of military high-performance aviators. *Aviation Space and Environmental Medicine,* 71: 496-500.

41. McCloskey, K., Albery, W. B., Zehner, G., Bolia, S. D., Hundt, T. H., Martin, E. J., & Blackwell, S. (1992). NASP re-entry profile: Effects of low-level $+G_z$ on reaction time, keypad entry, and reach error. (AL-TR-1992-0130). Wright-Patterson Air Force Base, Ohio.

42. McKinley, R.A., Tripp L.D. Jr., Bolia S.D., Roark M.R. (2005a). Computer Modeling of Acceleration Effects on Cerebral Oxygen Saturation. *Aviat Space Environ Med, 76*: 733-738.

43. McKinley R.A., Fullerton K.L., Tripp L.D. Jr., Esken R.L., Goodyear C. (2005b). A Model of the Effects of Acceleration on a Pursuit Tracking Task. AFRL-HE-WP-TR-2005-0008.

44. McKinley R.A., Fullerton K.L., Tripp L.D. Jr., Goodyear C. (2005c) "Effects of Acceleration on the Ability to Perceive Relative Motion", presented at the *76th Aerospace Medical Association Annual Scientific Meeting*, Kansas City, MO, May 8-12, 2005.

45. Miller, G. A. (1956). “The magical number seven, plus or minus two: some limits on our capacity for processing information”. *Psychological Review, 63*, 81-97.

46. Milner, B., Corkin, S., and Teuber, H.-L. (1968). Further analysis of the hippocampal amnesic syndrome: 14-year follow-up study of H.M. *Neurophysiologia*, *6*:317-338.

47. Milner, B. (1970). Memory and the temporal regions of the brain. In *Biology of Memory*, edited by K.H. Pribram and D.E. Broadbent. New York: Academic Press.

48. Naval Aerospace Medical Institute. G-Induced Loss of Consciousness (G-LOC). Chapter 7: Neurology. In: United States Naval Flight Surgeon's Manual: Third Edition; 1991.

49. Nethus, T. E., Werchan, P. M., Besch, E. L., Wiegman, J. F., & Shahed, A. R. (1993). Comparative effects of +Gz acceleration and maximal anaerobic exercise on cognitive task performance in subjects exposed to various breathing gas mixtures. Abstract, *Aviat Space Environ Med*, *64* (5): 422.

50. Newman D.G., White S.W., Callister R. (1998). Evidence of baroreflex adaptation to repetitive $+G_z$ in fighter pilot. *Aviat Space Environ Med, 69*:446-451.

51. Nichelli, P et al. (1996). Perceptual timing in cerebellar degeneration. *Neuropsychologia*, 34, 863-871.

52. Peuskins, H., Sunaert, S., Dupont, P., Van Hecke, P., and Orban, G.A. Human brain regions involved in heading estimation. *Journal of Neuroscience, 21*:2451-2461.

53. Phillips, C.A., Repperger, D.W., Kinsler, R., Bharwani, G., Kender, D. (2007). A quantitative model of the human–machine interaction and multi-task performance: A strategy function and the unity model paradigm. *Computers in Biology and Medicine 37*:1259 – 1271.

54. Porlier, G., Kelso, B., Landolt, J.P., and Fowler, B. (1987). "Study of the Effects of Hypoxia on P300 and Reaction Time", Proceedings of the 1987 Aerospace Medical Association Annual Meeting, May, pp. A14.

55. Ratino, D.A., Repperger, D.W.,Goodyear, C., Potor, G., and Rodriquez, L.E. Quantification of Reaction Time and Time Perception During Space Shuttle Operation, *Aviat Space Environ Med*, March, 1988.

56. Roach, R.C. (ed.) (1999). Chapter 14: The Hypoxic Brain: Insights from Ischemia Research. In Hypoxia: Into the Next Millennium. New York: Academic/Plenum Publishing.

57. Rogers, D. B. (2003). Design and safety analysis tool for amusement park rides. SAFE Symposium, Sept. 22-24. Jacksonville, FL.

58. Rogers, D. B., Ashare, A. B., Smiles, K. A., Frazier, J. W., Skowronski, V. D., & Holden, F. M. (1973). Effect of modifies seat angle on air-to-air weapon system performance under high acceleration. *Memorandum-AMRL-TR-73-5.* Wright-Patterson AFB, OH: AF Aerospace Medical Research Laboratory

59. Repperger, D. W., Frazier, J., Popper, S., and Goodyear, C. (1989). Attention Anomalies As Measured by Time Estimation Under G Stress, Proceedings of the NAECON Conference, Dayton OH, May, pp. 787-793.

60. Rubia., K., Smith, A. (2004). The neural correlates of cognitive time management: a review. *Acta Neurobiologica*, 64: 329-340.

61. Smith, K., Dickhaut, J., McCabe, K., Pardo, J.V. (2002). Neuronal Substrates for Choice under Ambiguity, Risk, Gains and Losses. *Management Science, 48*(6):711-718.

62. Stoll, A. M. (1956). Human tolerance to positive G as determined by the physiological end points. *Aviation Medicine*, August, p. 356.

63. Sugar, O., Gerard, R.W. (1938). Anoxia and brain potentials. *J Neurophysiol, 1*:558-572.

64. Tsao, Y., Wittlieb, E., Miller, B., & Wang, T. (1983). Time estimation of a secondary event. *Perceptual and Motor Skills*, 57: 1051-1055.

65. Tripp, L.D., Chelette, T, Savul, S.A., and Widman, B.S. (1998). Female exposure to high-G: Effects of simulated combat sorties on cerebral and arterial O2 Saturation. *Aviat Space Environ Med 69*(9): 869-874.

66. Tripp, L.D., Warm, J.S., Matthews, G., Chiu, P.Y., Deaton, J.E., Albery, W.B. +Gz acceleration loss of consciousness: Time course of performance deficits with repeated experience. Proceedings of the 46th Annual Meeting of the Human Factors and Ergonomics Society, Baltimore, MD 30 September – 4 October 2002. (130-134).

67. Tripp, L.D., Werchan, P., Deaton, J.E., Warm, J.S., Matthews, G., Chiu, P.Y. The Effect of repeated exposure to G-induced loss of consciousness on recovery time and psychomotor task performance 12th International Symposium on Aviation Psychology, Dayton, OH. 14-17 April 2003. (1166-1171).

68. Walsh, V., Ellison, A., Battelli, L., and Cowey, A. (1998). Task-specific impairments and enhancements induced by magnetic stimulation of human visual area V5. *Proceedings of the Royal Society of London (B), 265*:537-543.

69. Wang, J., Zhou, T., Qui, M., Du, A., Cai, K., Wang, Z., Zhou, C., Meng, M., Zhuo, Y., Fan, S., Chen, L. (1999). Relationship between ventral stream for object vision and dorsal stream for spatial vision: an fMRI + Erp study. *Human Brain Mapping*, *8*:170-181.

70. Warrick, M. J., & Lund, D. W. (1946). Effect of moderate positive acceleration (G) on the ability to read aircraft instrument dials. Memorandum-TSEAA-694-10. Wright-Patterson AFB, OH.

71. White, Susan, Mark Desantis, Bhavani Kashyap, Kevin Kelliher, and Michael Laskowski. "Basal Ganglia." Med. Sci 532. 24 Jan. 2007. University of Idaho. 15 Oct. 2007 <http://www.sci.uidaho.edu/med532/basal.htm>.

72. White, W. J. (1960). Variations in absolute visual thresholds during acceleration stress. ASD-TR-60-34 (DTIC-AD-243612).

73. White, W. J. (1962). Quantitative instrument reading as a function of illumination and gravitational stress. *Journal of Engineering Psychology*, *3*: 127-133.

74. Wickens, C.D., Self, B.P., Andre, T.S., Reynolds, T.J., Small, R.L. (2007). Unusual Attitude Recoveries with a Spatial Disorientation Icon. *International Journal of Aviation Psychology*, 17(2): 153-165.

75. Wickens, C.D. (1984). Processing resources in attention. In R. Parasuraman & D.R. Davies (eds.), Varieties of attention. (pp. 63-102). New York, NY: Academic Press.

76. Wilson, G.F. (2002). An analysis of mental workload in pilots during flight using multiple psychophysiological measures. *The International Journal of Aviation Psychology, 12*(1): 3-18.

77. Zakay, D., Fallach, E. (1984). Immediate and remote time estimation – a comparison. *Acta Psychologica*, 57: 69-81.

78. Zakay, D. (1990). The evasive art of subjective time measurement: Some methodological dilemmas. In R. A. Block (Ed.), Cognitive models of psychological time, (pp. 59-84). Hillsdale, NJ: Erlbaum.

APPENDIX A: ADDITIONAL DATA PLOTS FROM HIPDE EXPERIMENTS

Additional data plots were generated for several of the HIPDE experiments that did not warrant inclusion in the pervious chapters. However, the plots have been included in this appendix for reference purposes. Below are additional plots for the pursuit tracking task. The resulting RMSE, G_z, and time data from the three experimental test days were plotted for each of the eight subjects. The plots for the 3, 5, and 7 G_z 15-sec plateau profiles can be found in Figure 67. Figure 68 displays the resulting tracking RMSE data for the SACM profile for all subjects and experimental testing days.

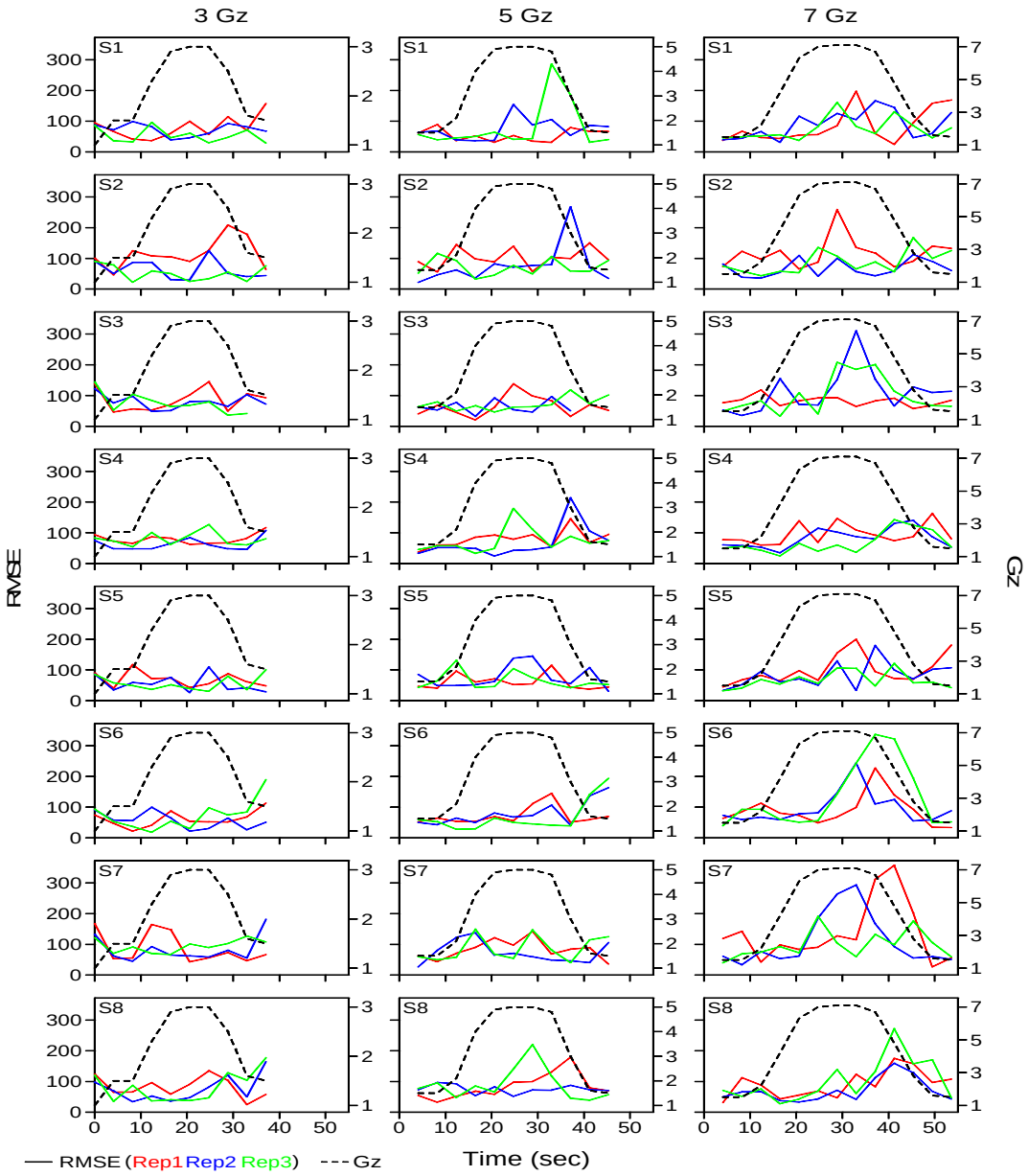

Figure 67: RMSE for Each Gz Plateau, Subject (N = 8), and Replication

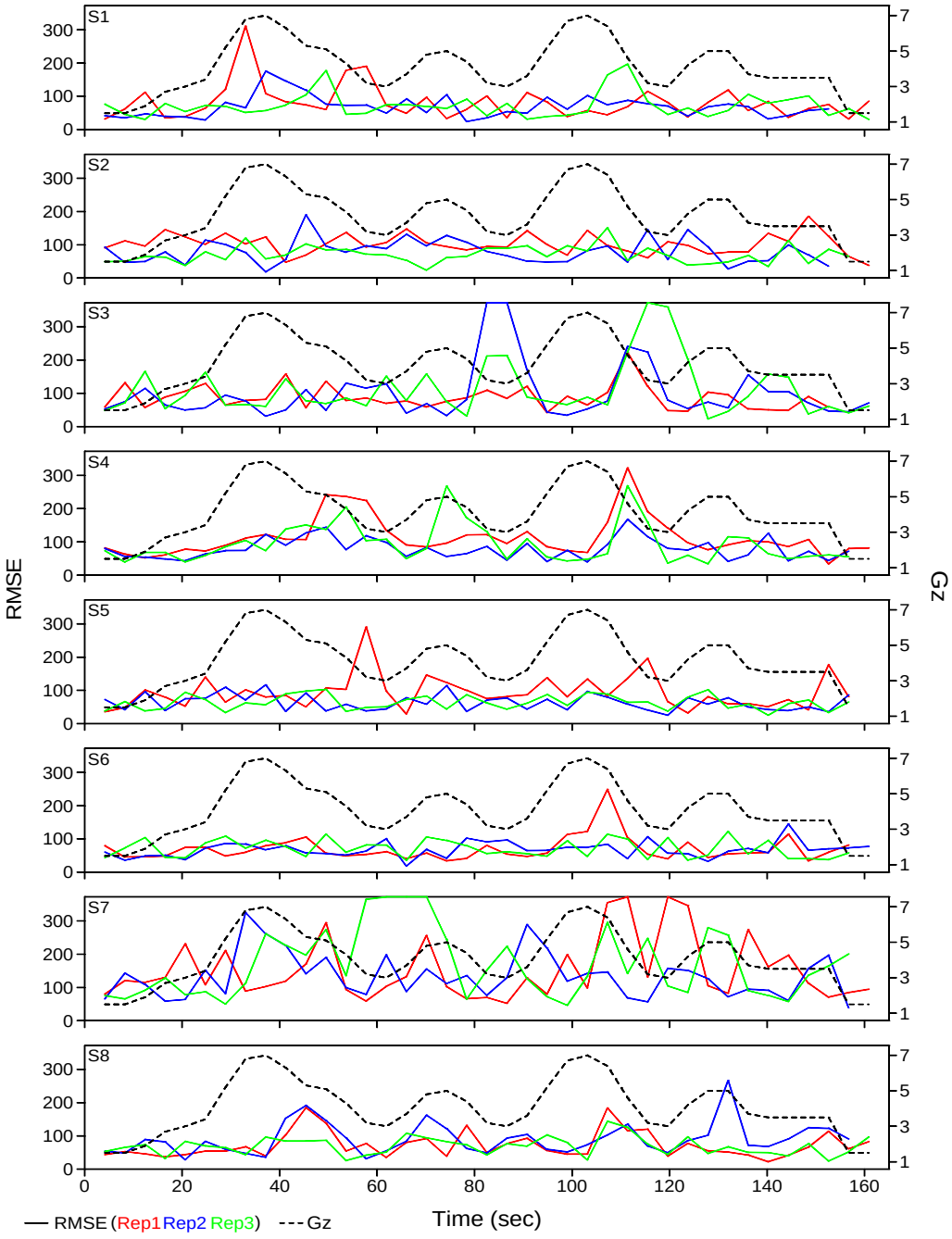

Figure 68: RMSE during SACM for Each Subject (N = 8), and Replication

The next plots detail results for each subject and trial for the precision timing task. For each block, the profiles are arranged in chronological order from top to bottom. Thus, day 1 runs are on top, day 2 runs in the middle, and day 3 runs on the bottom. The curves displayed in each

block represent the G_z profiles. The numbers presented on each curve represent the angle difference parameter.

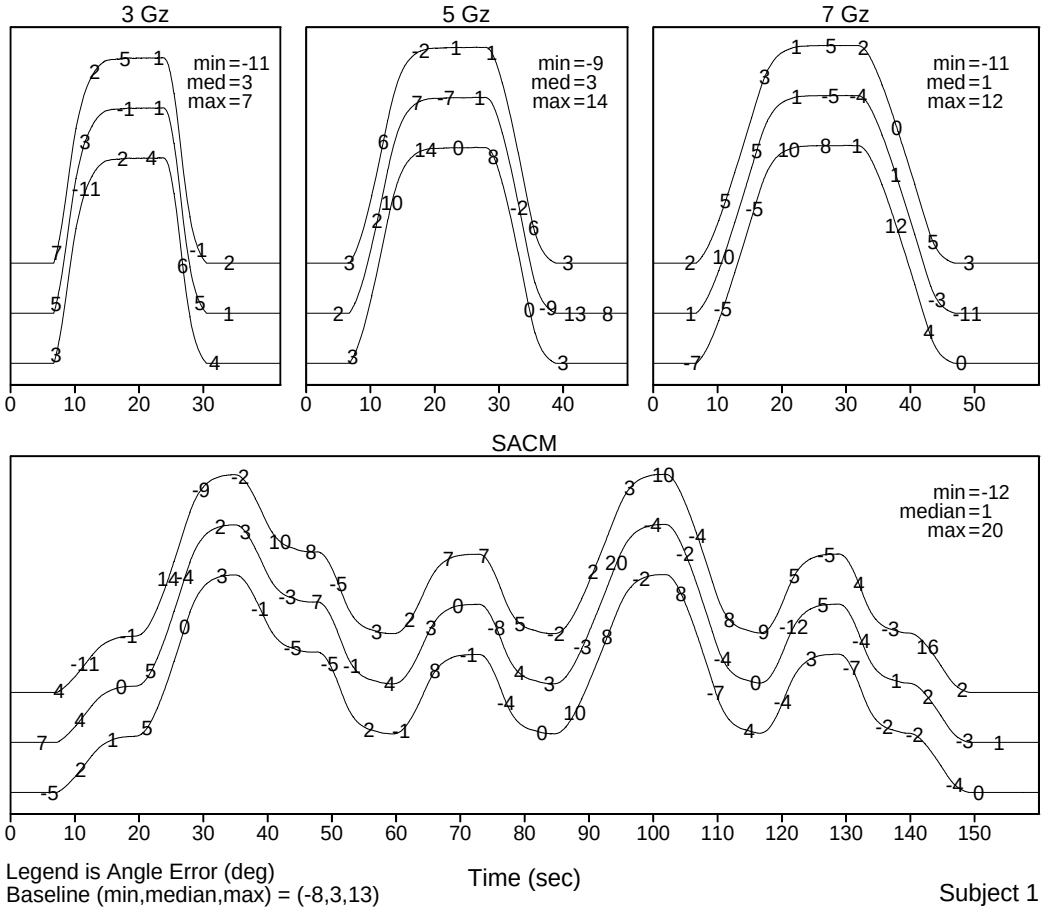

Figure 69: Angle difference data for subject 1 across all experimental test days

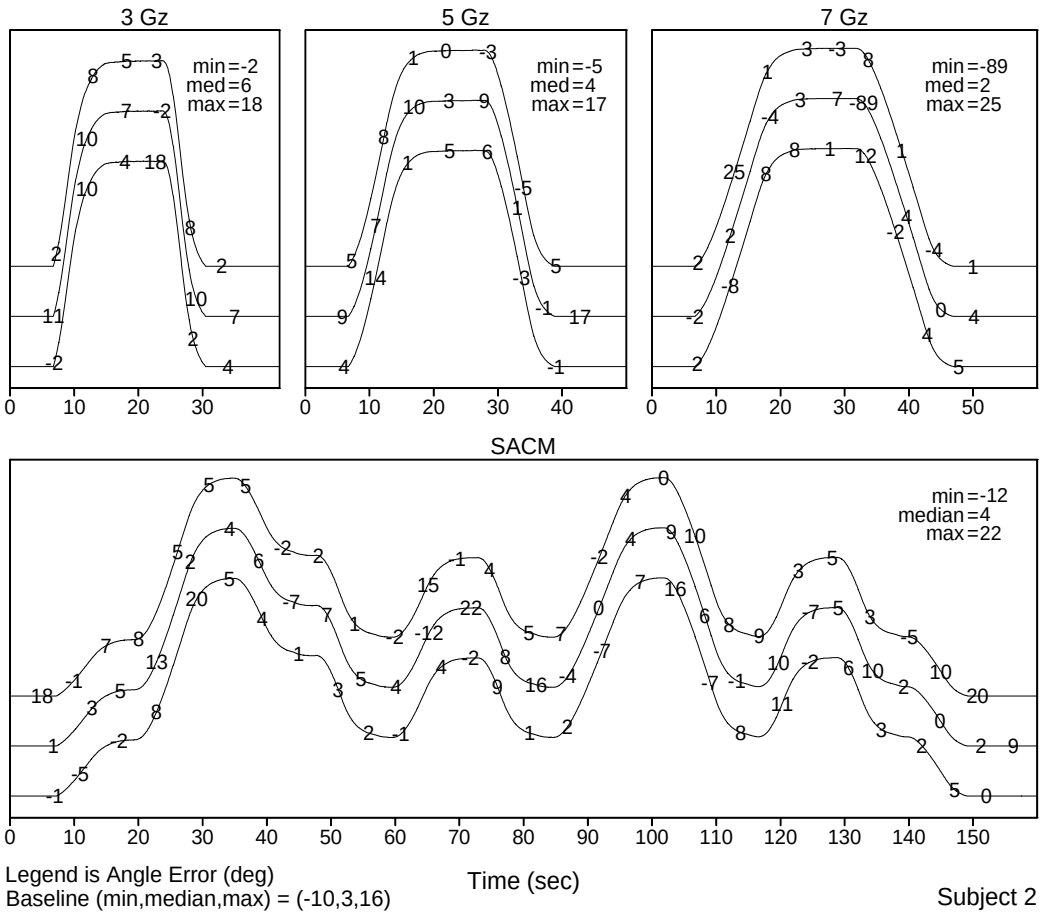

Figure 70: Angle difference data for subject 2 across all experimental test days

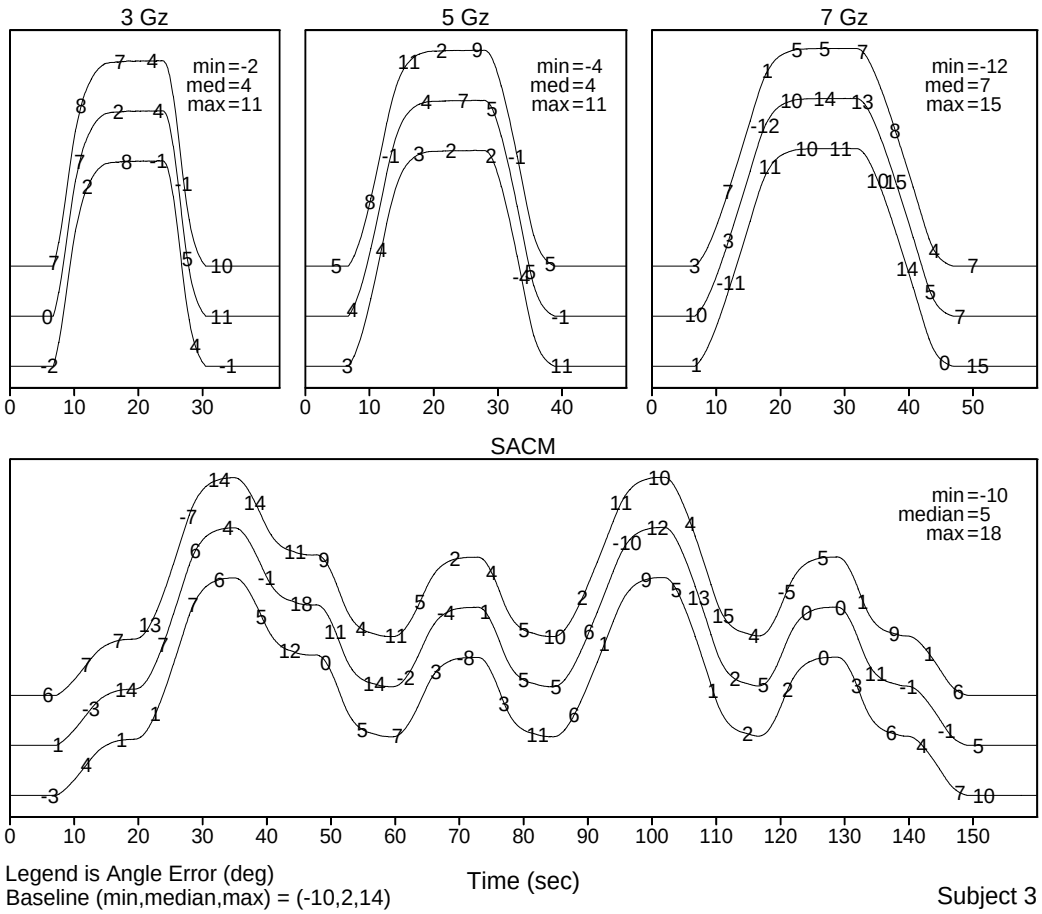

Figure 71: Angle difference data for subject 3 across all experimental test days

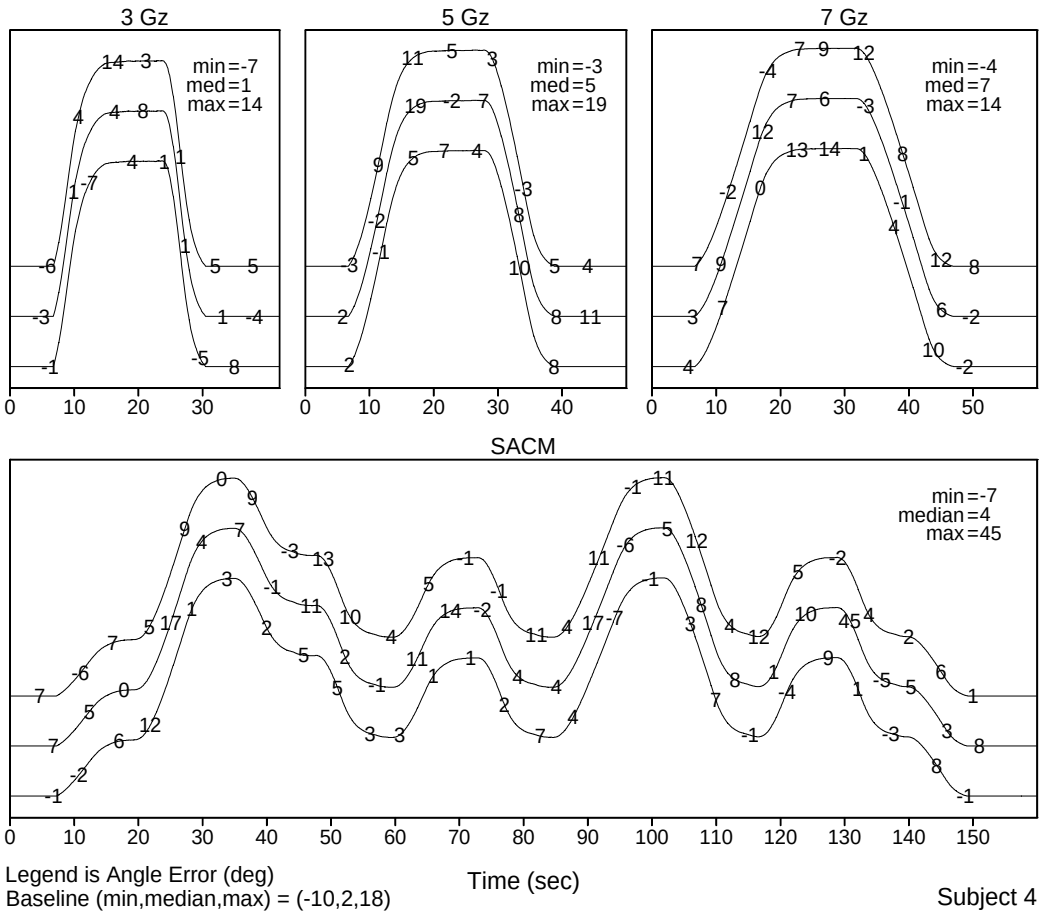

Figure 72: Angle difference data for subject 4 across all experimental test days

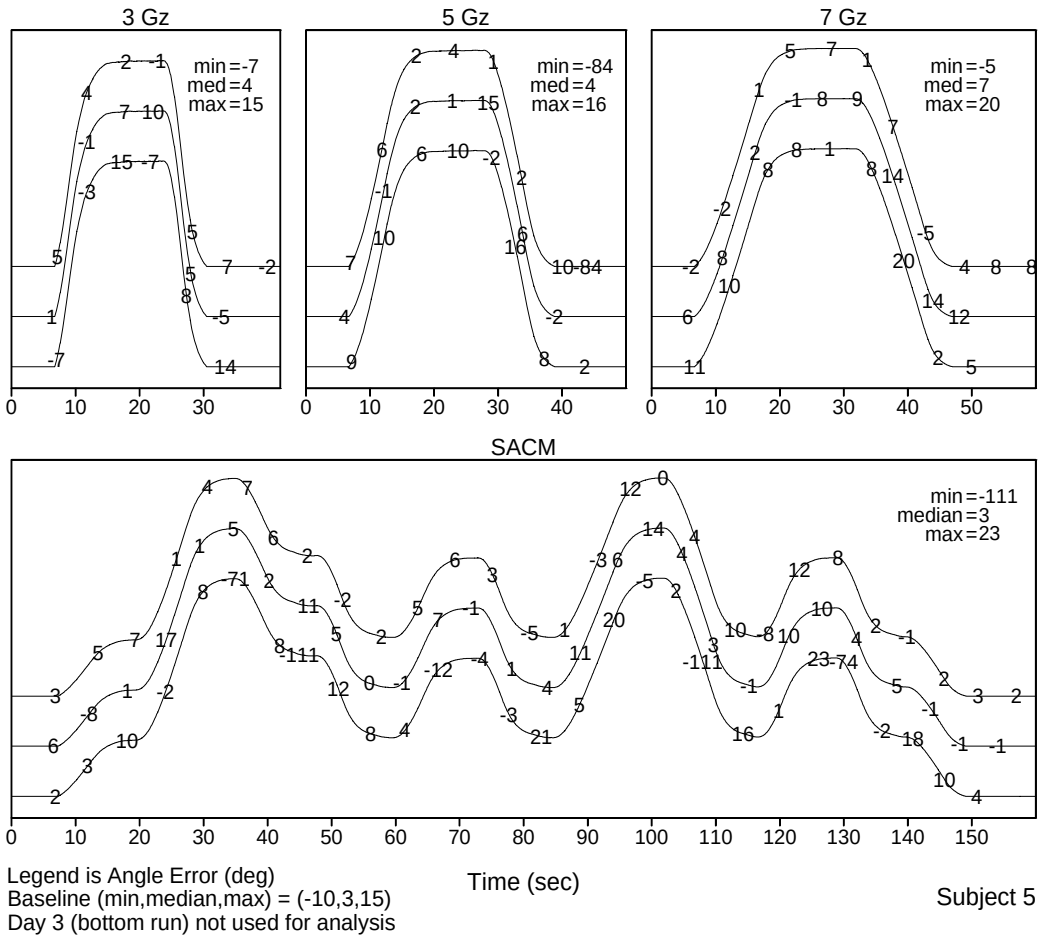

Figure 73: Angle difference data for subject 5 across all experimental test days

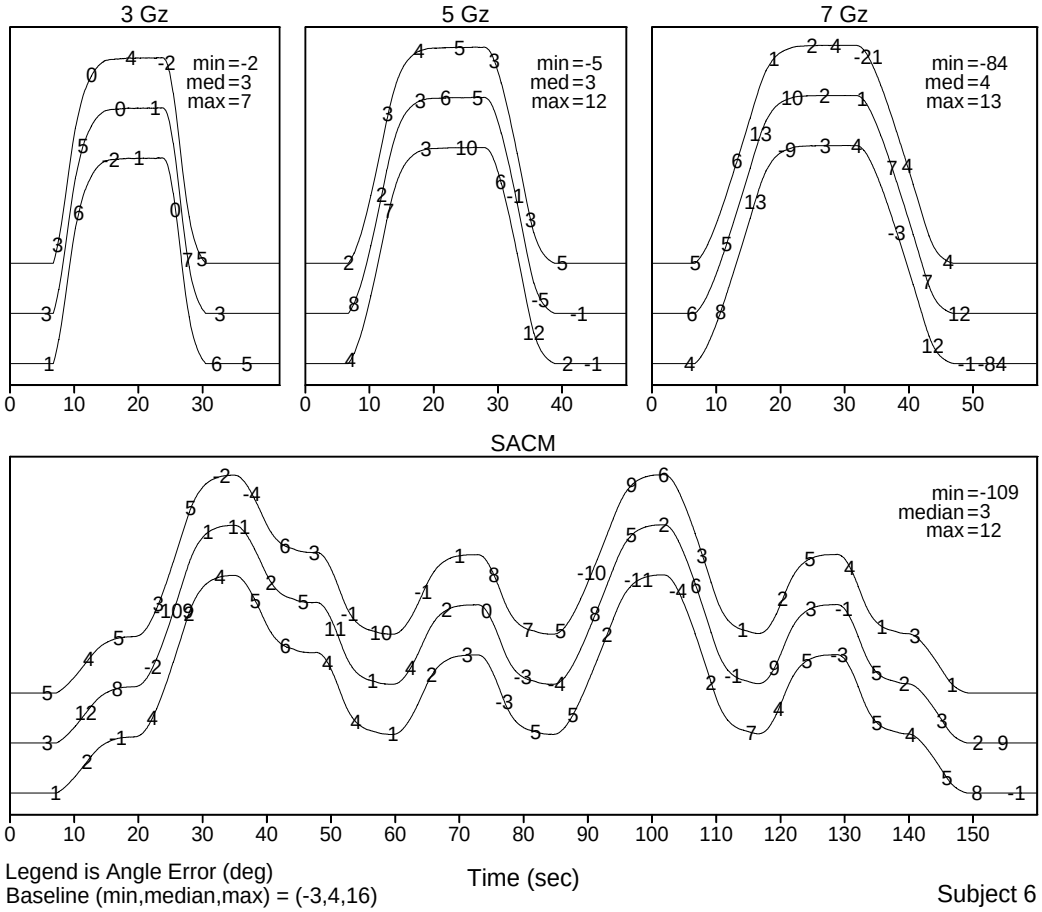

Figure 74: Angle difference data for subject 6 across all experimental test days

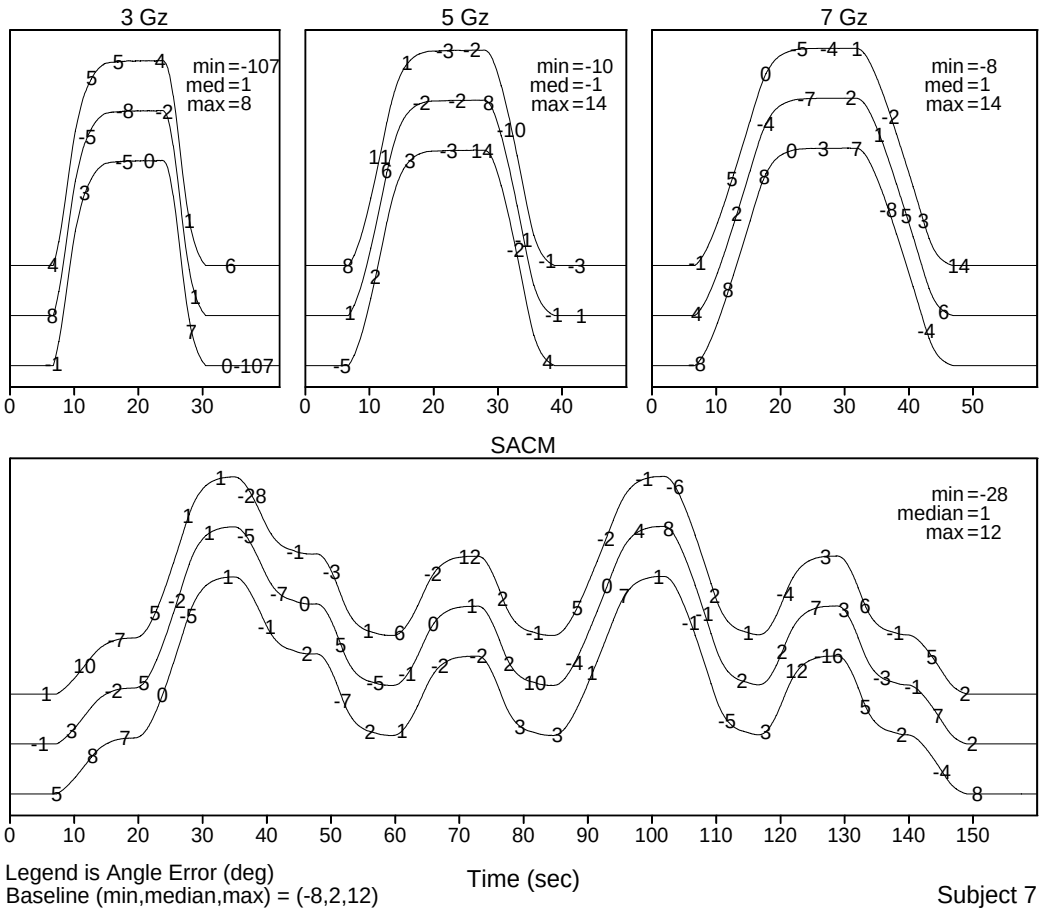

Figure 75: Angle difference data for subject 7 across all experimental test days

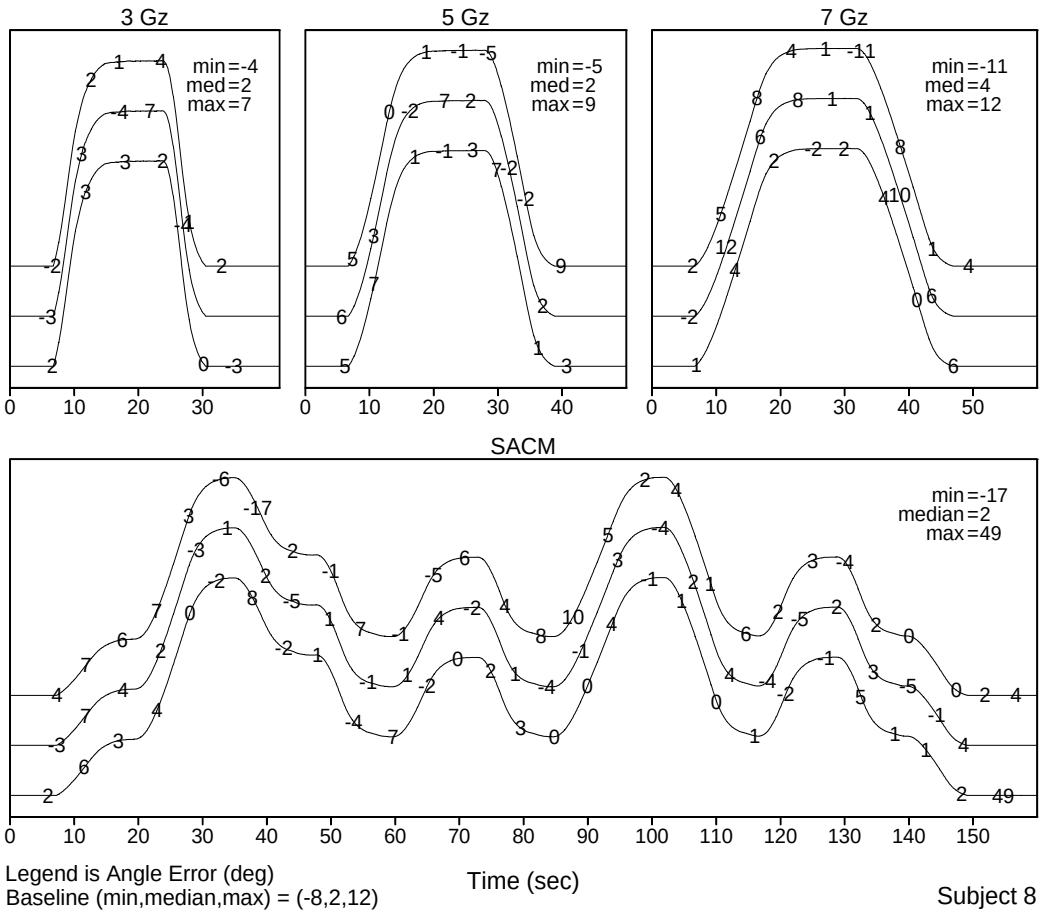

Figure 76: Angle difference data for subject 8 across all experimental test days

Additional plots were also generated for the motion inference study. Figure 77 shows the correlation between angle error and G_z, whereas Figure 78 displays the correlation between the angle error percent change from baseline. Above each panel is the p-value from a two-tailed t-test for H_o: correlation (or slope) = 0.

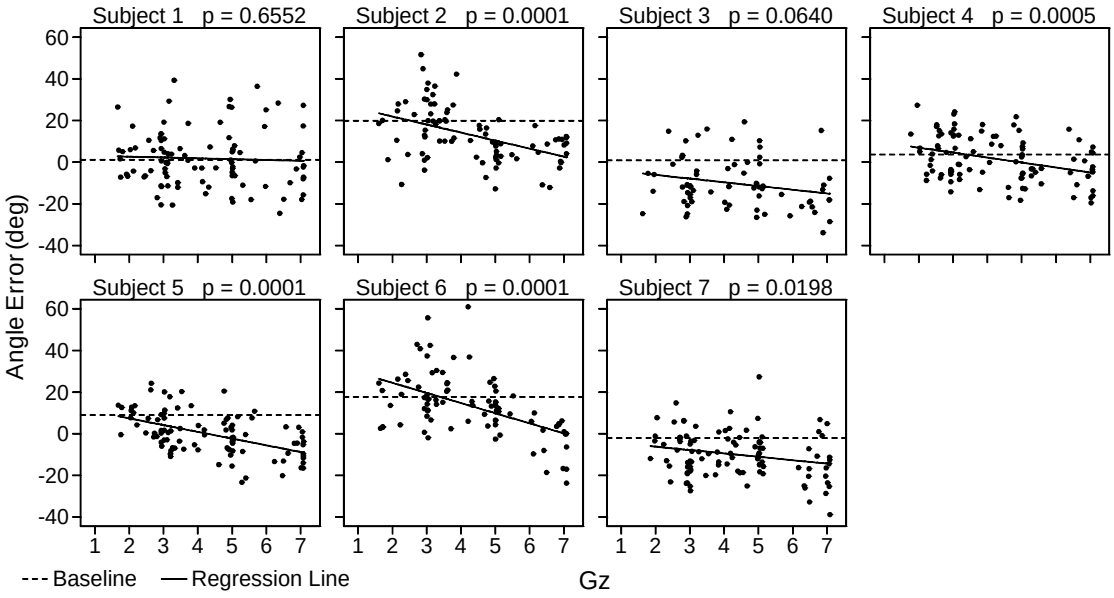

Figure 77: Correlation between angle error and G_z.

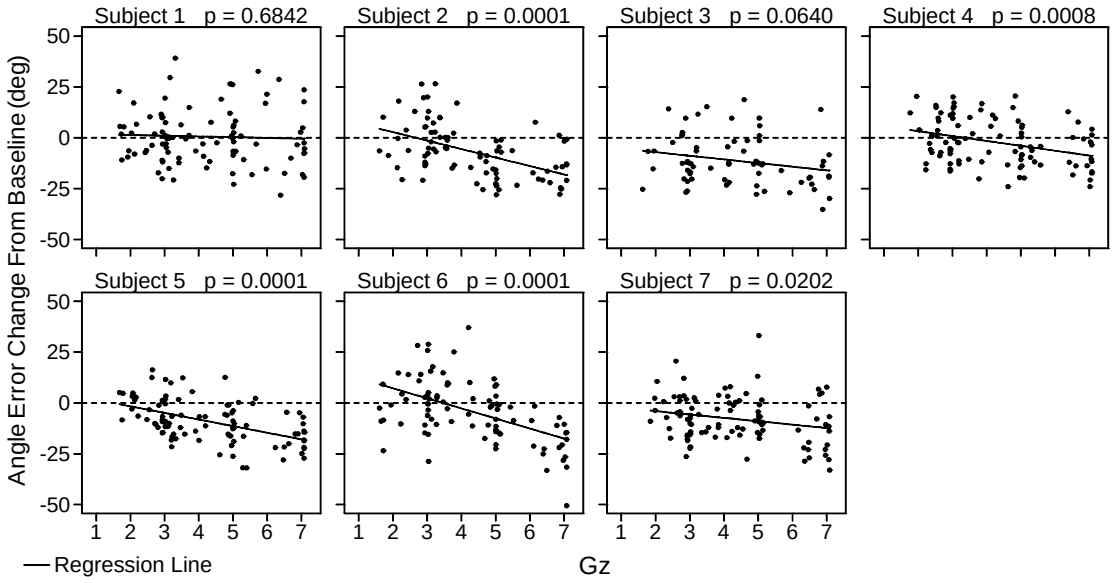

Figure 78: Correlation between angle error change from baseline and G_z.

The next set of plots provides the results from the "Capture Time" metric in the Relative Motion task for each individual subject. Again, the profiles are arranged in chronological order from top to bottom. Thus, day 1 runs are on top, day 2 runs in the middle, and day 3 runs on the bottom. The curves displayed in each block represent the G_z profiles. Numbers on the G_z profile

identify the starting position of the target with 1 = far left, 4 = straight ahead, and 7 = far right. The X = failure can be either improper contact (not circled) or no contact (circled) between planes. A square indicates trials not used in analyses for being too late in the profile.

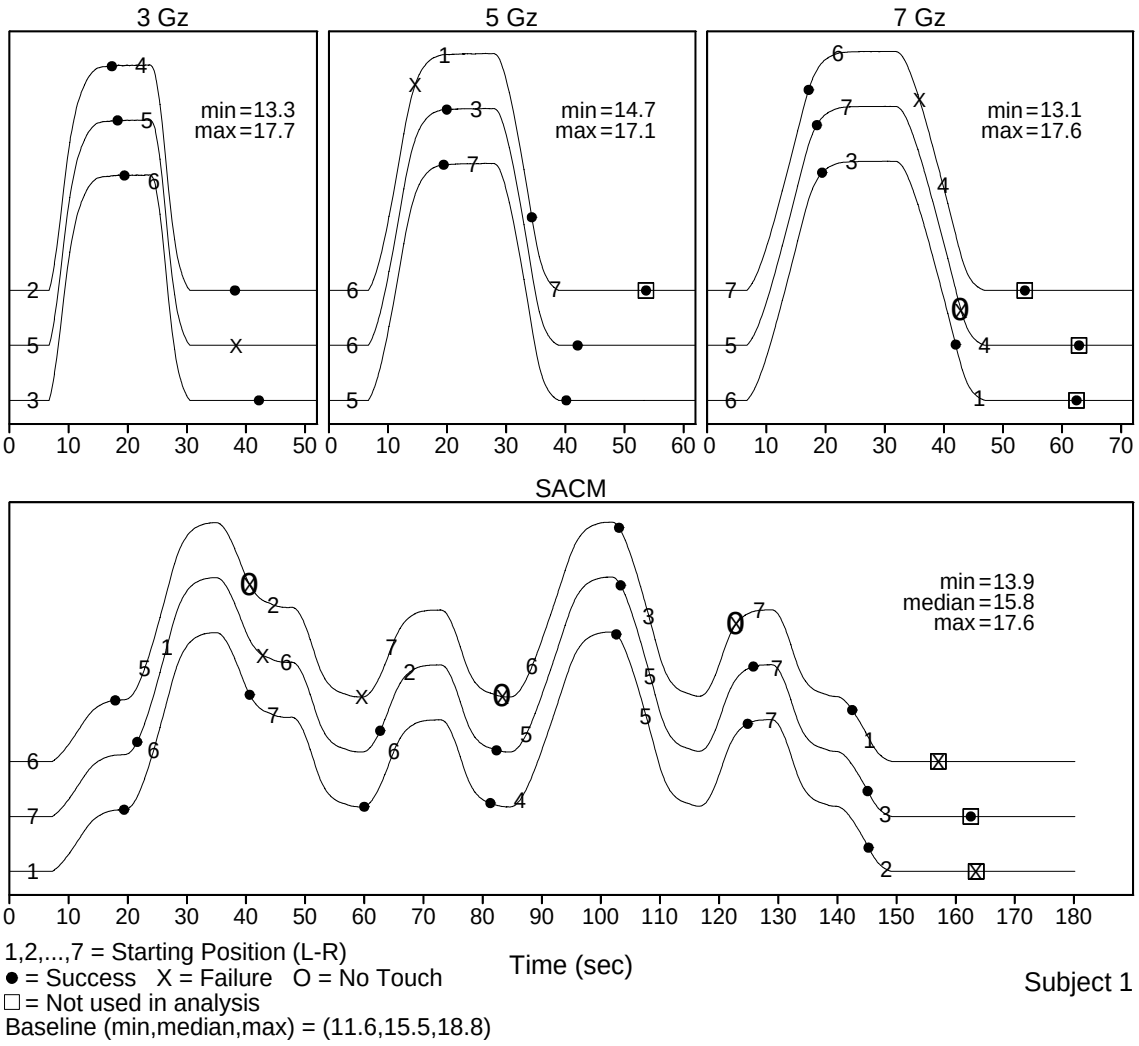

Figure 79: Performance of subject 1 on the relative motion task

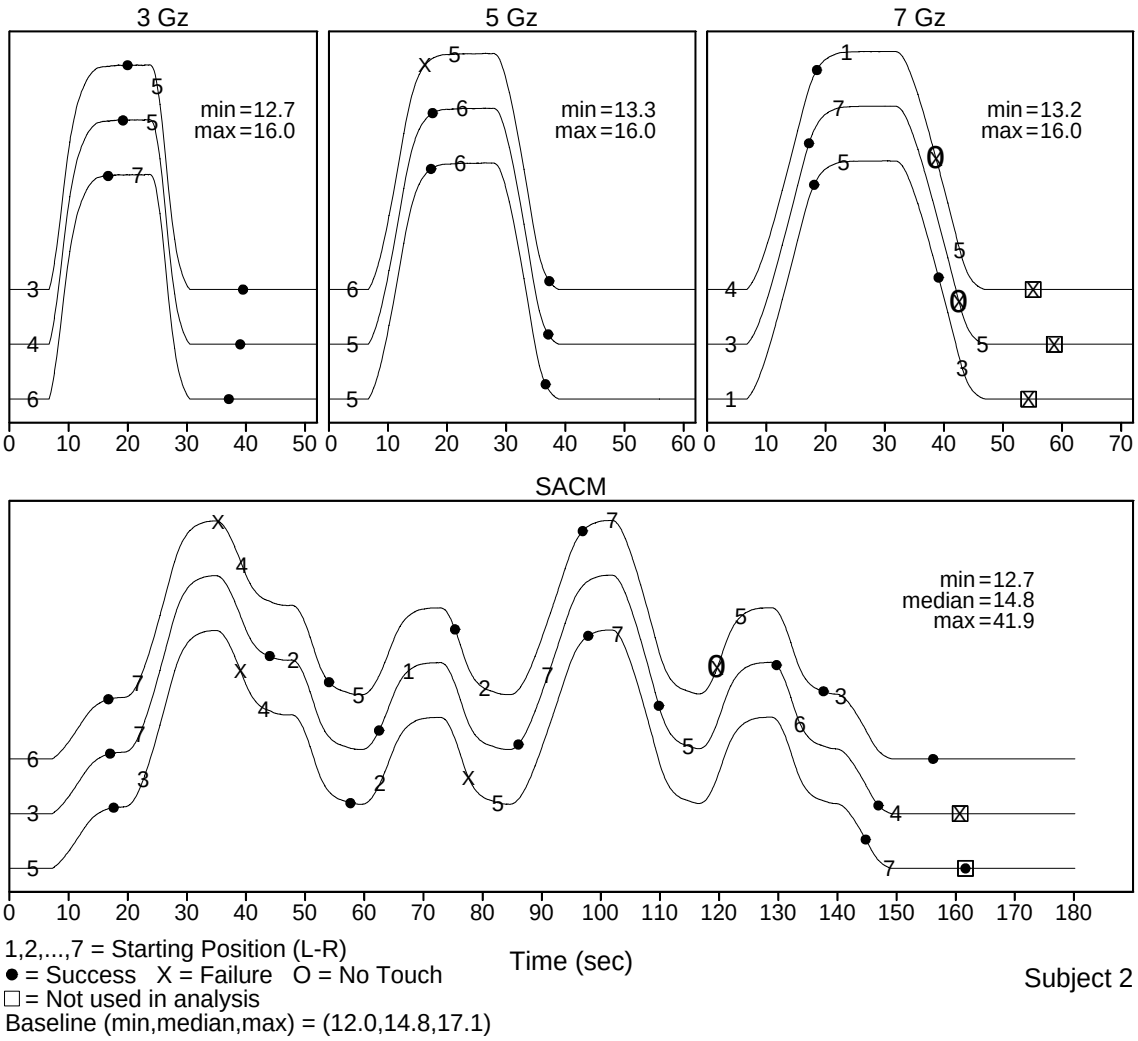

Figure 80: Performance of subject 2 on the relative motion task

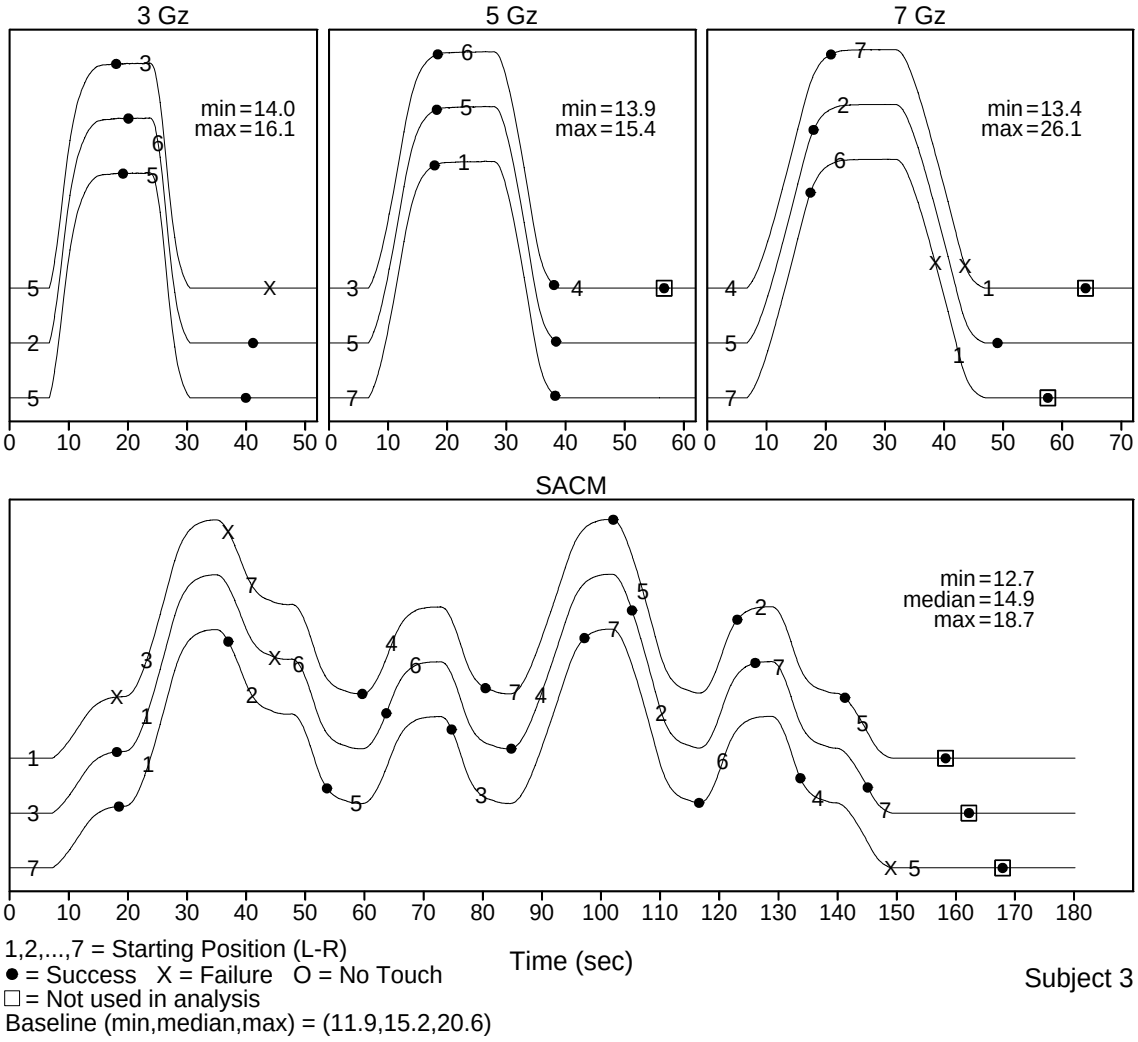

Figure 81: Performance of subject 3 on the relative motion task

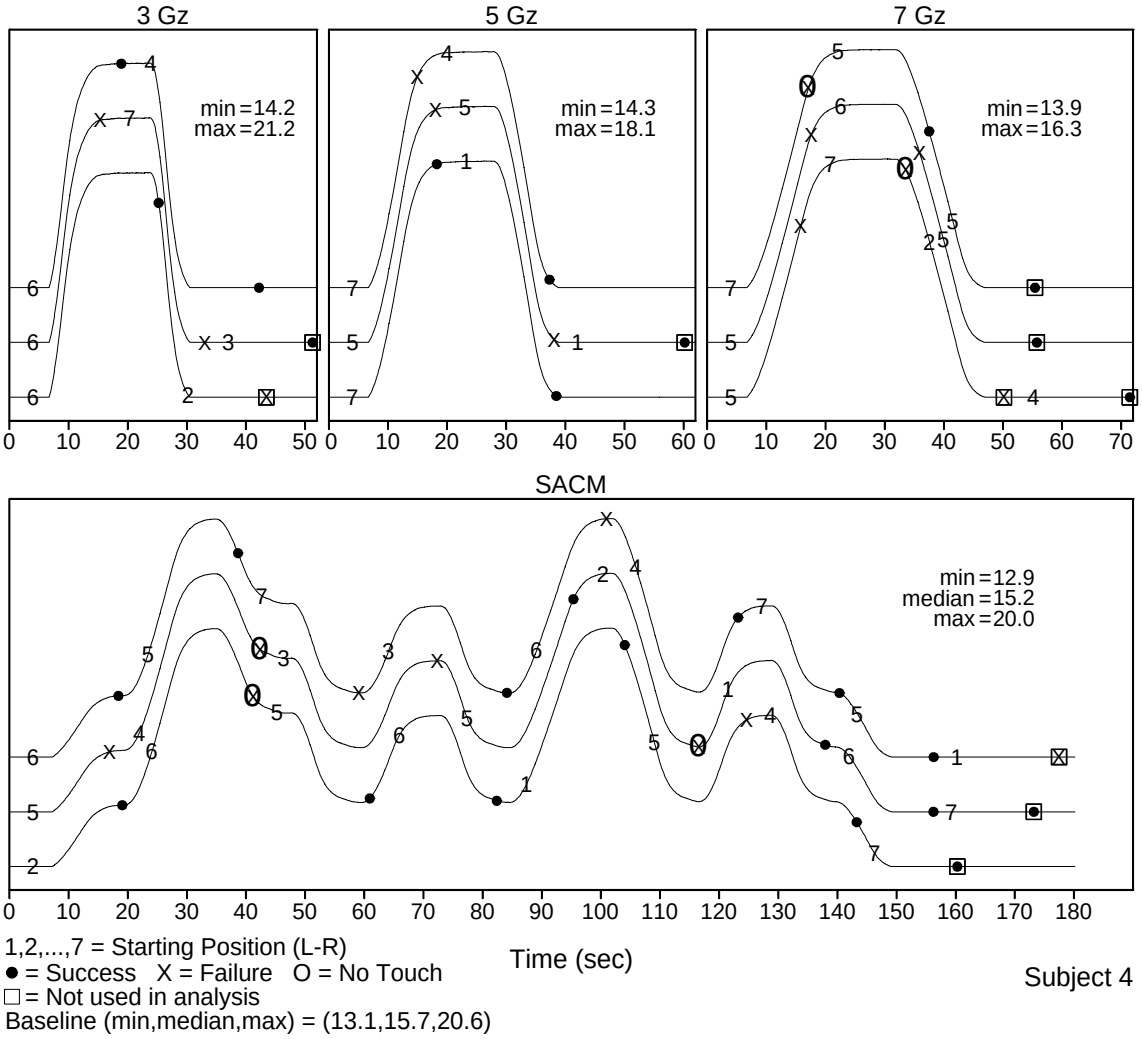

Figure 82: Performance of subject 4 on the relative motion task

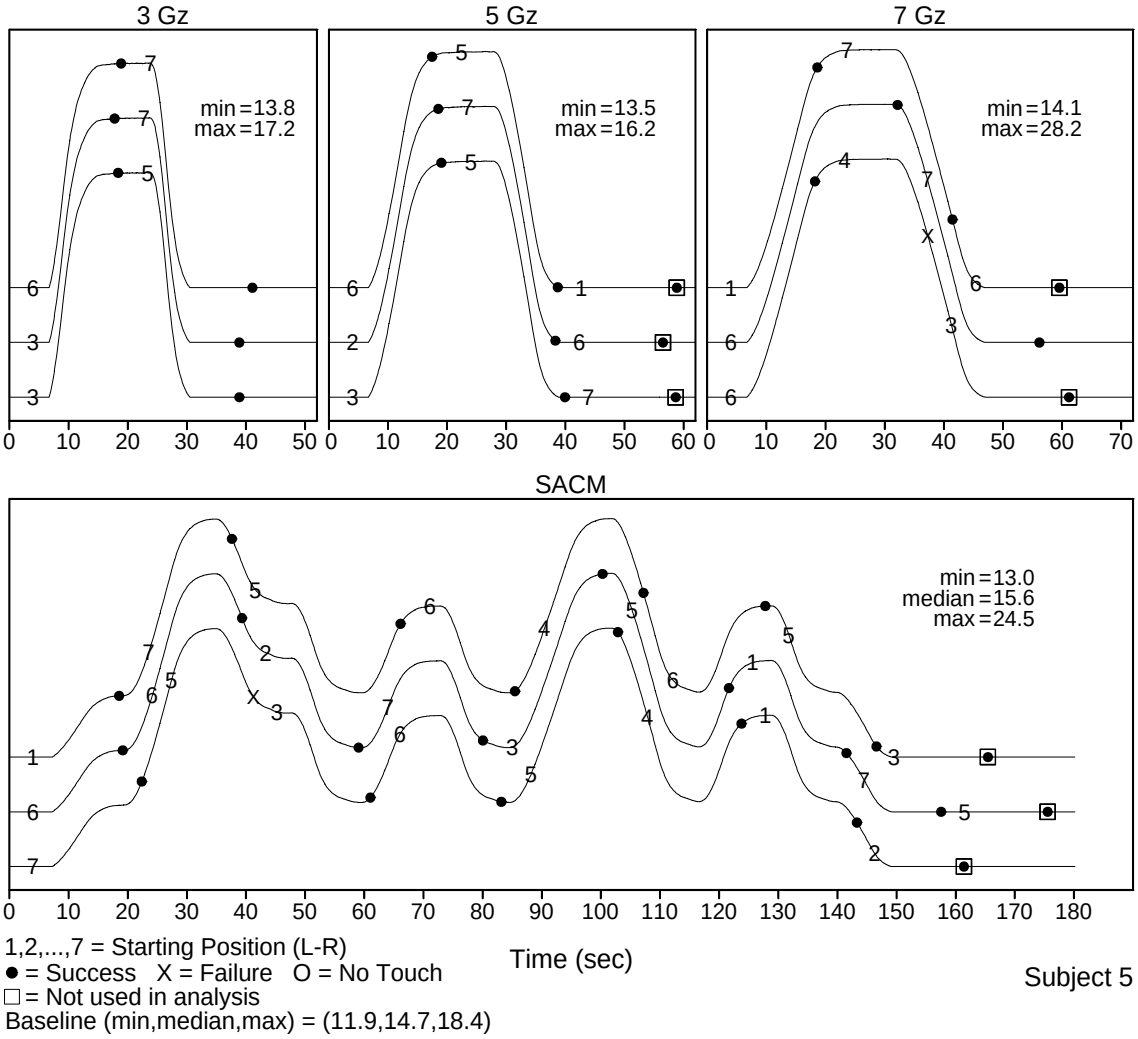

Figure 83: Performance of subject 5 on the relative motion task

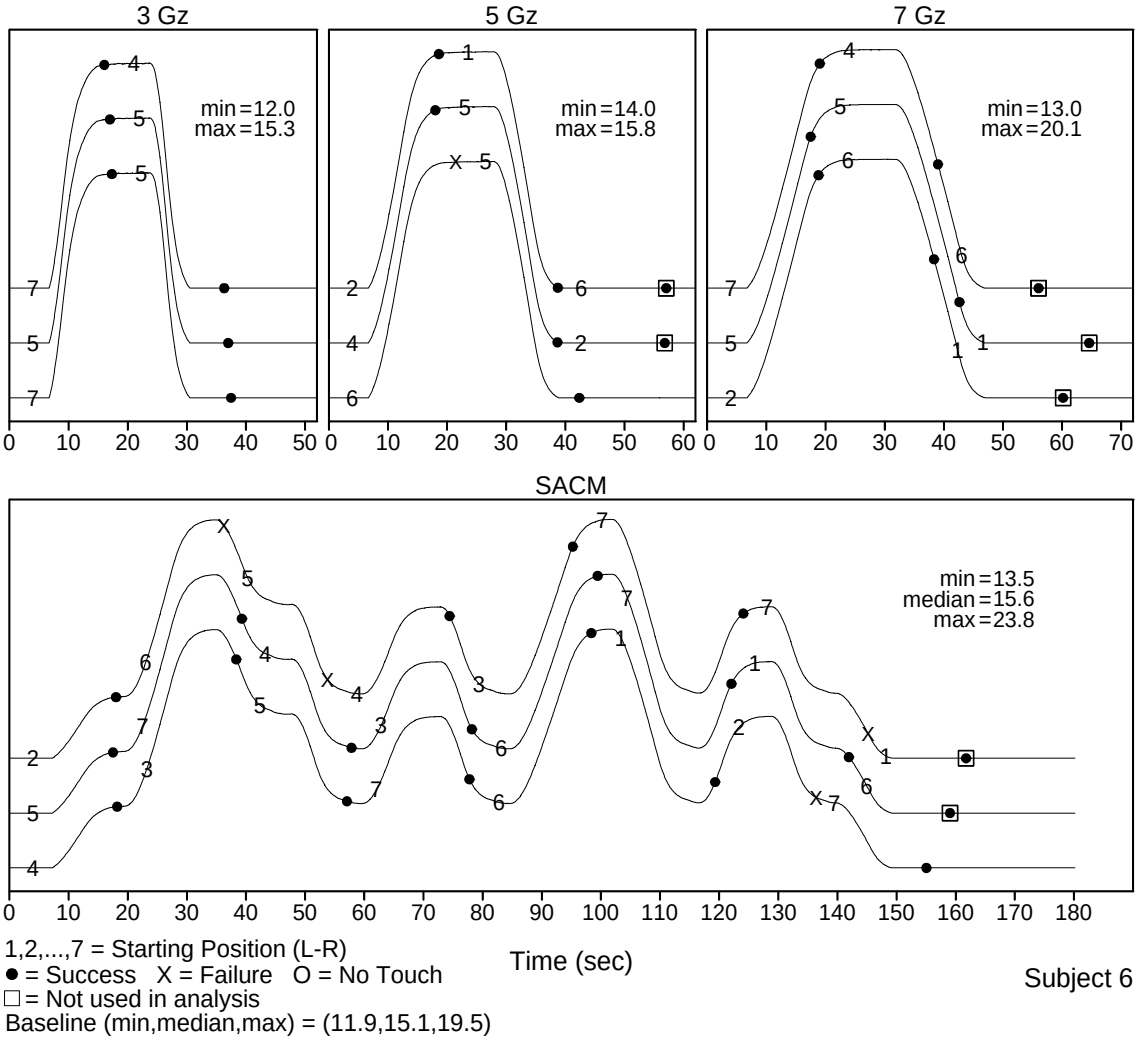

Figure 84: Performance of subject 6 on the relative motion task

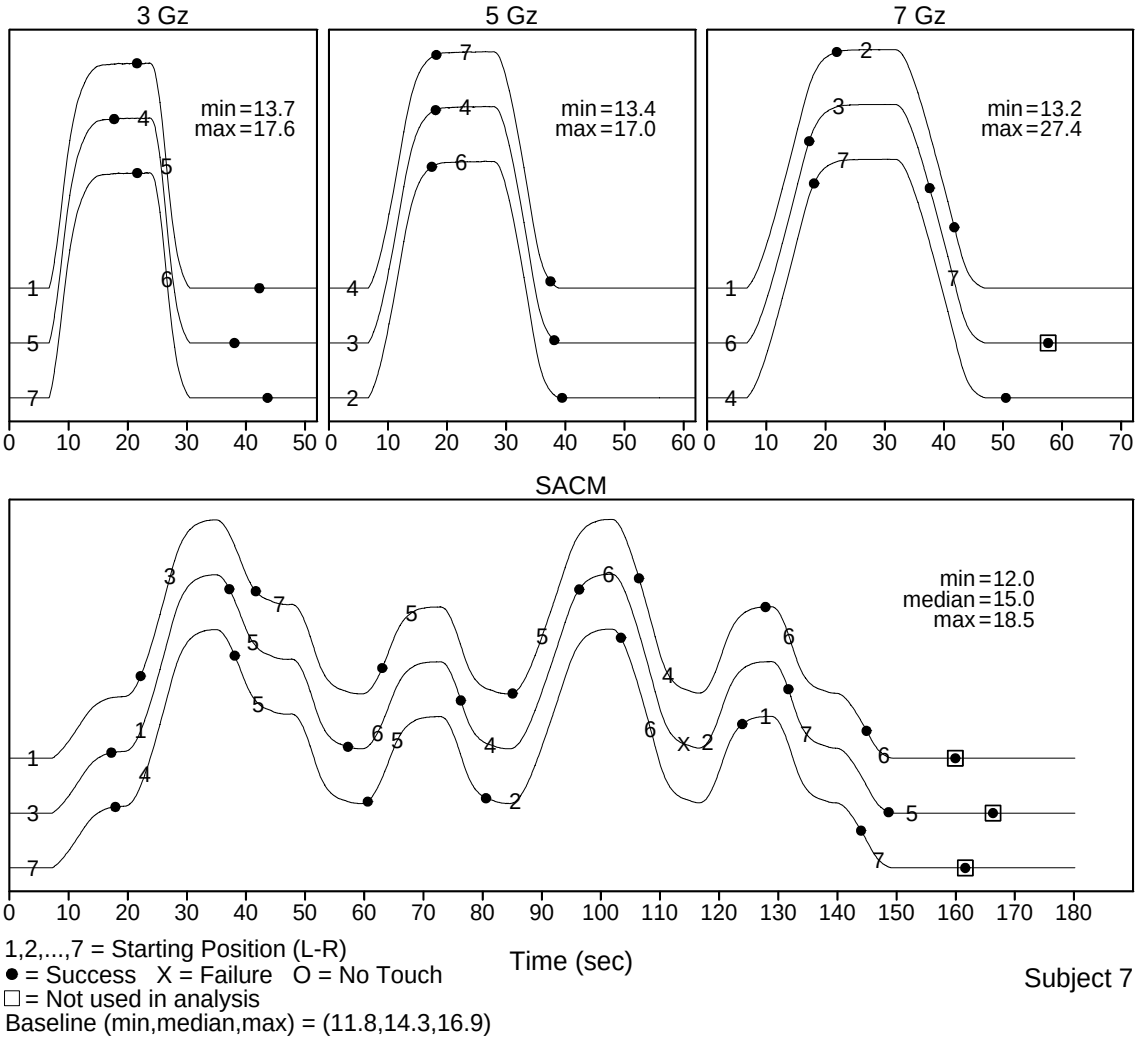

Figure 85: Performance of subject 7 on the relative motion task

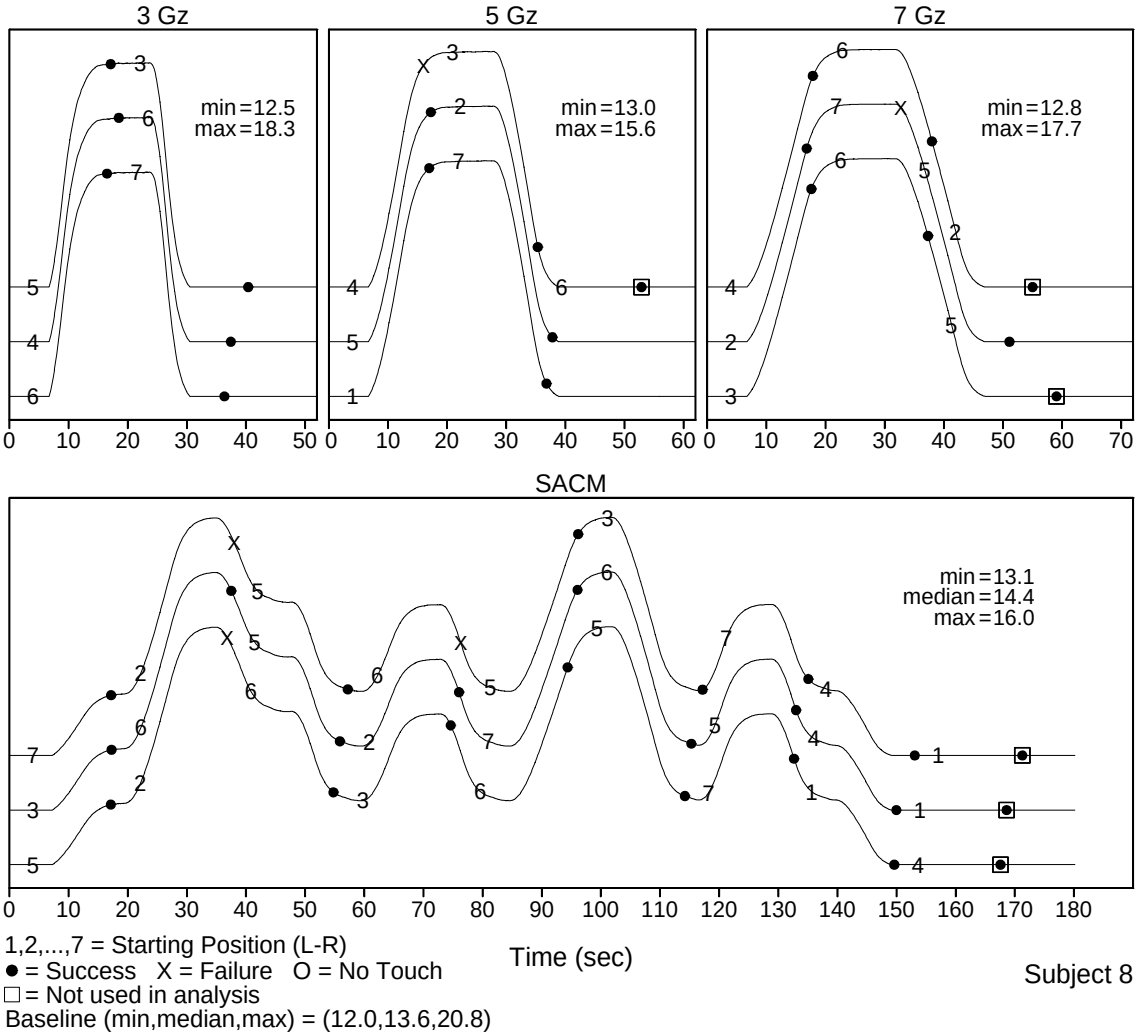

Figure 86: Performance of subject 8 on the relative motion task

The following two figures (87 & 88) provide additional detail for the recorded performance on the peripheral information processing task. Figure 87 provided the response time for each subject and plateau. The dashed horizontal reference line represents the geometric mean of baseline response time. Baseline response time statistics (min, geometric mean, max) are given above the top right of each plot. Figure 88 illustrates the reponse times for each subject and plateau during each half of the SACM. Again, the baseline angle error statistics (min, mean, max) are displayed above each plot and the dashed horizontal reference line represents the geometric mean of baseline response time.

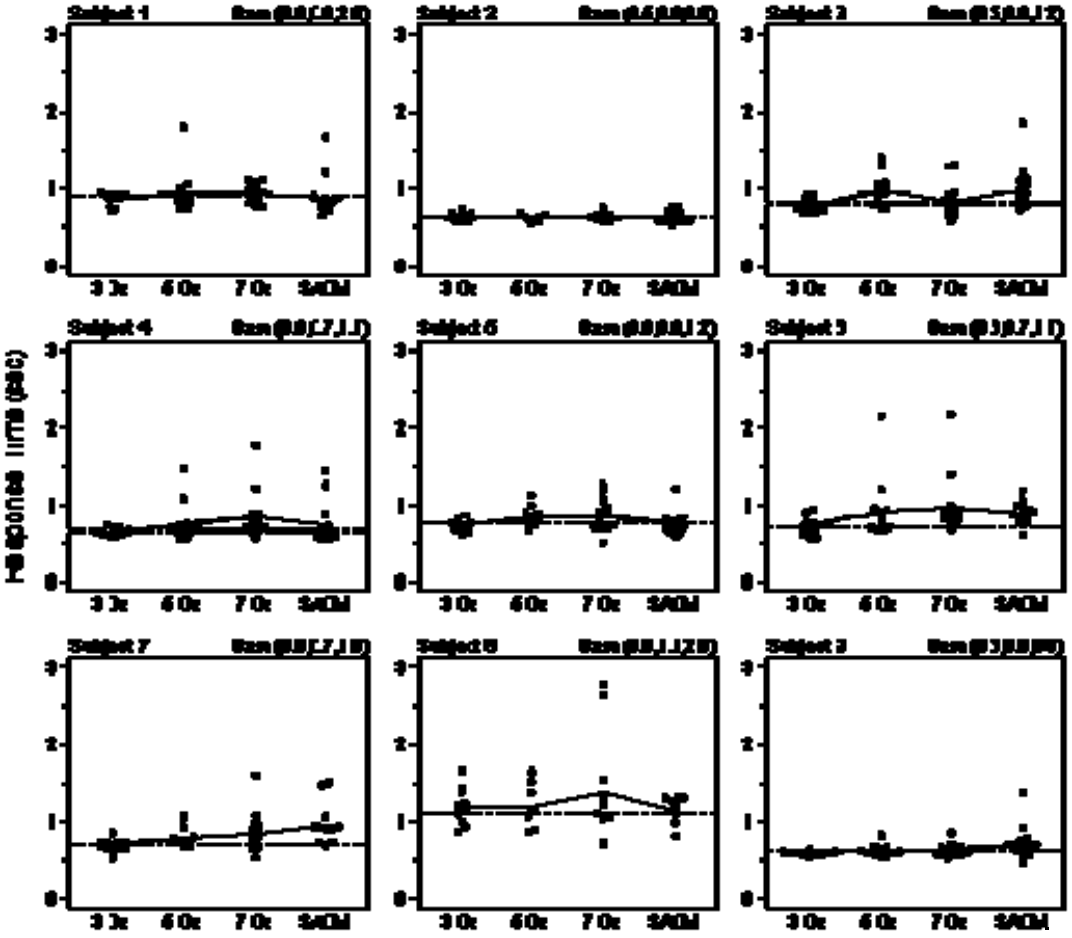

Figure 87: Peripheral information processing response time for each subject and plateau

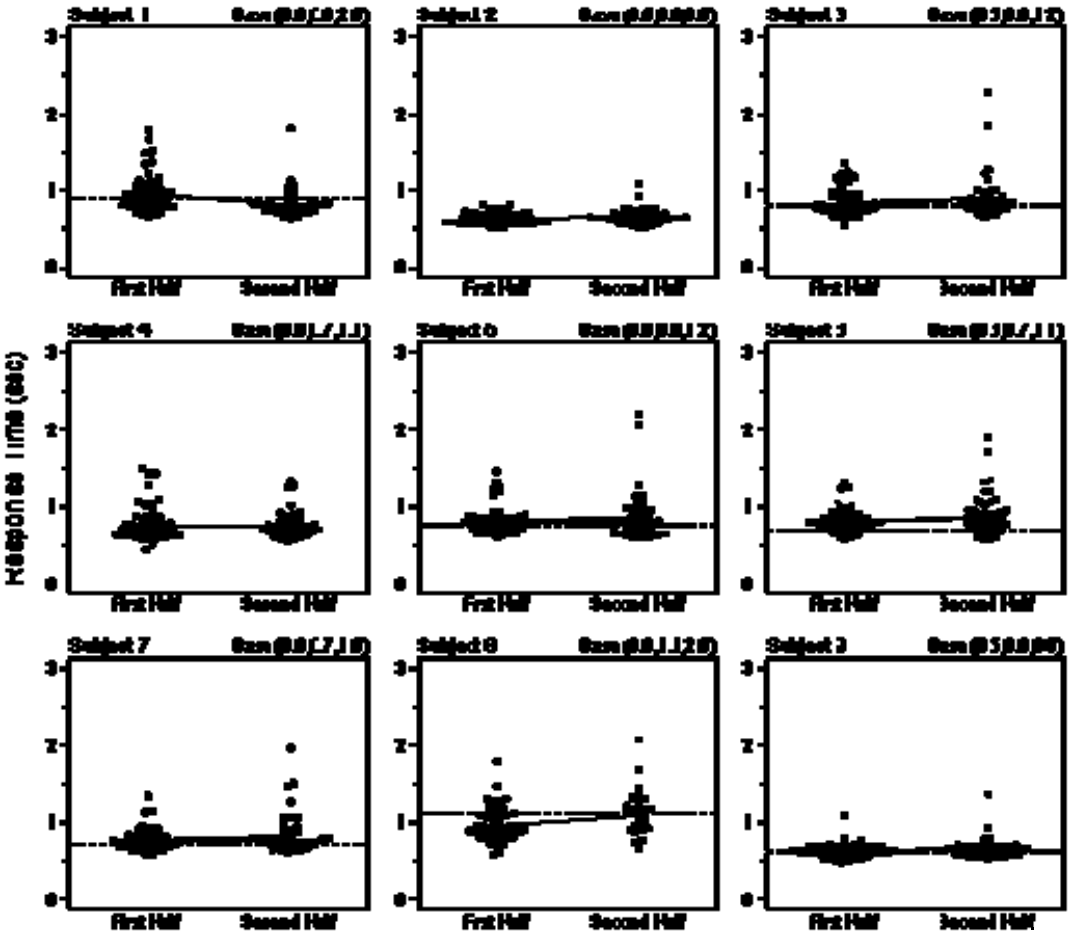

Figure 88: Peripheral information processing response times for each subject SACM half

Additional charts were also created for the pitch-roll capture task that provide additional detail. For Figures 89-92, the correlation between particular variables is shown for each subject. Above each panel is the p-value from a two-tailed t-test (H_o: correlation (or slope) = 0).

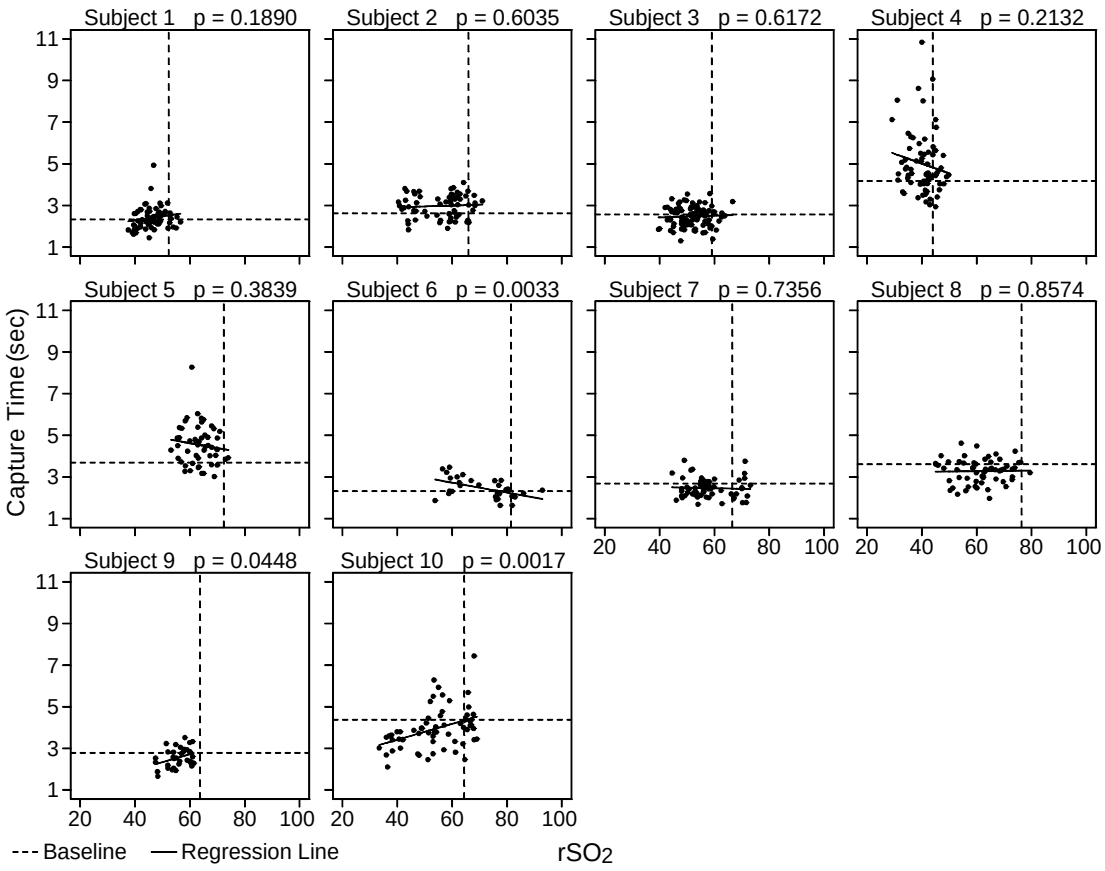

Figure 89: Correlation between capture time and rSO_2 for the pitch-roll capture task

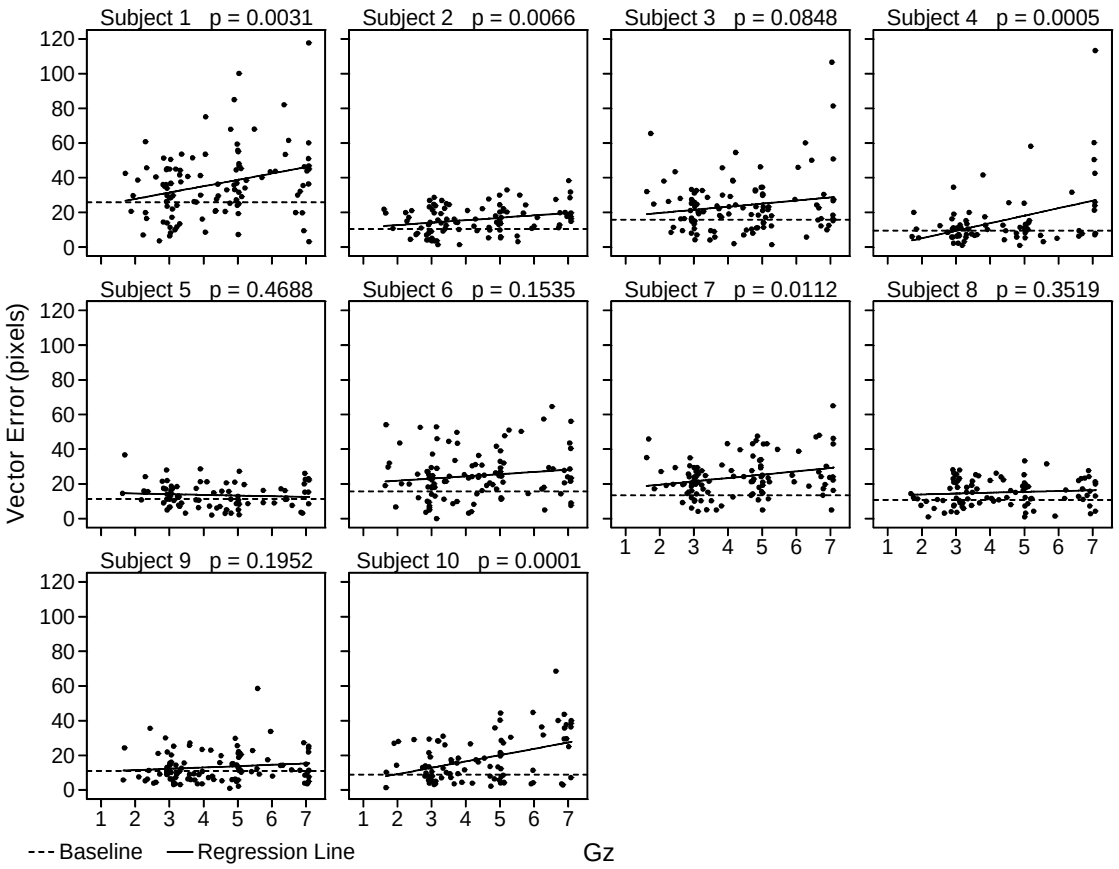

Figure 90: Correlation between vector error and G_z for the pitch-roll capture task

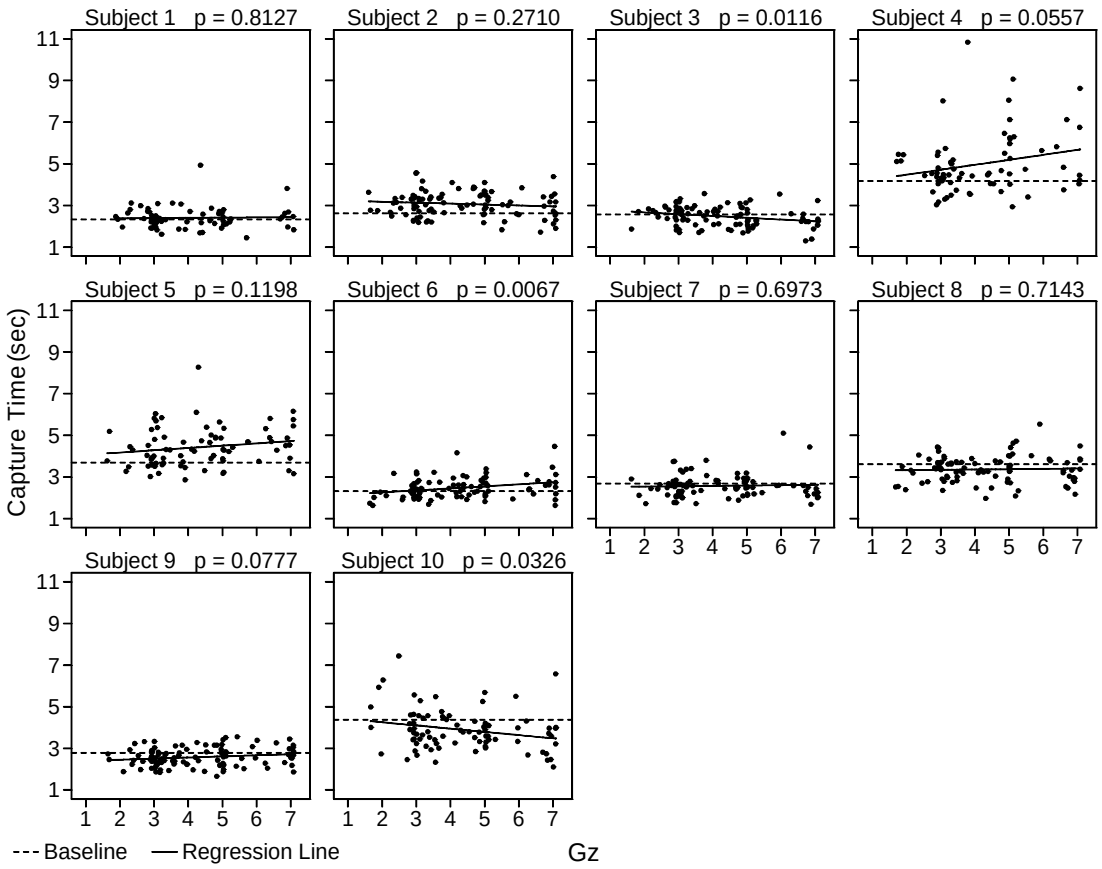

Figure 91: Correlation between capture time and G_z for the pitch-roll capture task

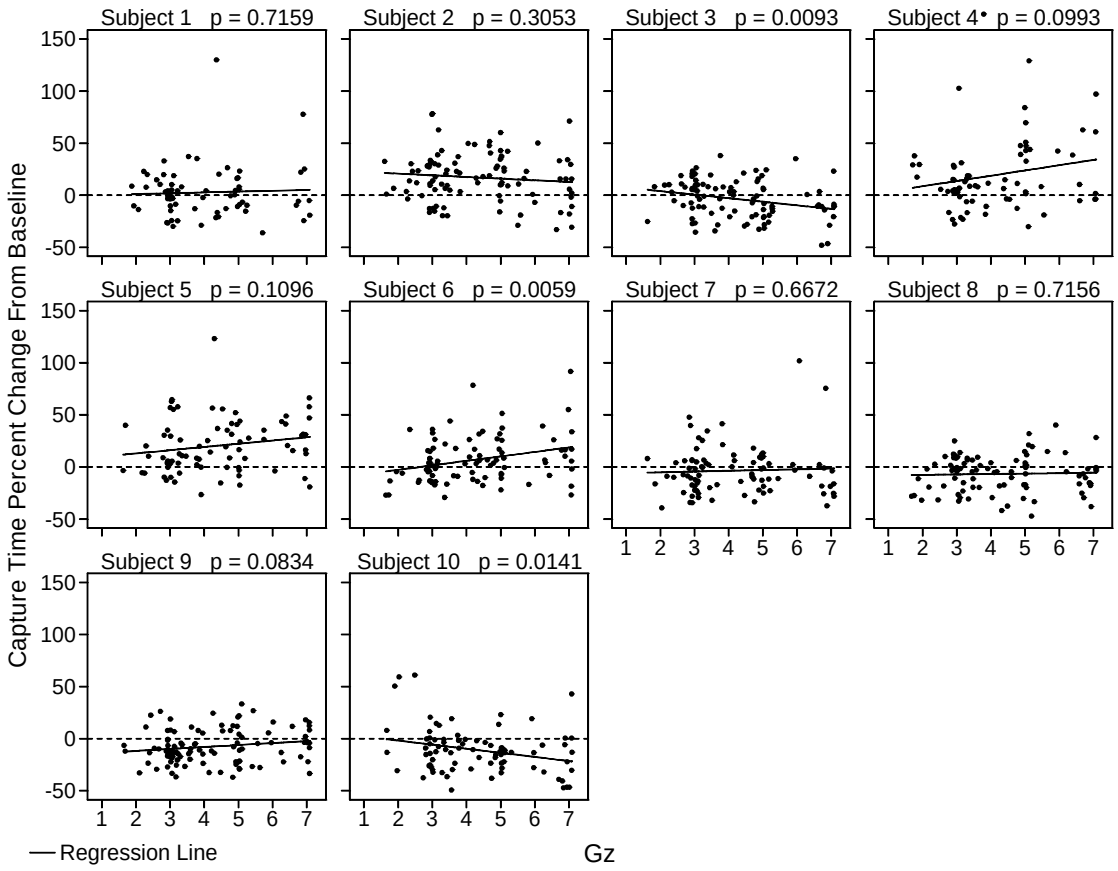

Figure 92: Correlation between capture time percent change from baseline and G_z for the pitch-roll capture task

Figure 93 contains capture times for each subject and trial during the plateaus of the 3 G_z, 5 G_z, and 7 Gz runs and the 7 G_z plateau of the SACM run while Figure 94 contains capture times for each subject and trial during the first and second half of the SACM.

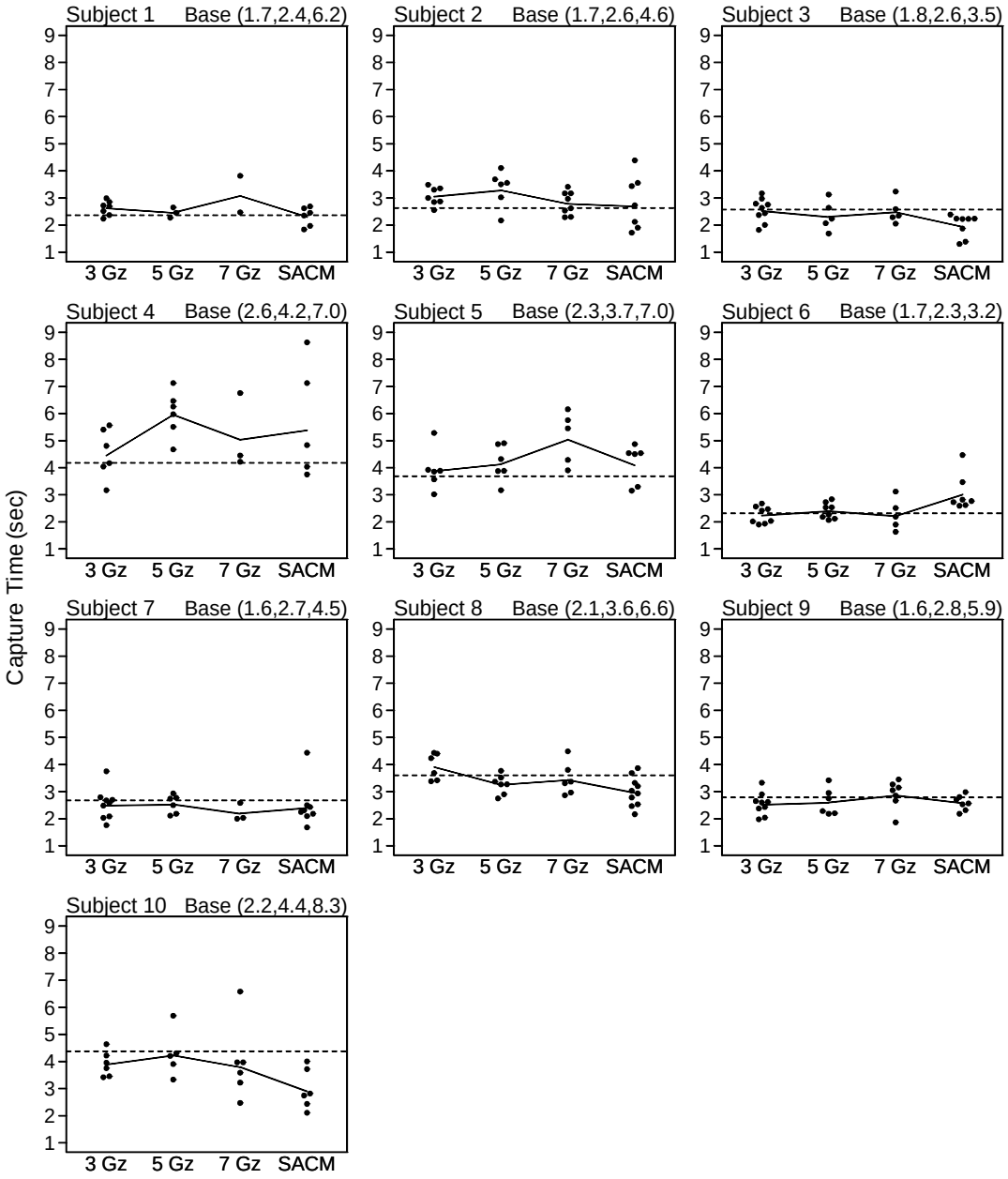

Figure 93: Pitch-roll capture time for each subject and plateau of each G_z profile

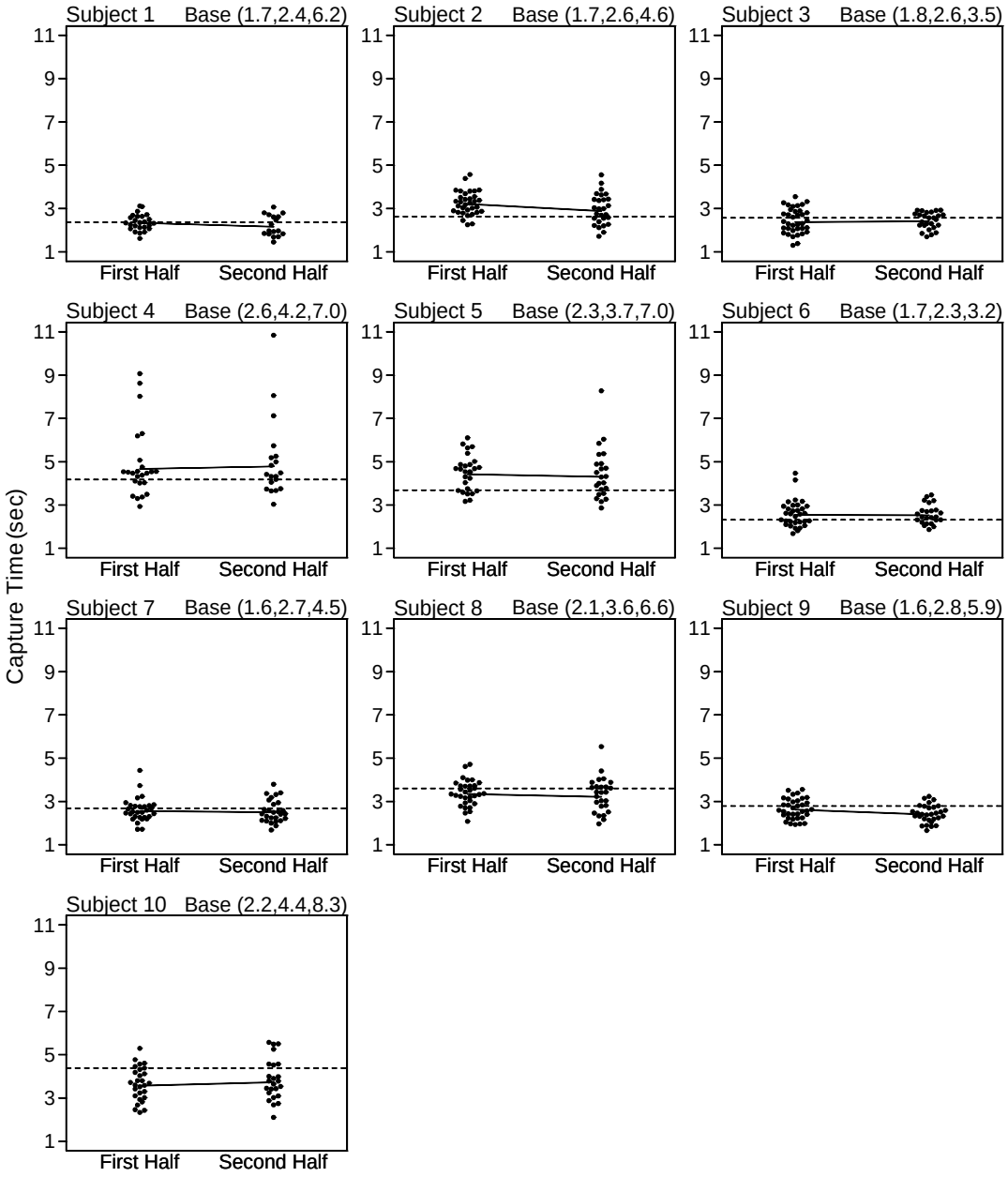

Figure 94: Pitch-roll capture time for each subject and first or second half of SACM

The non-baseline trials for each subject are shown in figures 95-104. For each panel in the top plot, day 1 runs are on top, day 2 runs in the middle, and day 3 runs on the bottom. The curve is the G_z profile. Numbers on the curve are capture time (rounded to the nearest integer). If the vector error was greater than 41.5 pixels (i.e., an error in performance), a rectangle was placed around the capture time. The rSO_2 profiles are shown below the performance panels.

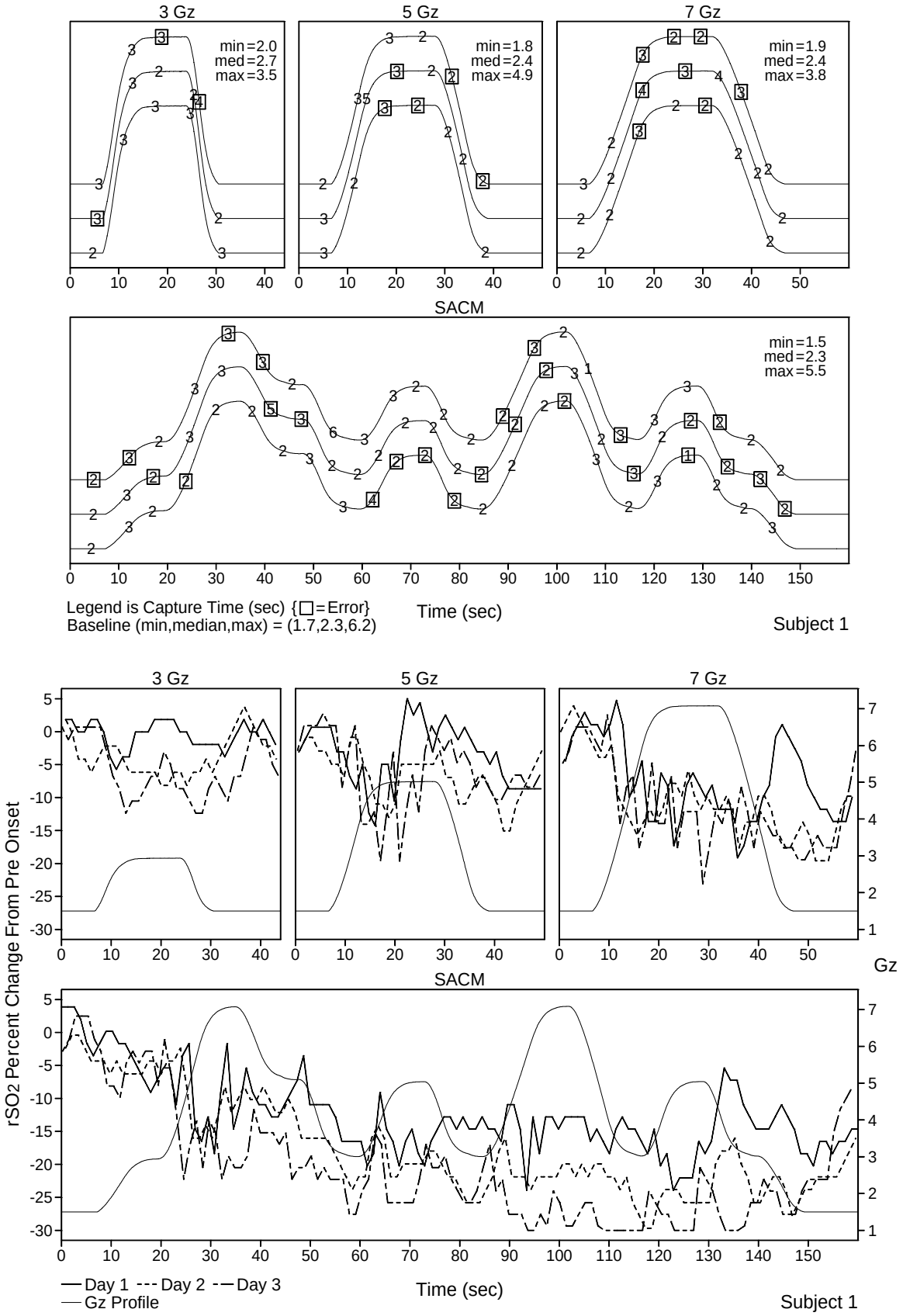

Figure 95: Pitch-roll capture time and rSO_2 data for subject 1

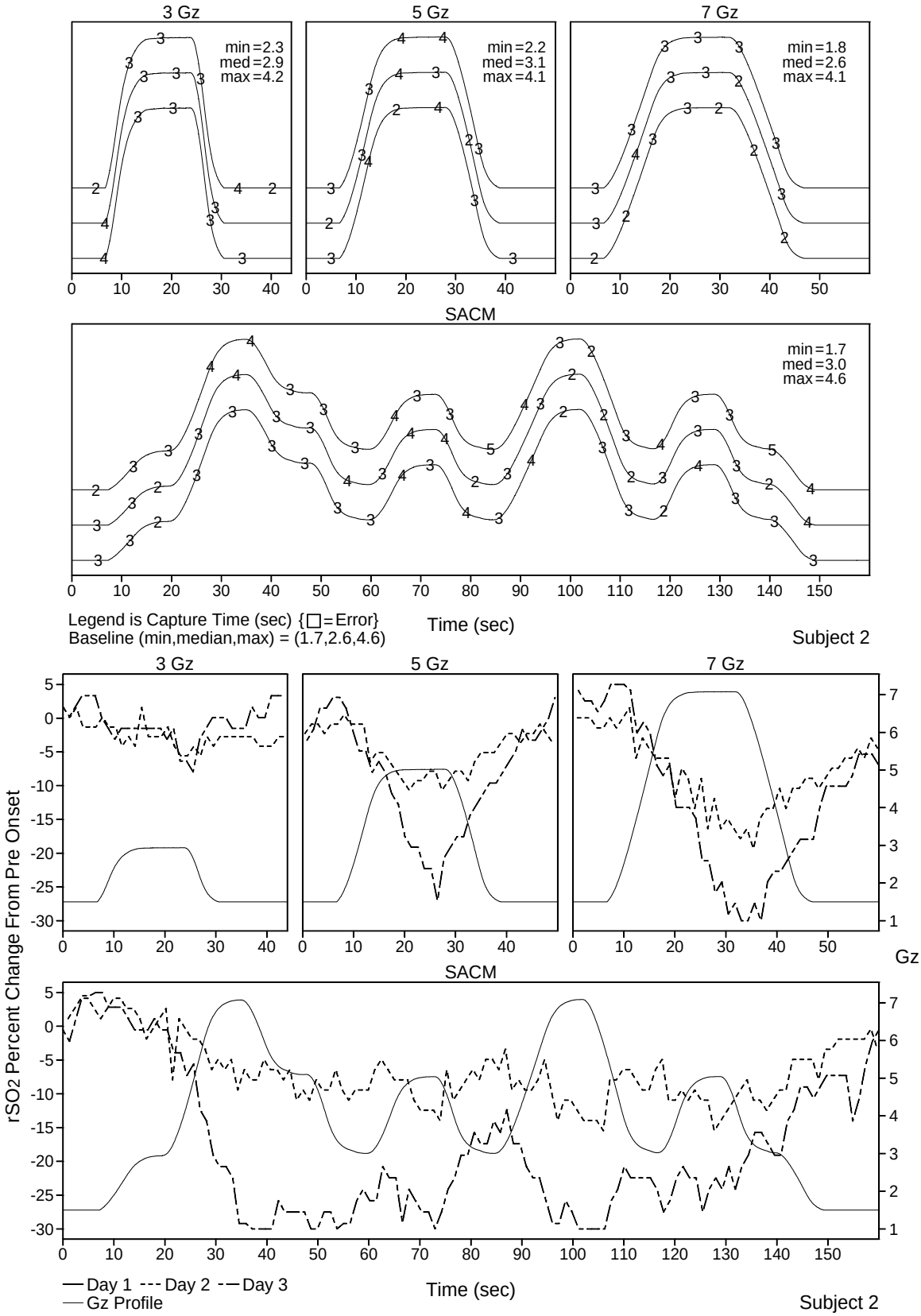

Figure 96: Pitch-roll capture time and rSO_2 data for subject 2

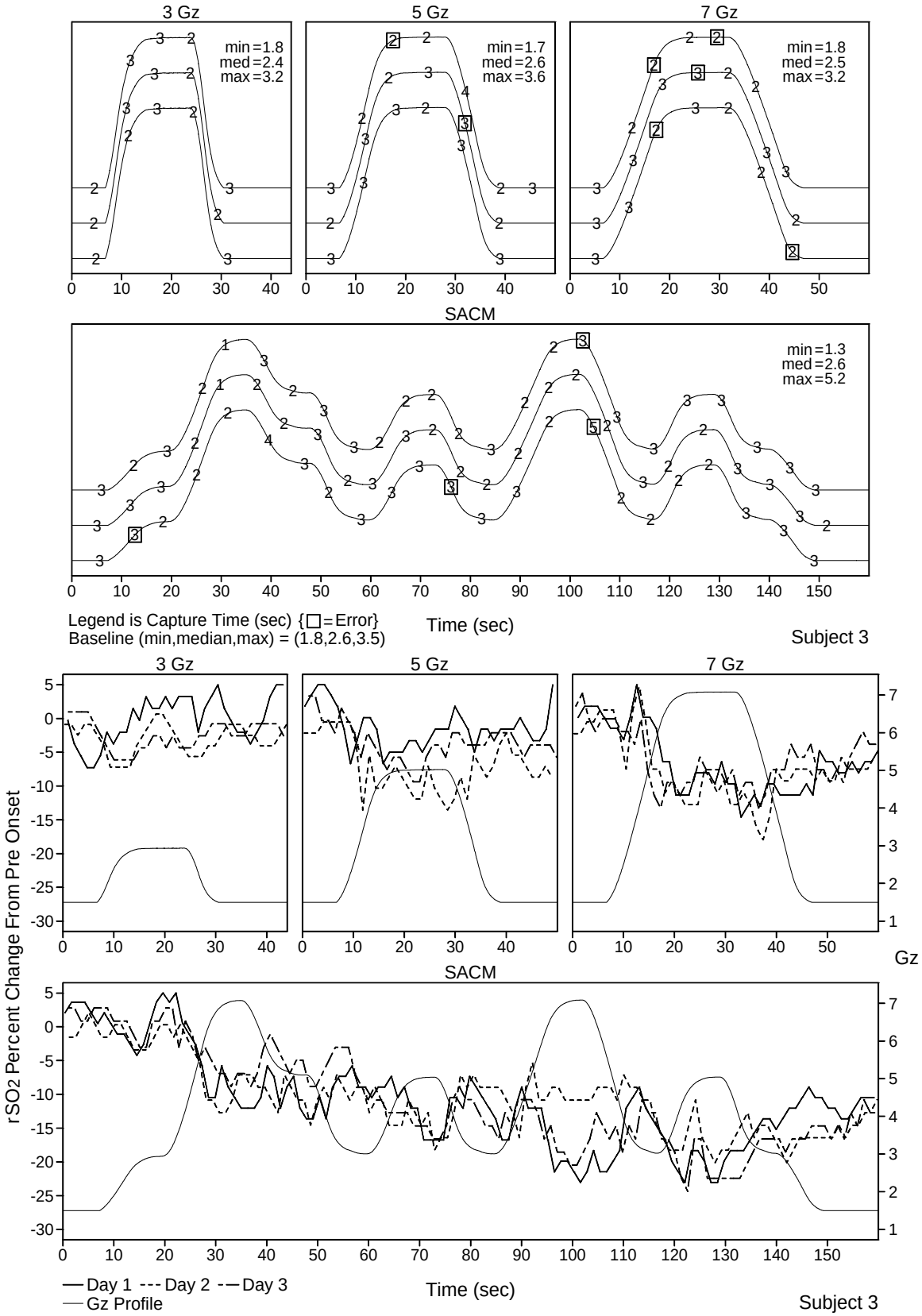

Figure 97: Pitch-roll capture time and rSO_2 data for subject 3

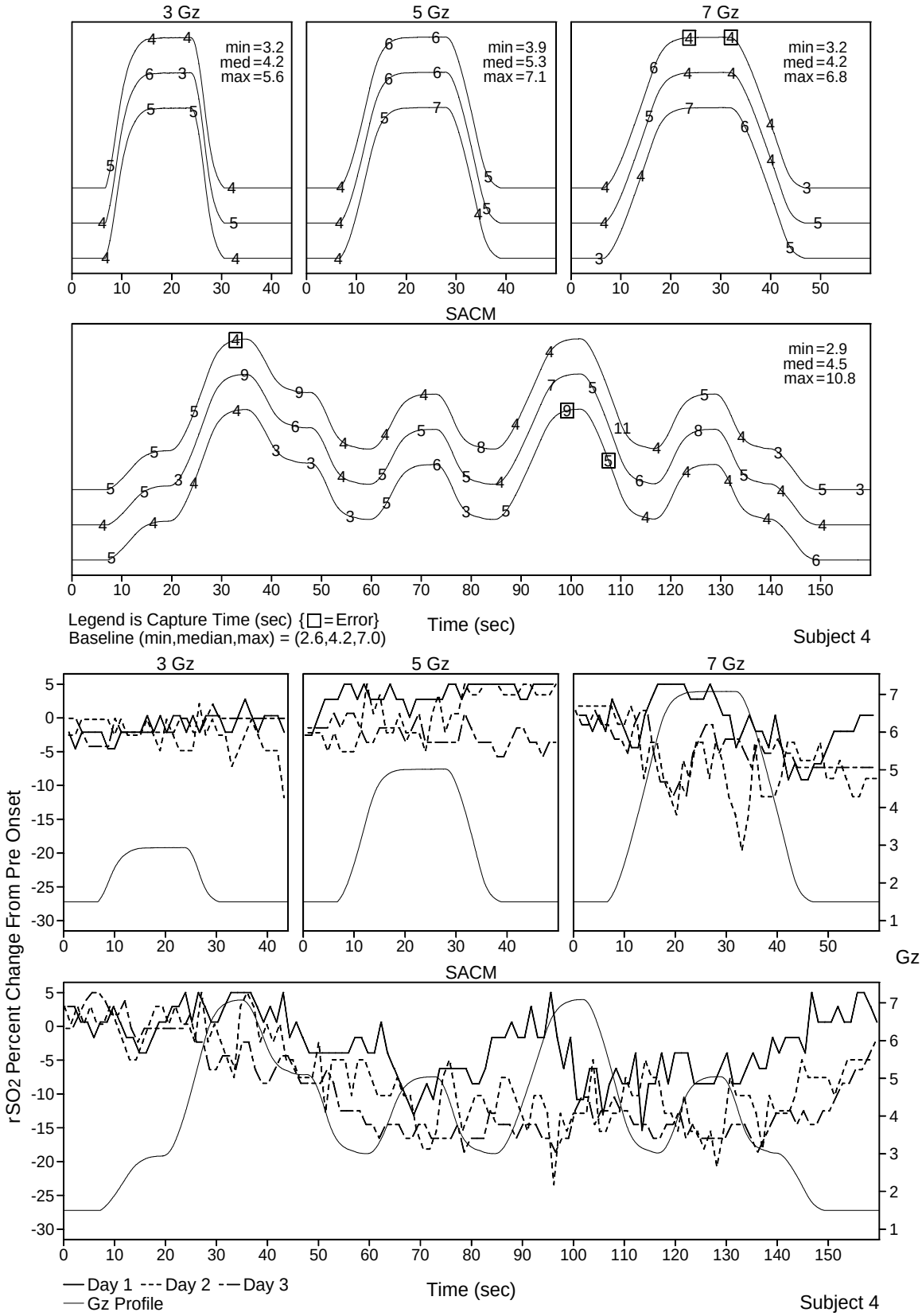

Figure 98: Pitch-roll capture time and rSO_2 data for subject 4

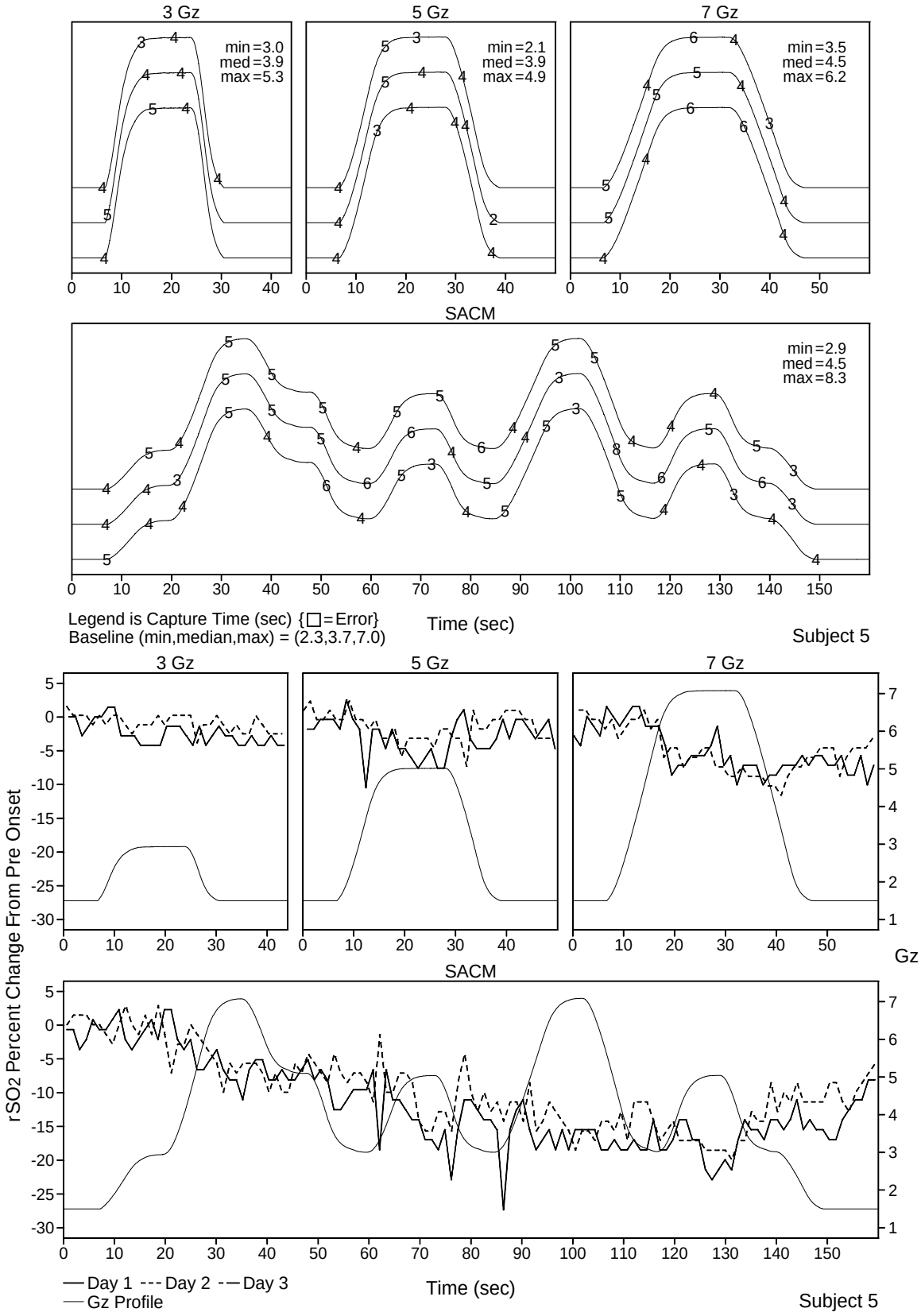

Figure 99: Pitch-roll capture time and rSO_2 data for subject 5

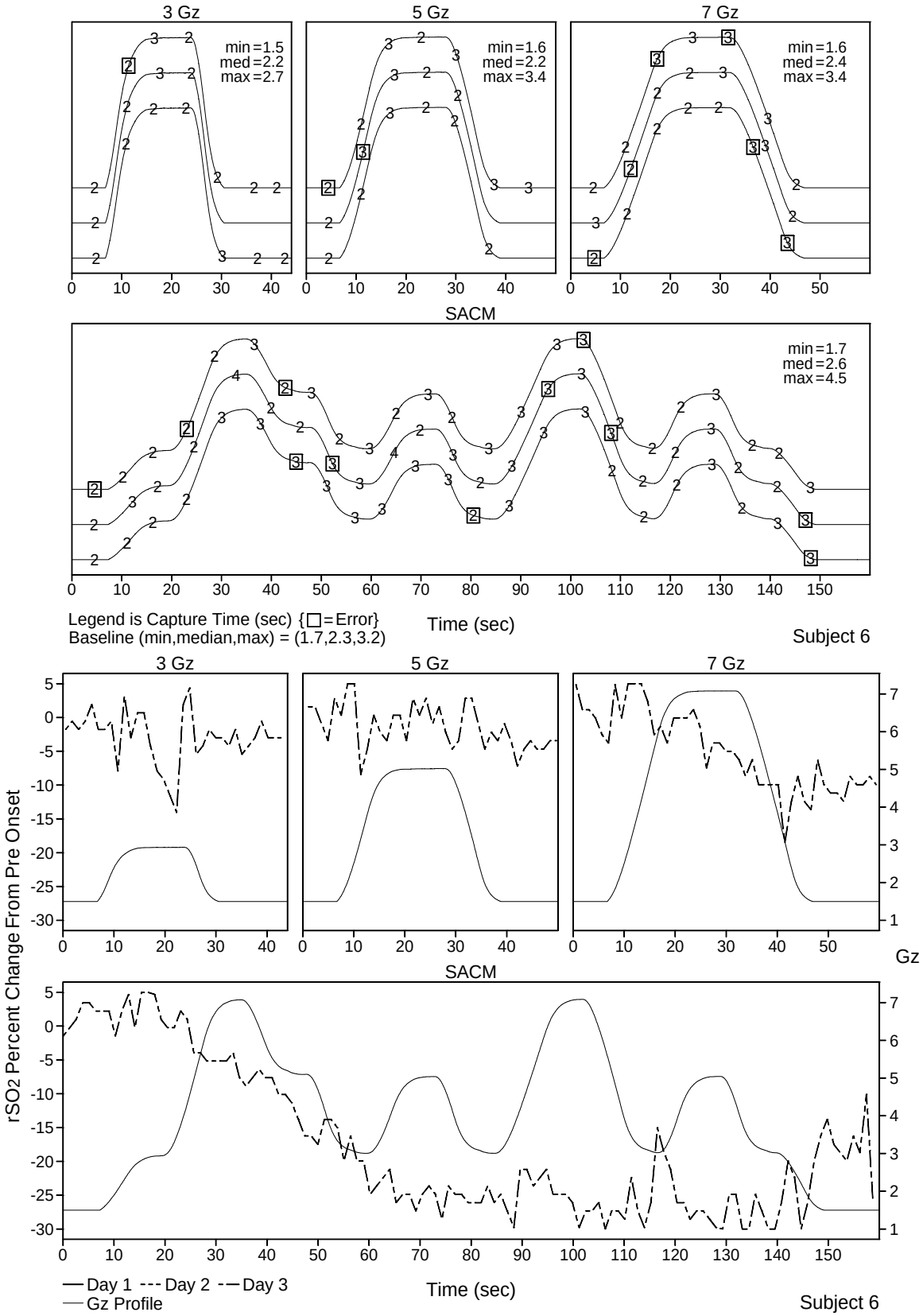

Figure 100: Pitch-roll capture time and rSO_2 data for subject 6

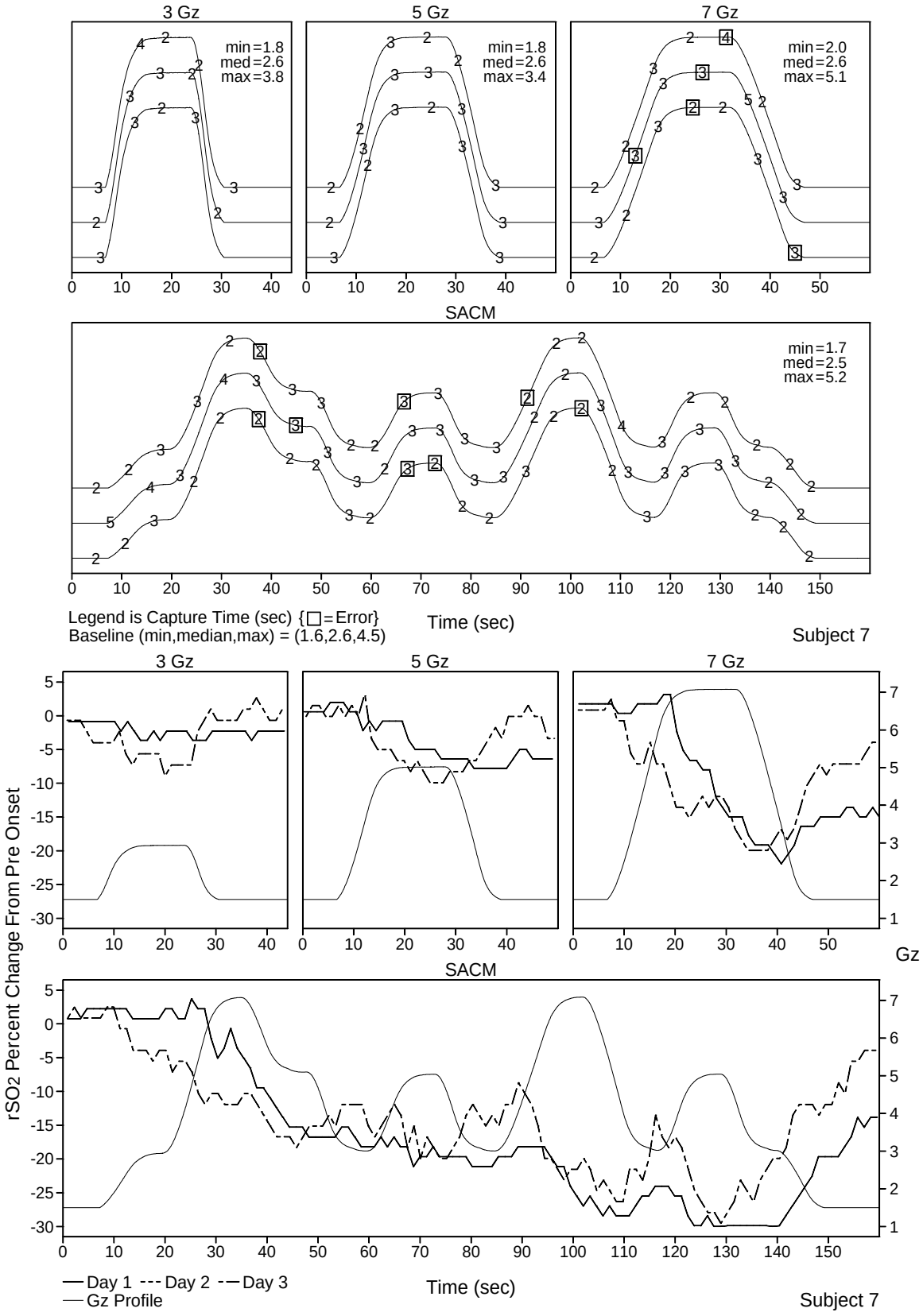

Figure 101: Pitch-roll capture time and rSO_2 data for subject 7

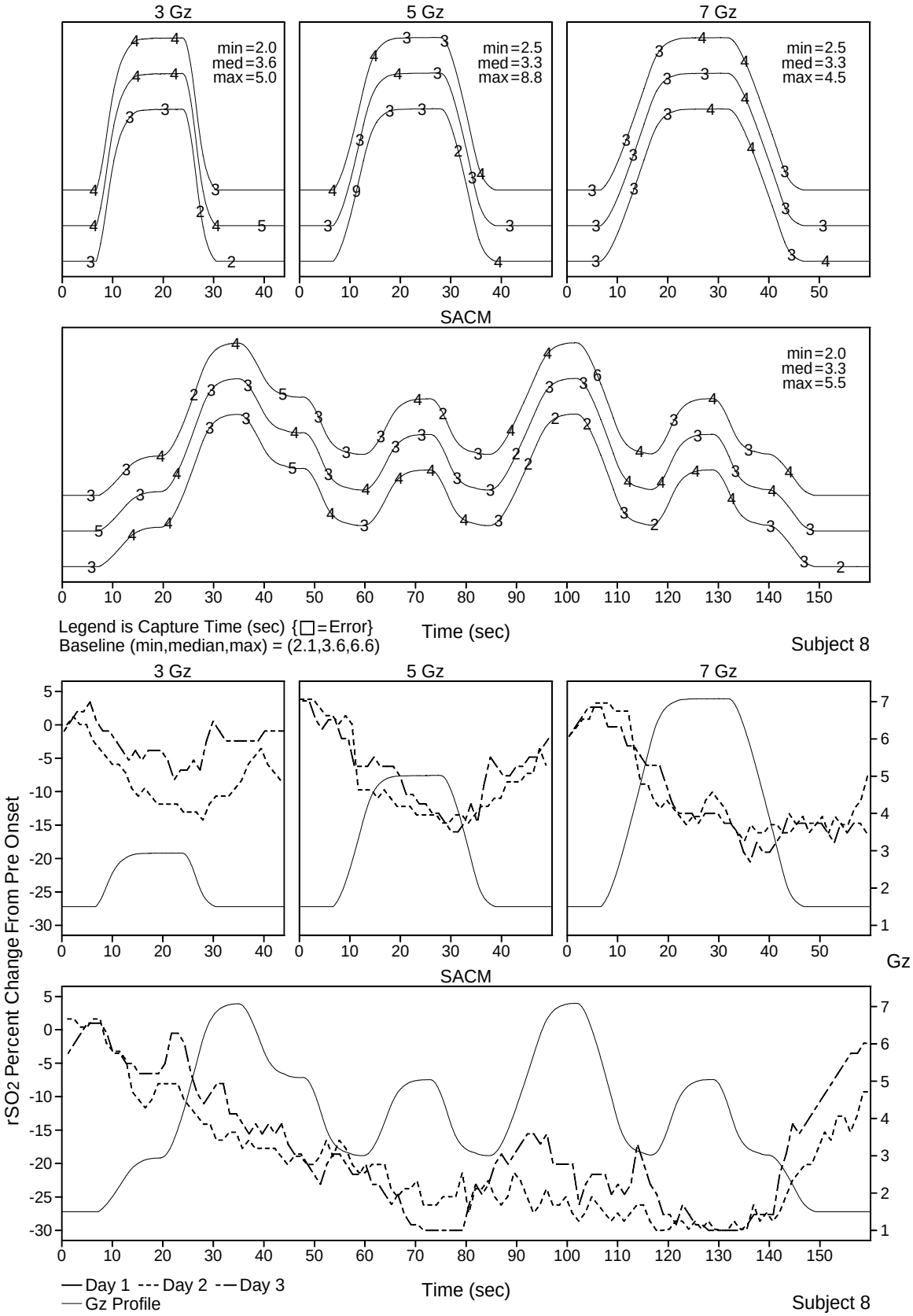

Figure 102: Pitch-roll capture time and rSO_2 data for subject 8

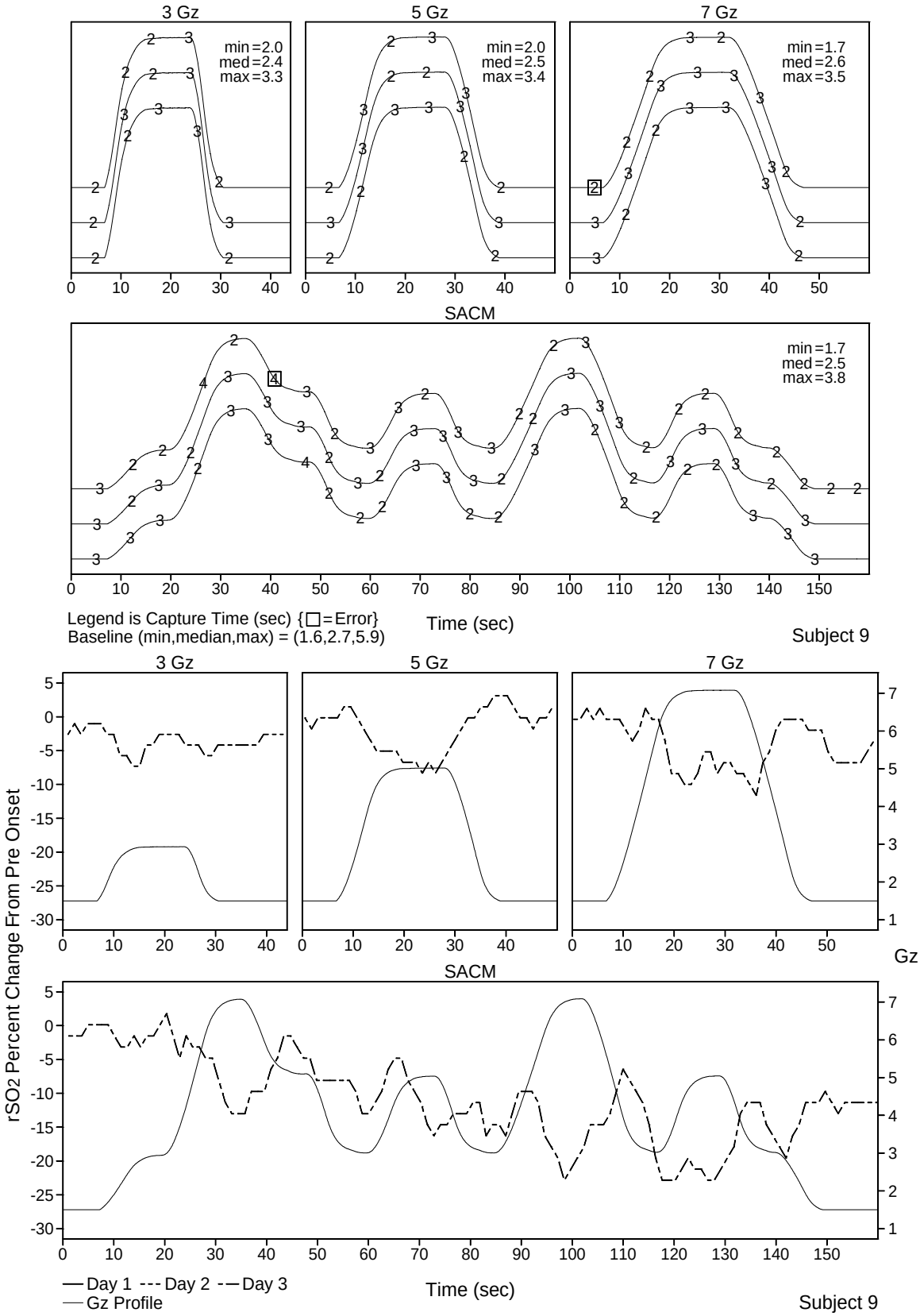

Figure 103: Pitch-roll capture time and rSO_2 data for subject 9

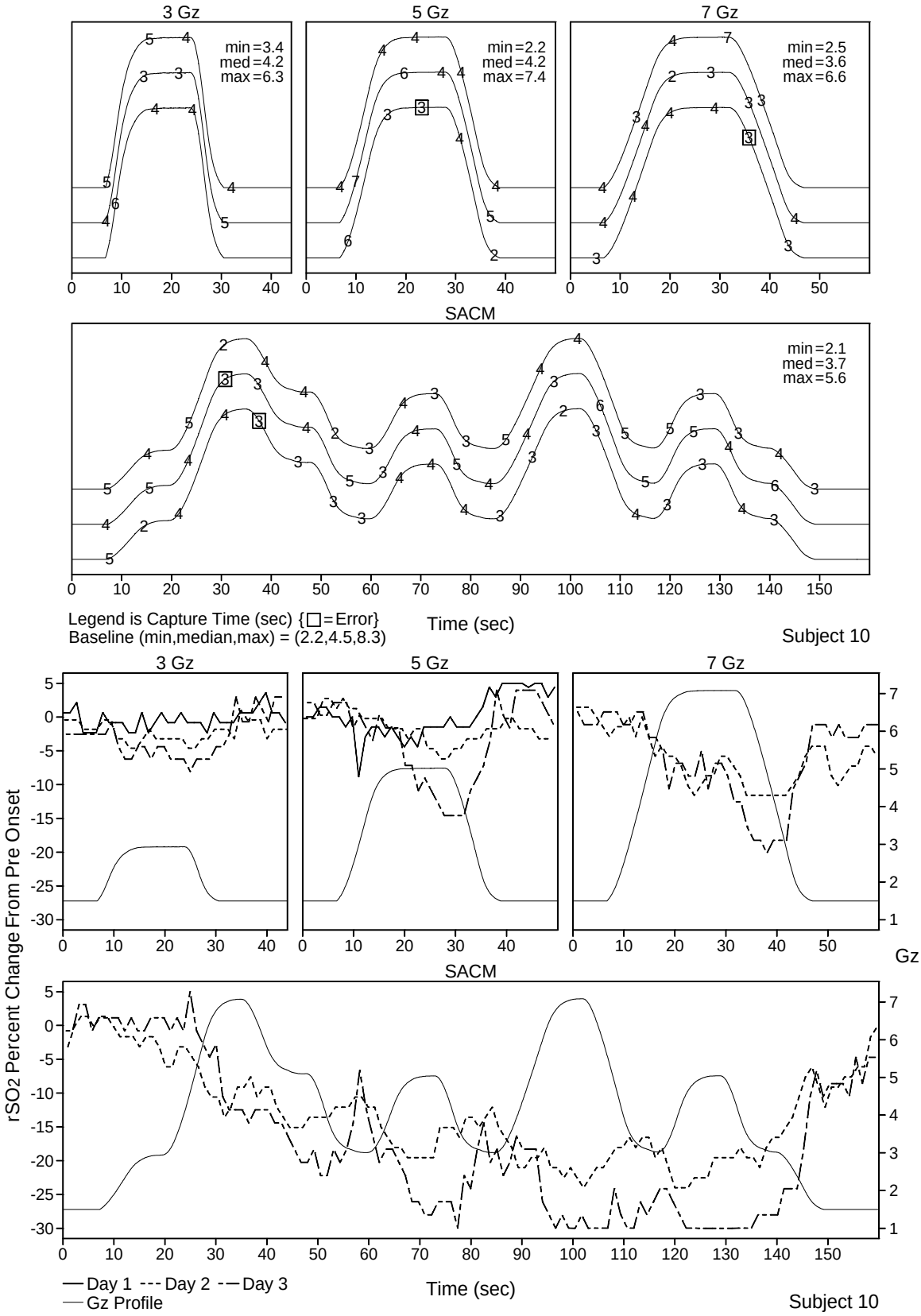

Figure 104: Pitch-roll capture time and rSO_2 data for subject 10

One additional plot was created for the unusual attitude recovery task. Figure 105 provides the recovery times for each subject and trial. The dashed horizontal line is mean baseline. The one recovery time too small to be reasonable (50 msec) and 9 timeouts (> 20 sec and placed at the top of the panel) are circled. The 3 combinations of pitch and roll used for a particular subject are identified above each panel and are color coded as indicated. S1 and S2 refer to the first and second half of the SACM.

Likewise, additional charts were created for the rapid decision making task. Figure 106 displays the response time percent change from baseline for each subject and plateau. The dashed horizontal reference line represents the geometric mean of baseline response time. Baseline response time statistics (min, geometric mean, max) are given above the top right of each plot. Figure 107 displays the response time for each subject and SACM half.

No additional plots or graphs were generated for the visual monitoring or short term memory tasks.

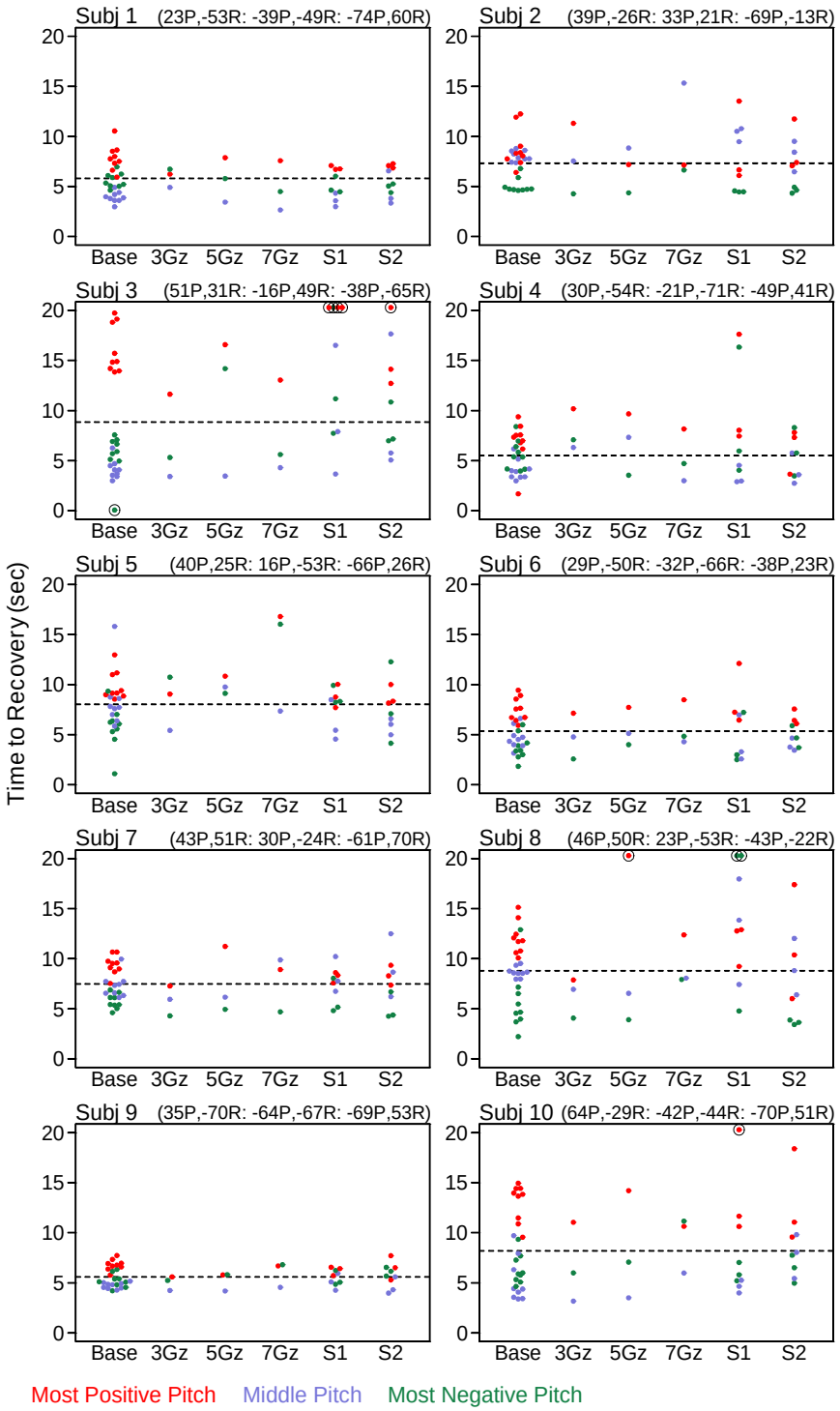

Figure 105: Time to recovery for each subject, condition, and trial

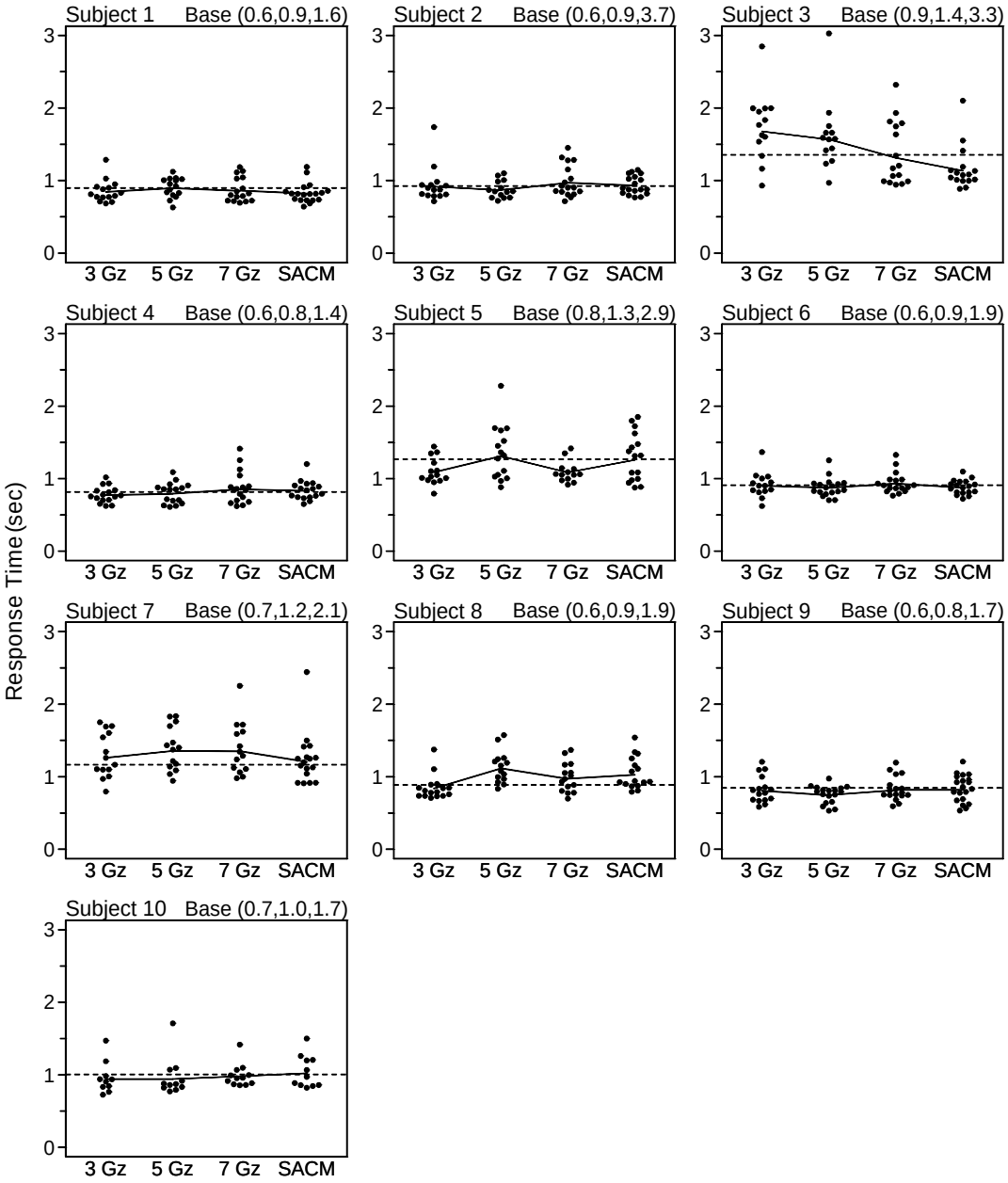

Figure 106: Rapid decision making task response time for each subject and plateau

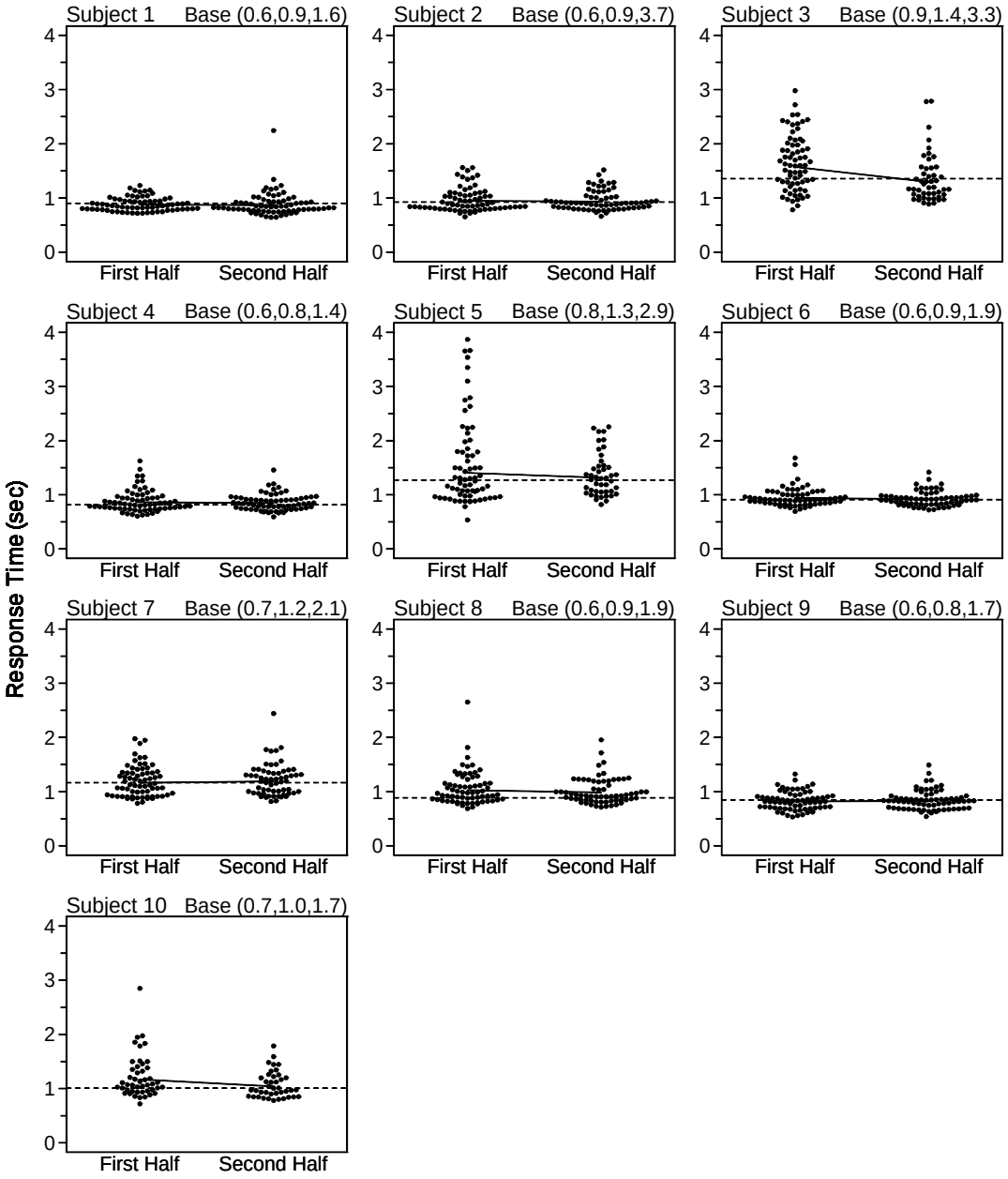

Figure 107: Response time for each subject SACM half